RIGA TECHNICAL UNIVERSITY
FACULTY OF TRANSPORT AND MECHANICAL ENGINEERING
INSTITUTE OF MECHANICS

Alexey KLOKOV
Candidate for a doctoral degree of study program "Mechanical Engineering"

Global Analysis of Dynamics of the Pendulum Systems, New Bifurcation Groups and Rare Attractors

Doctoral Thesis

Scientific supervisor
Dr. habil. sc. ing., Professor
Mikhail ZAKRZHEVSKY

Riga 2013

Klokov A. Global analysis of dynamics of the pendulum systems, new bifurcation groups and rare attractors. Doctoral Thesis. – R.: RTU, 2013 – 191 p.

Printed according to the decision of IM, the protocol No. 6, dated June 21, 2013.

The doctoral thesis submitted for the degree of Doctor of Engineering Sciences (Engineering Technology, Mechanics and Mechanical Engineering) and defended at the public session at the Faculty of Transport and Mechanical Engineering, Riga Technical University, at 29 of November 2013, room 302, at 6 Ezermalas Street, Riga, Latvia.

OFFICIAL REVIEWERS

Professor, Dr.habil.sc.ing., Honored Scientist of the Russian Federation, Grigory Panovko
Blagonravov Mechanical Engineering Institute of Russian Academy of Sciences, Russia

Professor, Dr.sc.ing., Jānis Auziņš
Riga Technical University, Institute of Mechanics, Latvia

Professor, Dr.habil.sc.ing., Juris Cimanskis
Latvian Maritime Academy, Latvia

This work has been supported by the European Social Fund within the project
«Support for the implementation of doctoral studies at Riga Technical University»

ESF
EIROPAS SOCIĀLAIS FONDS

EIROPAS SAVIENĪBA

Annotation

The doctoral thesis cover new previously unknown fundamental laws governing the behavior of the pendulum driven systems in the framework of the interdisciplinary science "nonlinear dynamics and chaos". The bifurcation theory of nonlinear dynamical systems and the method of complete bifurcation groups developed in Institute of Mechanics of Riga Technical University are used for the global analysis of driven damped pendulum systems with one or several degrees of freedom. New nonlinear effects have been found for parametrically excited pendulum systems with the periodically vibrating point of suspension in different directions (in vertical, in horizontal, in both directions and at a certain angle to the horizontal), pendulum with external harmonic excitation, rigid body pendulum with several equilibrium positions, centrifugal pendulum vibration absorber, pendulum model with a additional sliding mass, double pendulum with harmonic oscillations of the point of suspension in the vertical direction, six body pendulum system with several equilibrium positions and harmonic excitation. The birth of the previously unknown rare attractors has been shown for different pendulum systems, and new bifurcation groups with complex protuberances have been obtained. The new types of interaction of different oscillating and rotating orbits have been found as well as rare and chaotic rotating regimes. Also the process of formation of chaotic rotation through the cascade of period-doubling bifurcations for different groups has been studied within the framework of the research. Also attention is paid to stable periodic and chaotic oscillations of different type near unstable equilibrium position of the pendulum.

The doctoral thesis are intended for use in a course of ordinary differential equations, in courses on nonlinear dynamics and chaos and in nonlinear oscillation theory for students of different specialties who have basic knowledge to the extent of the 1st year of training at technical colleges and universities, as well as for those interested in contemporary issues and methods of nonlinear oscillation theory and nonlinear dynamics and chaos. This doctoral thesis obviously does not cover the topic fully and author will be grateful for remarks.

This doctoral thesis can be useful for illustrating the main statements of the bifurcation theory of nonlinear dynamical systems, which is a rather new section of the general theory of nonlinear dynamical systems.

Contents

Introduction

The doctoral thesis present the results of the global bifurcation analysis, new bifurcation groups, rare attractors and chaos for pendulum driven systems and researches conducted on "novelty bifurcation theory", developed in Institute of Mechanics of Riga Technical University (RTU). The method of complete bifurcation groups is developed (1993-2013) in Institute of Mechanics of Riga Technical University in the research group of Prof. M. Zakrzhevsky. This group is working in such scientific direction "Nonlinear dynamics, chaos, catastrophes and control". The method of complete bifurcation groups and complex of algorithms and software proposed on its basis allows finding for the archetypical and widely used classical nonlinear dynamic models qualitatively new previously unknown rare regular and chaotic attractors, new bifurcation groups and studying the interaction of different bifurcation groups.

A novelty bifurcation theory of nonlinear dynamical systems (BT NDS) and its application, intended for direct global bifurcation analysis of dynamical periodic systems is presented. The bifurcation theory is established for essential nonlinear dynamical periodic systems, described by models of ODE equations or by map-based models of discrete-time equations. Our approach is based on ideas of Poincaré, Andronov and other scientists' results concerning global dynamics, structural stability and bifurcations and chaotic responses of dynamical nonlinear systems and their topological properties.

The main idea of the novelty BT is a fact that the NDS in given parameters and state spaces has a finite number (usually not so many) of independent bifurcation groups S(p) with their own complex topology and bifurcations, chaotic behaviour, and, in many cases, with rare regular and chaotic attractors (RA). For each point of parameter space it is possible to find all essential fixed points of the periodic orbits (stable and unstable). This periodic skeleton allows to mark out the bifurcation groups and to start global analysis in state and parameter spaces.

One of the main elements of the method of complete bifurcation groups is a continuation of unstable periodic regimes in the parameter space that allows finding so-called rare stable dynamical regimes - rare chaotic and periodic attractors. These phenomena cannot be systematically detected by traditional methods of nonlinear dynamics: the Krylov-Bogolyubov, the small parameter method and the method of harmonic balance.

The main concepts of the novelty BT are: complete bifurcation group (BG); unstable periodic infinitium subgroups (UPI- or π- groups), responsible for chaos; complex protuberances; and periodic skeletons for a system with parameter p. For illustration of the advantages of the novelty bifurcation theory in this doctoral thesis such pendulum driven systems are used:

- The parametrically excited pendulum system with an additional linear restoring moment and with the periodically vibrating point of suspension in both directions;
- The pendulum system with the periodically vibrating point of suspension in the vertical direction;
- The pendulum with the vibrating point of suspension in the horizontal direction;
- The pendulum system with harmonic oscillations of the point of suspension at a certain angle to the horizontal;
- The pendulum with external harmonic excitation;
- Rigid body pendulum with linear spring and several equilibrium positions;
- Centrifugal pendulum vibration absorber with impact interactions;
- Driven damped pendulum model with a sliding mass and with the external periodic excited moment;
- Double pendulum with harmonic oscillations of the point of suspension in the vertical direction;
- Six body driven symmetric pendulum system with several equilibrium positions, linear dissipative forces between pendulums, additional linear elastic forces and harmonic excitation, applied to the first pendulum.

In all considered examples we have found that the novelty bifurcation theory's methods allow finding important unknown regular or chaotic attractors and new bifurcation groups with rare attractors. Additional illustration of the novelty bifurcation theory, it is possible to find in my colleague's papers where there is a rather complete bibliography on the bifurcation theory and rare attractors (see references).

A novelty of bifurcation theory used in the doctoral thesis is based on fundamental works of: H. Poincaré, J.D. Birkhoff, A.M. Lyapunov, L.I. Mandelstam, A.A. Andronov, N.N. Bogolyubov, N.M. Krylov, Yu. A. Mitropoloskii et.al.

The author of the doctoral thesis used the ideas and materials of many scientists of nonlinear dynamics, in particular: I.V. Adrianov, V.S. Afraimovich, A.S. Alekseev, H. Altenbach, V.S. Anishchenko, A.V. Aramov, V.I. Arnold, V.K. Astashev, J. Auzinsh, J. Awrejcewicz, V.I. Babitsky, J.M. Balthazar, R. Bansevicius, Z.S. Batalova, N.N. Bautin, V.V. Beletsky, V.N. Belix, L.N. Belustina, S. Bishop, I.I. Blekhman, V.V. Bolotin, A. Bubulis, N.V. Butenin, M.P. Cartmell, G.M. Chechin, F.L. Chernousko, L.O. Chua, L. Dai, M. di Bernardo, M.F Dimentberg., A.S. Dmitriev, J. Engelbrecht, M.J. Feigenbaum, M.I. Feigin, A. Fidlin, A.L. Fradkov, R.F. Ganiev, O. Gendelman, P.B. Goncalves, C. Grebogi, J. Guckenheimer, V.I. Gulyayev, T. Hayasi, K.S. Hedrih, M. Henon, T. Hikihara, S.J. Hogan, P.J. Holmes, E. Hopf, D.A. Indeitsev, A. Janushevskis, J.A. Jorke, L.V. Kantorovich, T. Kapitaniak, P.L. Kapitza, D. Klimov, A.N. Kolmogorov, M.Z. Kolovsky, V.O. Kononenko, E. Kreuzer, V.L. Krupenin, A.P. Kuznetsov, N.V. Kuznetsov, S.P. Kuznetsov, P.S. Landa, L.D. Landau, S. Lenci, G.A. Leonov, U. Lepik, Y. Levinson, E.N. Lorenz, A. J.C. Luo, A.I. Lurie, N.A. Magnitskii, G.G. Malinetskii, A.I. Manevich, L.I. Manevich, A.P. Markeev, Yu.V. Mikhlin, F.C. Moon, A.D. Morozov, E. Mosekilde, Yu. Mozer, Yu.I. Neimark, V.V. Nemickii, I. Newton, E. Ott, G.Ya. Panovko, Ya.G. Panovko, C. Pierre, L.S. Pontryagin, A.I. Potapov, I. Prigozin, L. Pust, M.I. Rabinovich, M. Rafikov, K. Ragulskis, M. Ragulskis, J.W.S. Rayleigh, G. Rega, O.E. Rösler, D. Ruelle, M.A.F. Sanjuan, G. Schmidt, D. Shalfeev, A.N. Sharkovskii, S.W. Shaw, L.P. Shilnikov, A.Yu. Shvets, Ya.G. Sinai, C.H. Skiadas, S. Smale, A. Stephenson, H.B. Stewart, J. Stokker, Yu.M. Svirezhev, W. Szemplińska-Stupnicka, J.M.T. Thompson, J.J. Thomsen, S. Timoshenko, A. Tondl, D.I. Trubetskov, S.L. Tsyfansky, Y. Ueda, A. Vakakis, D.H. Van Campen, Van der Heijden, B. Van der Pol, F. Verhulst, J. Viba, I.I. Vulfson, J. Warminski, M. Wiercigroch, J. Yorke, G.N. Zaslavsky, A.A. Zevin, V.F. Zuravlev.

This list is incomplete and the author apologizes to the scientists that are not mentioned.

The doctoral thesis has been written in English. It contains the introduction, 6 chapters, conclusions, reference list, 3 appendices, 113 figures and 8 tables; the total number of pages: 191. The reference list contains 152 items.

The first chapter **"Task description of the global bifurcation analysis of the pendulum systems"** covers the problems of global bifurcation analysis of the typical pendulum driven systems and characterizes models used in the research. The notions of the coefficient of nonlinear elastic characteristic, awareness of which enables the readers to foresee chaotic oscillations in the system, are introduced. Moreover, the chapter considers the notions of periodic skeleton and passport of periodic regime on the Poincaré plane, which assist in performing the global analysis of the system dynamics in the given point of parameter space, as well as during the global bifurcation analysis in case one or several system parameters are changed. The list of pendulum driven models, discussed in the present thesis, is provided for the convenience of the readers.

The second chapter **„Basic elements of the bifurcation theory of the pendulum systems"** presents the approaches and methods that will be used for a global analysis of driven damped pendulum systems in this doctoral thesis. These approaches include the algorithms for construction of periodic skeleton (periodic passport), the method of searching the fixed points with and without taking into account the cyclic coordinates, method of complete bifurcation groups, Poincaré mappings from a line and from a contour, Cell-to Cell mapping, the method of separatrices of the saddle point, the method of continuation of bifurcation boundaries for the construction of the two-parameter bifurcation diagrams. The above mentioned approaches and methods are realized in three different software NLO, ABC NDC and SPRING. All the results of numerical simulations for the pendulum systems with one and several degrees of freedom in this doctoral thesis were obtained using these software.

In the third chapter **"Forced and parametrical oscillations of the pendulum systems with one degree of freedom"** the bifurcation analysis of harmonically driven damped pendulum systems with one degree of freedom (with dimension D = 3) was performed. The effectiveness of the method of complete bifurcation groups were discussed for following pendulum driven systems: pendulum with additional linear elastic spring and vibrating point of suspension in both directions, pendulum with harmonic oscillations of the point of suspension in the vertical direction, pendulum with harmonic oscillations of the point of suspension in the horizontal direction, pendulum with harmonic oscillations of the point of suspension at a certain angle to the horizontal, pendulum with external harmonic excitation, rigid body pendulum with linear spring and several equilibrium positions, centrifugal pendulum vibration absorber with impact interactions. The birth of the previously unknown rare attractors has been shown for different harmonically driven damped systems, and new bifurcation groups with complex

protuberances have been obtained. The new types of interaction of different oscillating and rotating orbits have been found as well as rare and chaotic rotational regimes. In addition, the process of formation of chaotic rotation through the cascade of period-doubling bifurcations for different groups has been studied within the framework of the research.

In the fourth chapter **"New bifurcation groups and rare attractors of the pendulum systems with two degrees of freedom"** is demonstrated how the method of complete bifurcation groups is applied to the global analysis of studied pendulum systems with two degrees of freedom (with dimension D = 5). Among them are pendulum system with a sliding mass and with the external periodic excited moment, and double pendulum with the periodically vibrating point of suspension in vertical direction. The main aims of the research are to investigate the qualitative behaviour of the pendulum systems with 2ODF by varying the parameters of the systems and to obtain the new qualitative results of topology of bifurcation groups with rare regular and chaotic attractors. There are complex protuberances with many rare regular attractors of different types, chaotic transients and chaotic motions.

In the fifth chapter **"Analysis of forced oscillations in the pendulum systems with several degrees of freedom"** the most commonly studied model of forced oscillations in the driven damped pendulum systems with several degrees of freedom was investigated. The possibility of using the method of complete bifurcation groups for the global analysis of the six body symmetric driven pendulum systems with several equilibrium positions is demonstrated. The possible applications of six body symmetric driven pendulum systems with several equilibrium positions are design of prospective laboratory equipment for control education, vibration absorbing systems, mixing (liquids, washing machines), etc.

The six chapter **"Experimental investigations and animation of the pendulum systems by the method of complete bifurcation groups"** shows the possibility of performance of the experimental investigations in more realistic models of pendulum systems, which were discussed in the present doctoral thesis. For these purposes, the experimental setup for natural experimental investigations in the simplest pendulum system with the periodically vibrating point of suspension in vertical direction was developed and produced. The experimental and theoretical investigations were performed for the simple pendulum driven system, in which founded regimes have qualitative agreement with the theoretical investigations. The four different oscillating and rotating regimes were found in both cases. Bifurcation diagrams also correspond to the results of numerical simulations. The visualization possibility of the founded regimes by the method of complete bifurcation groups in the pendulum systems is shown as

well. It is implemented by the animation software created using Pascal programming language. The animation of nonlinear phenomena of pendulum systems can be useful not only for student as methodological material, but also for engineers who are working with real pendulum-like systems.

In the **conclusion** of the present doctoral thesis the new qualitative results of global bifurcation analysis of the pendulum systems with one or several degrees of freedom based on the method of complete bifurcation groups are presented. The usefulness of the study of the pendulum systems by the method of complete bifurcation groups for finding new bifurcation groups, rare periodic and chaotic attractors both oscillating and rotating.

In the **appendices** the list of the open problems, which have not been completely solved in the present doctoral thesis, is presented. However, these questions, of course, should be solved in future investigations.

The **main task** of the doctoral thesis is a theoretical and practical study of the nonlinear dynamics of the pendulum systems with one or several degrees of freedom by the method of complete bifurcation groups, which allow conducting the global bifurcation analysis and finding new bifurcation groups, rare periodic and chaotic attractors both oscillating and rotating. The results can provide guidance on the use of complex regular and chaotic regimes on real objects in vibroengineering, robotics, space dynamics, medicine etc.

The **main aim** of the present doctoral thesis is to show, that the method of complete bifurcation groups allows conducting the global bifurcation analysis of the pendulum systems with one or several degrees of freedom and finding new bifurcation groups and unknown before forced regular and chaotic oscillations, and showing the possibility of using new (found regimes) results in real pendulum-like systems.

The results obtained by the method of complete bifurcation groups in the pendulum systems, from my point of view have a great **practical significance**. The new types of interaction of different oscillating and rotating orbits have been found as well as rare and chaotic rotating regimes. In addition, the process of formation of chaotic rotation through the cascade of period-doubling bifurcations for different groups has been found within the framework of the research. Also attention is paid to stable periodic and chaotic oscillations of different type near unstable equilibrium position of the pendulum, which can be widely used in real objects. There complex protuberances with many rare regular attractors of different types, chaotic transients and chaotic motions have importance in the study of driven damped pendulum systems. The possibility of performance of the experimental investigations and visualization of the founded

regimes by the method of complete bifurcation groups in more realistic models of pendulum systems is shown.

The doctoral thesis **is intended for** use in a course of ordinary differential equations, in courses on nonlinear dynamics and chaos and in nonlinear oscillation theory for students of different specialties who have basic knowledge to the extent of the 1st year of training at technical colleges and universities, as well as for those interested in contemporary issues and methods of nonlinear oscillation theory and nonlinear dynamics and chaos. This doctoral thesis obviously does not cover the topic fully and author will be grateful for remarks.

This doctoral thesis **can be useful for** illustrating the main statements of the bifurcation theory of nonlinear dynamical systems, which is a rather new section of the general theory of nonlinear dynamical systems.

The **accuracy** of the presented results provided by the use of modern methods of analysis of strongly nonlinear systems developed a systematic approach to the investigation of forced oscillations in nonlinear dynamical systems, using the exact analytical solutions for testing and the coincidence of new results obtained by at least three different methods.

The results of the presented doctoral thesis were **presented** at seminars of Institute of Mechanics of RTU since 2007 till 2013 and at international scientific conferences in RTU, in University of Latvia, USA, Germany, Russia, Lithuania, Tallin, Lisbon, Prague, Łódź.

The materials of the present doctoral thesis were **published** in the 30 works:

- 4 monographs;
- 6 international journals;
- 20 proceedings of the international scientific conferences.

Acknowledgments

I want to express my sincere gratitude to my supervisor Mikhail V. Zakrzhevsky for suggesting the topic of the present doctoral thesis, ideas and tips that helped me a lot in the preparation and presentation of the results of this work, and for his patience and understanding.

The author express his sincere gratitude to his colleagues at the research group «Nonlinear dynamics, chaos, complexity and control»: Dr.sc.ing. Igor Schukin, Dr.sc.ing. Raisa Smirnova, Dr.sc.ing. Vladislav Yevstignejev, Dr.sc.ing. Yuri Ivanov, Dr.sc.ing. Valentin Frolov and doctoral candidate Eduard Shilvan for their help in preparing of this doctoral thesis and for their participating in common investigations.

The author is also grateful to the staff of the Institute of Mechanics of RTU and to participants of the scientific seminars of the Institute of Mechanics of RTU for a constructive discussion of basic results of this doctoral thesis and critical remarks.

The author express his sincere gratitude to the student Einars Deksnis from the Faculty of Electronics and Telecommunications of Riga Technical University for his help in performance the experiment, especially for using the Hall-effect 360° angle position encoder.

I would like to gratefully and sincerely thank my wife Jekaterina and my son Andrey for their patience, understanding and countenance as well.

Alexey V. Klokov,
Institute of Mechanics, RTU

1

Task Description of the Global Bifurcation Analysis of the Pendulum Systems

As was already mentioned, this doctoral thesis is devoted to the theoretical and practical study of the nonlinear dynamics of the pendulum system based on the method of complete bifurcation groups. Selection the direction of research is related to the fact that the current situation is such that many of the important orbits (attractors, regimes) in archetypical classical models are unnoticed by the modelling with traditional analytical and numerical methods in spite of the possibility of using modern high-speed computers.

The first chapter covers the problems of global bifurcation analysis of the typical pendulum driven systems and characterizes models used in the research. The notions of the coefficient of nonlinear elastic characteristic, awareness of which enables the readers to foresee chaotic oscillations in the system, are introduced. Moreover, the chapter considers the notions of periodic skeleton and passport of periodic regime on the Poincaré plane, which assist in performing the global analysis of the system dynamics in the given point of parameter space, as well as during the global bifurcation analysis in case one or several system parameters are changed. The list of pendulum driven models, discussed in the present thesis, is provided for the convenience of the readers.

In the following chapters the traditional methods of bifurcation analysis, a review of general known nonlinear phenomena in nonlinear dynamical systems under the external periodic excitation and formulated problem statement of the thesis are presented.

1.1 Introduction to global bifurcation analysis of the pendulum driven systems

In the study of dynamical systems, the change of the parameter of the system can cause a qualitative change in the behaviour of the system. To describe this phenomenon the notion of a bifurcation is used. In the bifurcation theory of nonlinear oscillations - a qualitative change in the structure of the phase space, which occurs as a result of some parameter changes of the system when it is going through some value [56, 69]. The value of the parameter for which there is a bifurcation, called a bifurcation value or point of bifurcation.

Nowadays great interest appears in the study of new nonlinear effects in the pendulum driven systems by the global bifurcation analysis. These effects can be used in vibroengineering, even in simple mechanical systems with a simple structure. It turns out that such nonlinear systems can have very complex regular and chaotic dynamics, which is insufficiently studied.

Let us first examine one-degree-of-freedom pendulum driven system with elastic linear restoring force $f(\varphi) = a_1 \sin \pi\varphi$ and linear dissipation performing forced oscillations under the impact of external harmonic force. Differential equation of this system is the following:

$$\ddot{\varphi} + b\dot{\varphi} + a_1 \sin \pi\varphi = h_1 \cos \omega t, \tag{1.1}$$

where φ – an angle of the pendulum, $\dot{\varphi}$ – an angular velocity of the pendulum, where $\dot{\varphi} = d\varphi / dt$; b – linear dissipation coefficient of visco-elastic characteristic; a_1 – gravitation parameter; h_1, ω – the amplitude and frequency of excitation, respectively.

It is a well-known fact that the behavior of a simple pendulum model as (1.1) with the external harmonic excitation can be very complex; moreover, sometimes sudden phenomena appear, such as stable oscillations with respect to the upper equilibrium position, complex subharmonic oscillations, different types of rotations [14, 15, 23,53, 57,76]. However, the tasks of global dynamics of pendulum models, such as the search of rare attractors and chaotic attractors, as well as rare chaotic rotational motions, require additional systematic research [99, 100,104, 147, 149, 150, etc.]. The process of formation of chaotic rotation through the cascade of period-doubling bifurcations for different groups has also been studied within the framework of research. Earlier, chaotic rotation was discovered in cosmic dynamics of Saturn's moon – Hyperion ["Astronomy Today"]. For the dynamical systems, operating under the conditions of the Earth, this phenomenon remains poorly studied. Apparently, rare regular and chaotic rotational regimes have been found in pendulum systems for the first time within the framework of this research, and the search of these regimes is the main task of the research.

The problem of the global analysis of the system (1.1) will be formulated in the following way. Let us assume that it is necessary to study the behaviour of the system in the given parameter space, for instance, on the plane of two parameters (ω, h). Let us denote $p_1 = \omega$ and $p_2 = h$ and set a task to find all stable and unstable periodic regimes (orbits) and possible other stationary regimes on the given parameter plane (p_1, p_2).

Since our task is three-dimensional, it is necessary to know possible values of all three phase coordinates ($\varphi, \dot{\varphi}$, t_0). In accordance with Poincaré's brilliant idea, this three-dimensional phase space in the process of study of trajectory motion can be reduced to the two-dimensional one – without loss of generality – by means of selecting respective Poincaré plane (plane point mapping) [56, 57, 81, 88, etc.]. In the present thesis, a (stroboscopic) plane ($\varphi, \dot{\varphi}$ and $t_0 = 0$) is chosen as the Poincaré plane. Therefore, when setting initial parameters, the phase of restoring force is by default accepted to be equal to zero and the system as if becomes two-dimensional with initial parameters φ_0 and $\dot{\varphi}_0$, where φ_0 and $\dot{\varphi}_0$ – the initial coordinate and its velocity, respectively [119].

Taking into account the set limitations on possible parameter variations and phase condition of the system, the task of global analysis of the pendulum system (1.1) is formulated as follows: on the given parameter plane (p_1, p_2) and the given plane of states ($\varphi, \dot{\varphi}$) it is necessary to find all stable and unstable periodic and other possible stationary regimes and to assess their stability numerically.

In the subsequent chapters, it will be demonstrated that it is possible to conveniently classify all found periodic orbits (stable and unstable) with the help of the notion of bifurcation group (see Chapter 2), which is a basic notion for the bifurcation theory of pendulum driven systems.

1.2 Choice of objects of study

To illustrate the effectiveness of the method of complete bifurcation groups in the present doctoral thesis, the following pendulum driven systems are discussed:

1) The classical model of the dissipative mathematical pendulum with additional linear elastic spring, the suspension point of which performs harmonic oscillations in both directions (Paragraph 3.2):

$$mL^2\ddot{\varphi} + b\dot{\varphi} + c\varphi + mL\left(\mu - A_2\omega^2 \cos\omega t\right)\sin\varphi + mLA_1\omega^2 \sin\omega t\cos\varphi = 0 \qquad (1.2)$$

m = 1, L = 1, b = 0.2, c = 1, μ = 9.81, ω = 1.5, A_2 = var., A_1 = var.

2) The classical model of the dissipative mathematical pendulum with harmonic oscillations of the point of suspension in the vertical direction (Paragraph 3.3):

$$\ddot{\varphi} + b\dot{\varphi} + \left(1 + h\cos\omega t\right)\sin\pi\varphi = 0 \qquad (1.3)$$

b = 0.2, h = var., ω = var.

3) The classical model of the dissipative mathematical pendulum with harmonic oscillations of the point of suspension in the horizontal direction (Paragraph 3.4):

$$\ddot{\varphi} + b\dot{\varphi} + a_1 \sin\pi\varphi = h\cos\omega t\cos\pi\varphi \qquad (1.4)$$

a_1 = -1, ω = 1.8, h = 5.5, b = var.

4) Pendulum system with harmonic oscillations of the point of suspension at a certain angle to the horizontal (Paragraph 3.5):

$$m\ell^2\ddot{\varphi} + b\dot{\varphi} + mg\ell\sin\pi\varphi + m\ell A\omega^2 \sin\omega t\cos\pi(\varphi + \alpha) = 0 \qquad (1.5)$$

m = 1, ℓ = 1, b = 0.2, g = 9.81, A = 2, α = var., ω =var.

5) Pendulum with external harmonic excitation (Paragraph 3.6):

$$\ddot{\varphi} + b\dot{\varphi} + a_1 \sin \pi\varphi = h_1 \cos \omega t \tag{1.6}$$

b = 0.2, a_1 = 1, h_1 = 5, ω = var.

6) Rigid body pendulum with linear spring and several equilibrium positions (Paragraph 3.7):

$$\ddot{\beta} + c\dot{\beta} + f(\beta) - p\sin\beta + \left[1 - \frac{1}{\sqrt{1+\alpha\sin\beta}} - \left(q + q_1 \sin\omega t\right)\right]\cos\beta = 0, \tag{1.7}$$

where $f(\beta) = k_0 + k_1\beta + k_2\beta^2 + k_3\beta^3$

c = 0.01, $k_0 = k_1 = k_2 = k_3$ = 0, q = 0.01, α = 0.8, ω = 0.8, q_1 = 0.05, p = var.

7) Centrifugal pendulum vibration absorber with impact interactions (Paragraph 3.8):

$$(1-\gamma)\ddot{\varphi} + f(\dot{\varphi}) + f_1(\varphi) + h\omega\cos\omega t + \omega^2(1+d)^2(1+2h\sin\omega t)\sin\varphi = 0, \tag{1.8}$$

where $f(\dot{\varphi}) = \begin{Bmatrix} b_2\dot{\varphi} & if & \varphi < -\varphi_r \\ b_1\dot{\varphi} & if & -\varphi_r \le \varphi < \varphi_r \\ b_2\dot{\varphi} & if & \varphi \ge \varphi_r \end{Bmatrix}$; $f_1(\varphi) = \begin{Bmatrix} c_r(\varphi + \varphi_r) & if & \varphi < -\varphi_r \\ 0 & if & -\varphi_r \le \varphi \le \varphi_r \\ c_r(\varphi - \varphi_r) & if & \varphi > \varphi_r \end{Bmatrix}$,

γ = 0.1, b_1 = 0.2, b_2 = 5, c_r = 5000, d = 0, ω = 3, h = var.

8) Driven damped pendulum model with a sliding mass and with the external periodic excited moment (Paragraph 4.2):

$$\begin{cases} \left[m_1 l^2 + m_2(l - l_0 + y)^2\right]\cdot\ddot{\varphi} + b_1\dot{\varphi} + 2m_2(l - l_0 + y)\dot{\varphi}\dot{y} + m_1 g l \sin\varphi + \\ \qquad + m_2 g(l - l_0 + y)\sin\varphi = h_1 \cos\omega_1 t, \\ m_2\ddot{y} + b_2\dot{y} + c_2 y - m_2(l - l_0 + y)\dot{\varphi}^2 + m_2 g(1 - \cos\varphi) = 0, \end{cases} \tag{1.9}$$

m_1 = 1, m_2 = 0.1, l = 1, l_0 = 0.25, b_1 = 0.2, b_2 = 0.1, c_2 = 2, μ = 10, h_1 = var., ω_1 = var.

9) Double pendulum with with harmonic oscillations of the point of suspension in the vertical direction (Paragraph 4.3):

$$\begin{cases} (m_1+m_2)\cdot l_1^2\cdot\ddot{\varphi}_1 + m_2 l_1 l_2\cos(\varphi_1-\varphi_2)\cdot\ddot{\varphi}_2 + b_1\dot{\varphi}_1 + b_2(\dot{\varphi}_1-\dot{\varphi}_2) + \\ + c_1\varphi_1 + c_2(\varphi_1-\varphi_2) + (m_1+m_2)\cdot\mu l_1\sin\varphi_1 + (m_1+m_2)\cdot l_1\ddot{y}(\omega t)\sin\varphi_1 + \\ + m_2 l_1 l_2\dot{\varphi}_2^2\sin(\varphi_1-\varphi_2) = 0, \\ m_2 l_2^2\cdot\ddot{\varphi}_2 + m_2 l_1 l_2\cos(\varphi_1-\varphi_2)\cdot\ddot{\varphi}_1 + b_2(\dot{\varphi}_2-\dot{\varphi}_1) + c_2(\varphi_2-\varphi_1) + \\ + m_2\mu l_2\sin\varphi_2 + m_2\cdot l_2\ddot{y}(\omega_2 t)\sin\varphi_2 - m_2 l_1 l_2\dot{\varphi}_1^2\sin(\varphi_1-\varphi_2) = 0 \end{cases} \quad (1.10)$$

where $y(\omega t) = h\cos\omega t$,

$m_1 = 1$, $m_2 = 0.1$, $l_1 = 1$, $l_2 = 0.25$, $b_1 = 0.2$, $b_2 = 0.1$, $c_1 = 1$, $c_2 = 0.5$, $\mu = 10$, $h = 3$, ω = var.

10) Six body driven symmetric pendulum system with several equilibrium positions, linear dissipative forces between pendulums, additional linear elastic forces and harmonic excitation, applied to the first pendulum (Chapter 5):

$$\begin{cases} m_1 l_1^2\ddot{\varphi}_1 = b_2(\dot{\varphi}_2-\dot{\varphi}_1) + c_2(\varphi_2-\varphi_1) - b_1\dot{\varphi}_1 - c_1\varphi_1 - m_1 g l_1\sin\varphi_1 + h\cos(\omega t+\phi_0), \\ m_2 l_2^2\ddot{\varphi}_2 = b_3(\dot{\varphi}_3-\dot{\varphi}_2) + c_3(\varphi_3-\varphi_2) - b_2(\dot{\varphi}_2-\dot{\varphi}_1) - c_2(\varphi_2-\varphi_1) - m_2 g l_2\sin\varphi_2, \\ m_3 l_3^2\ddot{\varphi}_3 = b_4(\dot{\varphi}_4-\dot{\varphi}_3) + c_4(\varphi_4-\varphi_3) - b_3(\dot{\varphi}_3-\dot{\varphi}_2) - c_3(\varphi_3-\varphi_2) - m_3 g l_3\sin\varphi_3, \\ m_4 l_4^2\ddot{\varphi}_4 = b_5(\dot{\varphi}_5-\dot{\varphi}_4) + c_5(\varphi_5-\varphi_4) - b_4(\dot{\varphi}_4-\dot{\varphi}_3) - c_4(\varphi_4-\varphi_3) - m_4 g l_4\sin\varphi_4, \\ m_5 l_5^2\ddot{\varphi}_5 = b_6(\dot{\varphi}_6-\dot{\varphi}_5) + c_6(\varphi_6-\varphi_5) - b_5(\dot{\varphi}_5-\dot{\varphi}_4) - c_5(\varphi_5-\varphi_4) - m_5 g l_5\sin\varphi_5, \\ m_6 l_6^2\ddot{\varphi}_6 = -b_6(\dot{\varphi}_6-\dot{\varphi}_5) - c_6(\varphi_6-\varphi_5) - m_6 g l_6\sin\varphi_6. \end{cases} \quad (1.11)$$

$m_1 = m_2 = \ldots = m = 1$, $b_1 = b_2 = \ldots = b = 0.2$, $c_1 = c_2 = \ldots = c = 10$, $l_1 = l_2 = \ldots = l = 0.5$, $h = 3$, $\varphi_0 = 0$, $g = 10$, ω = var.

Studies of these systems were conducted using the new methods of new bifurcation theory (see Chapter 2), which are intended not only to solve the driven pendulum systems with one degree of freedom, but also for systems with two or many degrees of freedom.

1.3 Main tasks of the doctoral thesis

It is well known that the simple nonlinear dynamical systems have quite complex behavior. To date, almost all archetypical models of nonlinear dynamical systems are understudied and many important stable regimes remain unknown. This is also applied fully to the driven damped pendulum systems with one or several degrees of freedom.

The main task of the doctoral thesis is a theoretical and practical study of the nonlinear dynamics of the pendulum system based on the method of complete bifurcation groups, which allow conducting the global bifurcation analysis and finding new bifurcation groups, rare periodic and chaotic attractors both oscillating and rotating. The results can provide guidance on the use of complex regular and chaotic regimes on real objects in vibroengineering, robotics, space dynamics, medicine etc.

In the present doctoral thesis it is planned to show the typical bifurcation groups and their topology change with varying of parameters in the driven damped pendulum systems with one or several degrees of freedom. The author hope that the materials of this thesis will be useful both for understanding the qualitative behavior of strongly nonlinear dynamical systems and for the practical use of new understudied phenomena in pendulum systems, in particular multiplicity, the coexistence of periodic and chaotic attractors, different chaotic attractors, rare attractors, as well as chaotic rotating regimes.

The materials of the doctoral thesis may be used in the teaching process: in courses of ordinary differential equations, nonlinear oscillations in nature and engineering, nonlinear theory of chaos and control.

2

Basic Elements of the Bifurcation Theory of the Pendulum Systems

As already mentioned, in addition to theoretical studies, the aim of the doctoral thesis is to show that the use of the method of complete bifurcation groups allows conducting the global bifurcation analysis of the pendulum systems and finding the new bifurcation groups and previously unknown regular and chaotic oscillating, oscillating-rotating and rotating orbits (regimes, attractors) by the example of the simplest systems with one or more degrees of freedom. The method and the methodology of its application are described further.

2.1 Introduction. Traditional methods of bifurcation analysis and the method of complete bifurcation groups (MCBG)

The task of studying the behavior of a system in the process of its parameter variation is one of the central tasks in the examining of pendulum driven damped systems. It is a well-known fact that nonlinear systems can have several or even many different periodic regimes in one and the same parameter range; periodic regimes P1 with a period of excitation and subharmonic regimes, as well as chaotic stable regimes can be found among these regimes. Another well-known fact is that in the process of parameter variation, periodic regimes can lose or acquire stability, and under certain conditions these regimes can disappear as a result of merging stable and unstable regimes. It is traditionally considered that the task of the global analysis is to find all stable periodic orbits in a certain area of phase space by using a natural transient. Hence, bifurcation diagrams, constructed on the basis of this data, reflect the dependence of condition of the system on a parameter only for the stable orbits.

However, such an approach is quite time-consuming, and it does not allow finding all existing attractors in the given range, since searching for all possible initial conditions and weak convergence of processes lead to extremely high processing overhead, particularly for weakly dissipative systems and systems with several and many degrees of freedom.

Therefore, bifurcation diagrams, constructed by traditional methods, are practically always incomplete, since, as a rule, not all attractors of the system under examination can be found and the branches of periodic regimes acquire discontinuities. The proposed bifurcation theory of pendulum driven damped systems reflects the physical laws of nonlinear systems. The method of complete bifurcation groups (MCBG) [108, 109, 147-150] allows carrying out a more in-depth global analysis in the space of system parameters than by applying traditional methods. MCBG practically always allows finding new and previously unknown periodic and chaotic attractors in typical nonlinear dynamical models. The method of complete bifurcation groups offers particular advantages for the systems with several and many degrees of freedom, since the method is based on the idea of motion along the branches of periodic regime in the parameter space, regardless of whether the regime is stable or unstable. This enables the construction of diagrams without discontinuities, the fact of which, in our opinion, corresponds to the nature of nonlinear phenomena.

2.2 Fundamental concept of the bifurcation theory

The cornerstone of the bifurcation theory is the fact that for the given parameters (let us assume that it is a point P_0 of the parameter space) the system has several periodic regimes, some of which are stable, while the others – unstable. All existing stable and unstable periodic regimes, found at the parameter $P = P_0$, will be used for the construction of bifurcation diagrams [147-150]. There may be situations, when in the system at the parameter $P = P_0$ there is only one stable regime, several stable regimes, no stable periodic regimes, and one or several unstable periodic regimes. In the bifurcation analysis, these regimes are associated with a fixed point of point mapping and its coordinates, and are used for the continuation of solution branches.

The proposed bifurcation theory is intended for periodic pendulum driven damped systems, described by the system of simple differential equations.

The nature of nonlinear dynamical systems lies in the fact that periodic regimes (stable and unstable) can belong to one or several independent bifurcation groups at $P = P_0$. The primary task of the global analysis in case of system parameter variations is to find all independent bifurcation groups, which are determined by the found periodic stable and unstable orbits at $P = P_0$. Solutions and solution branches, belonging to different bifurcation groups, cannot intersect in the state-parameter space. The use of the found periodic orbits (fixed points) at a parameter $P = P_0$ allows achieving motion along the solution branch in the parameter space and constructing a complete bifurcation diagram for the found bifurcation groups.

The present doctoral thesis is illustrated by a large number of bifurcation diagrams for the different pendulum damped driven systems listed in Section 1.2. In the bifurcation diagrams, stable regimes are represented in black, while unstable – in reddish. All orbits (solutions), located on one branch, are connected to each other at bifurcation points, out of which protuberances with the regimes of higher order appear during further research. In the bifurcation diagrams coordinates of fixed points are defined by $x = x_p$ and $v = \dot{x}_p$.

Thus, in the given range of parameters in a pendulum system there are independent bifurcation groups, the branches of which can have both stable and unstable solutions of different order, but joined together in a single unit [149].

2.3 Complete bifurcation group *nT* in the space of parameter *p*

Let us define bifurcation group *nT* as complete one, if all stable and unstable branches of periodic orbits, the branches of which are connected to each other at a bifurcation point, are found. Here, *n* represents a minimum order of periodic orbits of this group. For example, for periodic group 1T, $n = 1$, for periodic group 2T, $n = 2$, …, for periodic group 5T, $n = 5$. Solution branches, constructed from the bifurcation points, can continue branching in case of constructing periodic regimes of higher order and can create protuberances [147-150].

2.4 Basic and extended passport of periodic orbits (regimes, solutions)

When applying the Poincaré map, the found regime can be set in the form of data on the solution (orbit) order, number of loops on the projection of phase trajectory, coordinates of a fixed point and stability characteristics [121-137]. For example, the line below –

P5 (3/5), Fixed Point (2.815634, -0.293778), Multipliers $\rho_1 = -0.467$, $\rho_2 = -1.813$ (2.1)

a "basic passport" of periodic regime (in the given point of parameter space of the system under consideration). The subharmonic regime with the period $T = 5T_\omega$ has a projection of phase periodic trajectory with three loops; the coordinates of a fixed point on the Poincaré plane are presented in brackets. The unstable regime – inverted saddle – since $\rho_2 = -1.813$. It is worth pointing out that a basic passport of periodic regime was applied by T. Hayashi, J. Ueda and others in well-known works of Japanese scientists [59, 96].

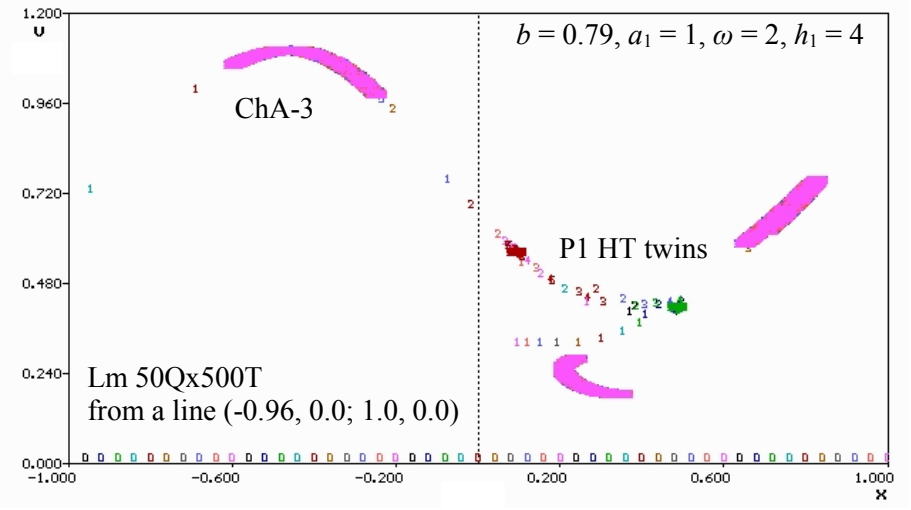

Fig. 2.1. Co-existence of P1 hilltop (HT) twin and chaotic ChA-3 attractors has been found in the harmonically driven damped pendulum system (1.1). Mapping Lm 50Qx500T from a line (-0.96, 0; 1, 0) on the Poincaré plane is shown. System parameters: $a_1 = 1$, $h_1 = 4$, $\omega = 2$, $b = 0.79$, $k = 7$.

Apart from the basic passport characteristics (2.1) of periodic regime, the "extended passport", in addition, includes the Poincaré mapping, time histories, phase trajectories, dependence of force variation, diagrams of work of forces, energy plane and spectral analysis. For the evaluation of the dissipation level, it is useful to include time dependent variation of phase coordinates and energy characteristics into the full passport of regime [102]. The examples of the extended passport of periodic and chaotic attractors in the harmonically driven damped pendulum system are shown on Figs. 2.1-2.4.

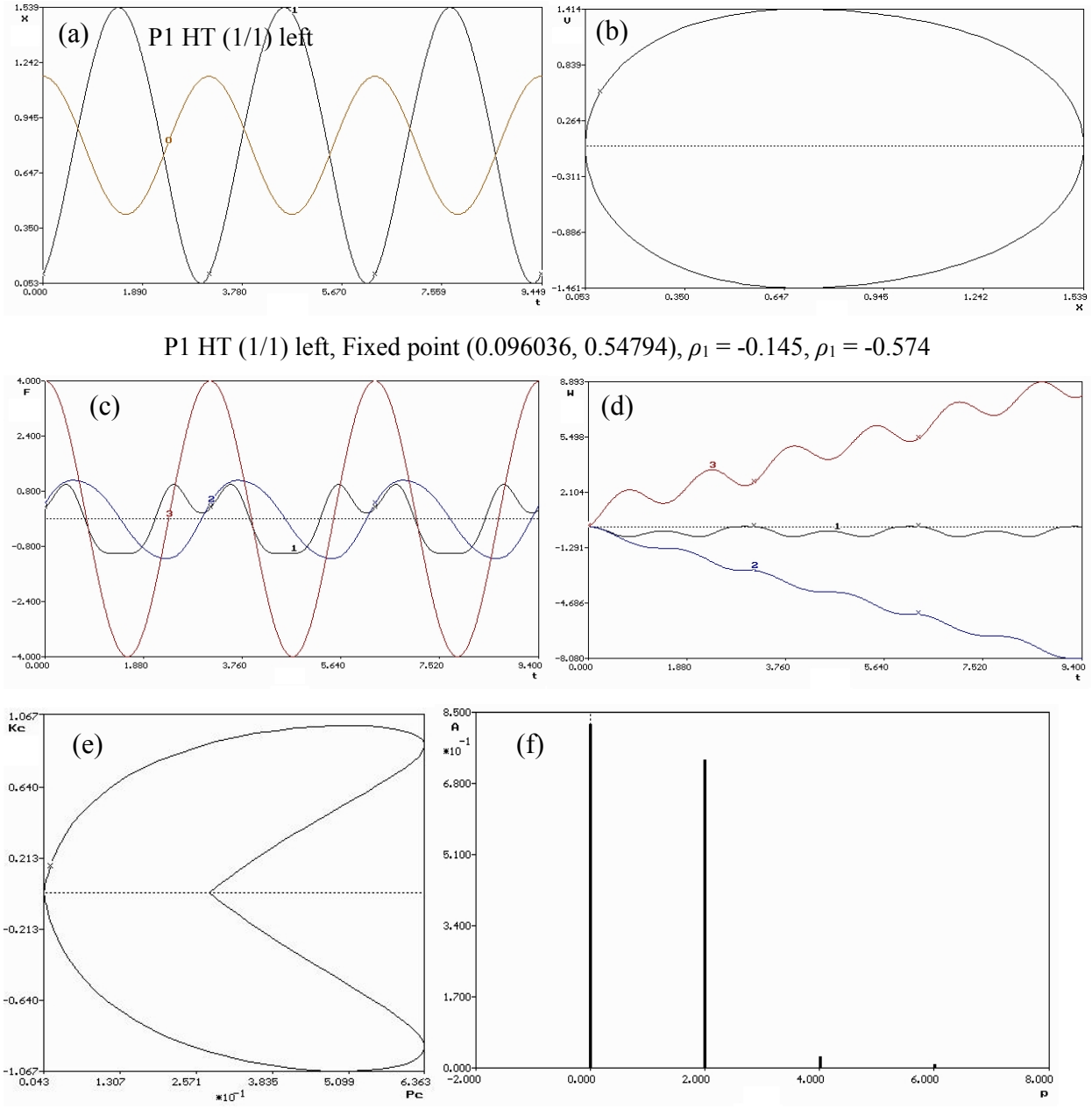

P1 HT (1/1) left, Fixed point (0.096036, 0.54794), ρ_1 = -0.145, ρ_1 = -0.574

Fig. 2.2. Extended passport of the periodic P1 hilltop left attractor: (a)-(b) time histories and phase trajectories; (c) time histories of applied forces; (d) work of forces depending on the time; (e) energy plane; (f) spectral analysis. System parameters: $a_1 = 1$, $h_1 = 4$, $\omega = 2$, $b = 0.79$, $k = 7$.

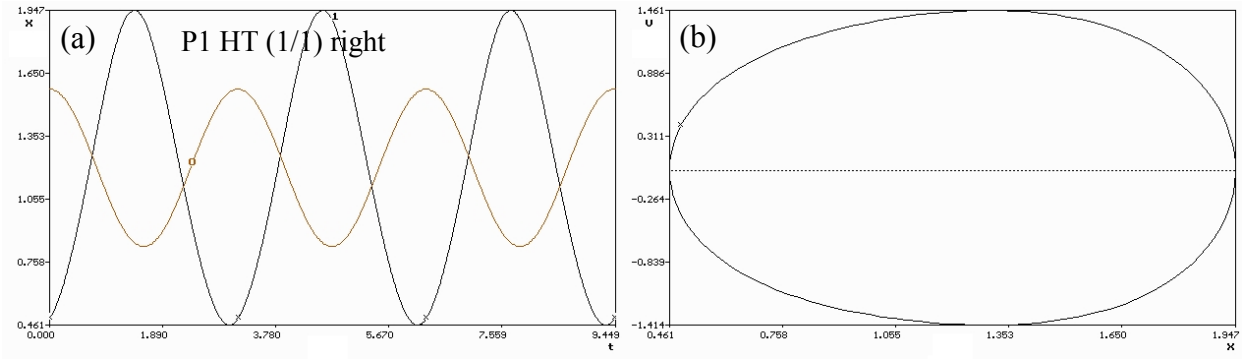

P1 HT (1/1) right, Fixed point (0.489581, 0.399980), ρ_1 = -0.145, ρ_1 = -0.574

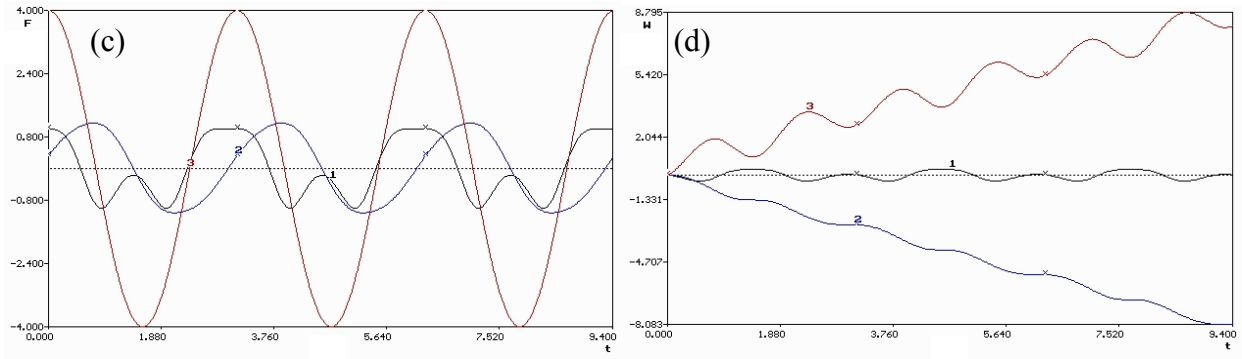

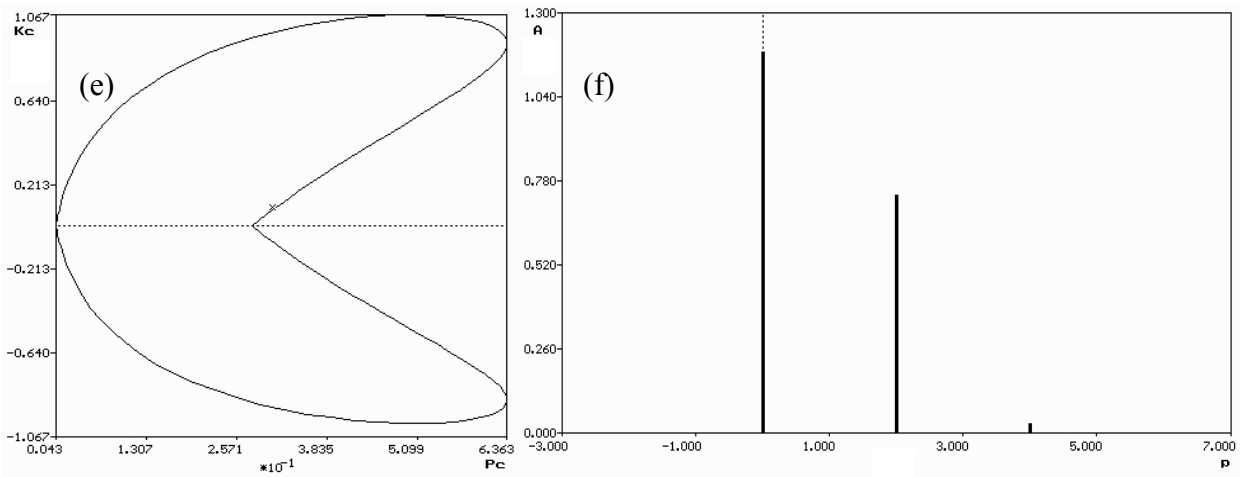

Fig. 2.3. Extended passport of the periodic P1 hilltop right attractor (the Poincaré mapping see on Fig. 2.1 and P1 hilltop left attractor on Fig. 2.2): (a)-(b) time histories and phase trajectories; (c) time histories of applied forces; (d) work of forces depending on the time; (e) energy plane; (f) spectral analysis. System parameters: $a_1 = 1$, $h_1 = 4$, $\omega = 2$, $b = 0.79$, $k = 7$.

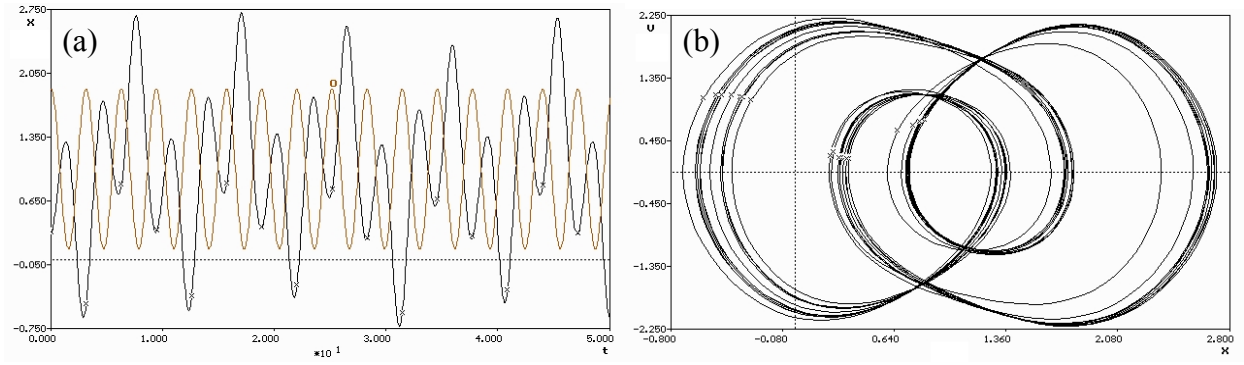

ChA-3, Initial conditions $x_0 = 0.25$, $v_0 = 0.20$, NT = 16T

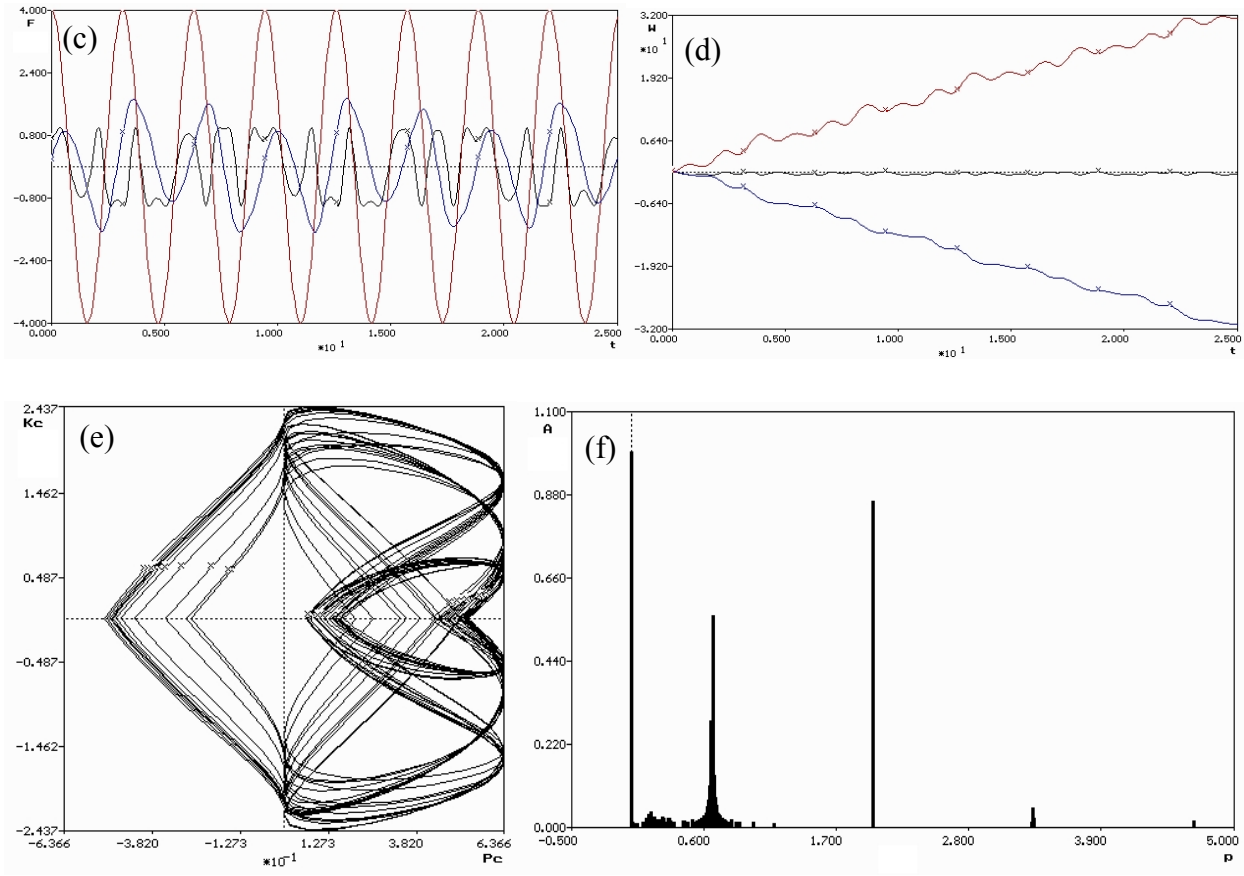

Fig. 2.4. Extended passport of the chaotic subharmonic ChA-3 attractor (the Poincaré mapping see on Fig. 2.1 and coexisting P1 hilltop twin attractors on Figs. 2.2-2.3): (a)-(b) time histories and phase trajectories; (c) time histories of applied forces; (d) work of forces depending on the time; (e) energy plane; (f) spectral analysis. System parameters: $a_1 = 1$, $h_1 = 4$, $\omega = 2$, $b = 0.79$, $x_0 = 0.25$, $v_0 = 0.20$, $k = 7$.

2.5 Periodic skeleton for the pendulum driven systems

At the present time a lot of scientists are searching only stable regimes by the natural transition process. In literature this approach is called by “brute force”. Lost by this approach an important information about the unstable regimes prevents or strongly complicates the study of the system in a given parameter space. In addition to the natural transition process for finding periodic regimes it is used a simple iteration, which in some cases can also search unstable solutions, and the Newton-Kantorovich [120,122], with the same success that allows us finding both stable and unstable regimes.

As aforementioned, for the global analysis of periodic regimes, before commencing the research it is useful to find – in the given point of parameter space – all stable and unstable orbits (solutions, regimes) and their basic passports for P1, P2, P3, ….. Pn, where n – a maximum order of findable solutions [147-150]. For this purpose, according to a certain rule, on the plane of states a certain number (sometimes a quite large number) of initial points is set, and they are used to find periodic regimes (coordinates of fixed points) of regimes on the basis of the Newton-Kantorovich method and to evaluate the stability of these regimes according to multiplicators. In the driven pendulum systems searching the fixed points or the rotational orbits the cylindrical phase space is taken into account with period Lx = 2 (see Fig.2.6). In case of recording of cyclic coordinates the sampling period matches with the period of the external excitation force ($T = 2\pi$), and then reduced phase portrait is the phase portrait of the rotating orbit R1 with period-1 [149].

The found stable and unstable regimes with their passports are used for the global analysis both in the state space and parameter space. Let us remind ourselves that the basic passport (see Section 2.4) of each periodic regime includes information about the order of the regime, coordinates of its fixed point and values of multiplicators, quantitatively characterizing stability or instability of the found periodic regimes. In our opinion, the most valuable information for the global analysis in the parameter space is presented by the found unstable regimes, the continuation of which along the branches of their solutions in the parameter space enables the discovery of new bifurcation groups and rare attractors. The procedures of constructing the periodic skeleton are included into the software ABC NDC and SPRING [107, 113], created in Institute of Mechanics of Riga Technical University.

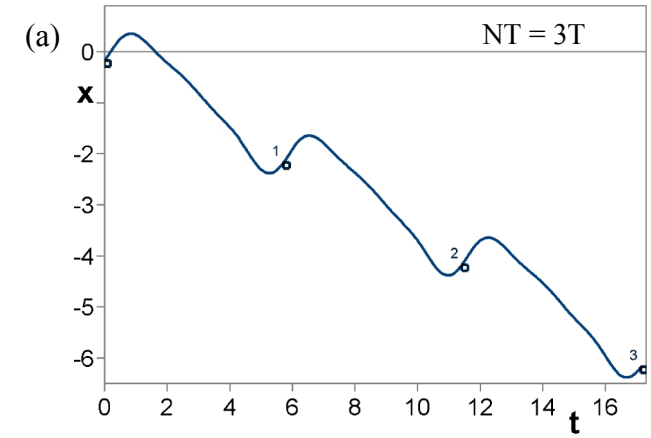

N	t	x	v
0	0.0	-0.177442	0.850614
1	5.711987	-2.177443	0.850615
2	11.423973	-4.177442	0.850614
3	17.13596	-6.177442	0.850614
	…		
10	57.119865	-20.177442	0.850614

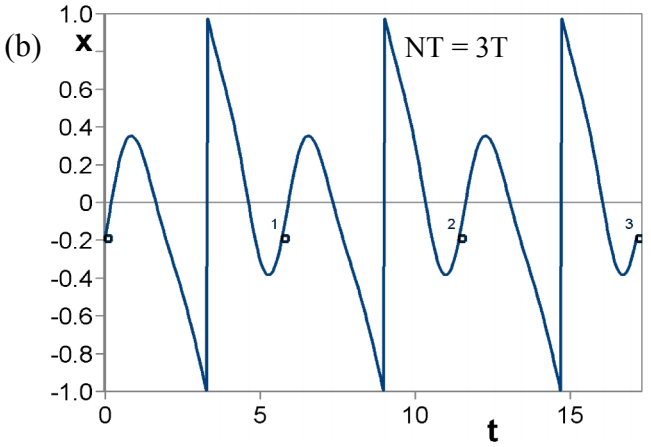

N	t	x	v
0	0.0	-0.177442	0.850614
1	5.711987	-0.177443	0.850614
2	11.423973	-0.177442	0.850615
3	17.13596	-0.177442	0.850614

Fig. 2.5. The example of calculation of periodic rotating orbit of period-1 without (a) and with (b) taking into account the cylindrical phase space with period $L_x = 2$.

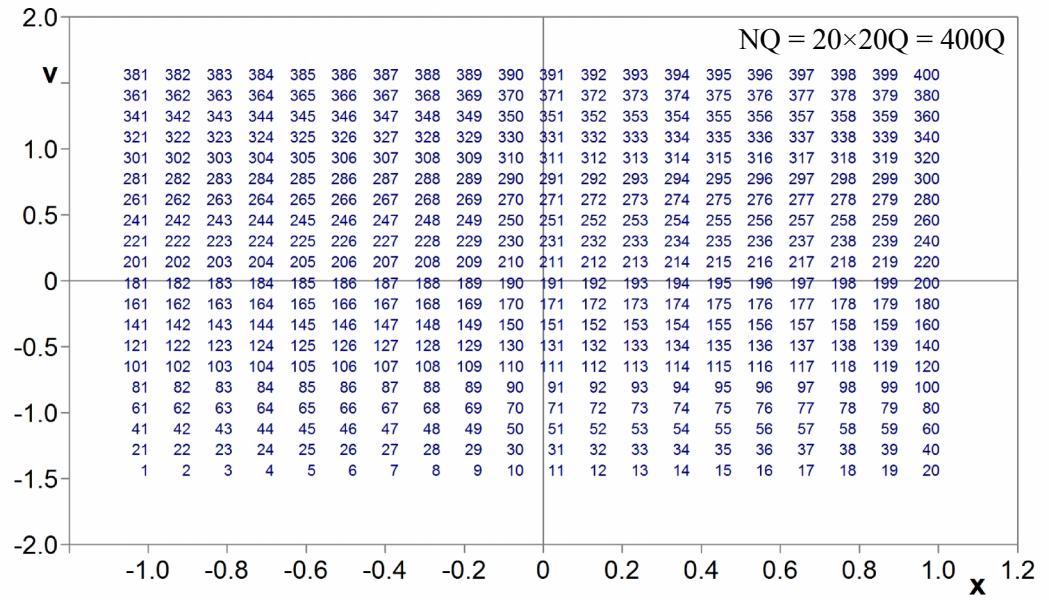

Fig. 2.6. A grid of 20×20 = 400Q initial conditions inside the rectangle (-1.0; -1.5 / 1.0; 1.5) for construction of periodic skeleton in the harmonically driven damped pendulum system (1.1). System parameters: $a_1 = 1$, $h_1 = 5$, $\omega = 2$, $b = 0.2$, $k = 7$.

Table 2.1. Periodic skeleton consists of 23 periodic oscillating and rotating orbits (regimes, attractors), among them are three stable regimes (one oscillating P1 (1/1), one left rotating R1– and one right rotating R1+) and twenty unstable regimes (one oscillating P1 (1/1) and other 19 left and right rotating of period-1, period-2, period-3, period-4, period-6, period-7, period-9) for the harmonically driven damped pendulum system (1.1). System parameters: $a_1 = 1$, $h_1 = 5$, $\omega = 2$, $b = 0.2$, $k = 9$.

Nr.	Orbits	x	v	ρ_1	ρ_2	α
1.	P1 (1/1) s +	-0.299692	0.303277	0.730402	0.730402	150.1°
2.	R1 s -	0.494430	-1.375354	0.730399	0.730399	170.4°
3.	R1 s +	0.185400	2.483508	0.730368	0.730368	170.4°
4.	R1 u -	-0.092941	-1.031110	-0.194663	-2.739857	0°
5.	R1 u -	0.732526	-1.292753	6.806660	0.078375	0°
6.	R1 u -	0.580883	-0.827837	19.154572	0.027840	0°
7.	P1 (1/1) u +	0.789310	0.212130	22.744366	0.023408	0°
8.	R1 u +	-0.511673	1.755808	-0.194663	-2.739857	0°
9.	R1 u +	-0.894933	1.472223	19.154572	0.027840	0°
10.	R2 u -	-0.363859	-1.050620	-0.025580	-11.106533	0°
11.	R2 u +	-0.636141	1.421742	-0.025580	-11.106533	0°
12.	R3 u -	0.428143	-1.422027	4.970083	0.030575	0°
13.	R3 u -	0.638218	-1.342504	-0.013882	-10.878729	0°
14.	R3 u -	0.484804	-0.821273	66.763020	0.003934	0°
15.	R3 u -	0.511005	-0.769334	-0.004877	-153.949713	0°
16.	R3 u +	-0.673072	1.805665	66.763020	0.003934	0°
17.	R3 u +	-0.863854	1.504888	-0.004877	-153.949713	0°
18.	R4 u -	0.688468	-1.310503	44.705645	0.001989	0°
19.	R4 u +	-0.511968	1.688329	-0.003424	-135.090165	0°
20.	R6 u -	0.649148	-1.336859	-0.002873	-65.324439	0°
21.	R7 u -	0.686130	-1.310525	-0.027549	-464.243132	0°
22.	R7 u -	0.605860	-1.261126	224.275914	0.007500	0°
23.	R9 u -	0.582779	-1.265010	-0.279498	-326.691283	0°

The example of the construction of periodic skeleton (PSK) [149, 152] in the harmonically driven damped pendulum system (1.1) for oscillating and rotating orbits (regimes, attractors) with order n = (1-16)T (see Table. 2.1) by using the Newton-Kantorovich method from the grid of initial conditions NQ = 20×20Q = 400Q (see Fig.2.6) inside the rectangle (-1.0, -1.5; 1.0, 1.5) is shown below. The maximum number of iterations is KIN = 64 with precision search of the

fixed point EPN = 1e-6 and parameter of discretisation DEN = 1e-5. Active boundaries are x_{min} = -1, x_{max} = 1, v_{min} = -10, v_{max} = 10. For rotational orbits the cylindrical phase space was taken into account with period Lx = 2. Time of calculation of periodic skeleton was about 1 hour (the PC characteristics: Intel(R) Core(TM) i3-2120, CPU - 3.30GHz, RAM - 4 GB, Windows 7 SP1).

Periodic skeleton (see Table 2.1) consists from 23 periodic oscillating and rotating orbits (regimes, attractors), among them are three stable regimes (one oscillating P1 (1/1) +, one left rotating R1– and one right rotating R1+) and twenty unstable regimes (one oscillating P1 (1/1) and other 19 left and right rotating of period-1, period-2, period-3, period-4, period-6, period-7, period-9) for the harmonically driven damped pendulum system (1.1).

2.6 Coefficient of nonlinear elastic characteristic

With the increase of nonlinearity, the number of nonlinear effects, as a rule, increases. It appears that the degree of nonlinearity of elastic characteristic can be conveniently evaluated with the help of a coefficient [119,147,149]:

$$k_a = \left| \frac{dp}{dA} \cdot \frac{A}{p} \right| \tag{2.2}$$

where p – the frequency of free oscillations of a partial system, A – the amplitude of oscillations.

In [119,147,146], the dependence of p on the amplitude A for several nonlinear systems with different f(x) is provided. For example, for the system with f(x) = x^3, a maximum coefficient of nonlinearity equals k_a = 1, for the symmetric system with f(x) = x^2sign(x), coefficient of nonlinearity equals 0.5. For the system with the symmetric trilinear characteristic, a maximum coefficient of nonlinearity can be significantly higher than 1 in the vicinity of fracture of the elastic characteristic.

2.7 Subgroup with an infinite number of unstable periodic orbits (regimes, solutions), unstable periodic infinitium (UPI) subgroup

It is a well-known fact that under certain parameters a system can have an infinite number of unstable periodic regimes of one group [109, 111, 137, etc.]. Construction of periodic skeleton allows finding parameter ranges, in case of which there is the infinite number of unstable periodic regimes of one group.

The formation of a group with an infinite number of periodic regimes (we call such a group UPI – Unstable Periodic Infinitium) occurs due to the cascade of period-doubling bifurcation. This mechanism is well-known and described in scientific literature; it is the basic mechanism for the creation of chaotic attractors or chaotic transients. As a result of the period-doubling cascade, distances between bifurcation points decrease exponentially; thus, a UPI subgroup with only unstable regimes of different order is found. The existence of such a UPI subgroup implies the existence of a chaotic attractor in the system under examination. Thus, the previously mentioned phrase "to find all stable and unstable periodic regimes" means finding stable and unstable regimes up to a certain order, for example, to the regimes $n = 16$, and finding bifurcation subgroups with UPI, i.e., only with unstable regimes.

2.8 Typical bifurcation topological groups and complex protuberances

Complete bifurcation groups can be simple, but more frequently they can be quite complex. The present paper is devoted exactly to the construction and analysis of complex bifurcation groups. As already pointed out, the branches of new periodic regimes of higher order "grow" from bifurcation points. These branches can curve in a complicated way, forming folds and creating new subgroups with UPI. Thus, a modern term "nonlinear dynamics, chaos and complexity" refers to the fact that even simple nonlinear dynamical systems have a complex topology of bifurcation groups [106, 112, 130]. Apparently, in the future it will be possible to classify the majority of different bifurcation groups, and author hope that the examination of certain driven damped pendulum systems, provided in Chapters 3 – 5, will contribute to this fact.

2.9 Rare attractors

The bifurcation theory and the method of complete bifurcation groups, implemented in the examination of certain damped pendulum systems, have enabled the systematic finding of new and previously unknown bifurcation groups with stable periodic or chaotic oscillating, oscillating-rotating and rotating attractors. These previously unknown stable regimes is called "rare attractors", since they exist, as a rule, in quite narrow ranges of system parameters [89-93].

Rare attractors can be systematically found as a result of continuation of unstable periodic regime nT along the solution branch in the parameter space. Rare attractors (RA) can be periodic, quasi-periodic or chaotic (ChA) and can be of different types [104, 105, 147-150].

Rare attractors of tip type (tip bifurcation subgroup) represent the main type of rare attractors. Both rare periodic attractors and rare chaotic attractors fall into this subgroup. Rare attractors can be in the form of egg-like or dumbbell, kink or hysteresis or in the form of small isolated island (isola isle). To find and prove the existence of rare attractors being important for theory and practice in all essentially nonlinear dynamical systems is one of the main tasks of the present research. The subsequent chapters will illustrate in detail the creation of rare attractors in the nonlinear dynamical systems as a result of systematic application of the method of complete bifurcation groups.

2.10 Construction of the basins of attraction

At coexistence of several orbits with given structure and parameters of the system, that is at multiplicity, it is necessary to divide the state space to the basins of attraction of coexisting regimes.

In the present doctoral thesis there are two methods construction of the basins of attraction are used: Cell-to-Cell mapping and method of separatrices of the saddle point. In the case of a system with many degrees of freedom it is talking about the core of domain of attraction, and to evaluate it the contour mapping in direct time can be used.

The most obvious and easiest to implement is a method known as cell-to-cell mapping [25, 107]. With this method, the studied region of the phase plane is divided evenly into cells. Each cell is assumed atomic, that means all its points are considered to belong to the same region of attraction. This assumption does not lead to significant errors at a cell with sufficiently small enough size. The natural transient process is used identify the cell to a concrete basin of attraction. This is done by the calculation of the transient process starting from the center of the cell. The process ends with one of the stationary orbit and thus defines to which basin of attraction source cell belongs. For example, the validation of one of the cells of the transient process completes by the P1 attractor, therefore, the tested cell belongs to the domain of attraction of the regime. If repeat the calculation for all cells of the plane and choose a fill color for them according to the attractor, the resulting mapping will determine the boundaries of the basins of attraction accurate to the size of the cell.

The second approach is the method of separatrices of the saddle point [106, 107]. The separatrices are the boundaries that divide the basins of attraction according to the different regimes. Therefore in this case the checking process of each point on the phase plane in the

algorithm of the Cell-to-Cell mapping is replaced by significantly faster process of constructing of separating lines.

The initial data for the beginning of the calculation are the coordinates of the saddle point, around which the algorithm is used to display a straight line in reverse time. If the line size is sufficiently small and the number of points on the line is big enough, the first few steps of mapping in reverse time will not lead to significant spread of the points. The points will be located on the separatrix and will determine its position. Such mapping allows getting the set of points (inset), which define the boundaries of the basins of attraction and the location of a saddle point between them. A similar mapping provided in the direct time (outset) shows the location of the fixed points of attractors, of which the basins of attraction are separated by the constructed boundaries.

The considered approaches of construction of basins of attraction are designed for the study of the systems with one degree of freedom (D3), although they can be used for systems with a large number of phase coordinates. In this case we are talking about the core of basin of attraction, and to evaluate it a contour map from some figure in the direct time can be used [147]. If all points of the contour will converge to the same attractor, then all the points inside the contour belong to the given attractor. The combination of these points forms the core of the basin of attraction of the corresponding regime.

2.11 Construction of the two-parameter bifurcation diagrams

The bifurcation diagrams show the state of the system (the coordinates of the fixed points of periodic regimes) versus a single simple parameter or a complex one. One of the important tasks of the bifurcation analysis of nonlinear dynamical systems is the construction of two-parameter bifurcation diagrams $M(p_1, p_2)$, dividing the plane of the two parameters of the system in a region with a qualitatively similar behavior. For example, the area can be allocated to the basic stable attractor or to the field with a chaotic behavior. The different approaches can be used for the construction of the two-parameter bifurcation diagrams. Most simple of them are enclosed to the grid scanning coverage of the whole parameter plane and to performing the complete analysis of the behavior in each cell of the grid for the nonlinear dynamical system with fixed parameters. This approach requires time consuming calculations and don't allow to quickly performing the bifurcation analysis. Another approach is similar to the algorithm of parameter continuation and it is enclosed to the continuation of bifurcation boundaries [59].

2.12 Conclusions

This chapter presents the approaches and methods that will be used for a global analysis of driven damped pendulum systems in this doctoral thesis. These approaches include the algorithms for construction of periodic skeleton (periodic passport), the method of searching the fixed points with and without taking into account the cyclic coordinates, method of complete bifurcation groups, Poincaré mappings from a line and from a contour, Cell-to Cell mapping, the method of separatrices of the saddle point, the method of continuation of bifurcation boundaries for the construction of the two-parameter bifurcation diagrams.

The above mentioned approaches and methods are realized in three different software NLO [100], ABC NDC [113] and SPRING [107]. All these results of numerical simulations in this doctoral thesis were obtained using these software.

Therefore this chapter describes the method of complete bifurcation groups and shows that the use of this approach allows conducting the global bifurcation analysis of the driven damped pendulum systems and finding new bifurcation group and previously unknown rare regular and chaotic attractors. The above mentioned methods will be used further in Chapters 3-5 for the study of pendulum systems with one and several degrees of freedom.

3

Forced and Parametrical Oscillations of the Pendulum Systems with One Degree of Freedom

3.1 Introduction

In the second chapter, it was noted that the purpose of the qualitative theory of multi-dimensional dynamical systems is a joint study of the structure of the separation of the phase space and parameter space. A qualitative study of dynamical systems involves the study of the steady motions and their bifurcations, identifying the basins of attraction of steady motions, as well as global pattern of their relative position and transition into each other by changing the

parameters. The main direction of the qualitative theory is that relying on a simple local research gradually it is possible to expand the studied region of the phase space and the parameter space.

This chapter provides a bifurcation analysis of the pendulum system with one degree of freedom and with forced and parametrical oscillations.

This chapter covers the most commonly studied models of forced and parametrical oscillations in the harmonically driven damped pendulum systems with one degree of freedom (with dimension D = 3). The main aim of the research is demonstrating how the method of complete bifurcation groups is applied to the global analysis of studied pendulum systems.

3.2 The parametrically excited pendulum system with an additional linear restoring moment and with the periodically vibrating point of suspension in both directions

The first studied dynamical model is shown in Fig.3.1a. The system has additional linear restoring moment with the harmonically vibrating point of suspension in both directions. The system has three equilibrium positions (Fig.3.1c). Restoring moment and backbone curves for the system are shown in Figs.3.1b, 3.1d. Close models have been examined in some works [8,15,19,23,25,29,43,53,55,61, etc.]. The aim of our bifurcation analysis is to find new rare attractors and new bifurcation groups. Some results of complete bifurcation analysis of the studied model have been examined in one of the previous works [126,131,137].

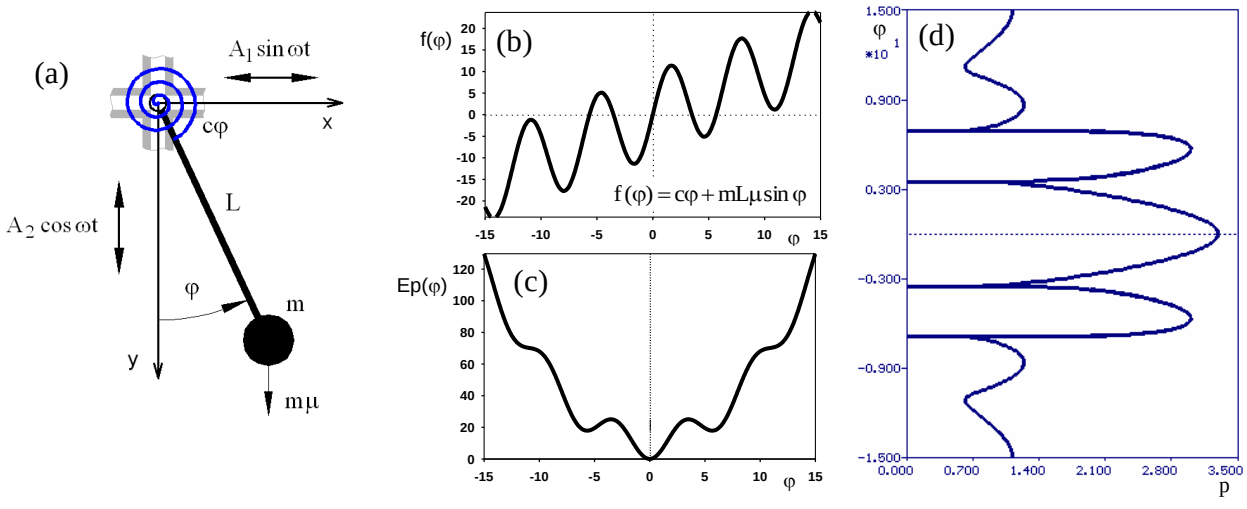

Fig. 3.1. The parametrically excited pendulum system with an additional linear restoring moment and with the periodically vibrating point of suspension in both directions. (a) Physical model; (b) restoring moment; (c) potential well; (d) backbone curve.

The equation of motion for mathematical pendulum (Fig.3.1a) is such:

$$mL^2\ddot{\varphi} + b\dot{\varphi} + c\varphi + mL\left(\mu - A_2\omega^2 \cos\omega t\right)\sin\varphi + mLA_1\omega^2 \sin\omega t\cos\varphi = 0, \quad (3.1)$$

where φ – angle of rotation, read-out from a vertical line; $\dot{\varphi}$ - angular velocity of the pendulum, where $\dot{\varphi} = d\varphi / dt$; t – time; m – mass, L – length of the pendulum; μ – gravitation constant; b – linear damping coefficient; c – linear stiffness coefficient; A_1, A_2 and ω – oscillation amplitudes and frequency of the point of suspension on a horizontal and a vertical direction. Equation (3.1) will be used for bifurcation analysis of the driven damped pendulum systems.

The results of bifurcation analysis of the model (3.1) are represented in Figs.3.2-3.14. In the first special case the model only with horizontal external force has three simple 1T bifurcation groups (Fig.3.2).

Phase projections for cross-section A_1 = 0.5 are shown in Fig.3.3. Dynamical wells built by Line mapping from a line (-10,-0.1; 10,-0.1) on the Poincaré map are represented on Fig.3.4a. Using Cell-to-Cell mapping with 501×501 grid of initial conditions, basins of attraction (Fig. 3.4b) have been obtained for cross-section A_1 = 0.5 of bifurcation diagram (see Fig.3.2a).

In the second special case the model only with vertical external force have three symmetric 1T, one 2T, one 4T and one 8T bifurcation groups (Fig.3.5). Bifurcation diagrams: state (φ, Amplitude) of the fixed periodic points versus vertical external force amplitude A_2, are shown in this figure. The system has many rare attractors of different kinds. The stable solutions are plotted by solid lines and unstable – by thin lines (reddish online). Two symmetric period one brunches near A_2 = 4 are not completed, because of problems of singularity. In Fig.3.6 coexistence of $P1_1$ twins stable solutions and $P1_1$ RA twins rare attractors (see Fig.3.5) in cross-section A_2 = 0.4882 is shown. Basins of attractions obtained using two different methods are shown in Fig.3.7: (a) insets and outsets from two symmetric 1T saddles; (b) Cell-to-Cell mapping with 501×501 grid of initial conditions for Eq.(1).

Five different 1T bifurcation groups and one 2T bifurcation group have been found (Fig.3.8) in general case for parametrically excited pendulum system with additional restoring moment and with the periodically vibrating point of suspension in both directions. Two of these groups are topologically similar and have rare attractors of a tip kind $P1_1$ RA and $P1_3$ RA. Two period one brunches near A_2 = 4 are not completed, because of problems of singularity. Other three 1T bifurcation groups have the own rare attractors $P1_4$ RA and $P1_5$ RA, which are stable in small parameter regions. Some cross-sections (A_2 = const) of bifurcation diagrams with dynamical characteristics from Fig.3.8 are represented in Figs.3.9, 3.10, 3.13, 3.14. All attractors

are of tip kind so each of them has not only periodic attractors, but also chaotic attractors as well.

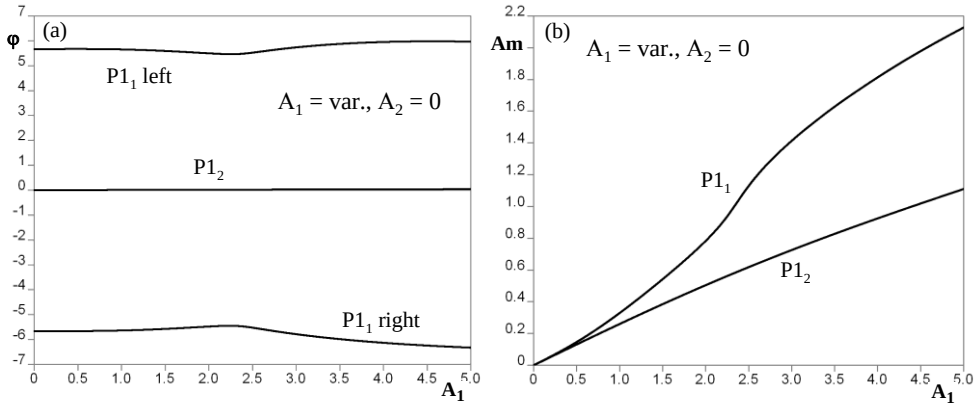

Fig.3.2. Parametrically excited pendulum system (see Fig. 3.1a) with linear restoring moment and with the periodically vibrating point of suspension in horizontal direction. Bifurcation diagrams: state (φ, Amplitude) of the fixed periodic points vs. horizontal external force amplitude A_1. There are three simple 1T bifurcation groups. Parameters: m = 1, L = 1, b = 0.2, c = 1, μ = 9.81, ω = 1.5, A_1 = var., A_2 = 0.

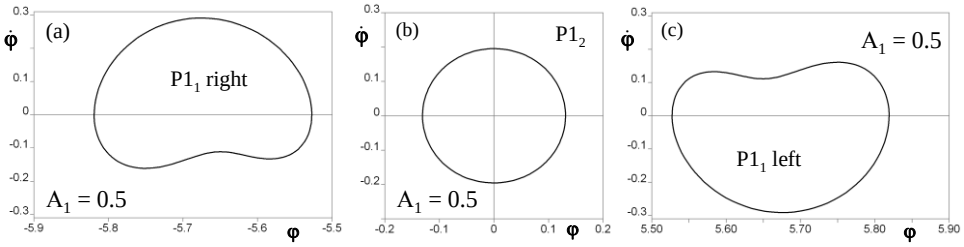

Fig.3.3. Parametrically excited pendulum system (see Fig. 3.1a) with linear restoring moment and with the periodically vibrating point of suspension in horizontal direction. Phase projections for cross-section A_1 = 0.5 (Fig. 2a). Parameters: m = 1, L = 1, b = 0.2, c = 1, μ = 9.81, ω = 1.5, A_1 = 0.5, A_2 = 0.

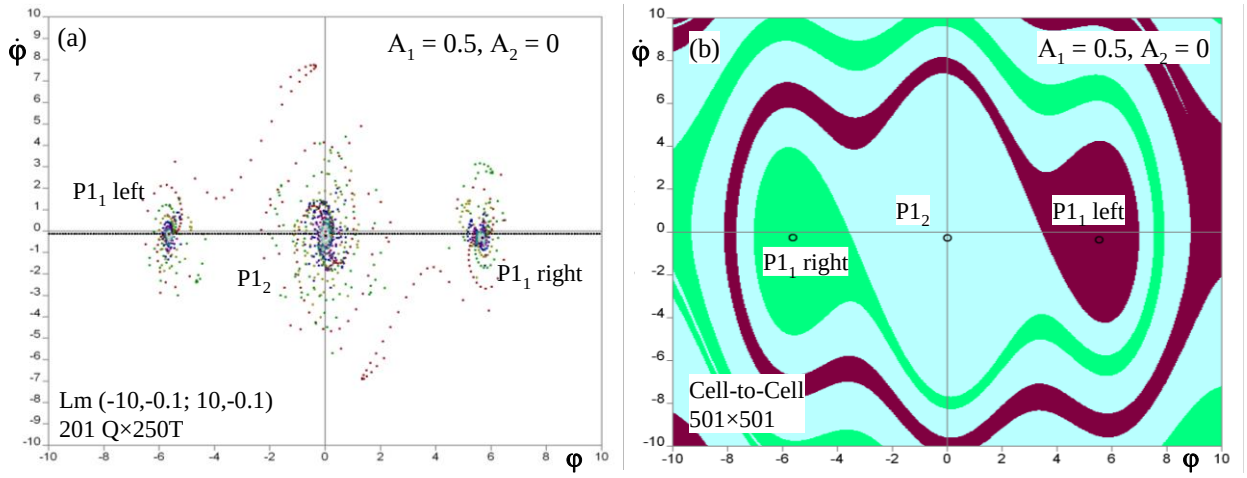

Fig.3.4. Parametrically excited pendulum system (see Fig.3.1a) with linear restoring moment and with the periodically vibrating point of suspension in horizontal direction. (a) Dynamical wells on the Poincaré map built by Lm (-10,-0.1; 10,-0.1) 201Q×250T. (b) Attractor-basin phase portrait with 501×501 grid of initial conditions for Eq.(1) of Fig. 3.2a. Parameters: m = 1, L = 1, b = 0.2, c = 1, μ = 9.81, ω = 1.5, A_1 = 0.5, A_2 = 0.

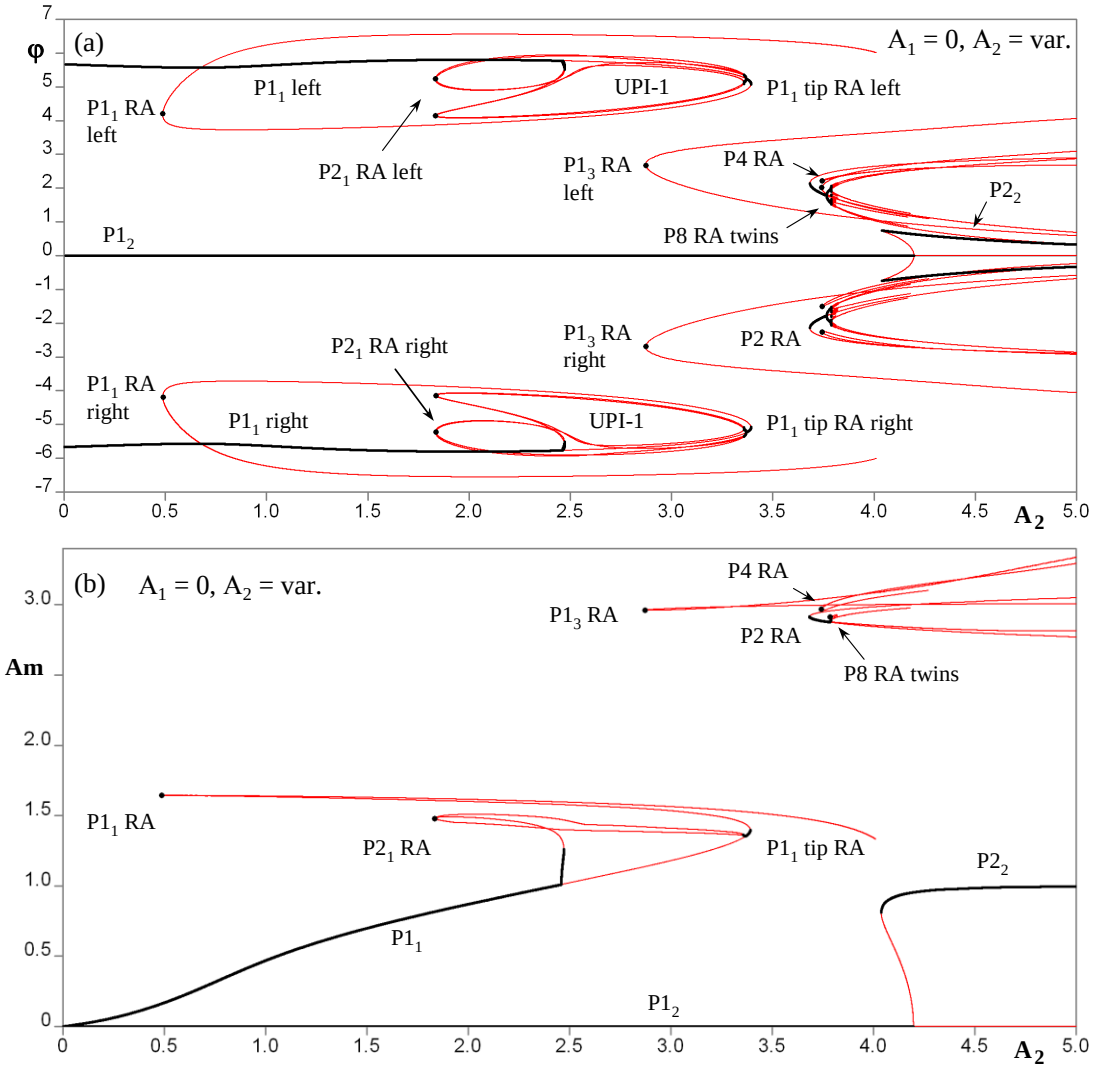

Fig.3.5. Parametrically excited pendulum system (see Fig. 3.1a) with linear restoring moment and with the periodically vibrating point of suspension in vertical direction. (a), (b) Bifurcation diagrams: state (φ, Amplitude) of the fixed periodic points versus vertical external force amplitude A_2. There are three symmetric 1T, one 2T, one 4T and one 8T bifurcation groups. The system has many rare attractors of different kinds. Parameters: $m = 1$, $L = 1$, $b = 0.2$, $c = 1$, $\mu = 9.81$, $\omega = 1.5$, $A_1 = 0$, A_2 = var.

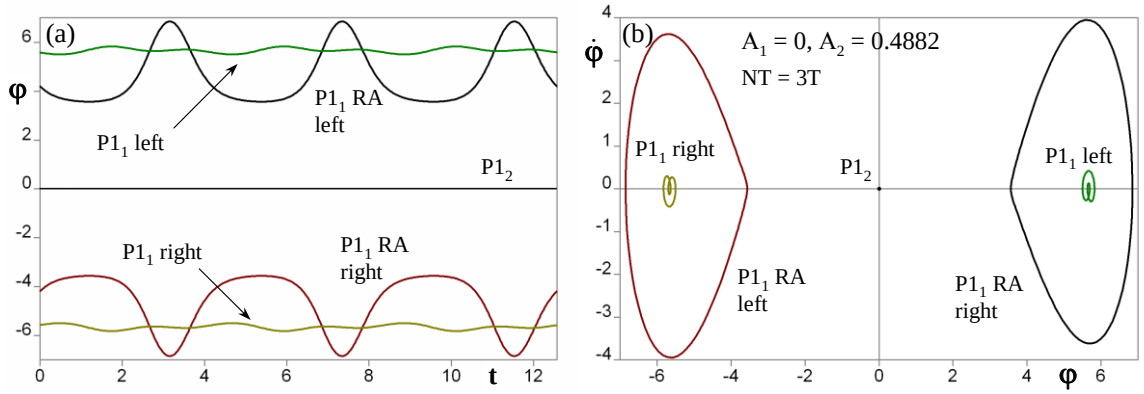

Fig.3.6. Coexistence of $P1_1$ twins stable solutions and $P1_1$ RA twins rare attractors (see Fig. 3.5) in cross-section $A_2 = 0.4882$. (a) Time histories, (b) phase projections. Parameters: $m = 1$, $L = 1$, $b = 0.2$, $c = 1$, $\mu = 9.81$, $\omega = 1.5$, $A_1 = 0$, $A_2 = 0.4882$.

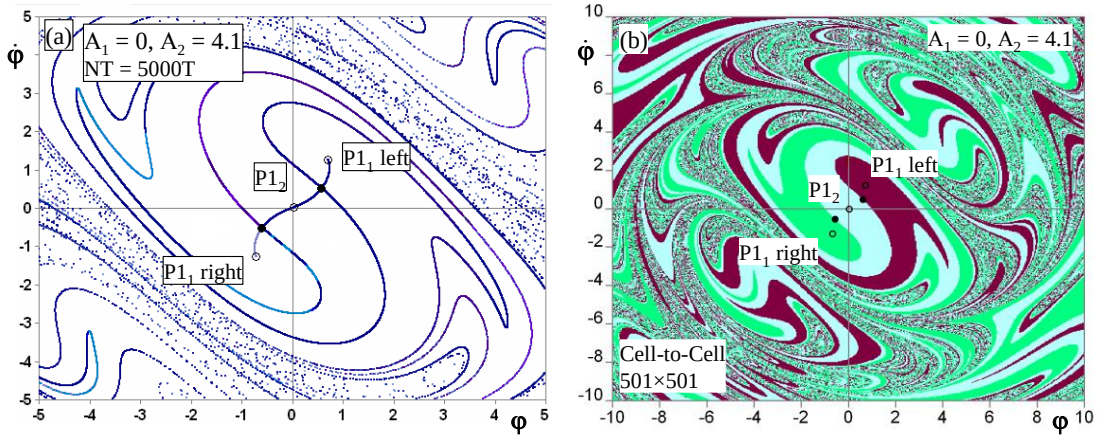

Fig.3.7. Parametrically excited pendulum system (see Fig. 3.1a) with linear restoring moment and with the periodically vibrating point of suspension in vertical direction. (a) Basins of attraction built by insets and outsets from two symmetric P1 saddles (±0.586055, ±0.516811; ρ_1 = 1.112, ρ_2 = 0.389). (b) Attractor-basin phase portrait with 501×501 grid of initial conditions for Eq.(3.1) of Fig. 3.5a. Parameters: m = 1, L = 1, b = 0.2, c = 1, μ = 9.81, ω = 1.5, A_1 = 0, A_2 = 4.1.

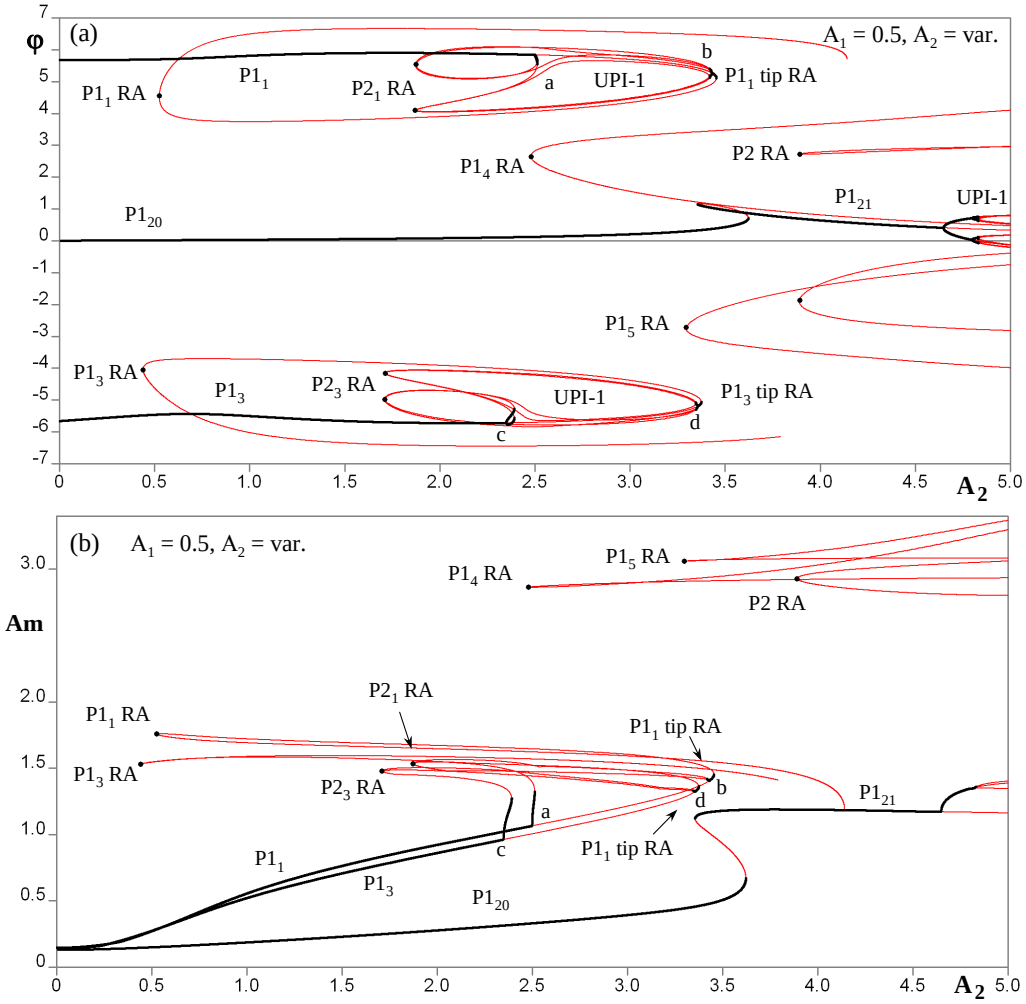

Fig.3.8. The parametrically excited pendulum system (Eq. 3.1) with linear restoring moment and with the periodically vibrating point of suspension in both directions. (a), (b) Bifurcation diagrams: state (φ, Amplitude) of the fixed periodic points versus vertical external force amplitude A_2. There are five 1T and one 2T bifurcation groups. The pendulum system has many rare attractors of different kinds. Parameters: m = 1, L = 1, b = 0.2, c = 1, μ = 9.81, ω = 1.5, A_1 = 0.5, A_2 = var.

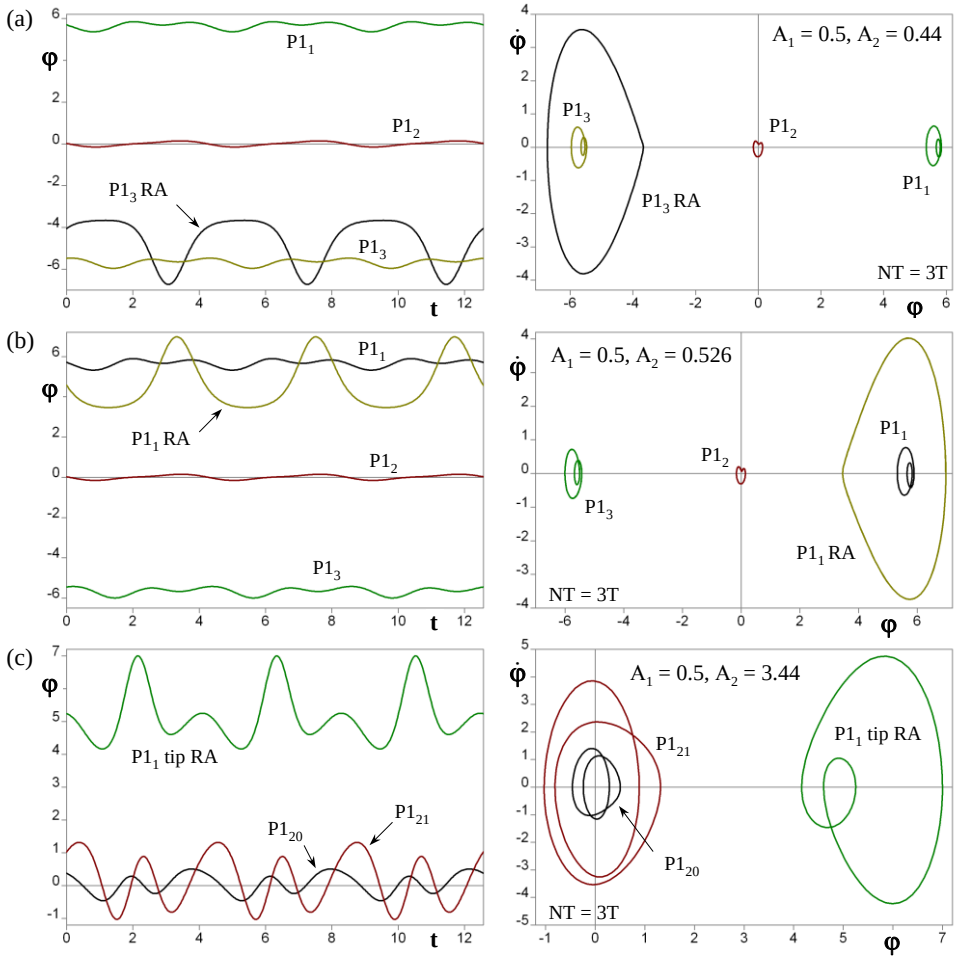

Fig.3.9. Coexistence of P1 usual and rare attractors P1 RA for three cross-sections (see Fig.3.8). (a) Time histories and phase projections for A_2 = 0.44. The rare attractor P1$_3$ RA has the fixed point FP (-4.05606/1.17632). (b) The same for cross-section A_2 = 0.526. The rare attractor P1$_1$ RA has the FP (4.56968/-2.60245). (c) The same for A_2 = 3.44. The rare attractor P1$_1$ tip RA has the FP (5.23616/-0.315143). Parameters: m = 1, L = 1, b = 0.2, c = 1, μ = 9.81, ω = 1.5, A_1 = 0.5, A_2 = var.

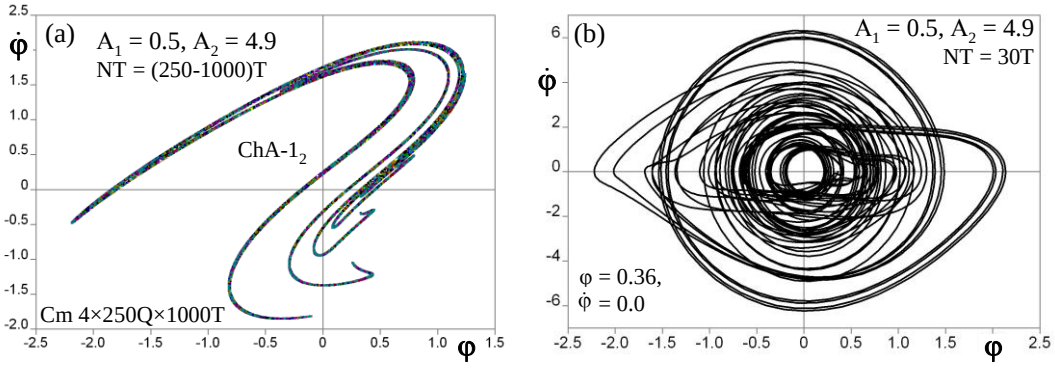

Fig.3.10. Chaotic attractor in the parametrically excited pendulum system for cross-section A$_2$ = 4.9 of bifurcation diagram Fig.3.8: (a) Poincaré map - Cm 4×250Q×(250-1000)T; (b) phase projection with NT = 30T. Parameters: m = 1, L = 1, b = 0.2, c = 1, μ = 9.81, ω = 1.5, A_1 = 0.5, A_2 = 4.9

The examples of coexistence of period-1 (P1) stable solutions and P1 RA rare attractors for three cross-sections A_2 = 0.44, A_2 = 0.526 and A_2 = 3.44 on bifurcation diagram (Fig.3.8a) with the time histories and phases projections are shown in Fig.3.9. Oscillation amplitudes of

rare attractors in some cases are tenfold bigger than oscillating amplitudes of stable P1 regimes. The examined system has also other bifurcation group of higher order with rare attractors, for example, 2T bifurcation group with P2 RA rare attractor with large oscillation amplitudes.

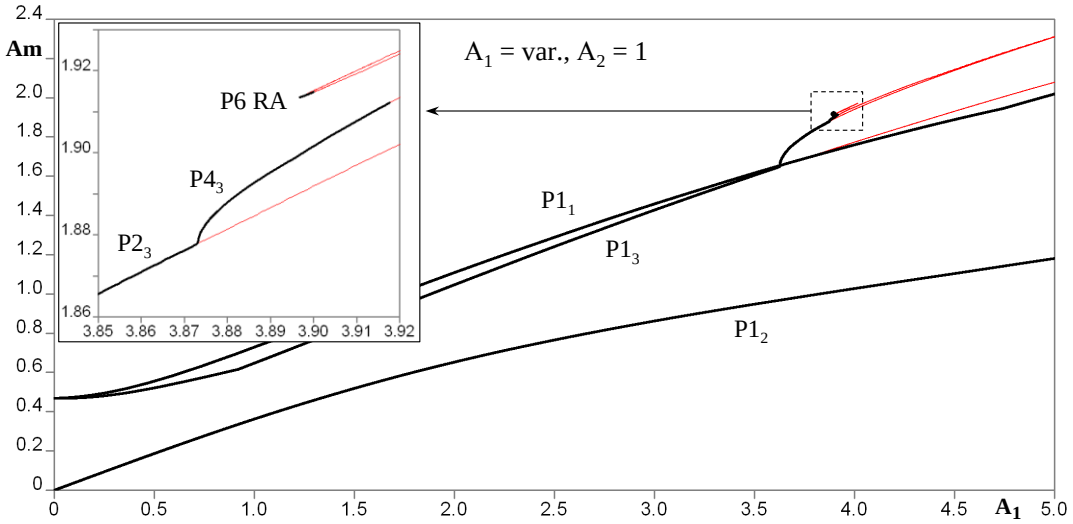

Fig.3.11. The parametrically excited pendulum system with linear restoring moment and with the periodically vibrating point of suspension in both directions. Bifurcation diagram - state (Amplitude) of the fixed periodic points versus horizontal external force amplitude A_1. There are three different 1T and one 6T bifurcation groups. Parameters: $m = 1$, $L = 1$, $b = 0.2$, $c = 1$, $\mu = 9.81$, $\omega = 1.5$, A_1 = var., $A_2 = 1$.

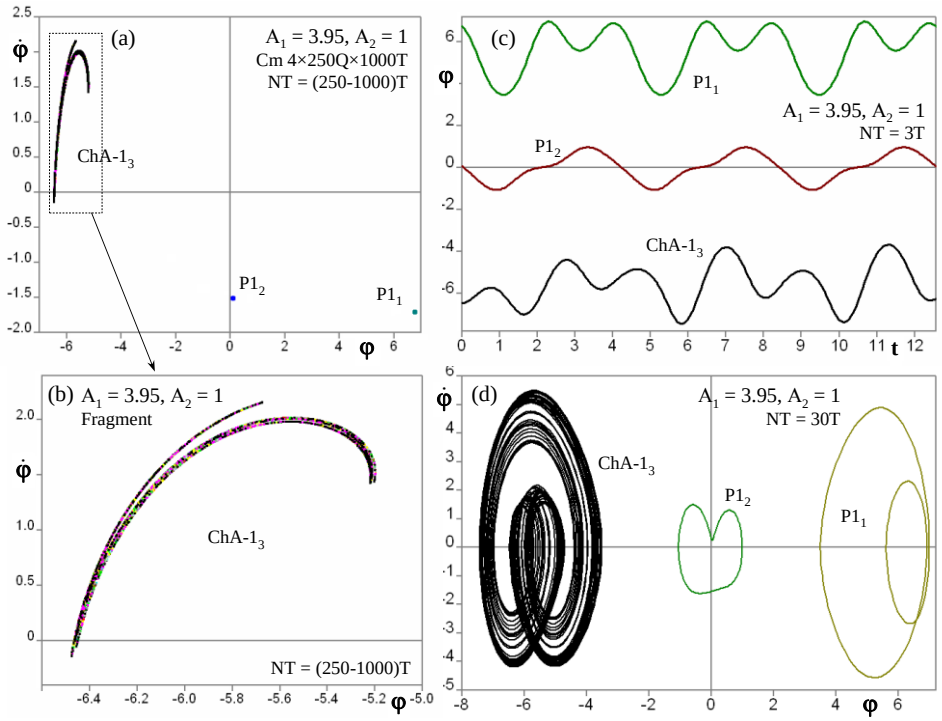

Fig.3.12. Coexistence of periodic regimes $P1_1$, $P1_2$ and ChA-1_3 chaotic attractor for cross-section $A_1 = 3.95$ in the parametrically excited pendulum system with additional linear restoring moment (see Fig. 3.11): (a) Poincaré map - Cm 4×250Q×1000T; (b) fragment of contour mapping; (c)-(d) time histories and phase projections. Parameters: $m = 1$, $L = 1$, $b = 0.2$, $c = 1$, $\mu = 9.81$, $\omega = 1.5$, $A_1 = 3.95$, $A_2 = 1$.

Each bifurcation group has its own unstable periodic infinitium (UPI) [109, 111, 137, etc.] with corresponding chaotic attractors. The example of globally stable chaotic attractor for cross-section with parameters A_1 = 0.5, A_2 = 4.9, obtained using the contour mapping, is shown in Fig.3.10a.

The system also has other nT subharmonic bifurcation groups with n = 3, not shown.

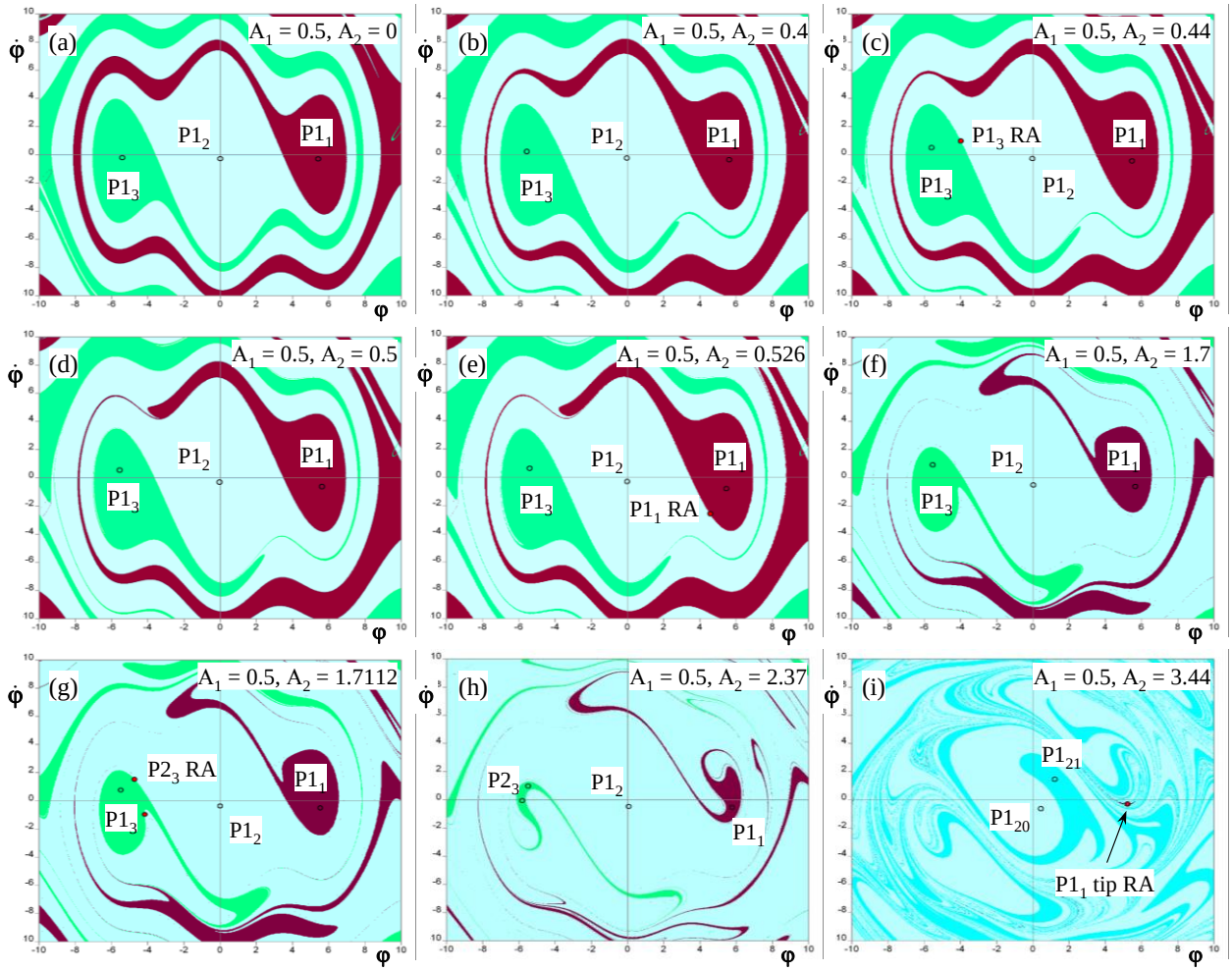

Fig. 3.13. Attractor-basin phase portraits with 501×501 grid of initial conditions for Eq.(3.1) of bifurcation diagram shown in Fig. 3.8a. Parameters: m = 1, L = 1, b = 0.2, c = 1, μ = 9.81, ω = 1.5, A_1 = 0.5, A_2 = var.

Coexistence of P1 stable solutions and ChA-1_3 chaotic attractor is shown on time histories, phase projections and on Poincaré map - Cm 4×250Q×1000T (Fig.3.12). At cross-section A_1 = 3.95 of bifurcation diagram (see Fig.3.11) in the parametrically excited pendulum system with additional linear restoring moment and vibrating point of suspension in both directions there are periodic regimes $P1_1$, $P1_2$ and chaotic attractor ChA-1_3.

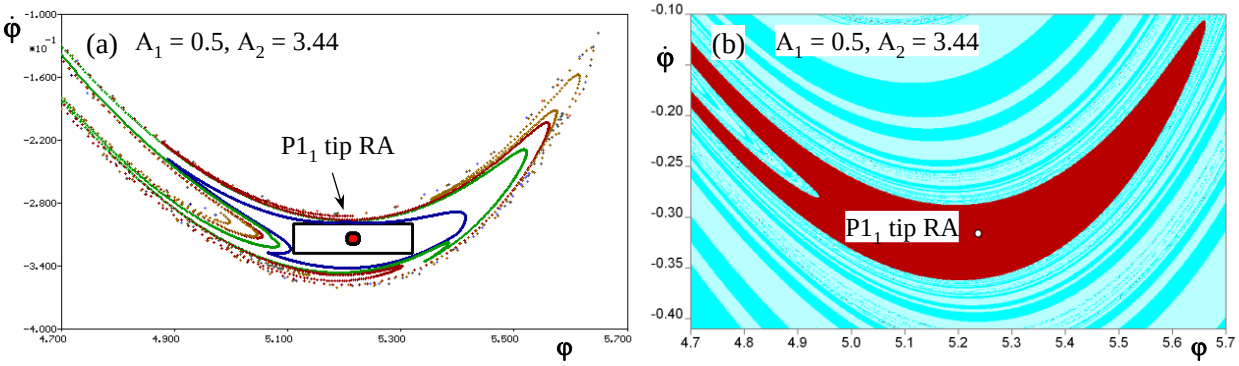

Fig. 3.14. Basins of attraction of period-1 tip rare attractor $P1_1$ tip RA (see Fig.3.8a and 3.13i) in a parametrically excited pendulum system: (a) obtained by using a reverse contour mapping from a rectangle; (b) obtained by using Cell-to-Cell mapping with 501×501 grid of initial conditions. Parameters: $m = 1$, $L = 1$, $b = 0.2$, $c = 1$, $\mu = 9.81$, $\omega = 1.5$, $A_1 = 0.5$, $A_2 = 3.44$.

Basins of attraction of periodic solutions in parametrically excited pendulum system for different cross-sections of bifurcation diagram (see Fig.3.8) obtained by Cell-to-Cell mapping, are shown in Fig.3.13. Comparison of two different methods for building basins of attraction of tip kind rare attractor $P1_1$ RA is represented in Fig.3.14: (a) reverse contour mapping from a rectangle; (b) Cell-to-Cell mapping with 501×501 grid of initial conditions. These methods show the same results of building basins of attraction.

It is shown that using of the method of complete bifurcation groups allows to conduct the bifurcation analysis of parametrically excited pendulum systems with several equilibrium positions, and to find new bifurcation groups with rare attractors and chaotic regimes. Obtained results of complete bifurcation analysis shows, that amplitudes of rare attractors are grater than once of regular attractors. It might be supposed that rare attractors can result in the loss of control and stability of oscillating systems, or in the other catastrophic or unexpected phenomena. Some obtained new effects can be used for the parametric stabilization of unstable oscillations in technological processes.

3.3 The pendulum systems with the periodically vibrating point of suspension in the vertical direction

The second studied pendulum model is shown in Fig.3.15. The system has the harmonically vibrating point of suspension in vertical direction. The same models have been examined in some works, see e.g. [15,17,19,23,25,29,40,41,43,52,53,54,61,62,70,72, etc.]. The aims of our bifurcation analysis are to find new bifurcation groups with unstable periodic infinitium (UPI) [109, 111, 137, etc.], rare regular and chaotic attractors, and to study obtained

nonlinear phenomena such as multiplicity, subharmonics (P2, P3 and P4) and different types of rotations (period-1, subharmonic and chaotic). Some results of complete bifurcation analysis of the studied model have been examined in [141,147,149,150].

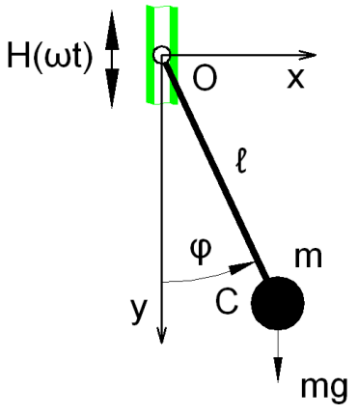

Fig. 3.15. The studied dynamical model of the pendulum system with the periodically vibrating point of suspension in vertical direction.

The equation of motion for pendulum (Fig.3.15) in dimensionless form is such:

$$\ddot{\varphi} + b\dot{\varphi} + (1 + h\cos\omega t)\sin\pi\varphi = 0\,, \qquad (3.2)$$

where φ – angle of the pendulum, read-out from a vertical line; $\dot{\varphi}$ - angular velocity, where $\dot{\varphi} = d\varphi / dt$; t – time; b – linear damping coefficient; h and ω – vertical vibrating amplitude and frequency of the support.

For simplification we accept that the angle of complete rotation is not equal 2π, but equal 2. The variable parameters of the system are dissipation b, frequency ω and amplitude h of periodical excitation.

The results of the bifurcation analysis for the pendulum with the vibrating point of suspension in the vertical direction (3.2) under variation of the excitation frequency ω are shown in Fig. 3.16-3.25.

First of all, the periodic skeleton, consisting of 87 oscillatory and rotational regimes, belonging to different bifurcation groups, has been constructed at fixed parameters b = 0.2, h = 1.5, ω = 1. Complete bifurcation diagrams have been constructed from some of the found fixed points, belonging to certain regimes. The complete bifurcation diagram, consisting of 8 different bifurcation groups, is shown in Fig. 3.16. The system has a period-doubling bifurcation, folds and different types of rare attractors.

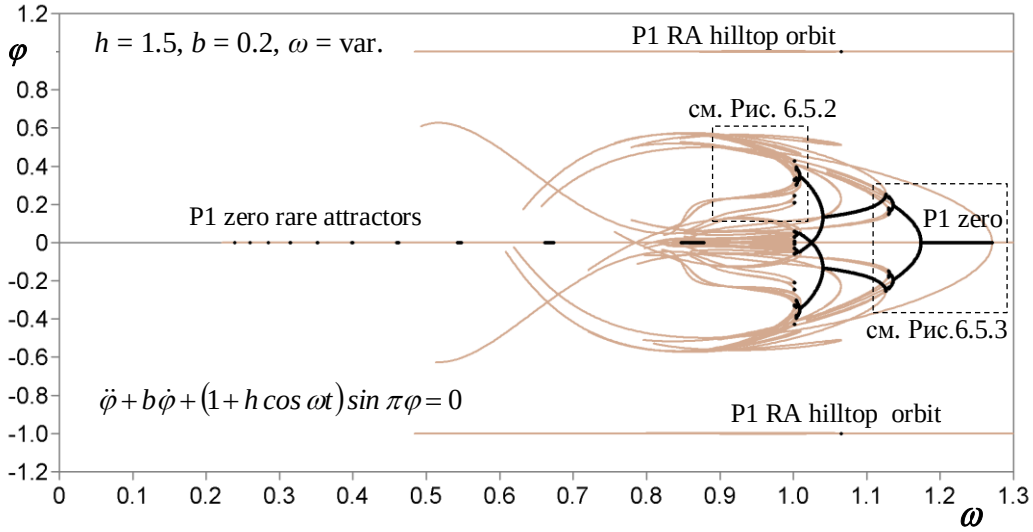

Fig. 3.16. Bifurcation diagram for the pendulum with the vibrating point of suspension in the vertical direction (Fig.3.15). 8 different bifurcation groups are also shown. The system has different types of rare attractors. System parameters: b = 0.2, h = 1.5, k = 7, ω = var.

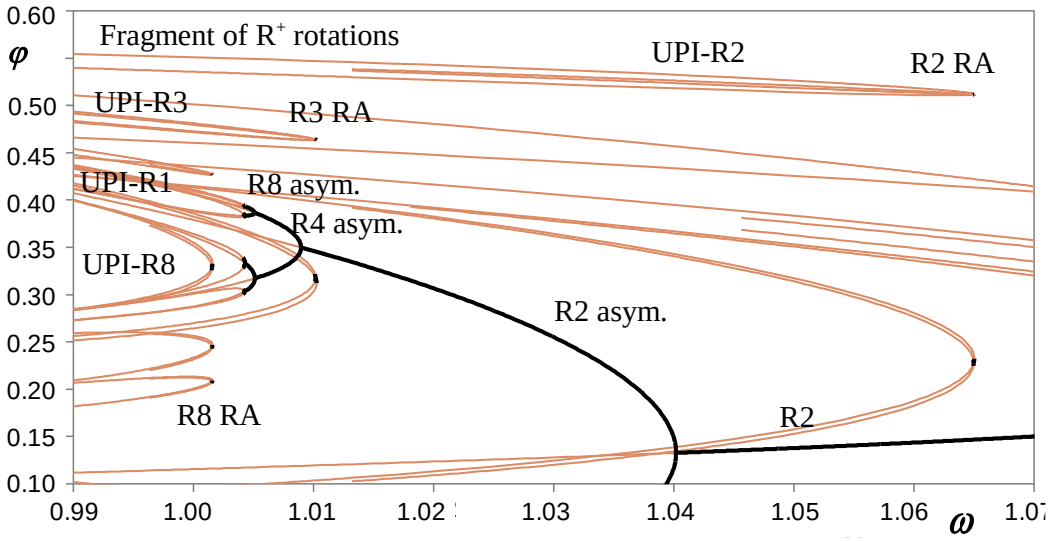

Fig. 3.17. Fragment of the bifurcation diagram (Fig. 3.16) for bifurcation groups 1T, 2T, 3T and 8T, formed by periodic rotations R1, R2, R3 and R8. The regions with the different types of chaotic rotations (UPI-R1, UPI-R2, UPI-R3 and UPI-R8) are born as a result of period-doubling bifurcations, illustrated in the figure.

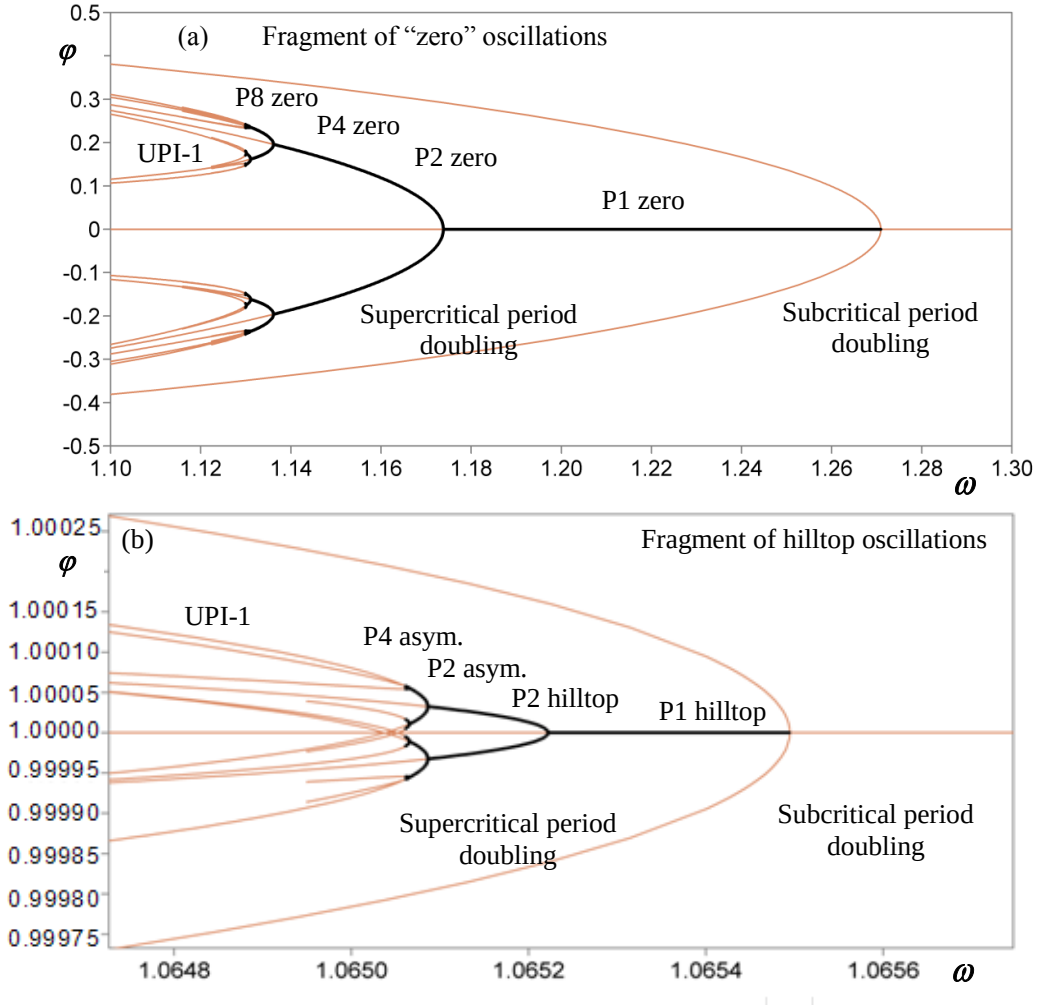

Fig. 3.18. Fragments of bifurcation diagrams (Fig. 3.16) for bifurcation groups 1T with regime P1 zero (a) and stable oscillations of pendulum with respect to the unstable equilibrium position (b). A scaled-up view of the period-doubling cascade and of the birth of an infinite number of unstable periodic solutions (UPI) is also provided. The structure of bifurcation groups is topologically similar in both cases.

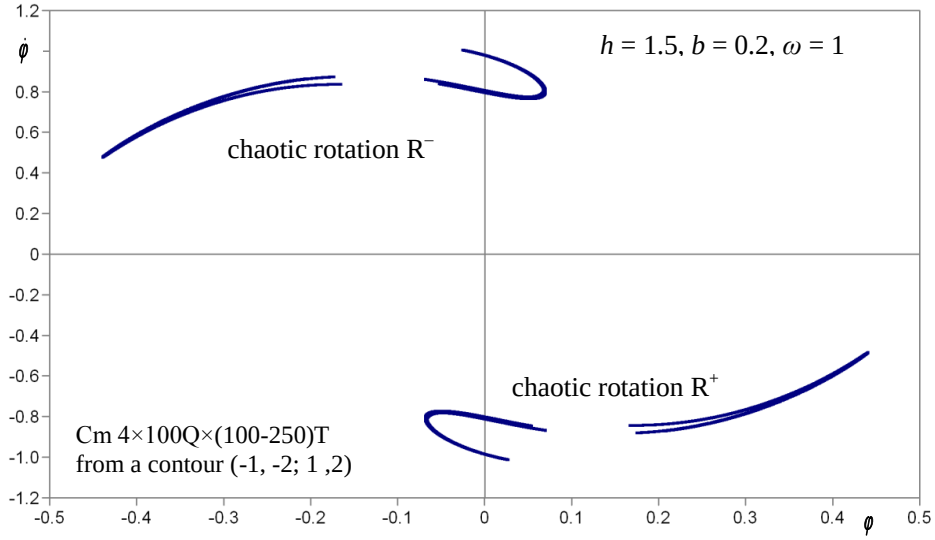

Fig. 3.19. Co-existence of chaotic attractors. A fragment of contour mapping Cm 4×100Q×(100-250)T on the Poincaré plane taking into account cyclicality. System parameters: $b = 0.2$, $h = 1.5$, $\omega = 1$.

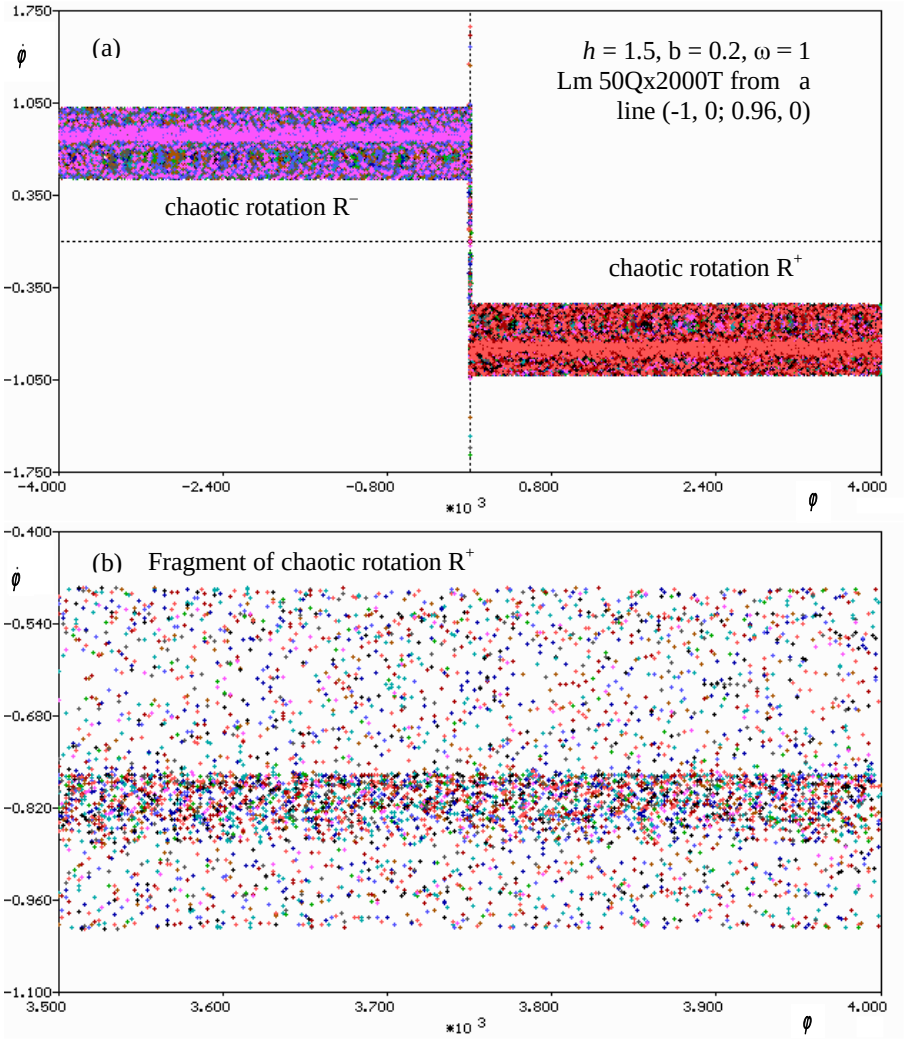

Fig. 3.20. Co-existence of chaotic attractors. Mapping from line Lm 50Q×2000T on the Poincaré plane without taking into account cyclicality. System parameters: b = 0.2, h = 1.5, ω = 1.

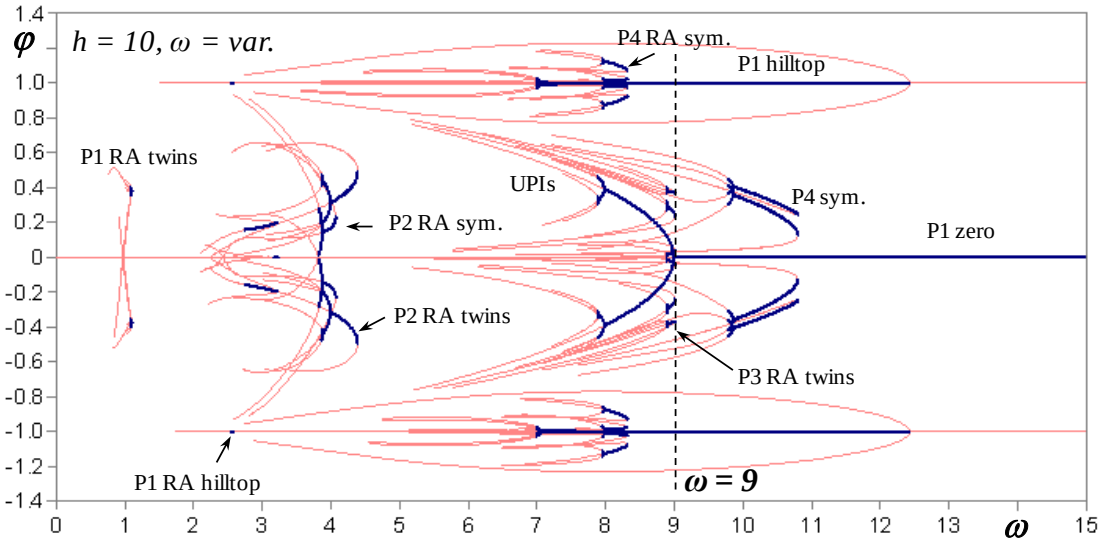

Fig. 3.21. Bifurcation diagram for the pendulum system with the vibrating point of suspension in the vertical direction (Fig.3.16) for 8 different bifurcation groups: three groups 1T, two groups 2T, one 3T and two 4T. The system has period-doubling bifurcations, folds and different types of rare attractors. Equation: $\ddot{\varphi} + b\dot{\varphi} + (1 + h\cos\omega t)\sin\pi\varphi = 0$. System parameters: b = 0.2, h = 10, k = 7, ω = var.

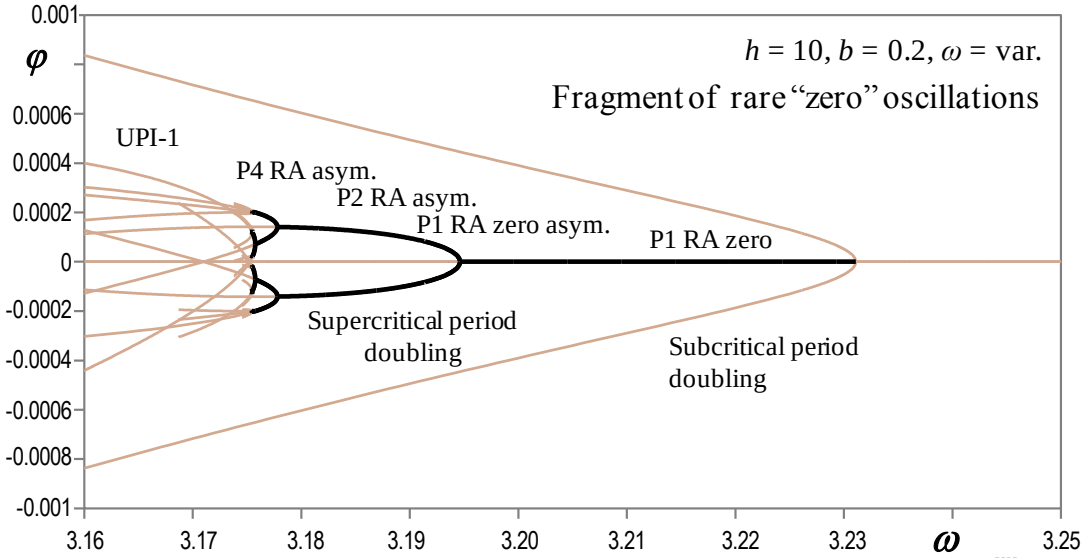

Fig. 3.22. Fragment of bifurcation diagram (Fig. 3.21) for bifurcation group 1T zero with regime P1 zero. A scaled-up view of the period-doubling cascade and of the birth of an infinite number of unstable periodic solutions (UPI) is provided. The structure of bifurcation group is topologically similar with other bifurcation groups in studied pendulum system.

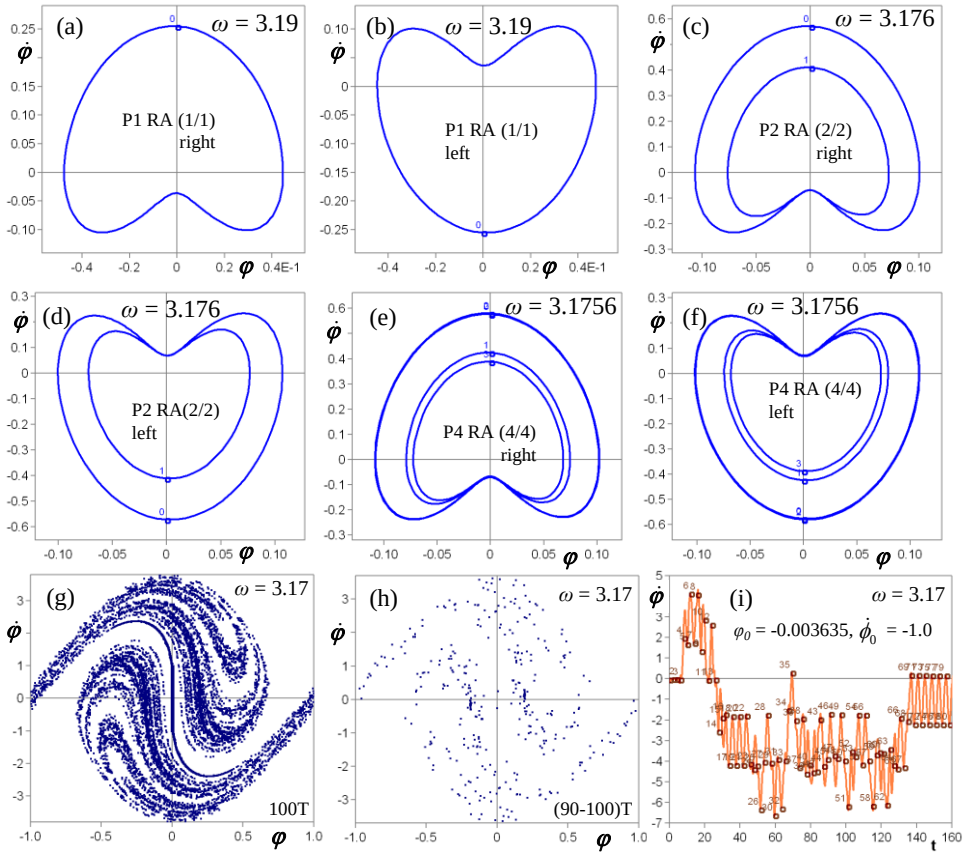

Fig. 3.23. The period-doubling cascade and the birth of an infinite number of unstable periodic solutions (UPI) for bifurcation group 1T zero with regime P1 zero (Fig. 3.22): (a)-(f) phase projections with period depth P1-P4; (g) Mapping from contour (-0.005, -1; 0.005, 1) Cm 4×250Q×100T on the Poincaré plane; (h) fragment of contour mapping NT = (90-100)T; (i) transient chaos to P2 attractor from an initial point φ_0 = -0.003635, $\dot{\varphi}$ = -1.0, NT = 80T. System parameters: h = *10*, b = 0.2, ω = var.

The fragments of bifurcation diagrams (Fig. 3.16) are shown in Fig. 3.17 and 3.18. The fragment of bifurcation group 1T of regime P1 zero with the period-doubling cascade, leading to the formation of a subgroup with an infinite number of unstable periodic solutions (UPI), is shown in Fig. 3.17. The presence of a subgroup with UPI indicates the existence of chaotic attractor or chaotic transient in this bifurcation group [147]. The fragment of a diagram for bifurcation groups 1T, 2T, 3T and 8T, formed by periodic rotations R1, R2, R3 and R8, can be seen in Fig. 3.16. The regions with different types of chaotic rotations (UPI-R1, UPI-R2, UPI-R3 and UPI-R8) are born as a result of period-doubling bifurcations, shown above. A chain of rare attractors for regime P1 zero corresponds to the Arnold's tongues. For cross-section of bifurcation diagram (Fig. 3.16-3.17) for ω = 1 co-existence of chaotic rotations is shown in a fragment of contour mapping Cm 4×100Q×(100-250)T on the Poincaré plane (Fig.3.19) taking into account cyclicality. The same chaotic rotational attractors are shown in Fig.3.20 by mapping from a line Lm 50Q×2000T on the Poincaré plane without taking into account cyclicality.

The pendulum model with vertical oscillations of the point of suspension at h = 10 has 8 different bifurcation groups (Fig. 3.21): three groups 1T, two groups 2T, one 3T and two 4T. The system has period-doubling bifurcations, folds and different types of rare attractors. The branches of bifurcation diagrams are not finished due to instability with the maximum value exceeding $9.7 \cdot 10^8$. The results of bifurcation analysis, obtained by applying the method of complete bifurcation groups, indicates not only the existence of stable oscillations with respect to the upper unstable equilibrium position with a period of excitation, but also more complex oscillations of subharmonic type, for example, P4 (Fig. 3.21). Bifurcation groups with tip and dumbbell rare attractors, each having not only periodic regimes, but also chaotic regimes, have 1

Fragment of bifurcation diagram (Fig. 3.21) for bifurcation group 1T zero with regime P1 zero is shown in Fig.3.22. A scaled-up view of the period-doubling cascade and of the birth of an infinite number of unstable periodic solutions (UPI) is provided. The structure of bifurcation group is topologically similar with other bifurcation groups in studied pendulum system. The period-doubling cascade and the birth of an infinite number of unstable periodic solutions (UPI) for bifurcation group 1T zero with regime P1 zero (Fig. 3.22) is shown in phase projections in Fig.3.23a-f with period depth P1-P4. As the result of period-doubling cascade and the birth of UPI the transient chaos to P2 attractor by mapping from a contour (-0.005, -1; 0.005, 1) Cm 4×250Q×100T on the Poincaré plane is shown in Fig.3.23g-h. Time history of transient chaos to P2 attractor from an initial point φ_0 = -0.003635, $\dot{\varphi}$ = -1.0 is shown in Fig.3.23i.

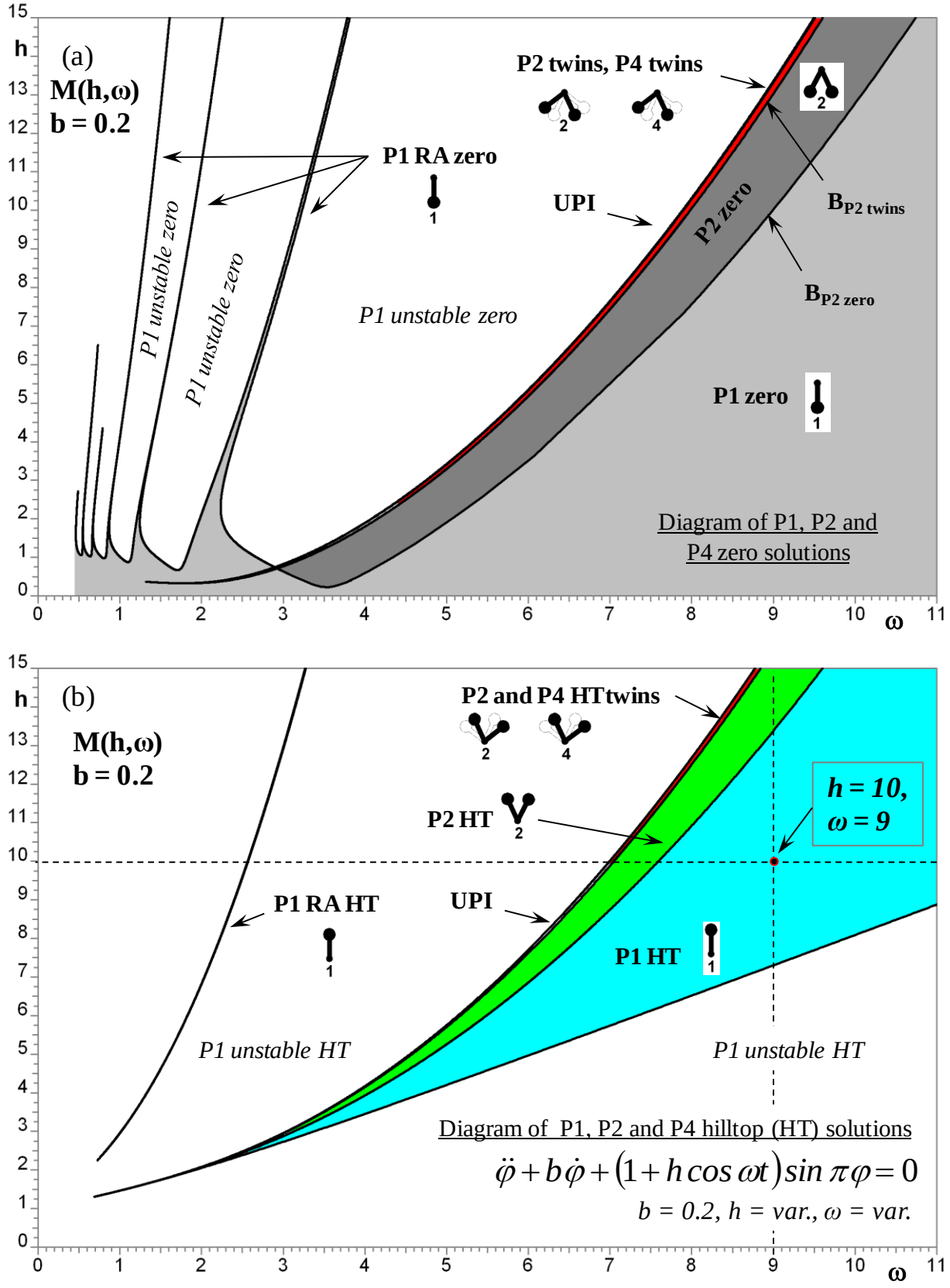

Fig. 3.24. The first steps of constructing two-parameter bifurcation diagrams in the plane (ω, h) for the pendulum system with the vibrating point of suspension in the vertical direction (Fig. 3.15). Bifurcation diagrams of regime P1 zero (a) and P1 hilltop (b) with the cascade of period-doubling bifurcations are also shown in the diagram. System parameters: b = 0.2, h = var, k = 7, ω = var.

The two-parameter bifurcation diagram shows the results of the research on oscillations with respect to the stable zero position and with respect to the upper unstable equilibrium position with a period of excitation (Fig. 3.24). Bifurcation borders of regime P1 with the respective cascade of period-doubling bifurcations are also shown in this diagram.

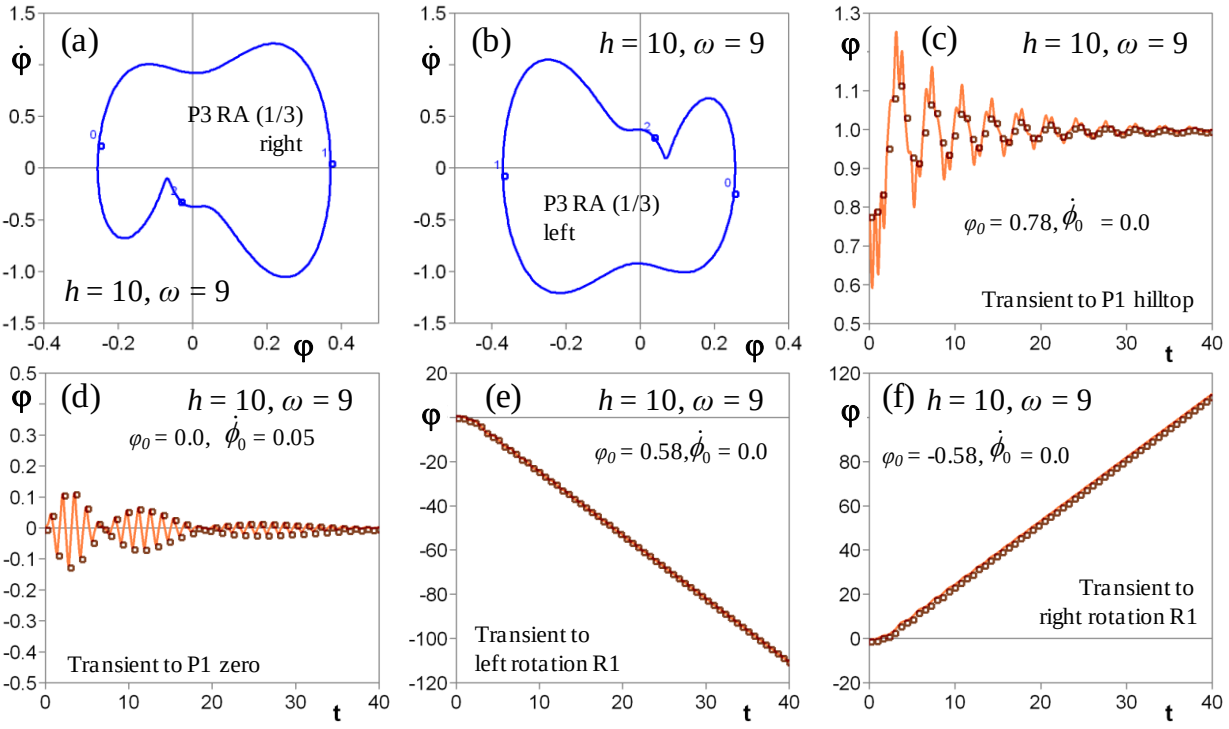

Fig. 3.25. Phase projections for P3 twin attractors (a)-(b) and transient processes - (c) to P1 hilltop; (d) to P1 zero; (e) to left rotation R1; (f) to right rotation R1, for cross-section of bifurcation diagram (see Fig.3.21). Parameters: *b = 0.2, h = 10, ω = 9.*

On the phase projections and by the transient processes Fig. 3.25 shows a coexistence of period-1 zero attractor, period-1 hilltop attractor, subharmonic P3 twin attractors, left and right rotations of period-1 declared by the cross-section $h = 10$, $\omega = 9$ of bifurcation diagrams (see Figs.3.21, 3.24).

Thus, rare regular and chaotic attractors and some other new nonlinear phenomena, such as co-existence of different types of periodic and chaotic attractors (rotation R1, P1 hilltop, subharmonic solutions and chaotic oscillations) and rare and chaotic rotational regimes (with a period of excitation, subharmonic and chaotic ones), oscillatory-rotational regimes, have been found for the pendulum system with the vibrating point of suspension in the vertical direction.

In Chapter 6 the software for animation of the dynamics of parametrically excited pendulum in vertical direction it discussed. The software was created using Pascal programming language. As the example of animation the P3 RA (1/3) right attractor (Fig. 3.25a) was shown. The results of experimental investigations of this pendulum are shown as well.

3.4 The pendulum with the vibrating point of suspension in the horizontal direction

The third studied pendulum model is shown in Fig.3.26. The methodology for constructing bifurcation diagrams and performing the global analysis in a pendulum system with the vibrating point of suspension in the horizontal direction is the same as in the previous systems. The equation of motion of this pendulum model (Fig. 3.26) is such:

$$\ddot{\varphi} + b\dot{\varphi} + a_1 \sin \pi\varphi = h \cos \omega t \cos \pi\varphi, \qquad (3.3)$$

where φ – the angle of deviation, measured from the vertical; $\dot{\varphi}$ – the pendulum angular velocity, $\dot{\varphi} = d\varphi / dt$; $b\dot{\varphi}$ – the linear dissipative force; b – the linear dissipation coefficient; a_1 – the coefficient, which includes the pendulum length and gravitation constant; h and ω – the amplitude and frequency of external harmonic excitation. All parameters of pendulum systems are dimensionless and normalized. For simplicity, the angle of a full pendulum turn is assumed to be equal to 2 in the given models. . The same models have been examined in work [43]. The results of bifurcation analysis of this pendulum were presented in works [147,149,150].

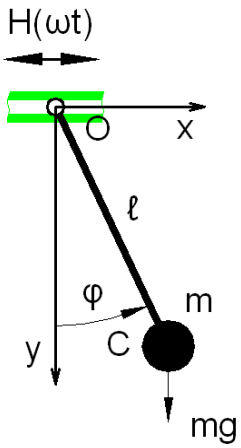

Fig. 3.26. Pendulum models: (a) with the periodically vibrating point of suspension in the vertical direction; (b) in the horizontal direction; (c) at a certain angle α with respect to the horizontal; (d) with harmonic excitation.

The results of bifurcation analysis for a pendulum under variation of the excitation frequency ω are shown in Fig. 3.27 – 3.30. The contour mapping from contour Cm 4×500Q×(100-500)T for the chaotic attractor in the Poincaré plane is shown in Fig. 3.27. Chaotic rotational regime for a pendulum system with the vibrating point of suspension in the horizontal direction (Fig. 3.26) in the time history diagram and phase projection from zero initial conditions is shown in Fig. 3.28. As seen from the diagrams, the rotational regime is of chaotic character on continuation of NT = 30T periods. The found chaotic rotational regime can be used in the design of vibration equipment.

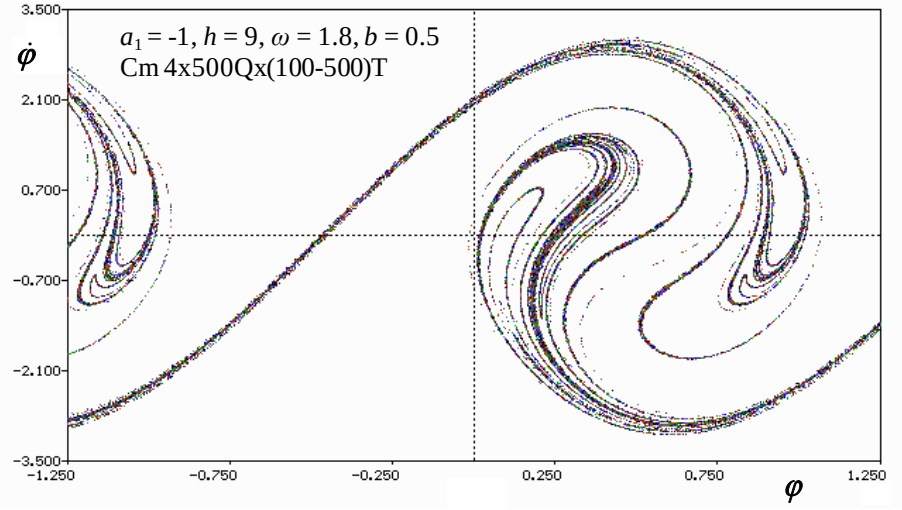

Fig. 3.27. Mapping from contour Cm 4x500Qx(100-500)T on the Poincaré plane for the pendulum system with the vibrating point of suspension in the horizontal direction (Fig.3.26). The system has a chaotic attractor. System parameters: a_1 = -1, h = 9, ω = 1.8, b = 0.5.

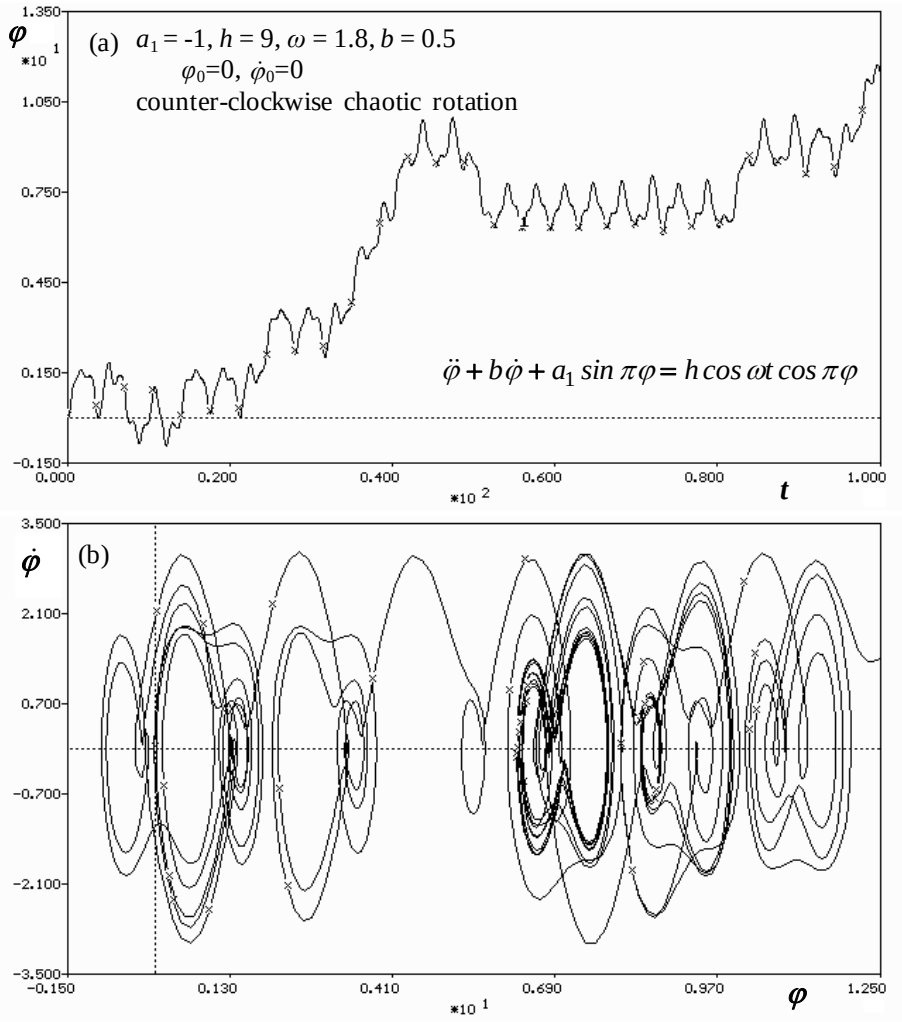

Fig. 3.28. Pendulum with the vibrating point of suspension in the horizontal direction. The counter-clockwise chaotic rotation: (a) time history; (b) phase trajectory. Equation: $\ddot{\varphi} + b\dot{\varphi} + a_1 \sin\pi\varphi = h\cos\omega t\cos\pi\varphi$. System parameters: a_1 = -1, h = 9, ω = 1.8, b = 0.5.

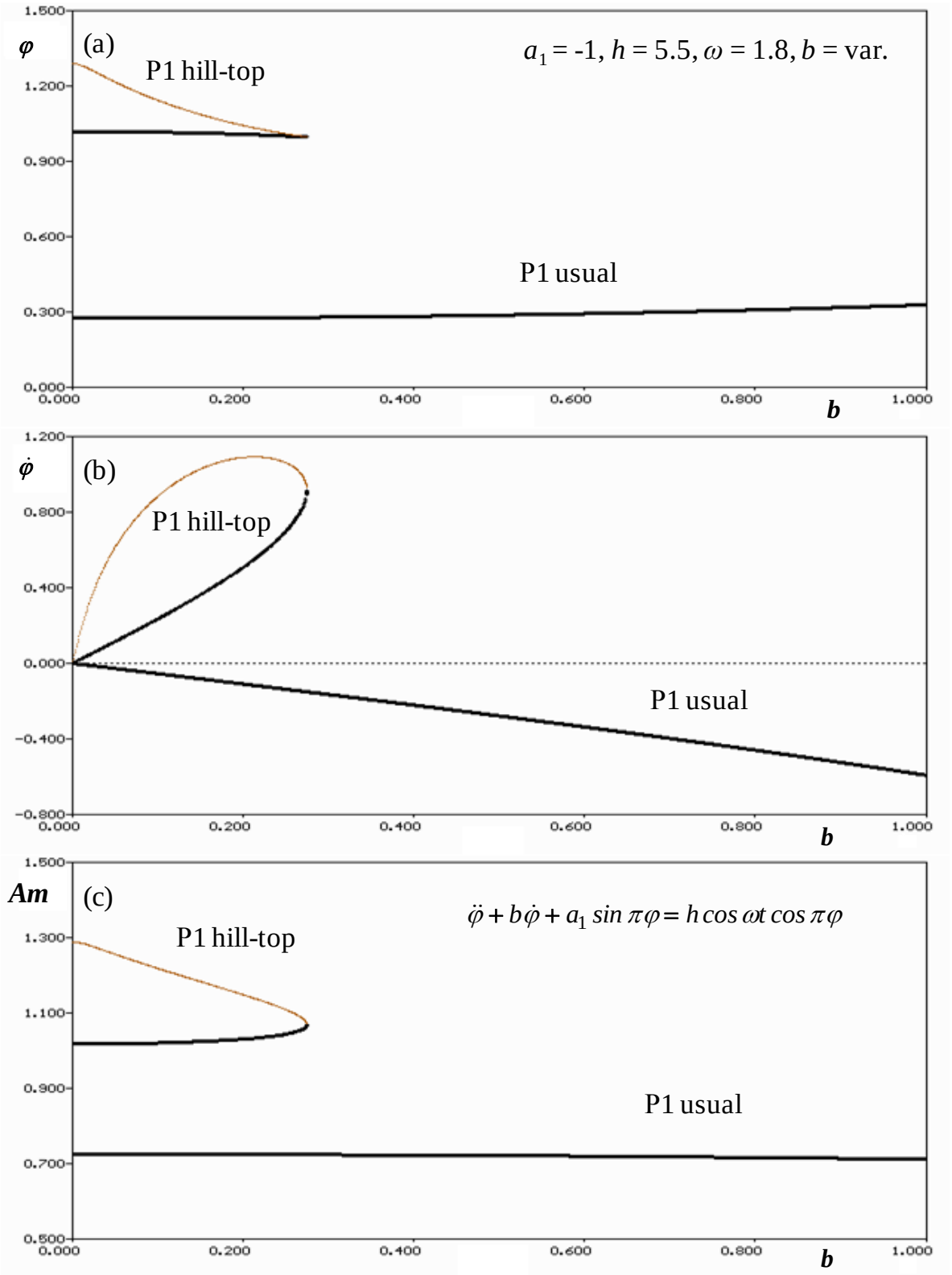

Fig. 3.29. Bifurcation diagrams under variation of dissipation coefficient b for regimes P1 usual and P1 hilltop for a pendulum system with the vibrating point of suspension in the horizontal direction. System parameters: a_1 = -1, h = 5.5, ω = 1.8, b = var.

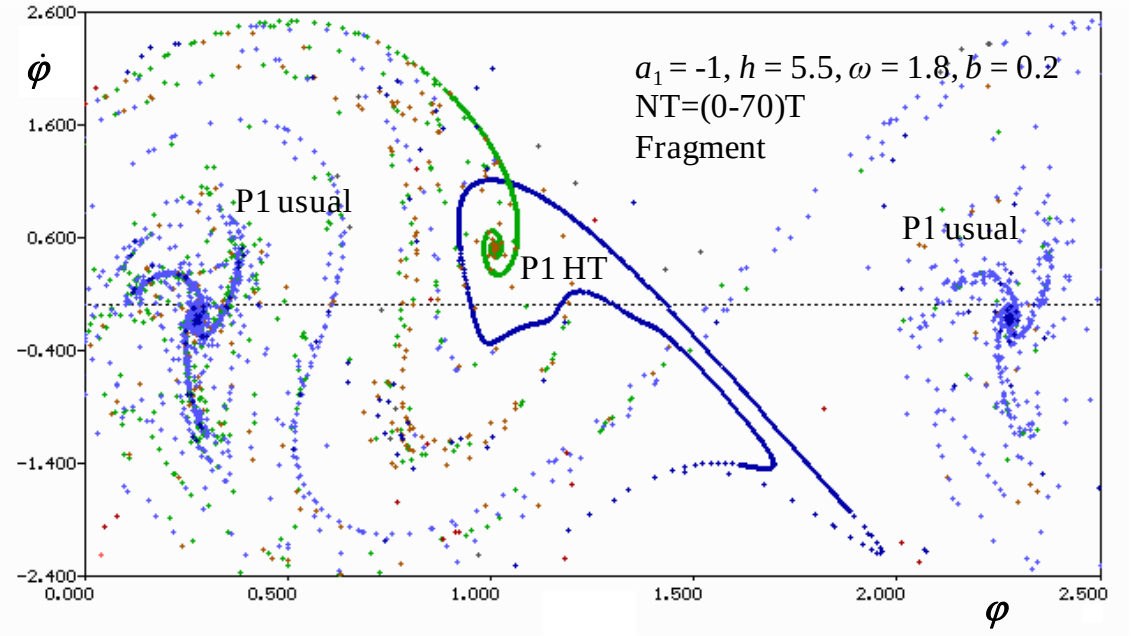

Fig. 3.30. The fragment of mapping from line NT = (0-70)T with the use of the properties of separatrix of the saddle point for a pendulum system with the vibrating point of suspension in the horizontal direction. The basins of attraction of regimes P1 usual and P1 hilltop are shown in the diagram. Equation: $\ddot{\varphi} + b\dot{\varphi} + a_1 \sin\pi\varphi = h\cos\omega t\cos\pi\varphi$. System parameters: a_1 = -1, h = 5.5, ω = 1.8, b = 0.2.

For a pendulum with the vibrating point of suspension in the horizontal direction, fixed points belonging to the corresponding bifurcation groups have been found and complete bifurcation diagrams have been constructed from the fixed points. Fig. 3.29 shows a complete bifurcation diagram, consisting of two bifurcation groups with a period of excitation (P1 usual and P1 hilltop), under variation of dissipation coefficient b. The amplitude of regime oscillations in the vicinity of the upper unstable equilibrium position (P1 hilltop) is higher than of usual regime P1. As seen from the bifurcation diagram, if the linear dissipation coefficient increases, rotational regime P1 hilltop disappears at b = 0.3, and there is only regime P1 usual in the system.

The basins of attraction for regime P1 usual and P1 hilltop in the cross-section of bifurcation diagram (Fig. 3.29) at b = 0.2 with the use of the properties of separatrix of the saddle point are shown in Fig. 3.30. As seen from the diagram, the basin of attraction of a stable oscillatory regime with respect to the upper stable equilibrium position is smaller than the basin of attraction of regime P1 usual.

3.5 The pendulum system with harmonic oscillations of the point of suspension at a certain angle to the horizontal

The fourth studied dynamical model is shown in Fig.3.31. The system has the harmonically vibrating point of suspension under some angle α from the horizontal direction to the vertical. Close models have been examined in some works [15,17,19,23,25,29,40,41, 43,52,53,54,61,62,72, etc.] The aim of our bifurcation analysis is to find new rare attractors and new bifurcation groups. Some results of complete bifurcation analysis of the studied model have been examined in one of the previous works [132,147,150].

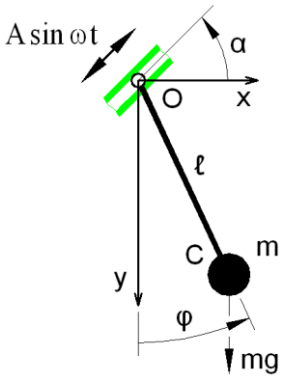

Fig. 3.31. The periodically driven damped pendulum with vibrating point of the support.

The equation of motion for mathematical pendulum (Fig.3.31) is such:

$$m\ell^2\ddot{\varphi} + b\dot{\varphi} + mg\ell \sin\pi\varphi + m\ell A\omega^2 \sin\omega t \cos\pi(\varphi + \alpha) = 0, \qquad (3.4)$$

where φ – angle of the pendulum, read-out from a vertical line; $\dot{\varphi}$ - angular velocity, where $\dot{\varphi} = d\varphi / dt$; α – angle of periodically excitation of the support, merged from the horizontal direction; t – time; m – mass, ℓ – length of the pendulum; g – gravitation constant; b – linear damping coefficient; A and ω – oscillation amplitude and frequency of the support.

For simplification we accept that the angle of complete rotation is not equal 2π, but equal 2. The same for the horizontal excitation $\alpha = 0$ and for vertical excitation $\alpha = 0.5$. The variable parameters of the system are frequency ω of periodical excitation and angle α of direction of vibrating of the support. Other parameters are fixed: $m = 1$, $\ell = 1$, $b = 0.2$, $g = 9.81$, $A = 2$.

Some results of bifurcation analysis of the model are represented in Figs.3.32-3.35. In the first special case the symmetric model only with horizontal external force has 11 bifurcation groups (Fig.3.32). In this figure stable solutions are plotted by solid lines and unstable – by thin lines (reddish online). One brunch of P1 unstable hilltop near ω = 1.75 is not completed,

because of problem of sufficiently high instability with maximal value less than 7200. Phase projections for four cross-sections of bifurcation diagram (see Fig.3.32) are shown in Fig.3.33: (a)-(c) for ω = 3.3, (d)-(e) for ω = 3.85, (f)-(i) for ω = 4.52, (j)-(l) for ω = 4.635. Using complete bifurcation analysis we have found different new rare regular and chaotic attractors, parameter regions with the coexistence of periodic attractors and subharmonic rotations.

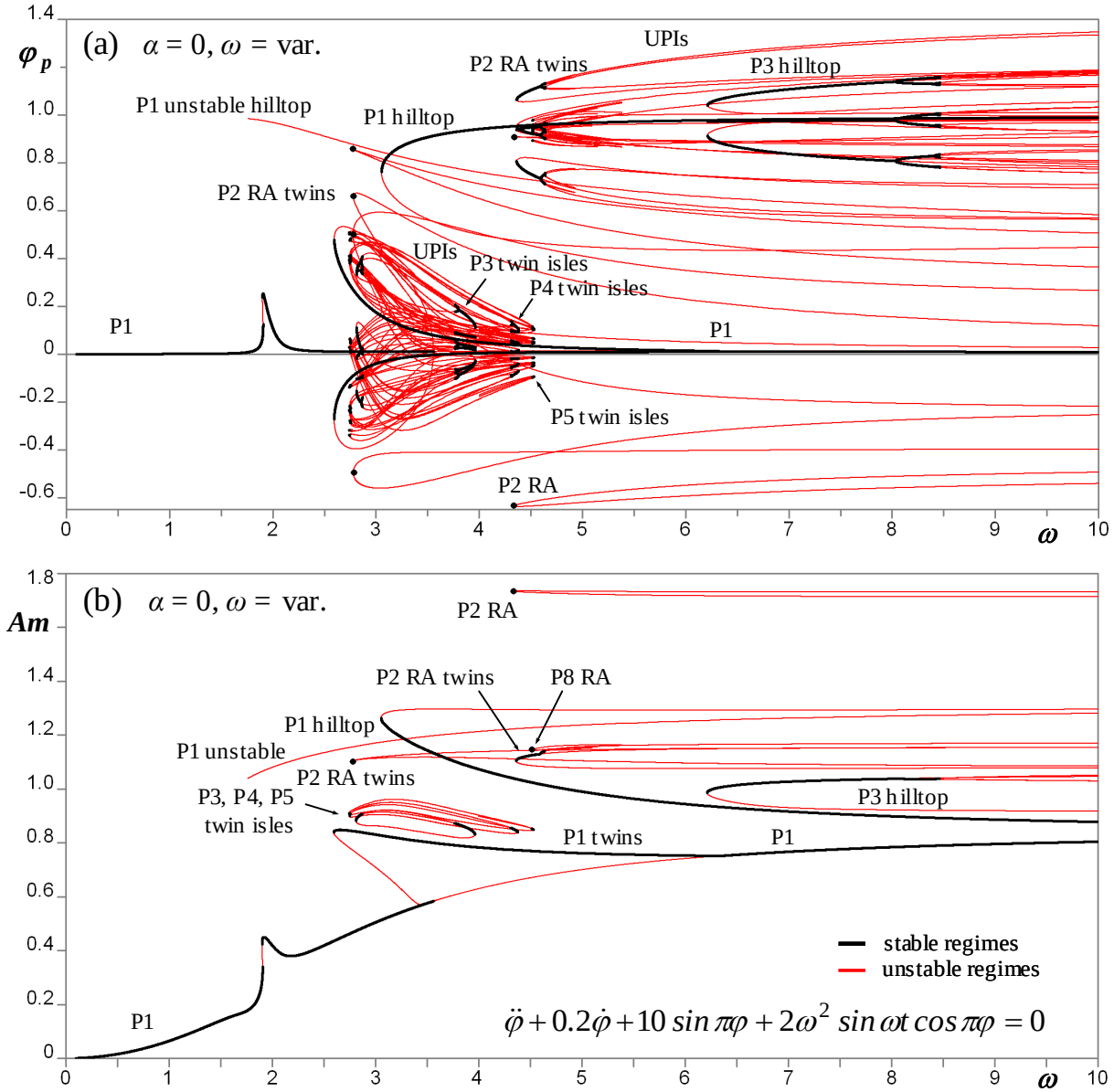

Fig. 3.32. The symmetric periodically driven damped pendulum (see Fig. 1) with the periodically vibrating point of suspension in horizontal direction. Bifurcation diagrams of the fixed periodic points of the angle of rotation φ_p and amplitude of rotation *Am* vs. oscillation frequency ω. Complete bifurcation diagrams of 11 bifurcation groups: three 1T, three 2T, two 3T, one 4T, one 5T and one 8T. There is submerged subharmonic twin isles 3T-5T form cluster. The system has many rare attractors of different kinds.

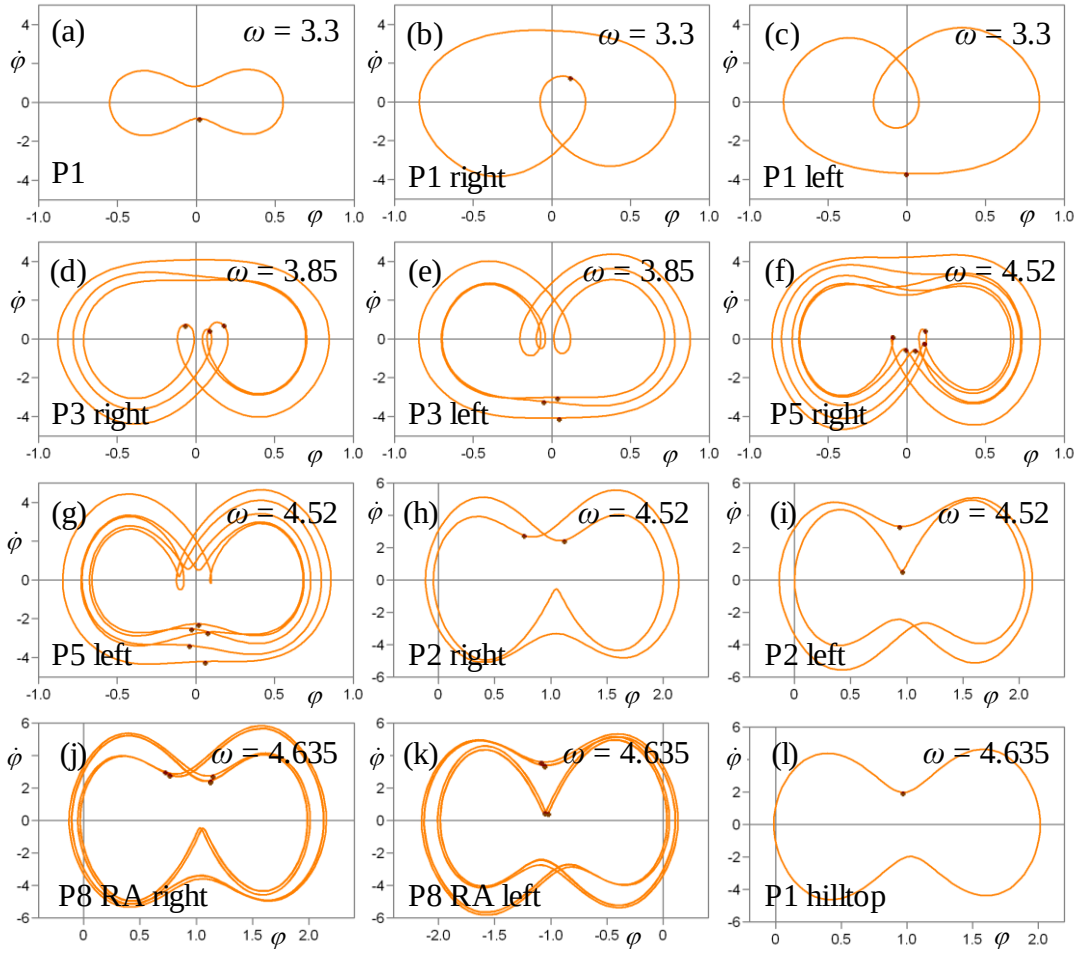

Fig. 3.33. Phase projections for four cross-sections of bifurcation diagram (see Fig.3.32): (a)-(c) for ω = 3.3, (d)-(e) for ω = 3.85, (f)-(i) for ω = 4.52, (j)-(l) for ω = 4.635.

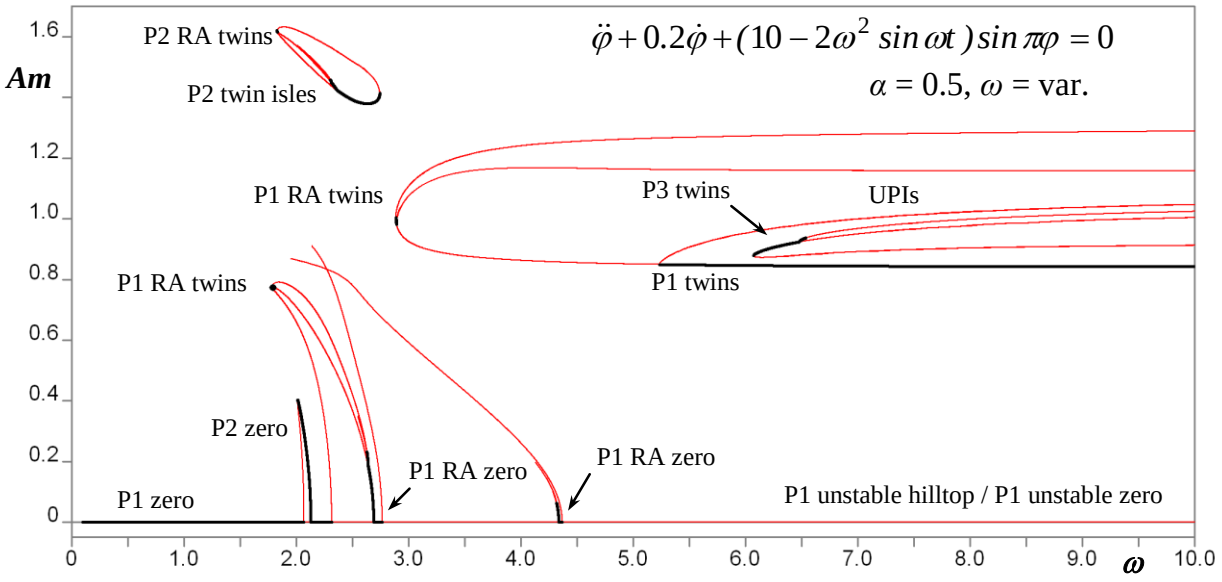

Fig. 3.34. The symmetric pendulum with the periodically vibrating point of suspension in vertical direction. Bifurcation diagrams of the fixed periodic points of the angle of rotation φ_p and amplitude of rotation *Am* vs. oscillation frequency ω. Complete bifurcation diagrams of 5 bifurcation groups: three 1T, one 2T and one 3T.

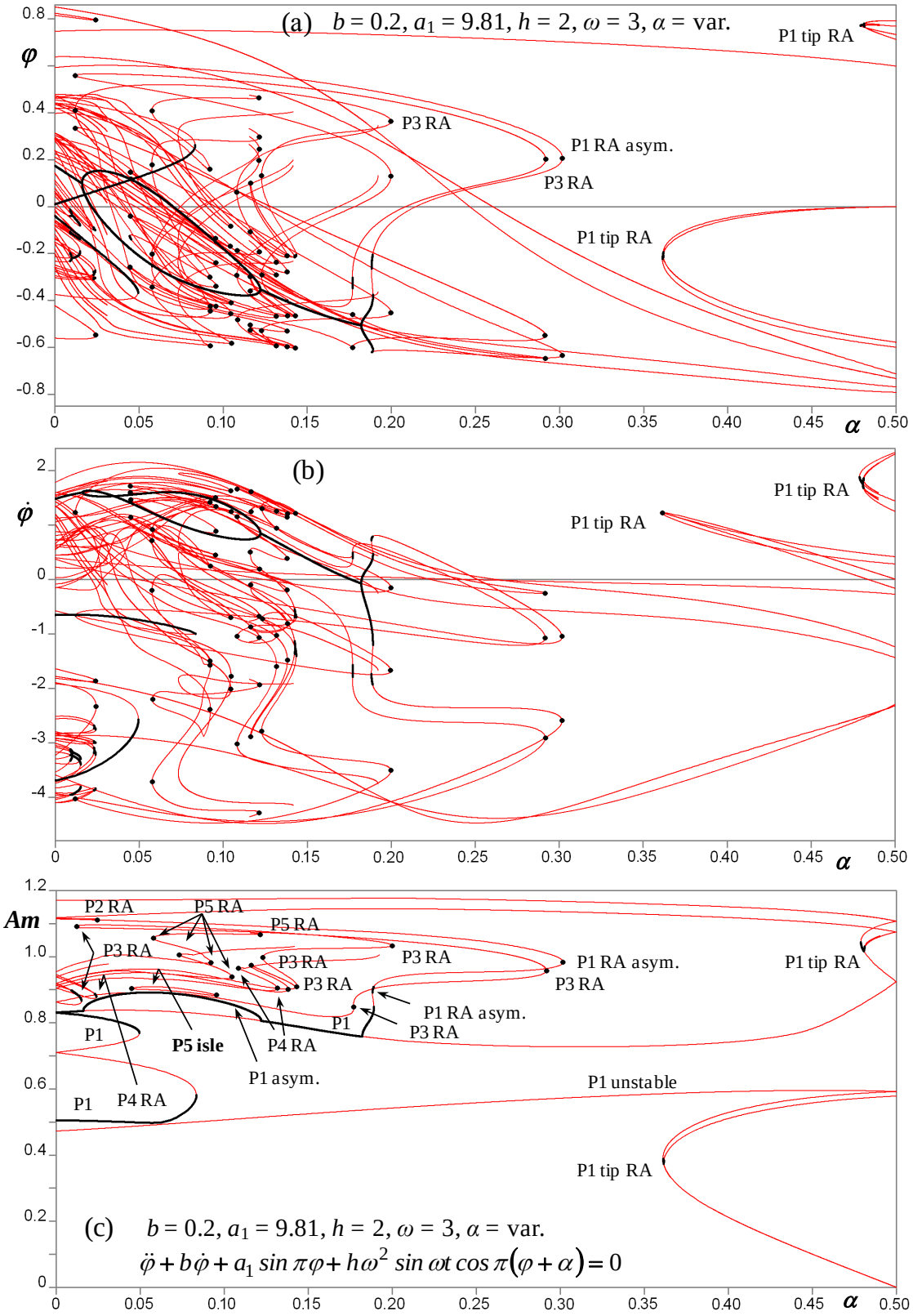

Fig. 3.35. Complex bifurcation diagrams for 15 different bifurcation groups for a pendulum system with the point of suspension vibrating at a certain angle α with respect to the horizontal (3.4). Many rare attractors, marked with black circles, have been found in the system. Inside each circle, there is a rare bifurcation subgroup with the period-doubling cascade and rare chaotic attractors. System parameters: $b = 0.2$, $a_1 = 9.81$, $h = 2$, $\omega = 3$, α = var.

In the second case the symmetric model only with vertical external force has 5 bifurcation groups (Fig.3.34): three 1T, one 2T and one 3T. Two brunches of P1 unstable zero twins near ω = 1.96 and ω = 2.13 are not completed, because of problem of sufficiently high instability with maximal value less than 2600.

The results received by the method of complete bifurcation groups show that there are stable hilltop solutions not only period-1, but more complicate subharmonic hilltop attractors, e.g. period-3, and hilltop chaotic attractors (see Fig.3.34). All bifurcation groups with rare attractors are of a tip kind and each of them has not only periodic attractors, but chaotic attractors as well. Fig.3.35 shows, that the direction α of the vibrating support is sufficient for global topology of the steady-state solutions of the system. Namely some subharmonical isles with rare attractors exist only for a case, where the support is vibrating under some angle α from 0.044 to 0.095.

It is shown that using of the method of complete bifurcation groups allows conducting the global bifurcation analysis of the periodically driven damped pendulum with the vibrating point of the support under some angle α from the horizontal direction to vertical direction, and finding new bifurcation groups with rare attractors and chaotic regimes. Some obtained new effects can be used for the parametric stabilization of unstable oscillations in technological processes or for other usages in the mechanics, mechanical engineering and other nonlinear dynamic systems.

3.6 The pendulum with external harmonic excitation

In contrast to the models discussed above, the following distinctive features, which can be seen in the bifurcation diagrams (Fig. 3.38 – 3.44), have been found in a pendulum system with external harmonic excitation (Fig. 3.36):

$$\ddot{\varphi} + b\dot{\varphi} + a_1 \sin \pi\varphi = h_1 \cos \omega t \qquad (3.5)$$

where φ – the angle of deviation, measured from the vertical; $\dot{\varphi}$ – the pendulum angular velocity, $\dot{\varphi} = d\varphi / dt$; $b\dot{\varphi}$ – the linear dissipative force; b – the linear dissipation coefficient; a_1 – the coefficient, which includes the pendulum length and gravitation constant; h_1 and ω – the amplitude and frequency of external harmonic excitation. All parameters of pendulum systems are dimensionless and normalized. For simplicity, the angle of a full pendulum turn is assumed to be equal to 2 in the given models. Close models have been examined in some works [15,23,29,53,54,55,61, etc.]. Some results of complete bifurcation analysis of the studied model have been examined in one of the previous works [99, 100, 138, 147, 149, 150].

The example of the construction of periodic skeleton in the pendulum system (3.5) for oscillating and rotating orbits (regimes, attractors) is shown in paragraph 2.5.

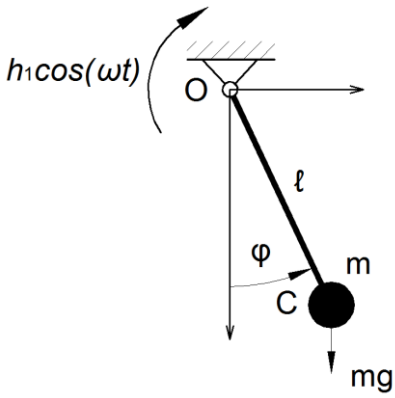

Fig. 3.36. The studied pendulum system with external harmonic excitation.

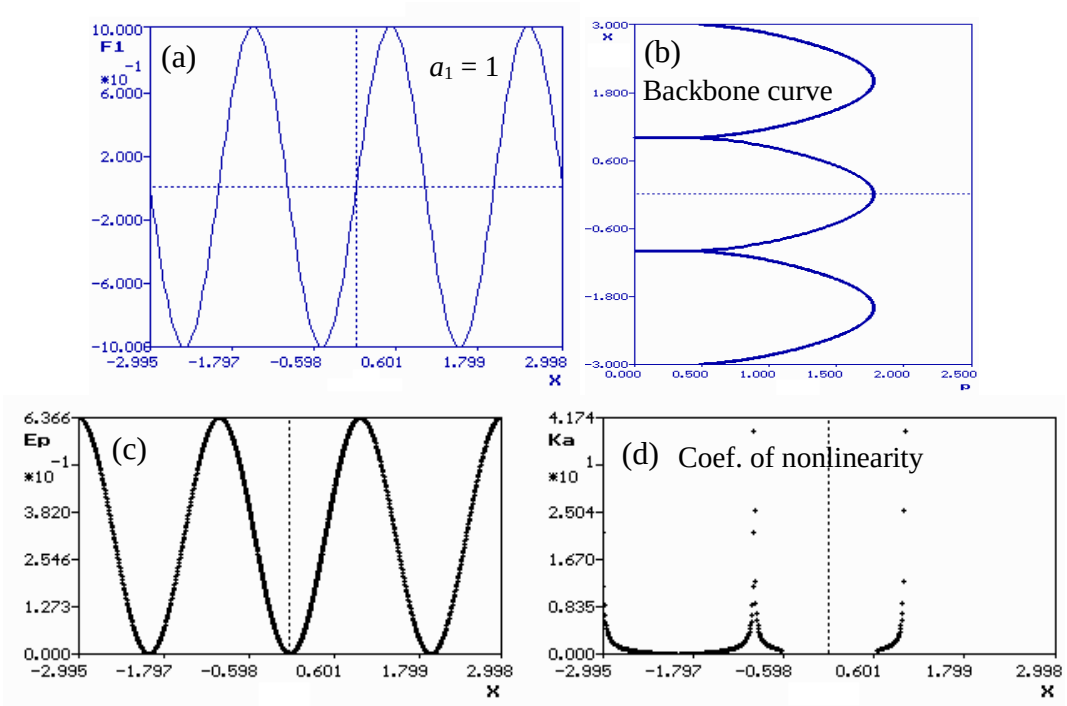

Fig. 3.37. Restoring force (a), backbone curves (b), potential well (c) and coefficient of nonlinearity $k_a = |dp/dA \cdot A/p|$ (d) for pendulum system with external harmonic excitation. Eq.: $\ddot{\varphi} + b\dot{\varphi} + a_1 \sin \pi\varphi = h_1 \cos \omega t$. Parameters: b = 0, a_1 = 1, h_1 = 0.

This paragraph includes a complete bifurcation analysis S1(ω) for the frequency ω of excitation force (in the diagrams coordinates of fixed points are defined by $\varphi = x = x_p$ and $\dot{\varphi} = v = \dot{x}_p$). Rare attractors and chaotic attractors and new nonlinear phenomena, such as new types of interaction of different types of oscillating and rotating orbits (rare subharmonic P2 twin attractors and subharmonic rotations R4, R6, R16), as well as rare and chaotic rotating regimes (usual P1 oscillating orbit and subharmonic rotational ChA-2 twin attractor) with the period of excitation or subharmonic have been found.

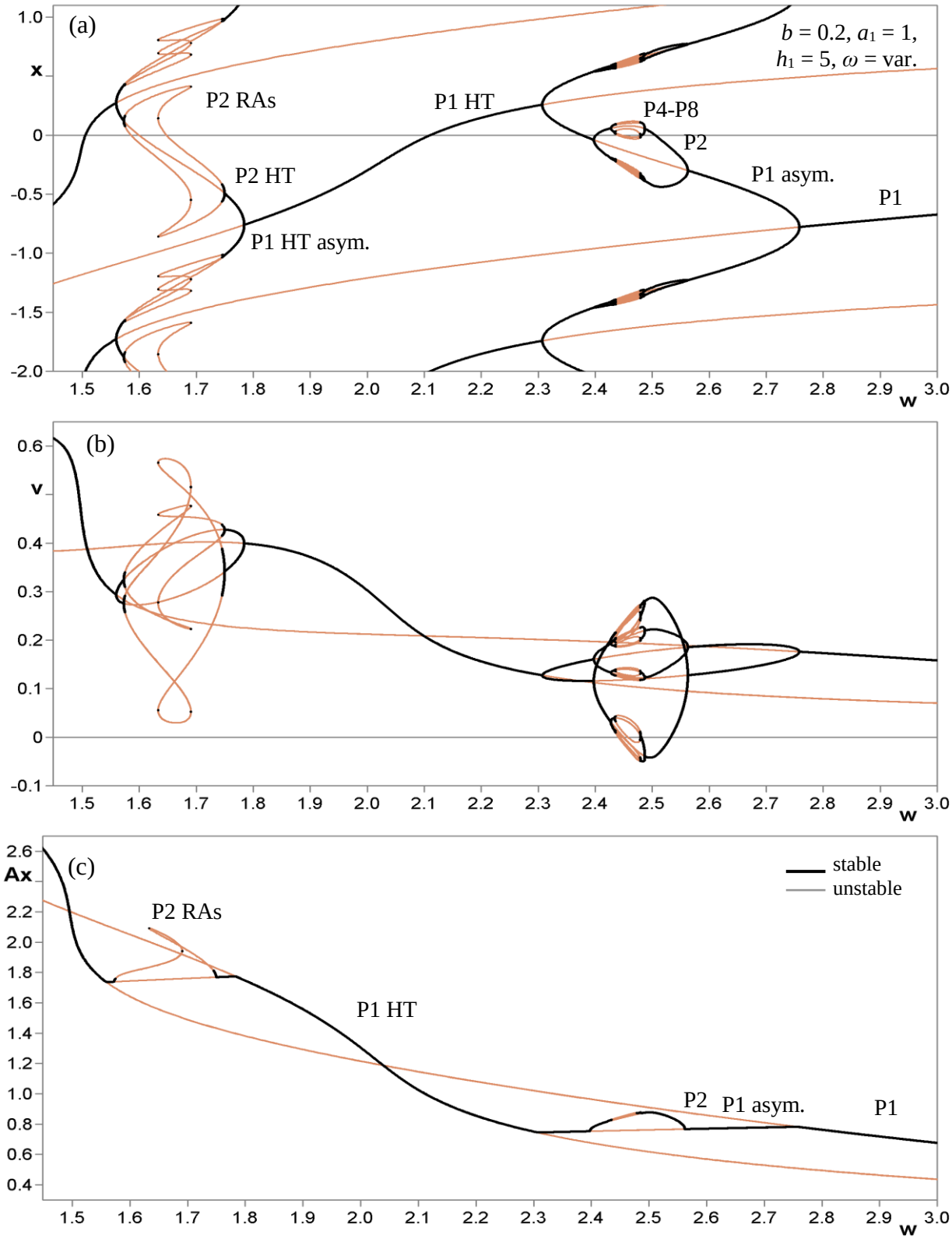

Fig. 3.38. Oscillating orbits on bifurcation diagrams S1(ω) of the fixed periodic points of the coordinates x, v and Am versus frequency ω of excitation force (in the diagrams coordinates of fixed points are defined by $\varphi = x = x_p$ and $\dot{\varphi} = v = \dot{x}_p$). There is one 1T bifurcation group (with P1, P2, P4 and P8 oscillating orbits) dependent form cyclic coordinate with complex protuberances, tip RAs and UPIs. Eq.: $\ddot{x} + b\dot{x} + a_1 \sin \pi x = h_1 \cos \omega t$. Parameters: b = 0.2, a_1 = 1, h_1 = 5, ω = var., k = 7.

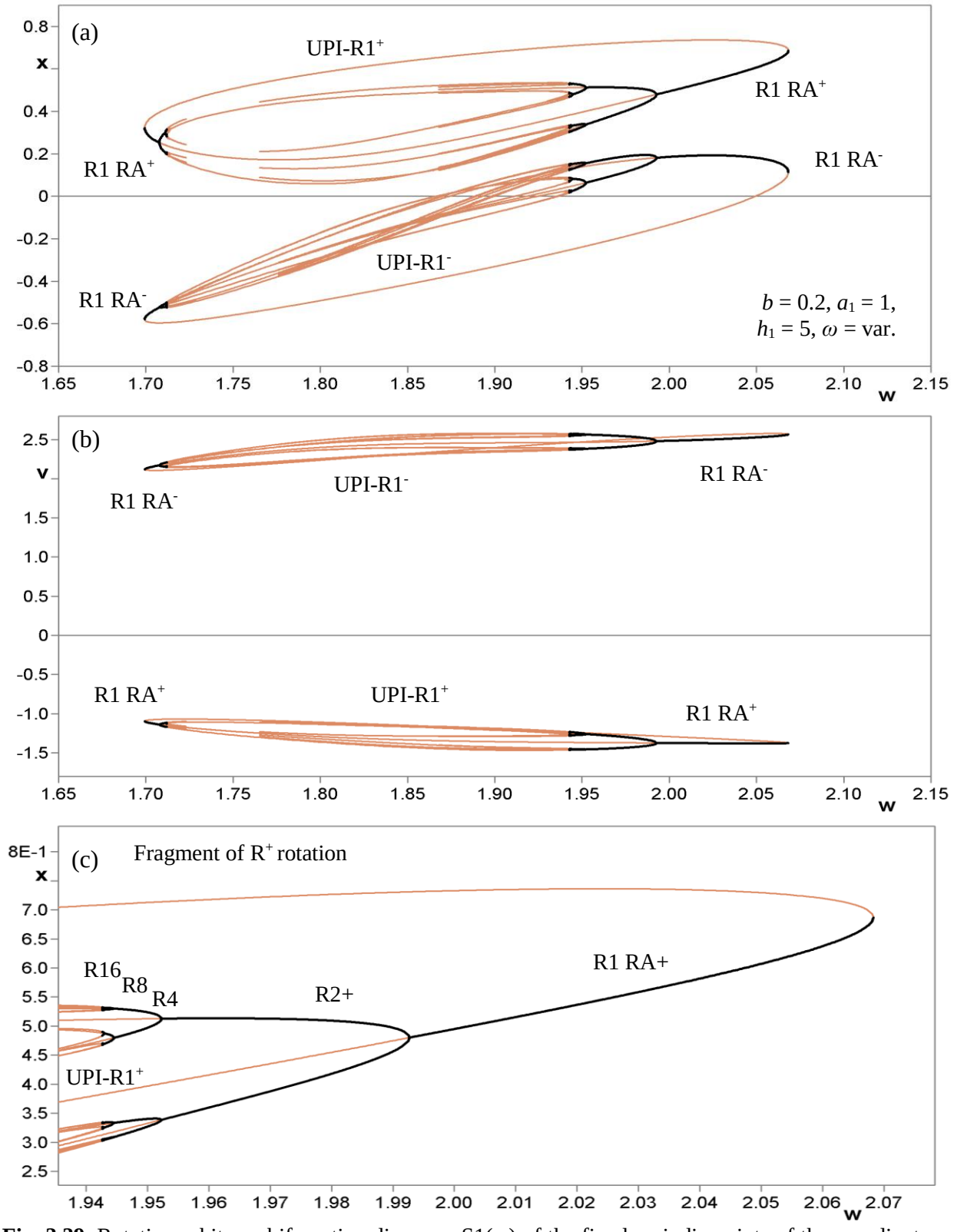

Fig. 3.39. Rotating orbits on bifurcation diagrams S1(ω) of the fixed periodic points of the coordinates x and v versus frequency ω of excitation force (in the diagrams coordinates of fixed points are defined by $\varphi = x = x_p$ and $\dot{\varphi} = v = \dot{x}_p$). There are two 1T bifurcation groups (with R1, R2, R4, R8 and R16 rotations) of rotating regimes with complex protuberances, tip RAs and UPIs. Eq.: $\ddot{x} + b\dot{x} + a_1 \sin \pi x = h_1 \cos \omega t$. Parameters: b = 0.2, a_1 = 1, h_1 = 5, ω = var., k = 7.

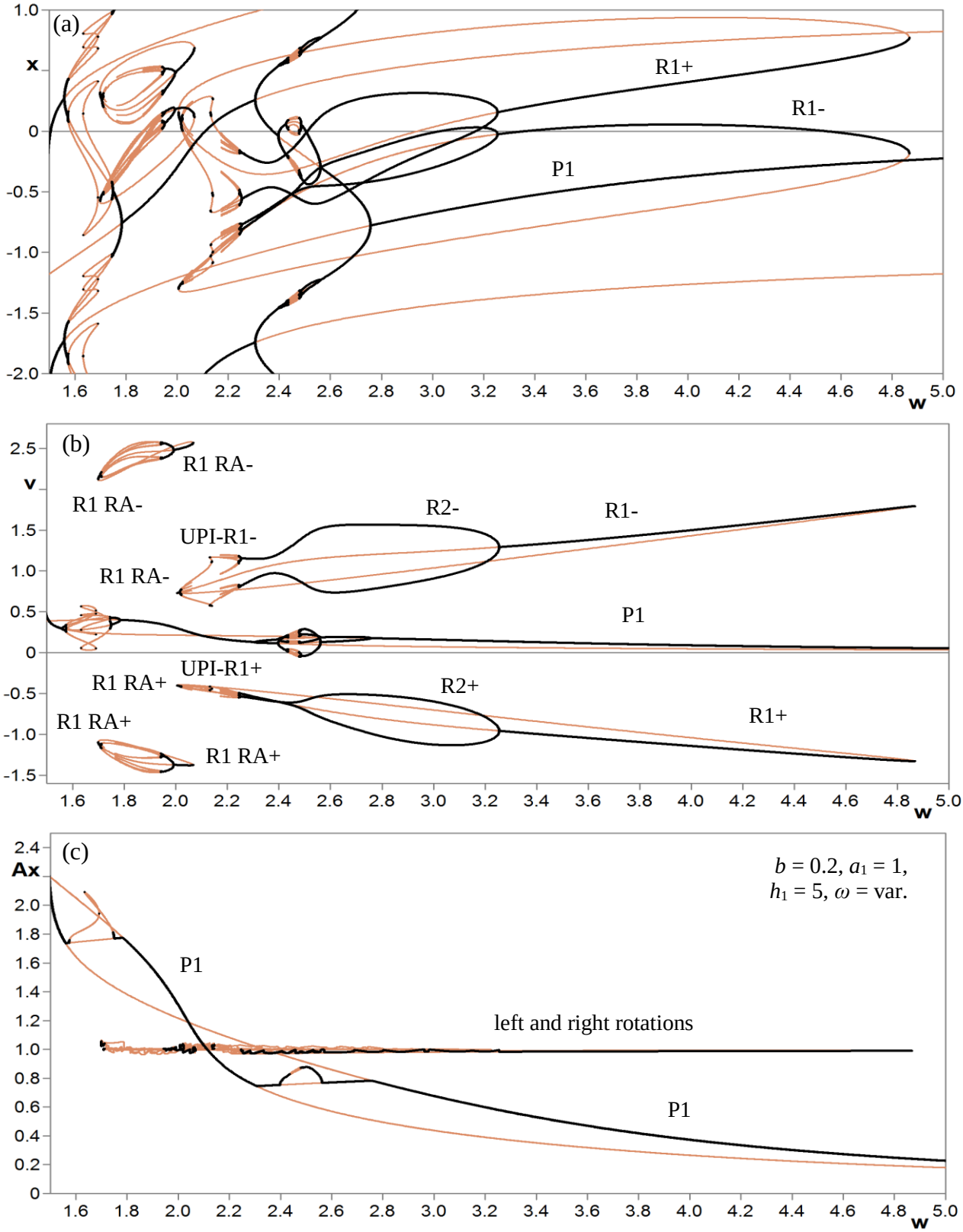

Fig. 3.40. Interaction of oscillating and rotating orbits on bifurcation diagrams of the fixed periodic points of the coordinates x and v versus frequency ω of excitation force (in the diagrams coordinates of fixed points are defined by $\varphi = x = x_p$ and $\dot{\varphi} = v = \dot{x}_p$). There are two 1T bifurcation groups (with R1, R2, R4, R8 and R16 rotations) of rotating regimes with complex protuberances, tip RAs and UPIs. Eq.: $\ddot{x} + b\dot{x} + a_1 \sin \pi x = h_1 \cos \omega t$. Parameters: b = 0.2, a_1 = 1, ω = var., h_1 = 5, k = 7.

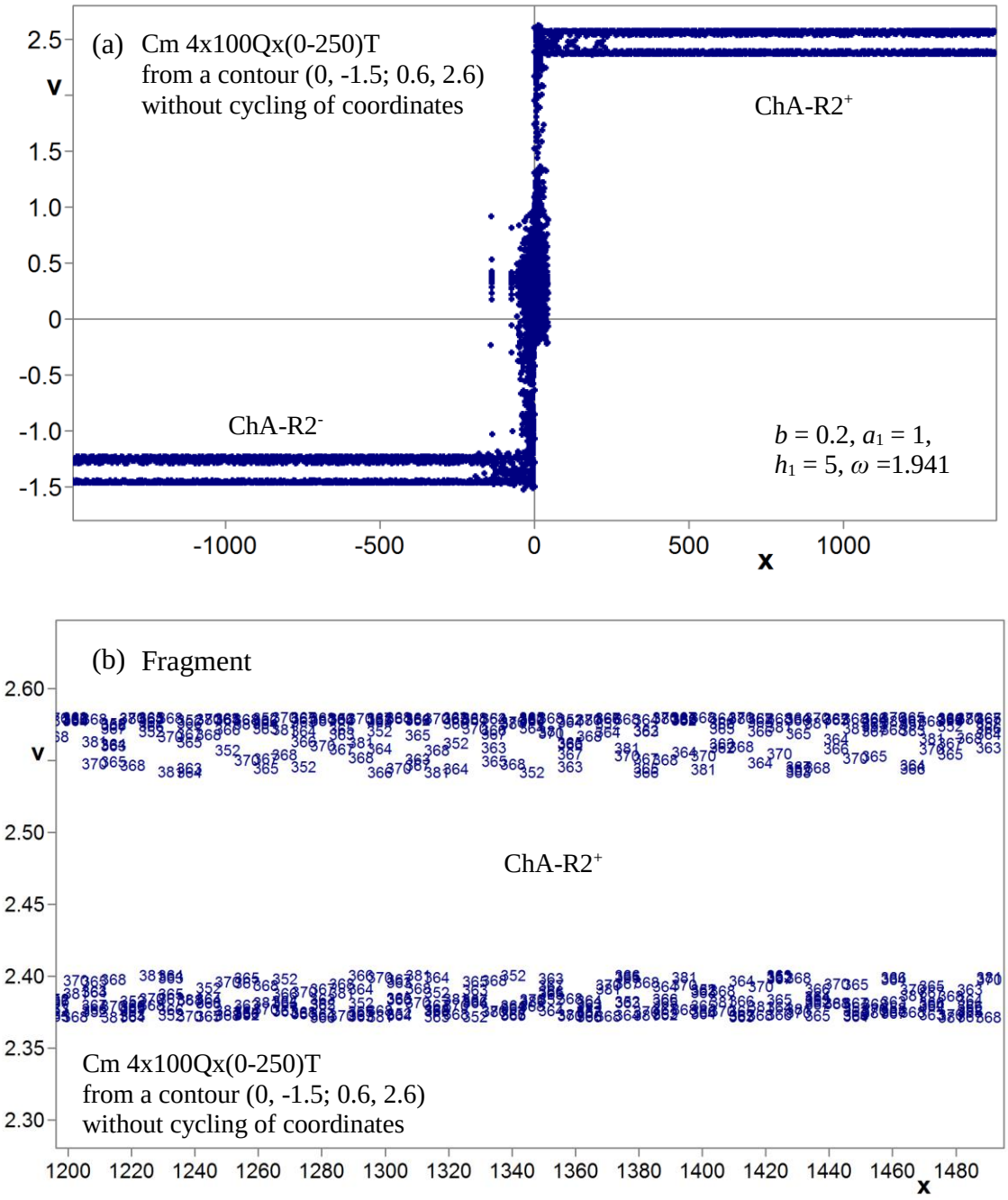

Fig. 3.41. Coexistence of usual P1 attractor and subharmonic rotational ChA-2 twin attractor on Poincaré map Cm 4x100Qx(0-250)T from a contour (0, -1.5; 0.6, 2.6) without taking into account the cycling of coordinates taking into account the cylindrical phase space with period Lx = 2. Except the periodic oscillating orbit the system has rotating subharmonic ChA-R2 twin attractors, which were formed through the cascade of period-doubling bifurcations of rare rotational R2 orbits (see bifurcation diagrams for 1T bifurcation groups shown on Fig. 3.39). Eq.: $\ddot{x} + b\dot{x} + a_1 \sin \pi x = h_1 \cos \omega t$. Parameters: b = 0.2, a_1 = 1, ω = 1.941, h_1 = 5, k = 7.

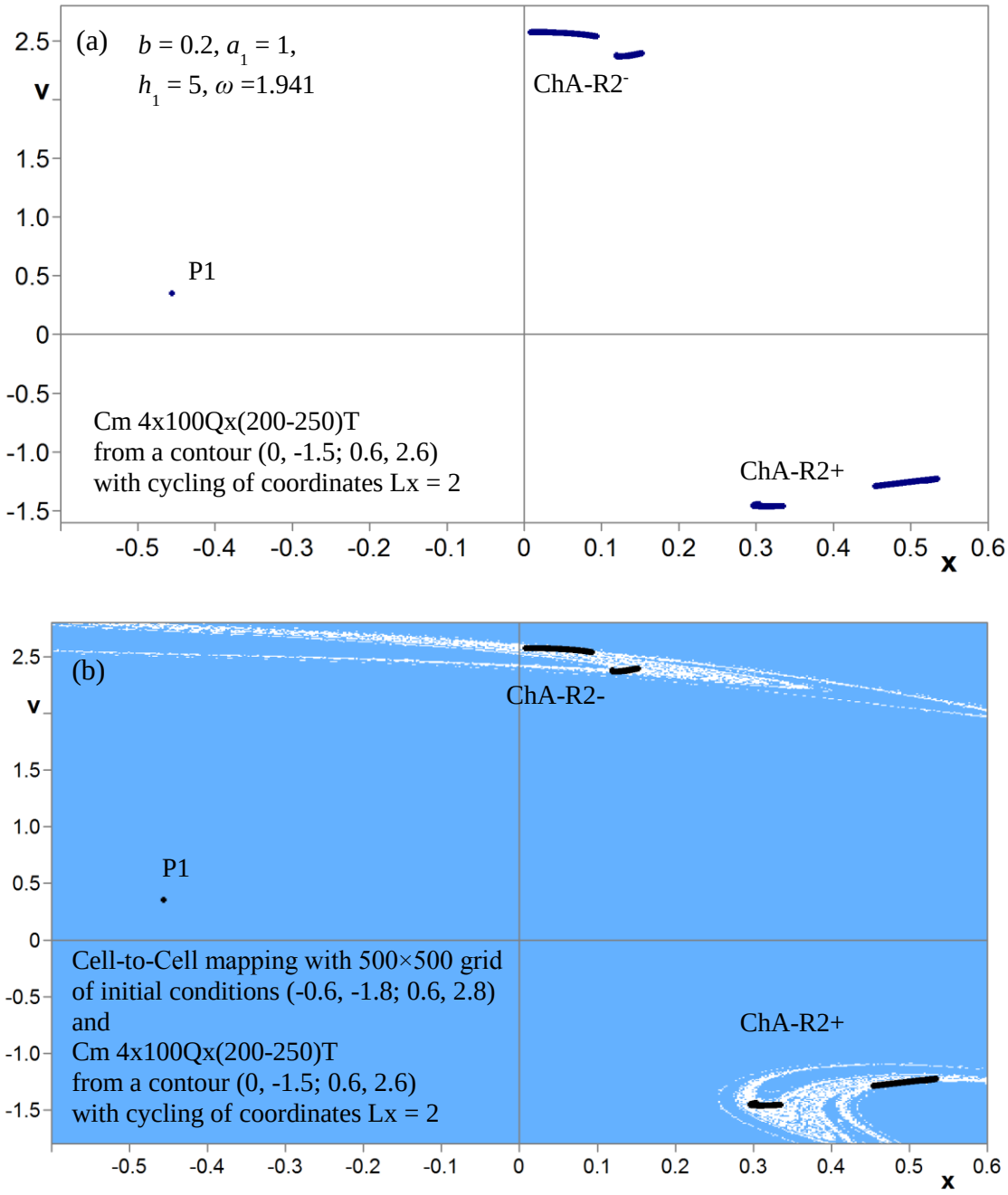

Fig. 3.42. (Continuation) Basins of attraction of coexistence of usual P1 attractor and subharmonic rotational ChA-2 twin attractor on Cell-to-Cell mapping with 500×500 grid of initial conditions (-0.6, -1.8; 0.6, 2.8) together with Poincaré map Cm 4x100Qx(200-250)T from a contour (0, -1.5; 0.6, 2.6) taking into account the cycling of coordinates. Except the periodic oscillating orbit the system has rotating subharmonic ChA-R2 twin attractors, which were formed through the cascade of period-doubling bifurcations of rare rotational R2 orbits (see bifurcation diagrams for 1T bifurcation groups shown on Fig.3.39). Parameters: $b = 0.2$, $a_1 = 1$, $\omega = 1.941$, $h_1 = 5$, $k = 7$.

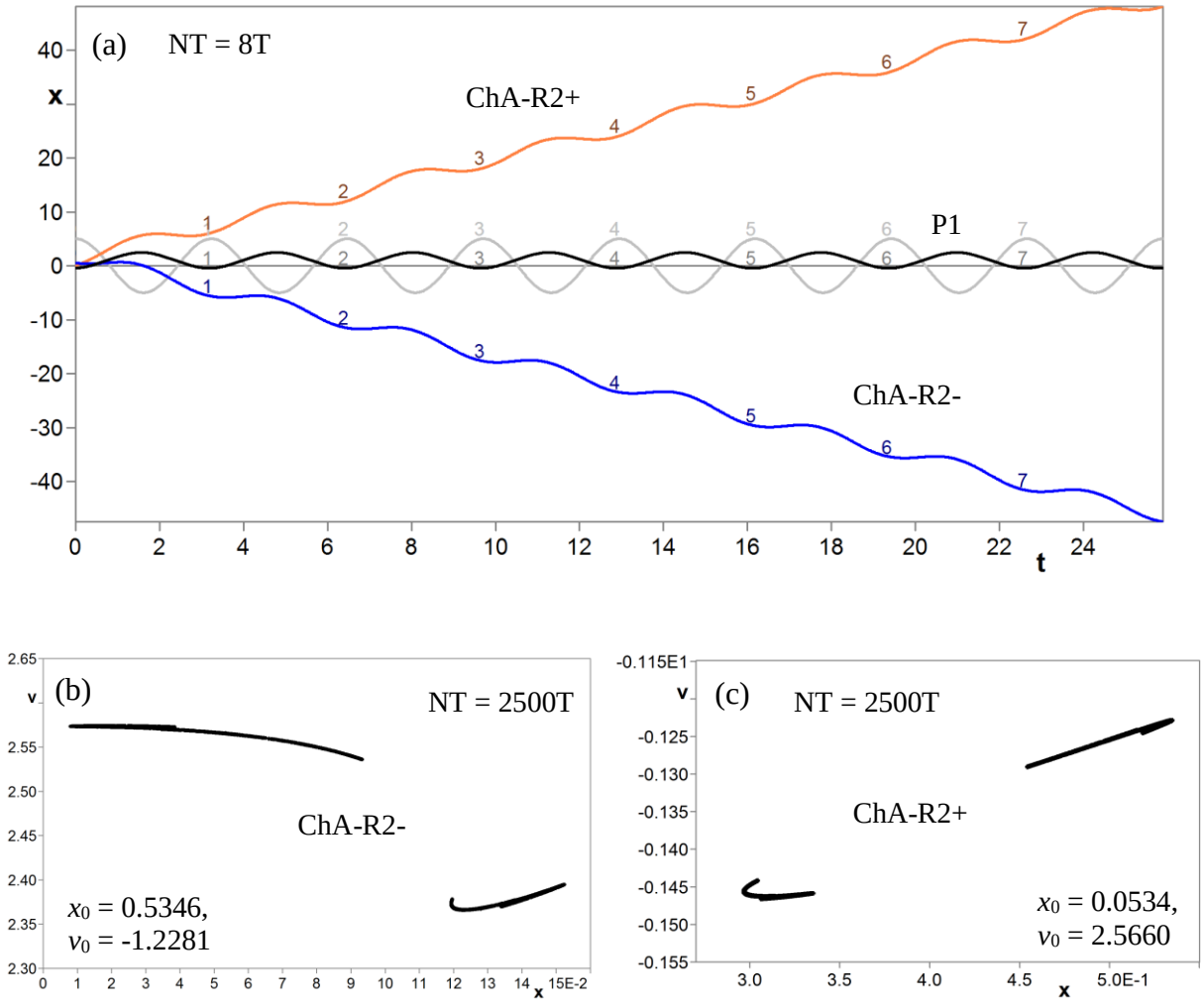

1	P1 (1/1)	-0.455840	0.349801	ρ_i = 0.723462, α = 177.9
2	ChA-R2-	x_0 = 0.534600	v_0 = -1.228100	—
3	ChA-R2+	x_0 = 0.053400	v_0 = 2.566000	—

Fig. 3.43. (a) Interaction of usual P1 attractor and subharmonic rotational ChA-2 twin attractors on time history diagram NT = 8T. Except the periodic oscillating orbit the system has rotating subharmonic ChA-R2 twin attractors (see Fig. 3.41). (b)-(c) Poincaré mappings during NT = 2500T for subharmonic chaotic ChA-R2 twin rotational attractors. Eq.: $\ddot{x} + b\dot{x} + a_1 \sin \pi x = h_1 \cos \omega t$. Parameters: b = 0.2, a_1 = 1, ω = 1.941, h_1 = 5, k = 7.

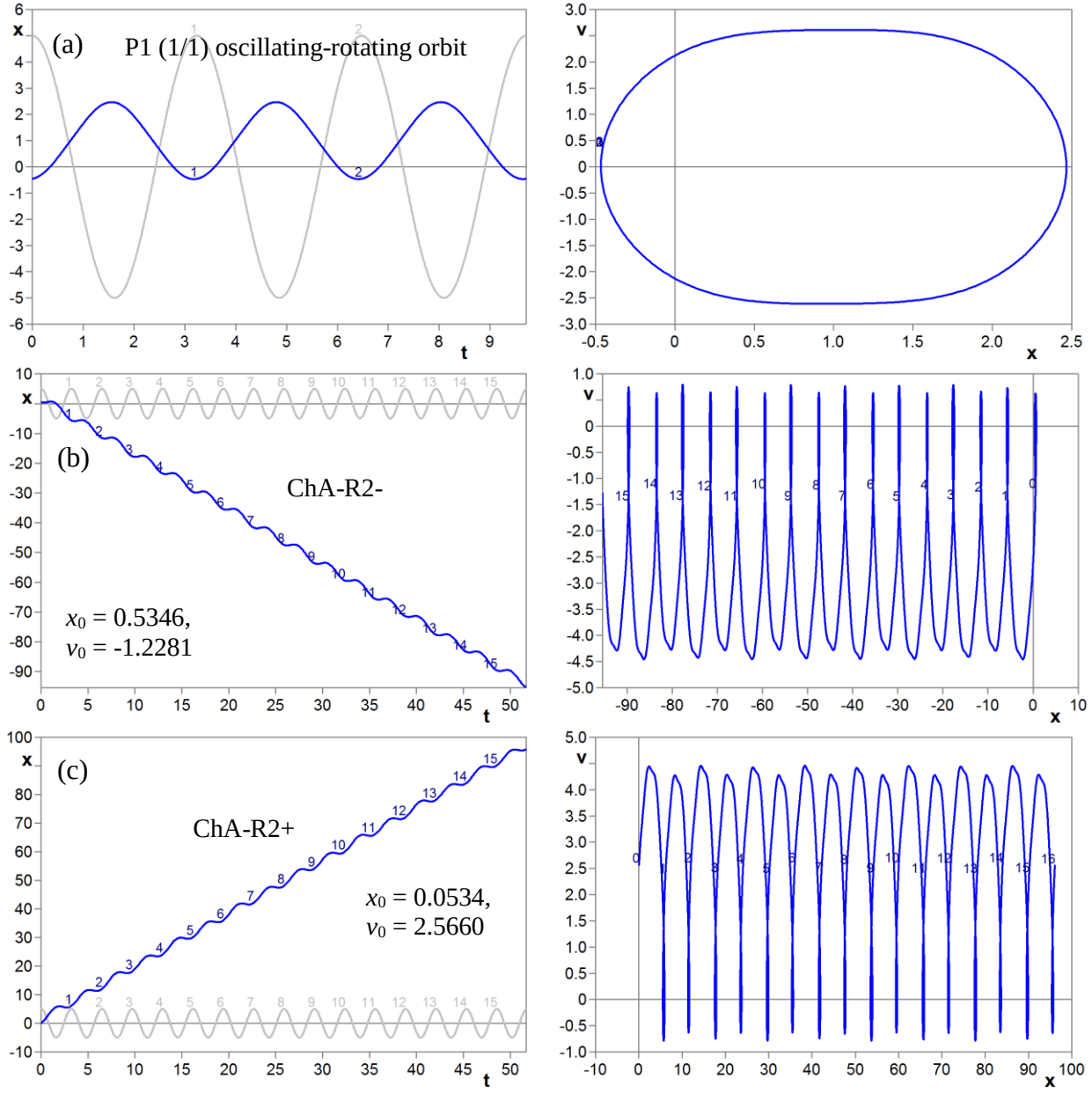

Fig. 3.44. (Continuation) Interaction of usual P1 (1/1) attractor and subharmonic rotating ChA-2 twin attractor on time history diagrams and phase portraits. Eq.: $\ddot{x} + b\dot{x} + a_1 \sin \pi x = h_1 \cos \omega t$. Parameters: b = 0.2, a_1 = 1, ω = 1.941, h_1 = 5, k = 7.

The process of formation of chaotic rotation [147,149,150] through the cascade of period-doubling bifurcations for different groups has also been studied within the framework of research. The interaction of oscillating and rotating orbits [149] in the pendulum system with external harmonic excitation will be demonstrated. The bifurcation diagrams S1(ω), phase portraits, mappings from a point and from a contour on Poincaré plane will be constructed. It is shown that in the considered models, except oscillating regimes, there are also the rotating and oscillating-rotating regimes.

Fig. 3.37 shows the restoring force, backbone curves, potential well and coefficient of nonlinearity $k_a = |dp/dA \cdot A/p|$ for the pendulum system with external harmonic excitation. There is one 1T bifurcation group (with P1, P2, P4 and P8 oscillating orbits) dependent form cyclic coordinate with complex protuberances, tip RAs and UPIs (Fig. 3.38).

The process of formation of chaotic rotation through the cascade of period-doubling bifurcations for the 1T bifurcation groups (with R1, R2, R4, R8 and R16 rotations) of rotating regimes with complex protuberances, tip RAs and UPIs (see Fig. 3.39). Interaction of oscillating and rotating orbits on bifurcation diagrams is shown on Fig. 3.40.

The coexistence of usual P1 attractor and subharmonic rotational ChA-2 twin attractor on Poincaré map Cm 4x100Qx(0-250)T from a contour (0, -1.5; 0.6, 2.6) without taking into account the cycling of coordinates taking into account the cylindrical phase space with period Lx = 2. Except the periodic oscillating orbit the system has rotating subharmonic ChA-R2 twin attractors, which were formed through the cascade of period-doubling bifurcations of rare rotational R2 orbits (see bifurcation diagrams for 1T bifurcation groups shown on Fig. 3.39). Basins of attraction of coexistence of usual P1 attractor and subharmonic rotational ChA-2 twin attractor on Cell-to-Cell mapping with 500×500 grid of initial conditions (-0.6, -1.8; 0.6, 2.8) together with Poincaré map Cm 4x100Qx(200-250)T from a contour (0, -1.5; 0.6, 2.6) taking into account the cycling of coordinates were shown on Fig.3.42. Except the periodic oscillating orbit the system has rotating subharmonic ChA-R2 twin attractors, which were formed through the cascade of period-doubling bifurcations of rare rotational R2 orbits (see bifurcation diagrams for 1T bifurcation groups shown on Fig.3.39).

Interaction of usual P1 attractor and subharmonic rotational ChA-2 twin attractors on time history diagram during NT = 8T is shown in Fig.3.43. Separately these orbits are shown on time history diagrams and phase portraits in Fig.3.44. The rotating subharmonic ChA-R2 twin attractors (see Figs. 3.41-3.42) are shown by the Poincaré mappings during NT = 2500T in Fig. 3.43(b, c).

Thereby the bifurcation diagrams with complex protuberances, phase portraits, basins of attraction and mappings from a contour on Poincaré plane were constructed.

Rare attractors and chaotic attractors and new nonlinear phenomena, such as new types of interaction of different types of oscillating and rotating orbits (rare subharmonic P2 twin attractors and subharmonic rotations R4, R6, R16), as well as rare and chaotic rotational regimes (usual P1 oscillating orbit and subharmonic rotational ChA-2 twin attractor) with the period of excitation or subharmonic have been found.

3.7 Rigid body pendulum with linear spring and several equilibrium positions

The present section includes a complete bifurcation analysis S*n*(*p*) for the longitudinal excitation force amplitude *p* (in the diagrams coordinates of fixed points are defined by $\beta = \beta_p$ and $\dot{\beta} = \dot{\beta}_p$). In previous sections it was shown, that the global bifurcation analysis based on new bifurcation theory and using the method of complete bifurcation groups helps finding new rare regular and chaotic oscillating, rotating and oscillating-rotating regimes. In this chapter the considered rigid body pendulum, except for torsional spring, has the linear spring that is connected to the end of the pendulum. Close model was investigated in the works [30, 31]. Some results of complete bifurcation analysis of the studied model have been examined in work [149].

Periodic skeleton was constructed for the rigid body pendulum with linear spring and several equilibrium positions. The coexistence of different types of oscillating, rotating and oscillating-rotating orbits (rare subharmonic P6 attractor, other different regular periodic oscillating regimes P*n*, different types of rotations R*n* and subharmonic oscillating-rotating orbits OR6, OR10 and OR13).

The collection of basins of attraction of bifurcation diagrams was shown for illustrating the system's behaviour with varying the longitudinal excitation force amplitude *p*.

The studied pendulum system with linear spring and several equilibrium positions is shown on Fig.3.45, where β is the angle of rotation, $f(\beta)$ is torsional restoring force, *c* the stiffness coefficient of the linear spring, *H* the length of the pendulum, *L* the horizontal distance between the end *B* of the pendulum and the extreme point of the spring *A*, *p* and *q* are the longitudinal and lateral excitation forces accordingly.

The equation of motion of studied pendulum system in dimensionless form is

$$\ddot{\beta} + c\dot{\beta} + f(\beta) - p\sin\beta + \left[1 - \frac{1}{\sqrt{1+\alpha\sin\beta}} - (q_0 + q_1\sin\omega t)\right]\cos\beta = 0, \qquad (3.6)$$

where $f(\beta) = k_0 + k_1\beta + k_2\beta^2 + k_3\beta^3$ and k_i - the stiffness coefficients of the torsional spring; α is the geometrical coefficient which depends from the length of the pendulum *H* and the horizontal distance *L*; q_0 is an offset of amplitude of excitation force; ω is the frequency of external excitation force.

In this paragraph the torsional restoring force $f(\beta)$ will be equal to 0. The same model was investigated in the works [30, 31].

The example of the construction of periodic skeleton (PSK) in studied pendulum system with linear spring and several equilibrium positions (3.6) for oscillating and rotating orbits (regimes, attractors) with order n = (1-16)T (see Table. 3.1) by using the Newton-Kantorovich method from the grid of initial conditions NQ = 25×25Q = 625Q inside the rectangle ($-\pi$, -1.5; π, 1.5) is shown. The maximum number of iterations is KIN = 64 with precision search of the fixed point EPN = 1e-6 and parameter of discretisation DEN = 1e-5. Active boundaries are x_{min} = - π, x_{max} = π, v_{min} = -10, v_{max} = 10. For rotational orbits the cylindrical phase space was taken into account with period $L_\beta = 2\pi$. Time of calculation of periodic skeleton was about 1 hour 20 minutes (the PC characteristics: Intel(R) Core(TM) i3-2120, CPU - 3.30GHz, RAM - 4 GB, Windows 7 SP1).

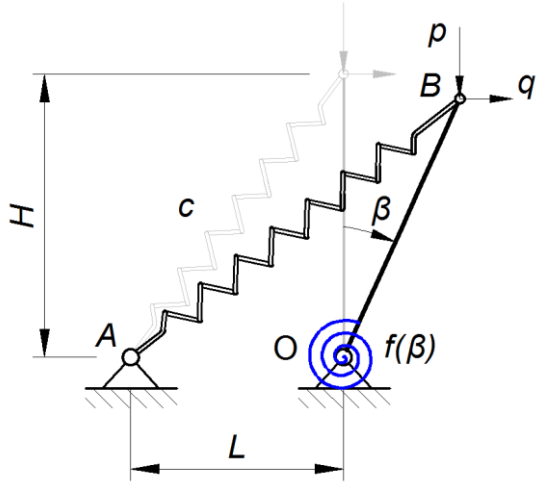

Fig. 3.45. The studied rigid body pendulum system with linear spring and several equilibrium positions.

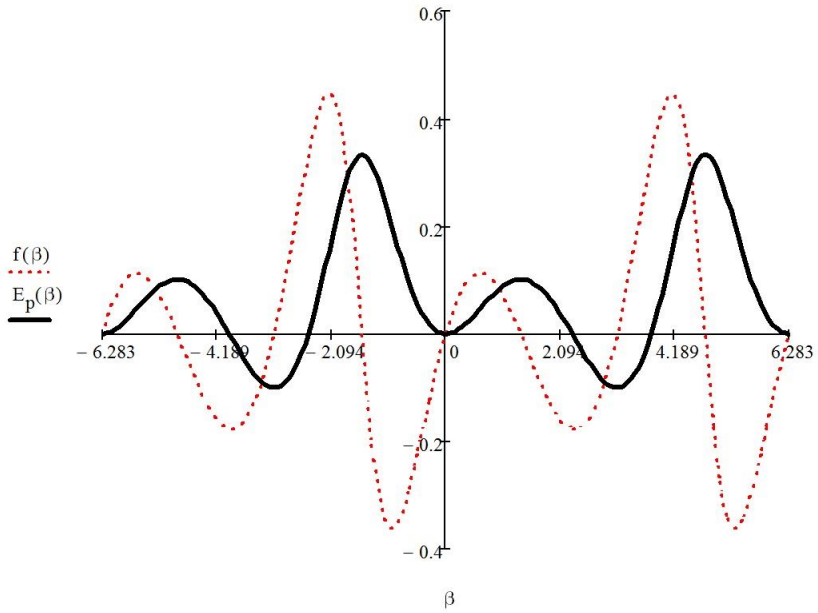

Fig. 3.46. Restoring force $f(\beta)$ and potential well $E_p(\beta)$. These curves underline the 2π periodicity with respect to β.

Table 3.1. Periodic skeleton consists of 101 oscillating and rotating orbits (regimes, attractors), among them are five stable regimes (two P1, R1+, R1- and P6 which is the period doubling of P3) and other unstable regimes (different types o oscillating P*n* and rotating orbits R*n* and four oscillating-rotating OR*n*) for the base parameters of the studied pendulum system with linear spring and several equilibrium positions. The base parameters: $c = 0.01$, $q_0 = 0.01$, $a = 0.8$, $p = 0.05$, $\omega = 0.8$, $q_1 = 0.05$, $k = 7$.

N	Orbits	β	$\dot{\beta}$	ρ_1	ρ_2	α	Bif.group
1.	R1 u-	-0.585939	-0.86374	3.745	0.247	0°	R1 -
2.	R1 s-	-2.497295	-0.911182	0.961	0.961	160.1°	R1 -
3.	P1 (1/1) s	0.036278	-0.127843	0.961	0.961	211.4°	1T (β=0)
4.	R1 s+	-0.595455	0.832939	0.962	0.962	160.3°	R1 +
5.	P1 (1/1) s	3.109178	0.185429	0.961	0.961	142.3°	1T(β=π)
6.	R1 u+	-2.504114	0.93539	3.749	0.246	0°	R1 +
7.	P1 (1/1) u HT	1.365171	-0.009294	44.55	0.021	0°	1T HT
8.	P2 (1/2) u	-0.211737	-0.450565	-0.065	-12.96	0°	1T (β=0)
9.	P2 (1/2) u	1.754762	0.137929	19.57	0.044	0°	1T (β= π)
10.	P2 (1/2) u	-0.252706	0.277075	10.50	0.081	0°	1T (β=0)
11.	P2 (1/2) u	1.666397	-0.09969	-0.041	-20.91	0°	1T (β=π)
12.	P3 u	-0.174072	-0.577977	-0.079	-10.05	0°	
13.	P3	-1.512201	-0.114262	0.001	-1392	180°	
14.	P3	0.337261	-0.614093	13.92	0.057	0°	
15.	P3	1.451579	-0.26293	-0.410	-1.928	0°	
16.	P3	-0.606221	0.270325	-0.435	-1.905	0°	
17.	P3	1.578892	-0.2458	6.468	0.122	0°	
18.	P3	-1.357123	-0.188566	306.0	0.004	0°	
19.	P3	-3.091269	-0.434448	-0.630	-1.253	0°	
20.	P3	-2.488326	0.049483	5.138	0.154	0°	
21.	P3 u	2.848215	-0.334384	5.139	0.154	0°	3T
22.	P3	1.309345	-0.032703	0.005	-707.2	180°	
23.	P3	-1.734824	0.225193	190.2	0.002	0°	
24.	P3	1.425309	-0.030425	884.8	0.003	0°	
25.	P3	0.337274	-0.614093	13.92	0.057	0°	
26.	P4 (1/4) u	0.140326	-0.561378	0.042	-308.1	180°	4T (2)
27.	P4 (2/4) u	0.203109	-0.451581	-0.013	-67.82	0°	1T (β=0)
28.	P4 (1/4) u	1.563273	-0.150578	515.2	-0.015	180°	4T (3)
29.	P4	1.472688	-0.020768	-0.002	-297.9	0°	
30.	P4 (1/4) u	1.396862	0.044483	-0.002	-259.2	0°	4T (3)
31.	P4 (1/4) u	1.455768	0.047283	306.1	0.003	0°	4T (2)
32.	P4 (1/4) u	1.642483	0.182567	206.6	0.004	0°	4T (1)
33.	P5	-1.714984	-0.290741	7.207	0.094	0°	
34.	P5	1.517236	0.212342	43.74	0.015	0°	
35.	P5	-1.650121	-0.150292	-0.007	-91.32	0°	
36.	P5	-0.543832	0.243715	-0.164	-38.80	0°	
37.	P5	1.446868	-0.174547	-0.008	-88.70	0°	
38.	P5	-2.721118	-0.519868	-0.007	-22.10	0°	
39.	P5	-1.613165	-0.523948	7.207	0.094	0°	
40.	P5	2.015245	0.263052	63.31	0.011	0°	
41.	P5	-1.330497	0.293888	7.603	0.089	0°	
42.	P5	1.440011	-0.120121	50.73	0.013	0°	
43.	P5	-1.832256	0.556424	0.011	-98.98	180°	
44.	P5	1.797907	-0.146099	76.68	0.007	0°	

Table 3.2. (Continuation 1 of Table 3.1) Periodic skeleton consists of 101 oscillating and rotating orbits (regimes, attractors), among them are five stable regimes (two P1, R1+, R1- and P6 which is the period doubling of P3) and other unstable regimes (different types of oscillating P*n* and rotating orbits R*n* and four oscillating-rotating OR*n*) for the base parameters of the studied pendulum system with linear spring and several equilibrium positions. The base parameters: $c = 0.01$, $q_0 = 0.01$, $a = 0.8$, $p = 0.05$, $\omega = 0.8$, $q_1 = 0.05$, $k = 7$.

N	Orbits	β	$\dot{\beta}$	ρ_1	ρ_2	α	Bif.group
45.	P5	-1.685008	0.293164	545.9	0.006	0°	
46.	R6 u-	-1.588768	-0.163273	92.28	0.007	0°	R6
47.	OR6 u+	1.479956	-0.246998	-0.261	-2.395	0°	
48.	P6 u	1.226772	0.005186	976.8	0.034	0°	
49.	P6	-1.434939	0.116515	-0.008	-756.6	0°	
50.	P6	-1.459596	0.164477	97.79	0.006	0°	
51.	P6	0.018571	-0.662248	0.008	-128.8	180°	
52.	P6	1.36762	-0.053579	3205.	0.064	0°	
53.	P6 (4/6) s	1.992033	0.107937	0.790	0.790	106.1°	3T
54.	P6	1.282022	0.014798	-0.002	-239.9	0°	
55.	P6	1.459469	-0.015492	0.040	-5599	180°	
56.	P7	-0.906797	-0.762434	480.4	0.258	0°	
57.	P7	0.785917	0.024167	525.8	0.126	0°	
58.	P7	1.369121	0.06738	248.0	0.003	0°	
59.	P7	1.904612	-0.046972	320.0	-0.014	180°	
60.	P7	1.612184	0.186994	-0.002	-238.5	0°	
61.	P7	1.135842	-0.183418	507.1	0.001	0°	
62.	P7	1.152732	0.014724	241.3	0.020	0°	
63.	P7	1.669328	-0.092918	1965	-0.381	180°	
64.	P7	1.46606	-0.092948	59.77	0.011	0°	
65.	P7	1.376409	0.074823	-0.001	-270.9	0°	
66.	P7	1.770354	0.142784	1188	-0.006	180°	
67.	P7	-1.481232	0.142261	509.0	0.002	0°	
68.	P7	1.849287	0.029214	-0.049	-791.6	0°	
69.	P7	1.543291	0.014814	-0.018	-2076	0°	
70.	P8	-0.175697	-0.600145	184.1	-0.0003	180°	
71.	P8	2.780972	-0.336747	-0.057	-174.2	0°	
72.	P8	1.487654	-0.122763	-0.005	-166.9	0°	
73.	P9	3.127835	-0.371776	-0.021	-24.09	0°	
74.	P9	1.420652	-0.062069	348.7	-0.001	180°	
75.	P9	1.384155	0.058916	2508	0.073	0°	
76.	P9	1.97555	0.127727	9.477	0.052	0°	
77.	P9	1.432084	-0.288305	-0.009	-57.88	0°	
78.	OR10 (1/10) u -	-1.774454	-0.231528	4.209	0.108	0°	OR10
79.	P10	-1.466065	-0.46202	4.209	0.108	0°	
80.	P10	-1.865119	0.580428	0.336	-489.3	180°	
81.	P10	-1.065249	0.401875	4.208	0.109	0°	
82.	OR10 (1/10) u-	-1.318986	-0.501562	-0.019	-33.76	0°	OR10
83.	P10	1.342841	-0.09676	0.001	-526.4	180°	
84.	P10	1.987711	-0.10414	-0.549	-1452	0°	
85.	P10	-1.681237	-0.149903	2658	0.055	0°	
86.	P10	1.250085	0.100281	-0.069	-427.6	0°	
87.	P10	-1.747881	0.499274	0.028	-87.91	180°	

Table 3.3. (Continuation 2 of Table 3.1) Periodic skeleton consists of 101 oscillating and rotating orbits (regimes, attractors), among them are five stable regimes (two P1, R1+, R1- and P6 which is the period doubling of P3) and other unstable regimes (different types of oscillating P*n* and rotating orbits R*n* and four oscillating-rotating OR*n*) for the base parameters of the studied pendulum system with linear spring and several equilibrium positions. The base parameters: c = 0.01, q_0 = 0.01, a = 0.8, p = 0.05, ω = 0.8, q_1 = 0.05, k = 7.

N	Orbits	β	$\dot{\beta}$	ρ_1	ρ_2	α	Bif.group
88.	P11	-1.339383	-0.628329	-0.529	-1226	0°	
89.	P11	1.55267	0.128264	318.5	0.001	0°	
90.	P11	-1.657079	-0.117144	258.8	0.002	0°	
91.	P11	-1.762392	0.637494	152.1	0.008	0°	
92.	P11	2.07299	0.234941	857.3	0.017	0°	
93.	P12	-0.780396	0.941169	-3.793	-460.8	0°	
94.	P12	1.942415	0.148414	87.35	0.003	0°	
95.	P12	1.096761	-0.058909	2927	-0.055	180°	
96.	OR13 u	-1.209325	-0.668096	293.0	0.010	0°	
97.	P13	1.573369	-0.096447	-0.964	-4180	0°	
98.	P13	0.379328	0.228023	298.6	0.018	0°	
99.	P14	1.636651	0.057129	-0.002	-1634	0°	
100.	P15	1.937202	0.152024	502.5	-0.023	180°	
101.	P16 (8/16) u	1.061444	-0.117872	2075	0.011	0°	

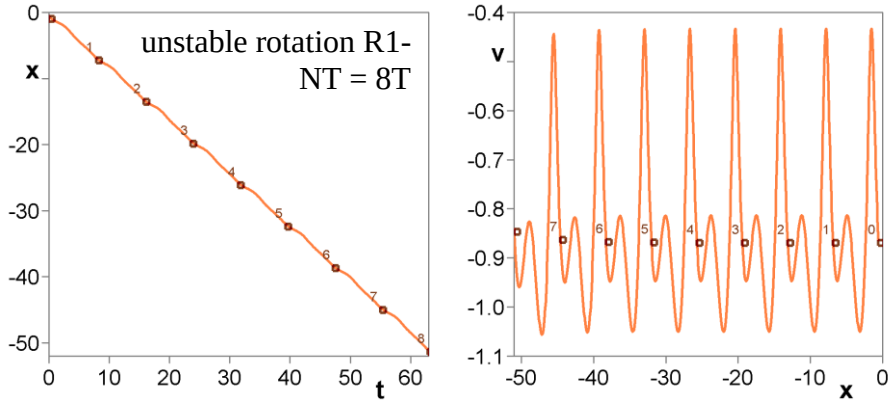

(a) R1 *u*- (-0.585939; -0.86374), ρ_1 = 3.745; ρ_2 = 0.247; α = 0°, bif. goup: R1 -.

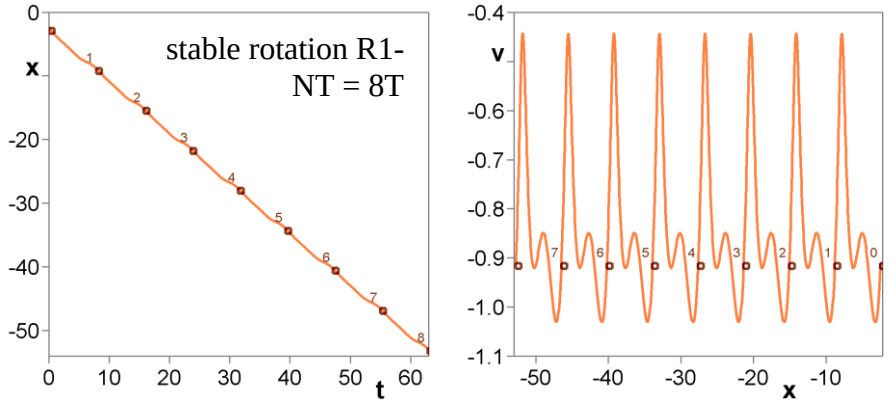

(b) R1 *s*- (-2.497295; -0.911182), ρ_1 = 0.961; ρ_2 = 0.961; α = 160.1°, bif. goup: R1 -.

Fig. 3.47. Time histories and phase portraits for the stable and unstable R1 left rotations in the studied pendulum system (3.6) with linear spring and several equilibrium positions. Parameters: c = 0.01, q_0 = 0.01, a = 0.8, p = 0.05, ω = 0.8, q_1 = 0.05, k = 7.

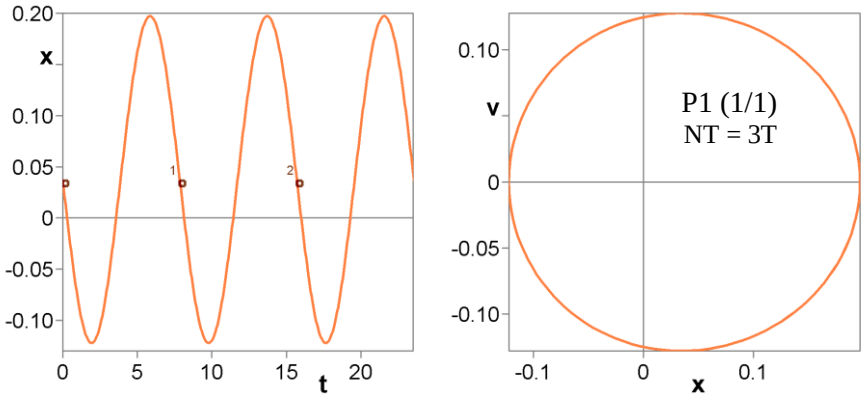

(c) P1 (1/1) s (0.036278; -0.127843), $\rho_1 = 0.961$; $\rho_2 = 0.961$; $\alpha = 211.4°$, bif. goup: 1T ($\beta = 0$).

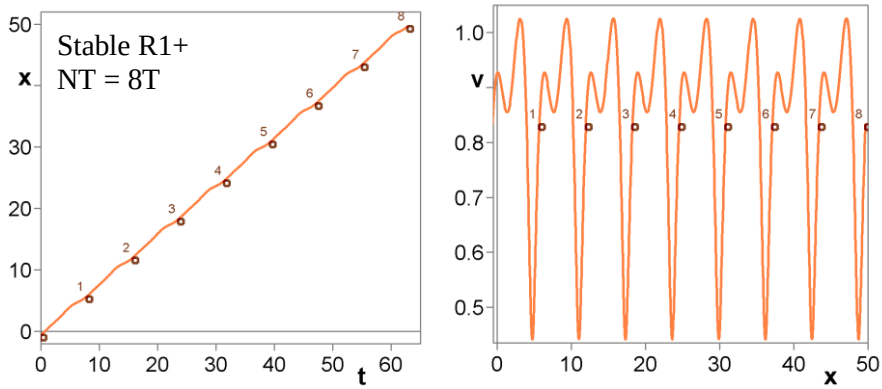

(d) R1 s+ (-0.595455; 0.832939), $\rho_1 = 0.962$; $\rho_2 = 0.962$; $\alpha = 160.3°$, bif. goup: R1 +.

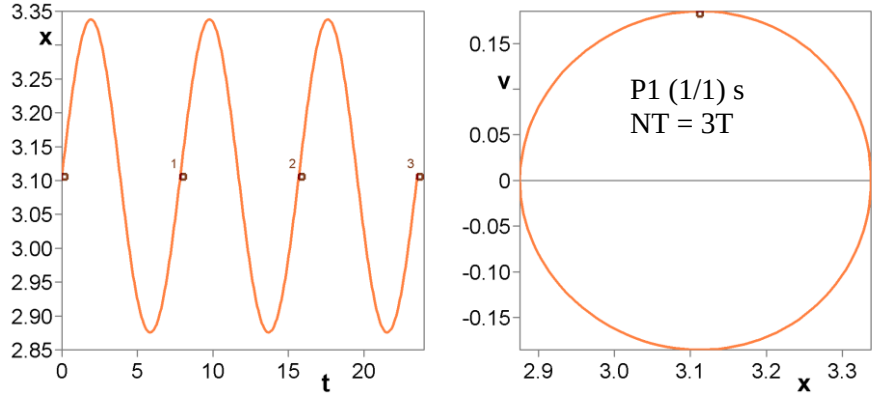

(e) P1 (1/1) s (3.109178; 0.185429), $\rho_1 = 0.961$; $\rho_2 = 0.961$; $\alpha = 142.3°$, bif. goup: 1T ($\beta=\pi$).

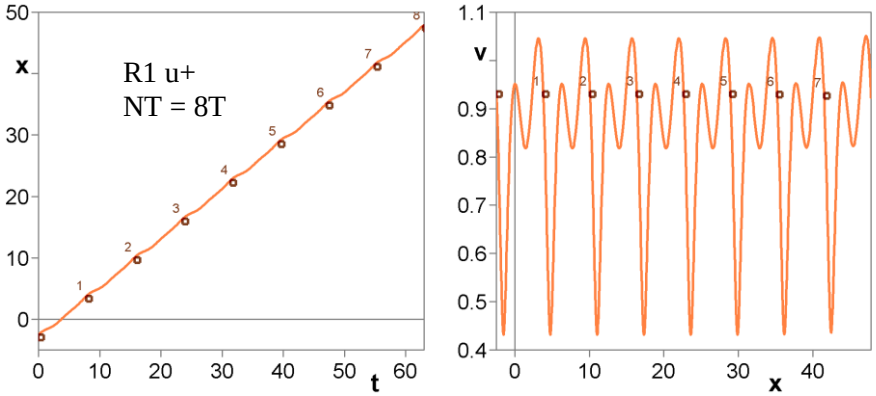

(f) R1 u+ (-2.504114; 0.93539), $\rho_1 = 3.749$; $\rho_2 = 0.246$; $\alpha = 0.0$ bif. goup: R1 +.

Fig. 3.48. Time histories and phase portraits for the two stable P1 oscillating attractors, for the stable and unstable R1 right rotations in the studied pendulum system (3.6) with linear spring and several equilibrium positions. Parameters: $c = 0.01$, $q_0 = 0.01$, $a = 0.8$, $p = 0.05$, $\omega = 0.8$, $q_1 = 0.05$, $k = 7$.

Previously the periodic skeleton for the rigid body pendulum system with linear spring and several equilibrium positions was constructed and it will be used for performing the global bifurcation analysis in this section by the method of complete bifurcation groups.

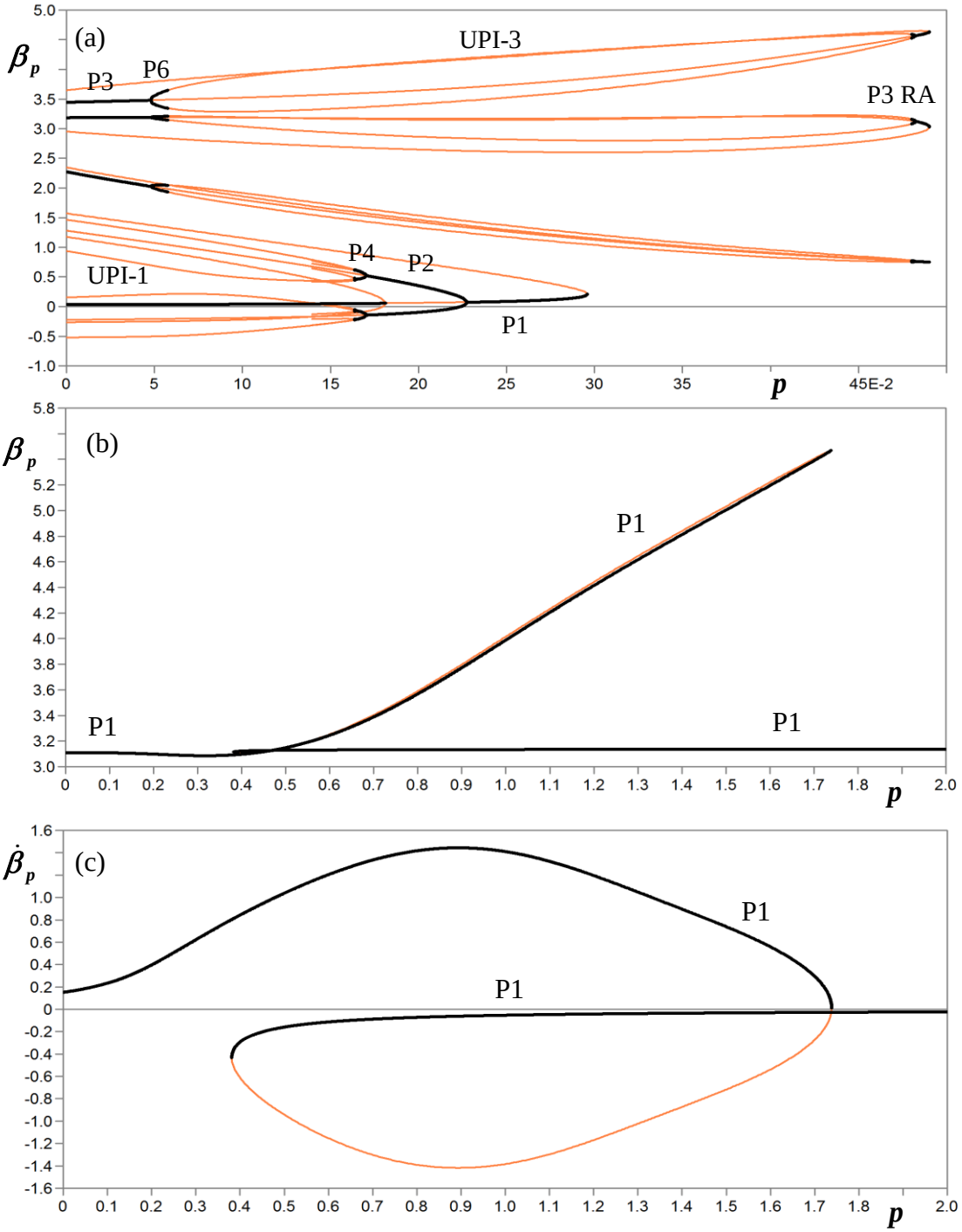

Fig. 3.49. Bifurcation diagrams S1(p) and S3(p) of the fixed periodic points of the coordinates β_p and $\dot{\beta}_p$ versus gravitation coefficient p. There is coexistence of 1T and 3T bifurcation groups (a) with their own rare attractors (RA) and UPIs. There is 1T (b)-(c) bifurcation group with hysteresis effect. Parameters: c = 0.01, q_0 = 0.01, a = 0.8, p = var., ω = 0.8, q_1 = 0.05, k = 7.

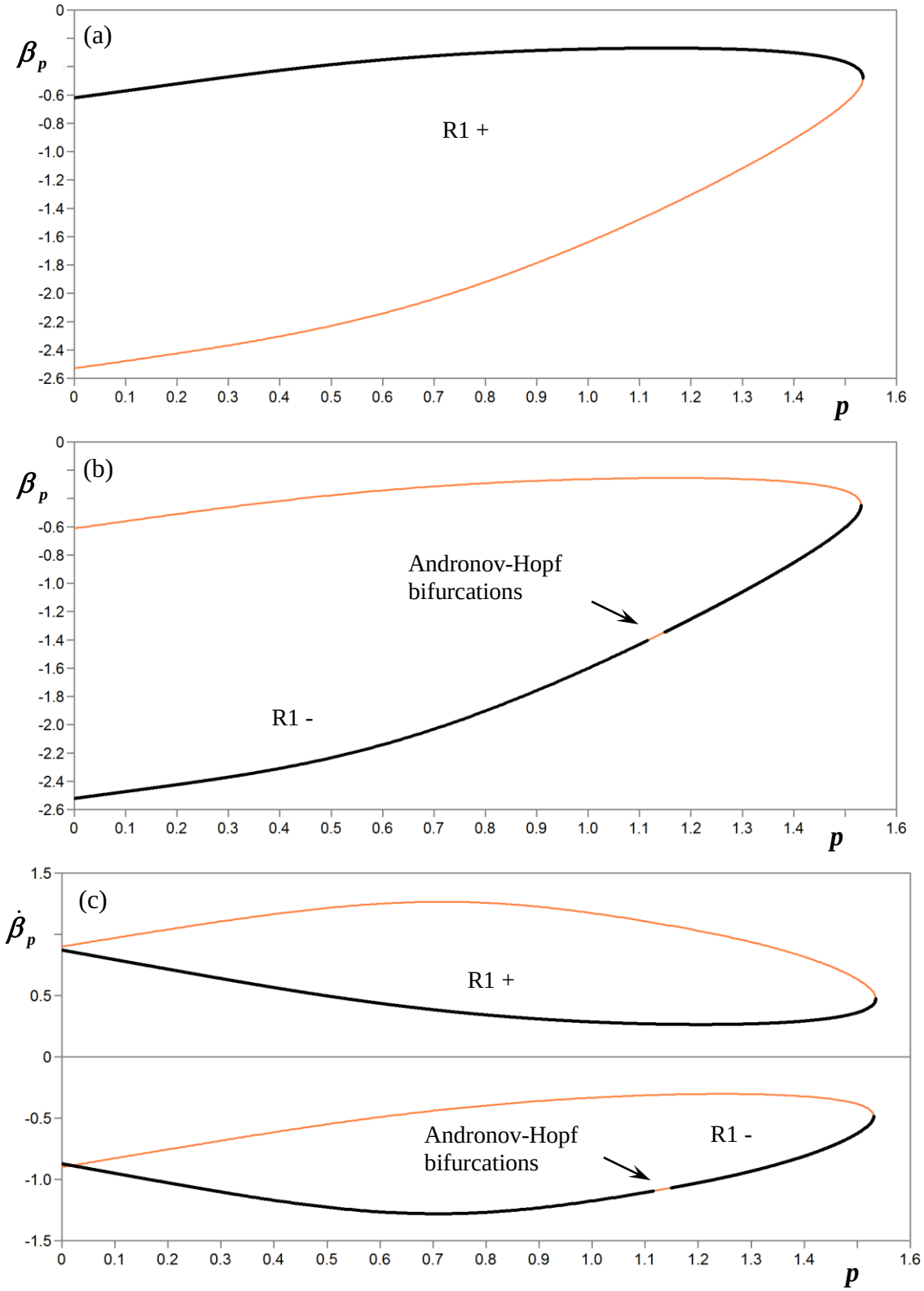

Fig. 3.50. Bifurcation diagrams S1(p) of the fixed periodic points of the coordinates β_p and $\dot{\beta}_p$ versus gravitation coefficient p. There is coexistence of two rotations: clockwise R1+ and counter-clockwise R1- rotations. For left rotating orbit R1- the Andronov-Hopf bifurcations are found. Parameters: c = 0.01, q_0 = 0.01, a = 0.8, p = var., ω = 0.8, q_1 = 0.05, k = 7.

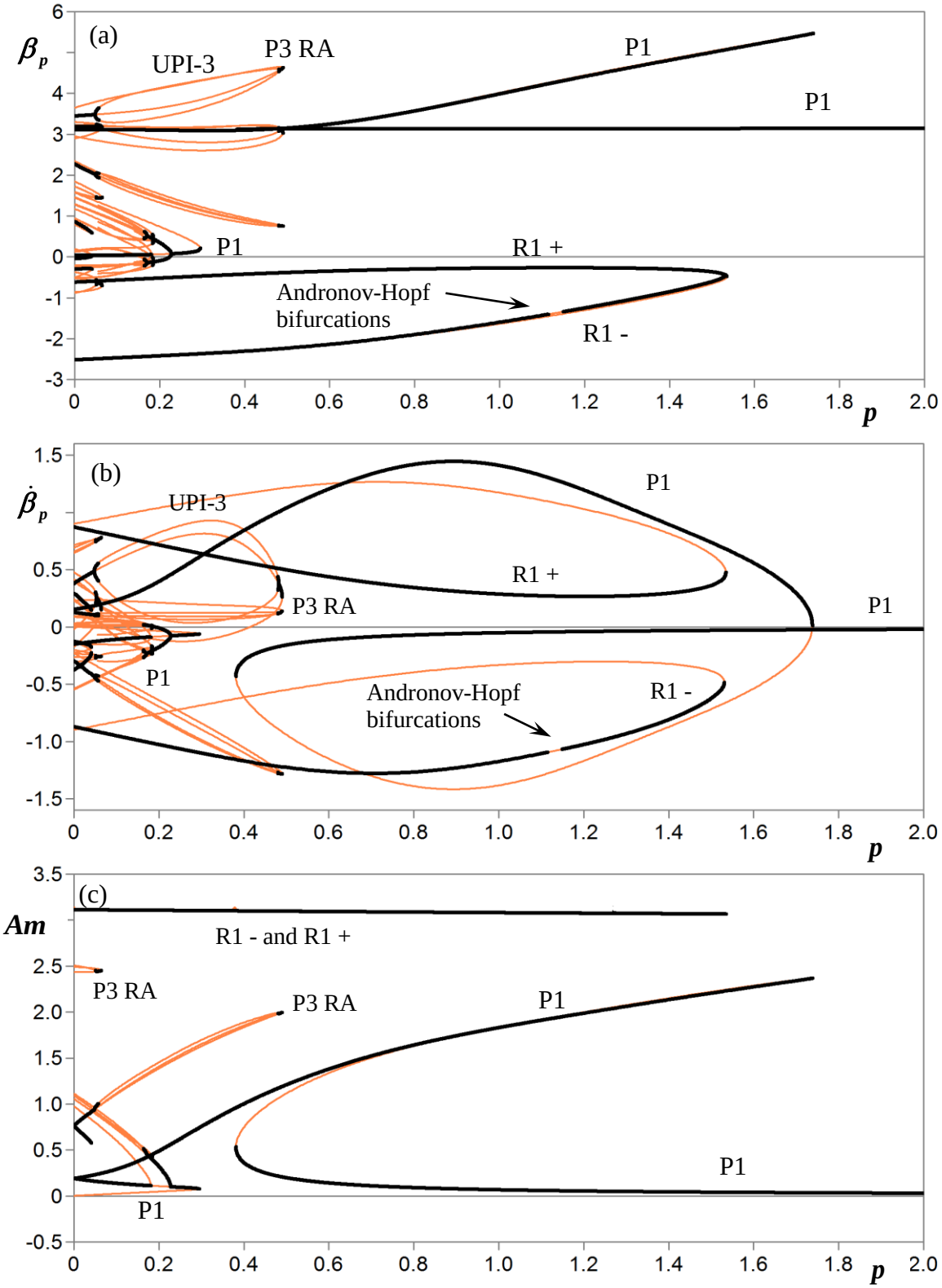

Fig. 3.51. Bifurcation diagrams S1(p) of the fixed periodic points of the coordinates β_p and $\dot{\beta}_p$ versus gravitation coefficient p. There are 7 bifurcation groups: two 1T, two 3T, one 6T, clockwise R1 and counter-clockwise R1 rotations. All groups are shown with orbits P1-P2-P4, P3-P6 and P6-P12 by period doubling bifurcations. Parameters: c = 0.01, q_0 = 0.01, a = 0.8, p = var., ω = 0.8, q_1 = 0.05, k = 7.

Using previously obtained complete bifurcation diagrams (Figs. 3.49-3.51) the topology of basins of attraction with varying coefficient $p = 0.00…2.00$ was investigated by 89 Cell-to-Cell mappings. But only 10 of them were shown on Figs. 3.52-3.62 due to space constraints of doctoral thesis. More results of the Cell-to-Cell mapping are presented in work [149].

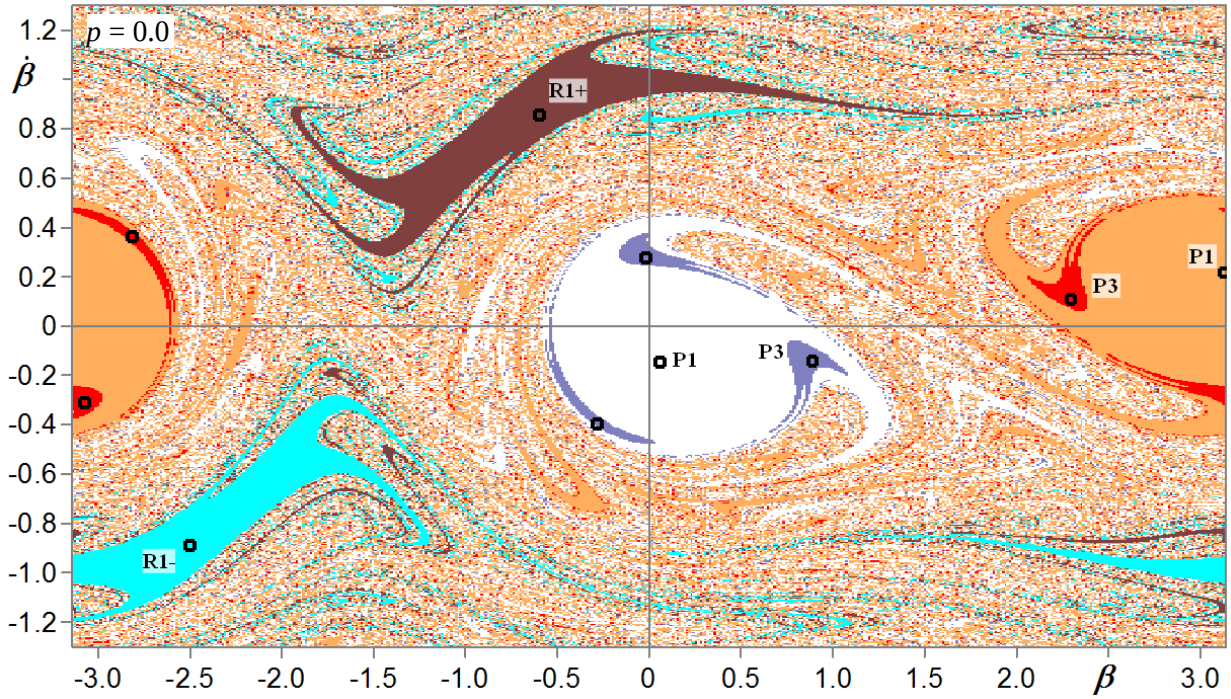

Fig. 3.52. Cell-to-Cell mapping with 500×500 grid of initial conditions ($-\pi$, -1.3; π, 1.3) for $p = 0.00$. The 6 stable regimes (two P1, two P3, R1+ and R1-) were found.

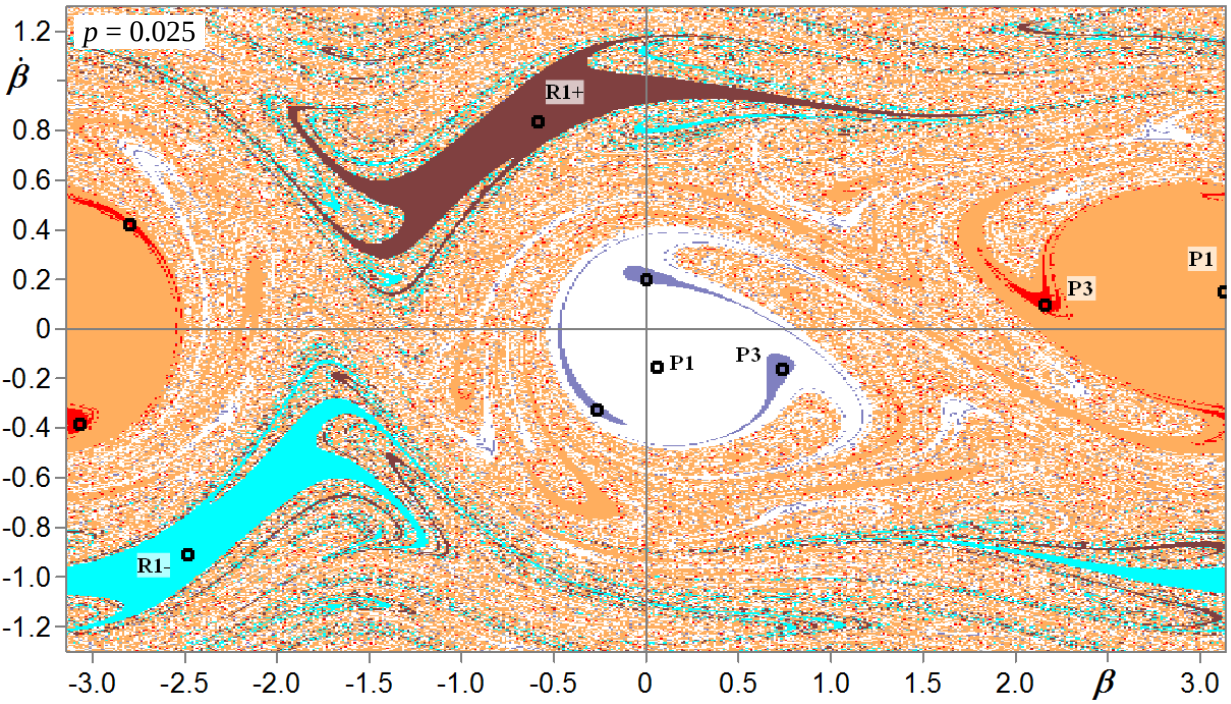

Fig. 3.53. Cell-to-Cell mapping with 500×500 grid of initial conditions ($-\pi$, -1.3; π, 1.3) for $p = 0.025$. The 6 stable regimes (two P1, two P3, R1+ and R1-) were found.

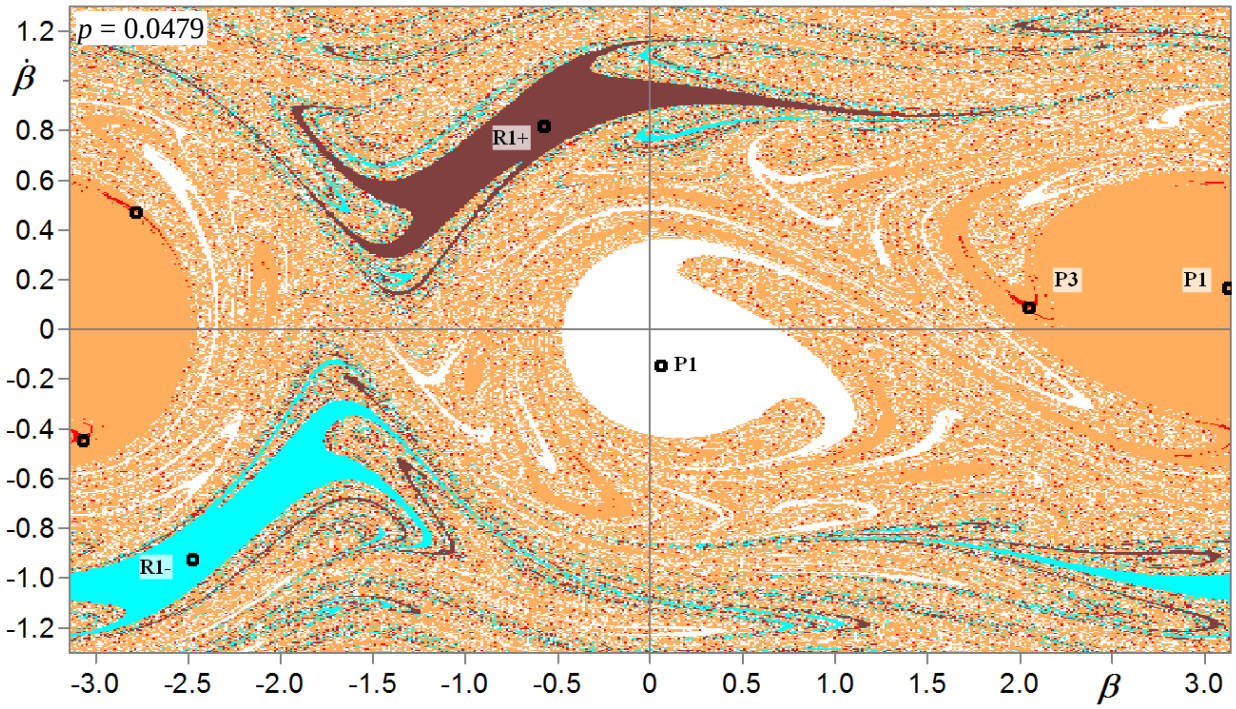

Fig. 3.54. Cell-to-Cell mapping with 500×500 grid of initial conditions ($-\pi$, -1.3; π, 1.3) for p = 0.0479. The 5 stable regimes (two P1, P3, R1+ and R1-) were found.

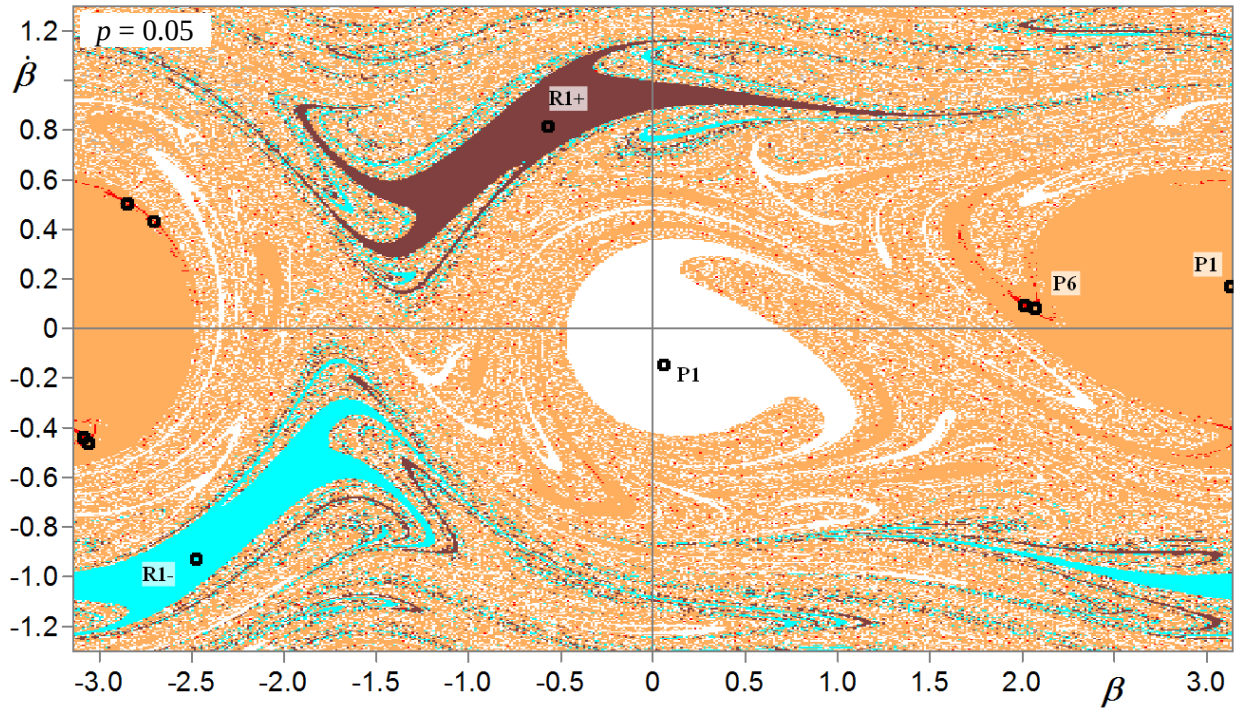

Fig. 3.55. Cell-to-Cell mapping with 500×500 grid of initial conditions ($-\pi$, -1.3; π, 1.3) for p = 0.05. The 5 stable regimes (two P1, P3, R1+ and R1-) were found.

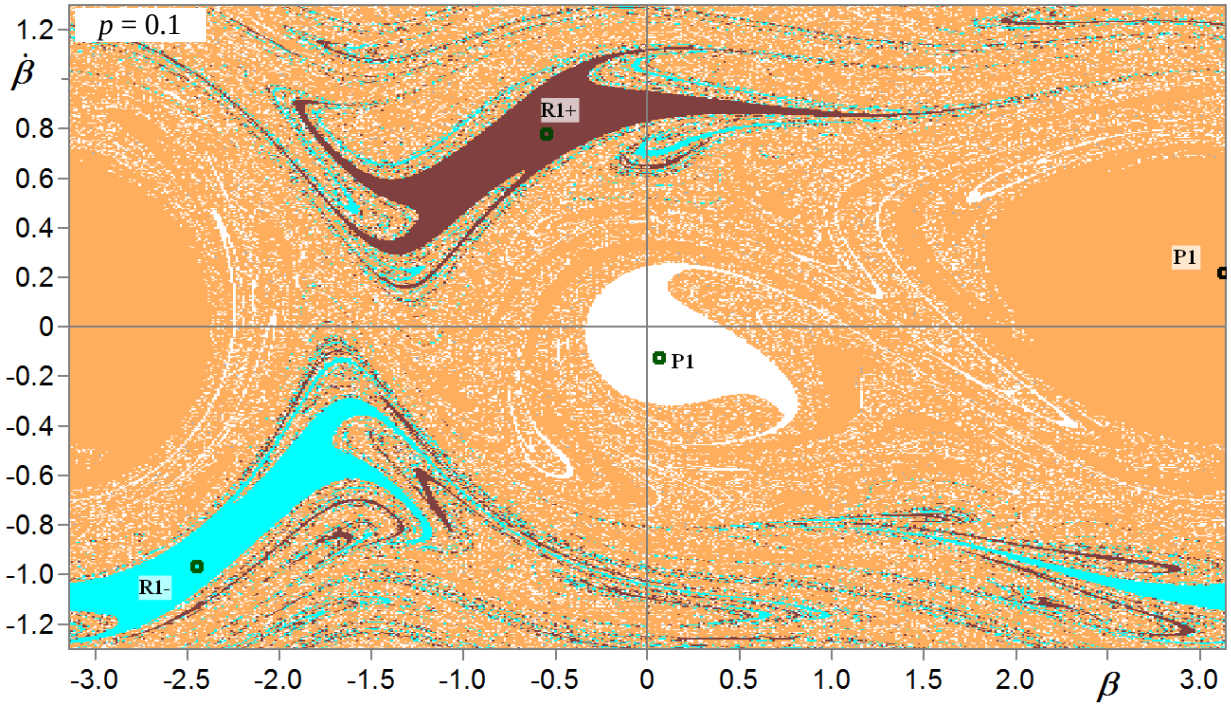

Fig. 3.56. Cell-to-Cell mapping with 500×500 grid of initial conditions ($-\pi$, -1.3; π, 1.3) for p = 0.10. The 4 stable regimes (two P1, R1+ and R1-) were found.

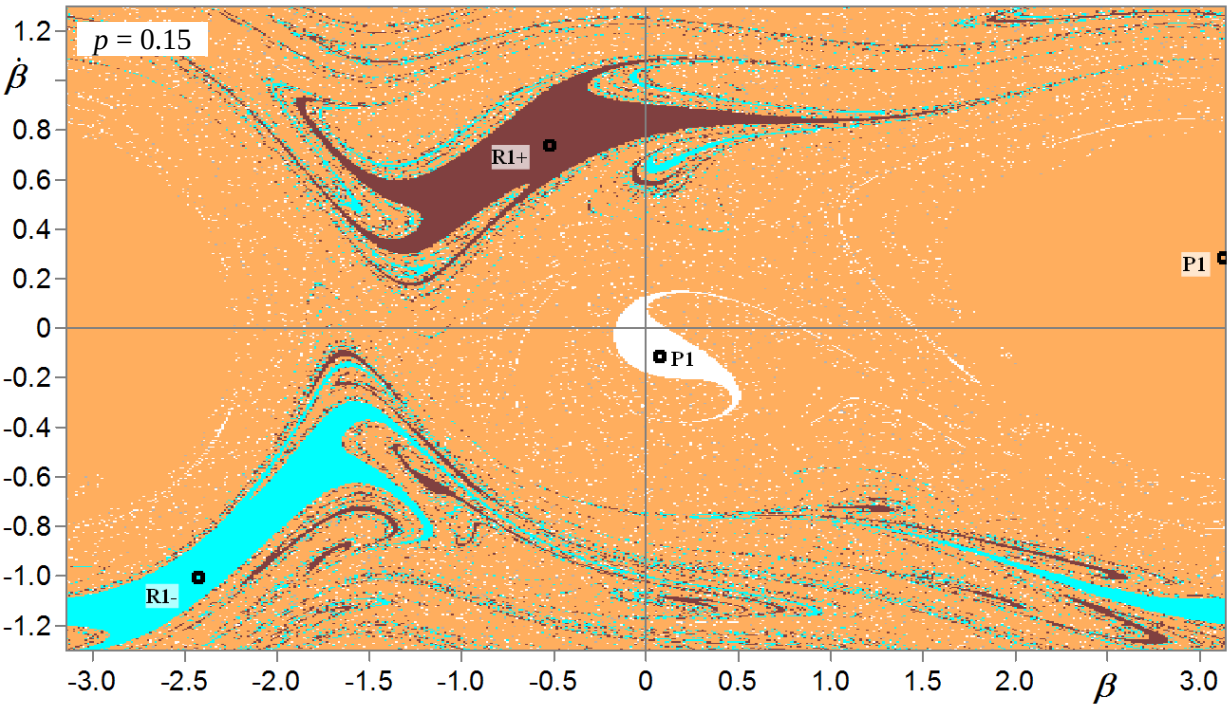

Fig. 3.57. Cell-to-Cell mapping with 500×500 grid of initial conditions ($-\pi$, -1.3; π, 1.3) for p = 0.15. The 4 stable regimes (two P1, R1+ and R1-) were found.

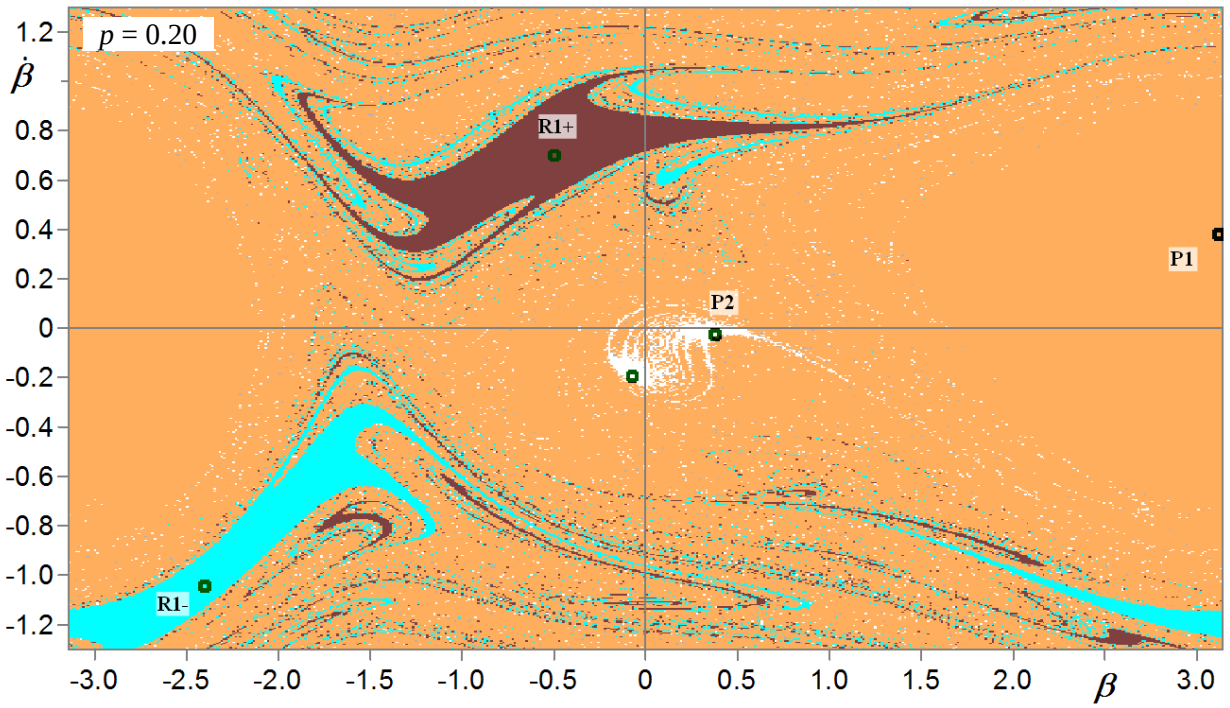

Fig. 3.58. Cell-to-Cell mapping with 500×500 grid of initial conditions ($-\pi$, -1.3; π, 1.3) for p = 0.20. The 4 stable regimes (one P1, one P2, R1+ and R1 -) were found.

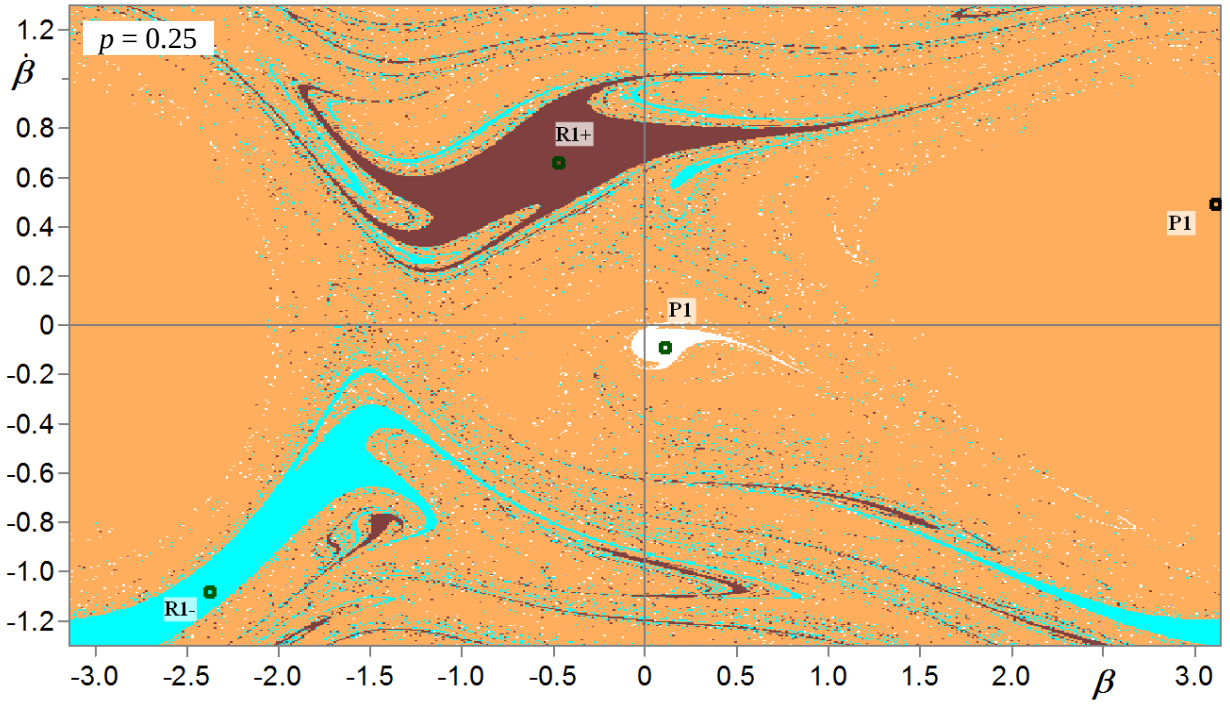

Fig. 3.59. Cell-to-Cell mapping with 500×500 grid of initial conditions ($-\pi$, -1.3; π, 1.3) for p = 0.25. The 4 stable regimes (two P1, R1+ and R1 -) were found.

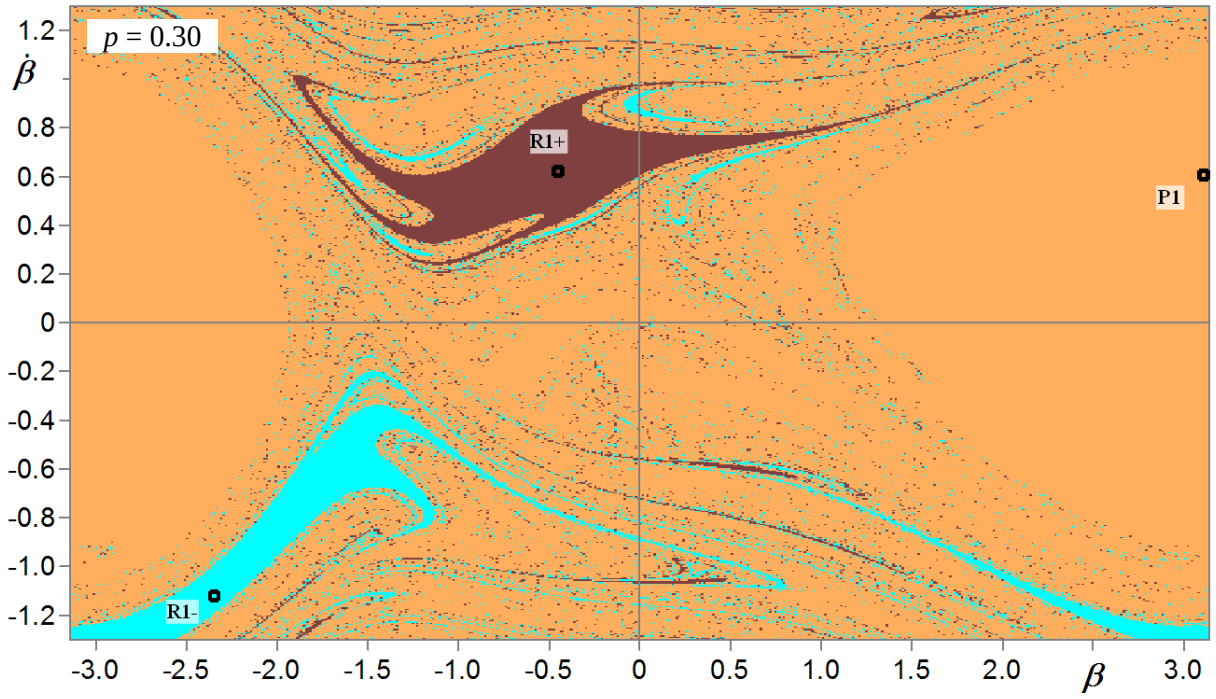

Fig. 3.60. Cell-to-Cell mapping with 500×500 grid of initial conditions (-π, -1.3; π, 1.3) for p = 0.30. The 3 stable regimes (one P1, R1+ and R1 -) were found.

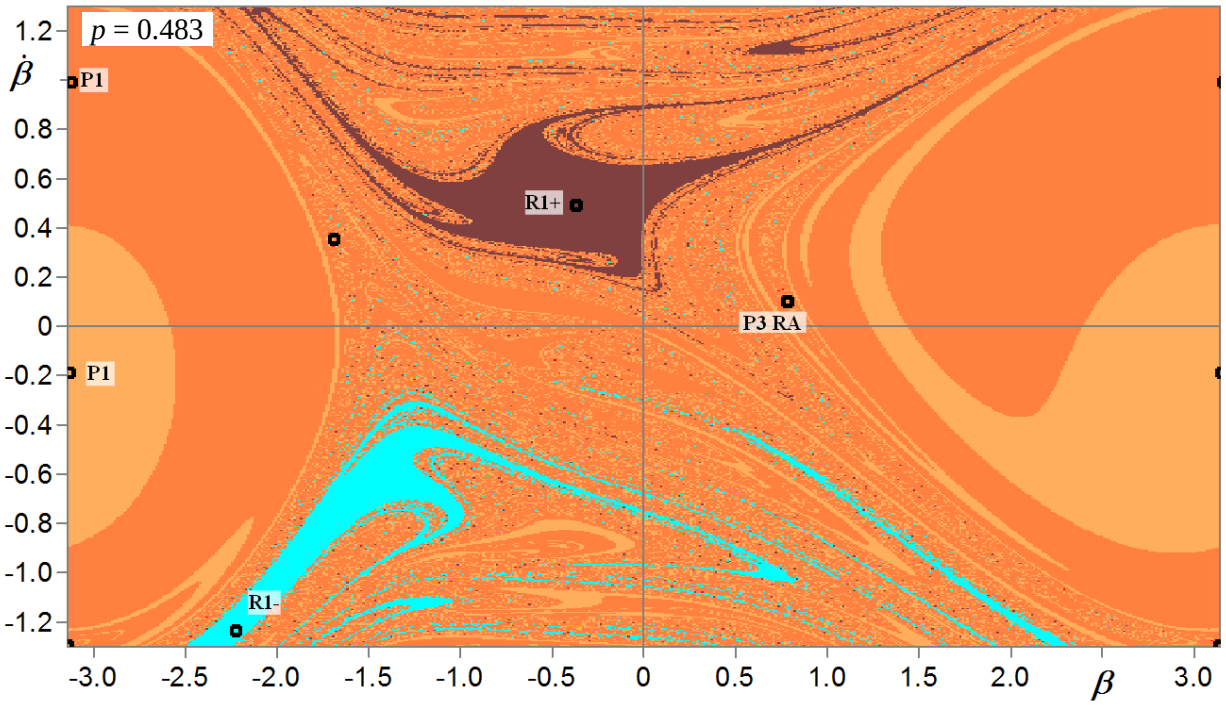

Fig. 3.61. Cell-to-Cell mapping with 500×500 grid of initial conditions (-π, -1.3; π, 1.3) for p = 0.483. The 5 stable regimes (two P1 of the common 1T bifurcation group, P3 rare attractor, R1+ and R1 -) were found.

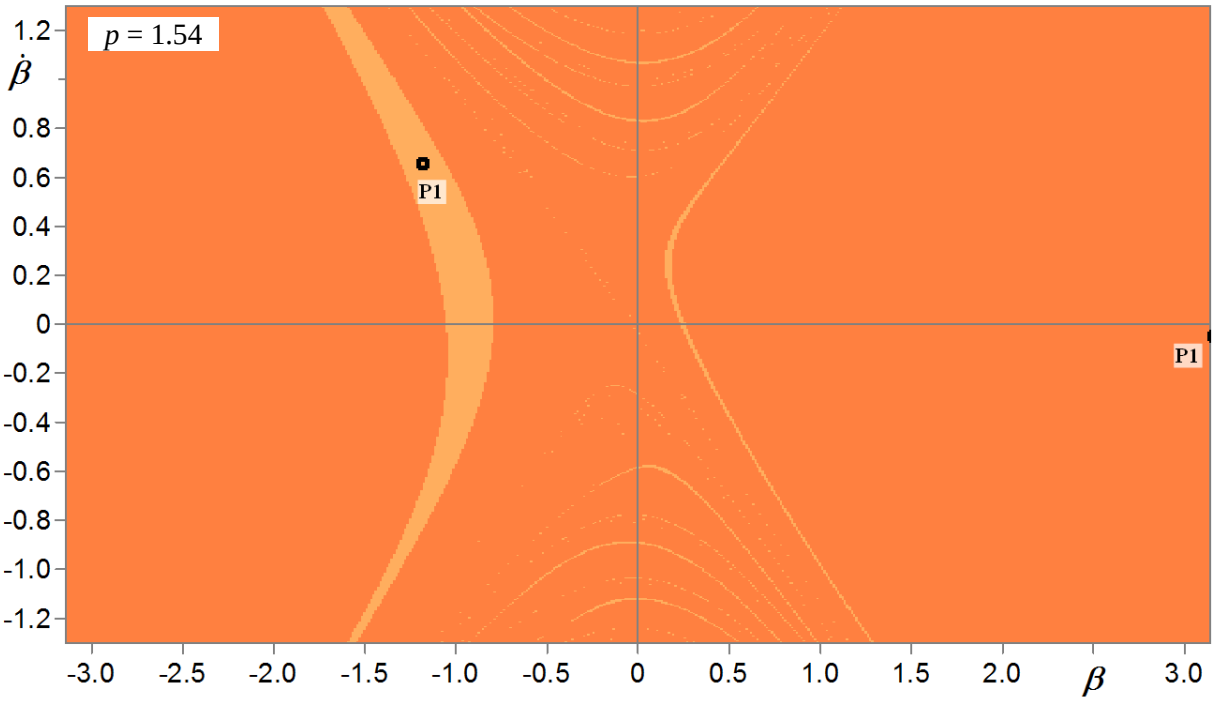

Fig. 3.62. Cell-to-Cell mapping with 500×500 grid of initial conditions ($-\pi$, -1.3; π, 1.3) for p = 1.54. The 2 stable oscillating regimes (two P1 of the common 1T bifurcation group) were found.

The construction process of these basins of attraction was time consuming and for the same parameters of PC, as it was done for the periodic skeleton, the calcullation time of one diagram was about 4 hours.

Global bifurcation analysis Sn(p) with varying longitudinal excitation force amplitude p based on new bifurcation theory and using the method of complete bifurcation groups is done for the rigid body pendulum with linear spring and several equilibrium positions. The system, except for torsional spring, has the linear spring that is connected to the end of the rigid body pendulum.

Periodic skeleton for oscillating and rotating orbits by using the Newton-Kantorovich method was constructed for the studied pendulum system. The coexistence of different types of oscillating, rotating and oscillating-rotating orbits (rare subharmonic P6 attractor, other different regular periodic oscillating regimes Pn, different types of rotations Rn and subharmonic oscillating-rotating orbits OR6, OR10 and OR13) is shown.

The collection of basins of attraction of bifurcation diagrams was shown for illustrating the system's behaviour with varying the longitudinal excitation force amplitude p.

3.8 Centrifugal pendulum vibration absorber with impact interactions

In previous paragraphs it is shown that the behavior of the driven damped pendulum systems may be complex and sometimes with the unexpected phenomena such as stable hilltop vibrations, complex subharmonical and quasi-periodical vibrations, different rotations and other.

In this section the illustration of the advantages of the new bifurcation theory is used for the pendulum vibration absorber model [27] with soft impact (Fig.3.63c). We have found important unknown regular or chaotic attractors and new bifurcation groups with rare attractors. The method of complete bifurcation groups gives robust stability to the pendulum vibration absorber by changing the system parameters, that allows saving characteristics of the vibration absorber system and excluding other amazing regimes.

The results of bifurcation analysis of studied pendulum vibration absorber with impact interactions were obtained as a result of joint research with Prof. Eugen Kremer form company LuK GmbH & Co. OHG from Germany. It is well-known in industry and automotive systems. These investigations are devoted to the centrifugal pendulum vibration absorber for neutralizing the irregularity of the engine torque in automotive. It is an effective device for damping vibrations in power train especially in combination with Dual-Mass Flywheel (DMFW), and its qualitative behavior with taking into account non-linear effects is very important.

The aim of this paragraph is doing complete bifurcation analysis for important parameter of pendulum vibration absorber systems by using the fundamental concepts of the bifurcation theory: a periodic skeleton, complete bifurcation group nT, subgroup of unstable periodic infinitium (UPI), concepts of rare attractors, complex protuberances, construction of basins of attraction, typical bifurcation topological groups and the topological structure of chaotic attractors and chaotic transients [147].

In present paragraph there are three cases of a flywheel with pendulum vibration absorber without impact (Fig.3.63,a), with stiff impact (Fig.3.63,b) and with soft impact (Fig.3.63,c). The studied nonlinear dynamical model of the pendulum vibration absorber [27] with soft impact (see Fig.3.63c) is represented. System has trilinear dissipation and restoring forces (Fig.3.63,d). The equation of motion for studied pendulum system is such:

$$(1-\gamma)\cdot\ddot{\varphi}+ f(\dot{\varphi})+ f_1(\varphi)+ h\omega\cos\omega t+\omega^2(1+d)^2(1+2h\sin\omega t)\cdot\sin\varphi=0, \qquad (3.7)$$

where φ – angle of the pendulum relative to basic disk (flywheel); $\dot{\varphi}$ – angular velocity of the pendulum relative to basic disk, where $\dot{\varphi}=d\varphi/dt$; b_1, b_2 – linear dissipation coefficients,

accordingly to linear subregions of visco-elastic characteristic; c_r – stiffness coefficient of linear elastic characteristic at soft impact in coordinate $\varphi_r = \pm 15^o$:

$$f(\dot{\varphi}) = \begin{Bmatrix} b_2\dot{\varphi} & if & \varphi < -\varphi_r \\ b_1\dot{\varphi} & if & -\varphi_r \le \varphi < \varphi_r \\ b_2\dot{\varphi} & if & \varphi \ge \varphi_r \end{Bmatrix}, \quad f_1(\varphi) = \begin{Bmatrix} c_r(\varphi + \varphi_r) & if & \varphi < -\varphi_r \\ 0 & if & -\varphi_r \le \varphi \le \varphi_r \\ c_r(\varphi - \varphi_r) & if & \varphi > \varphi_r \end{Bmatrix} \tag{3.8}$$

γ – ratio of moments of inertia of the pendulum and disk ($\gamma < 1$); h – dimensionless torque from the engine (oscillating component) ($h \le 1$); ω – excitation order (ω = 2 or 3, respectively for 4-cylinder and 6-cylinder engine); d – error in setting up the absorber at anti-resonance (mistuning) ($-0.1 \le d \le 0.1$); R – coefficient of restitution of stiff impact in coordinate $\varphi_r = \pm 15^o$; $\dot{\varphi}^+ = -R\dot{\varphi}^-$; $\dot{\varphi}^+, \dot{\varphi}^-$ – velocities before and after impact respectively.

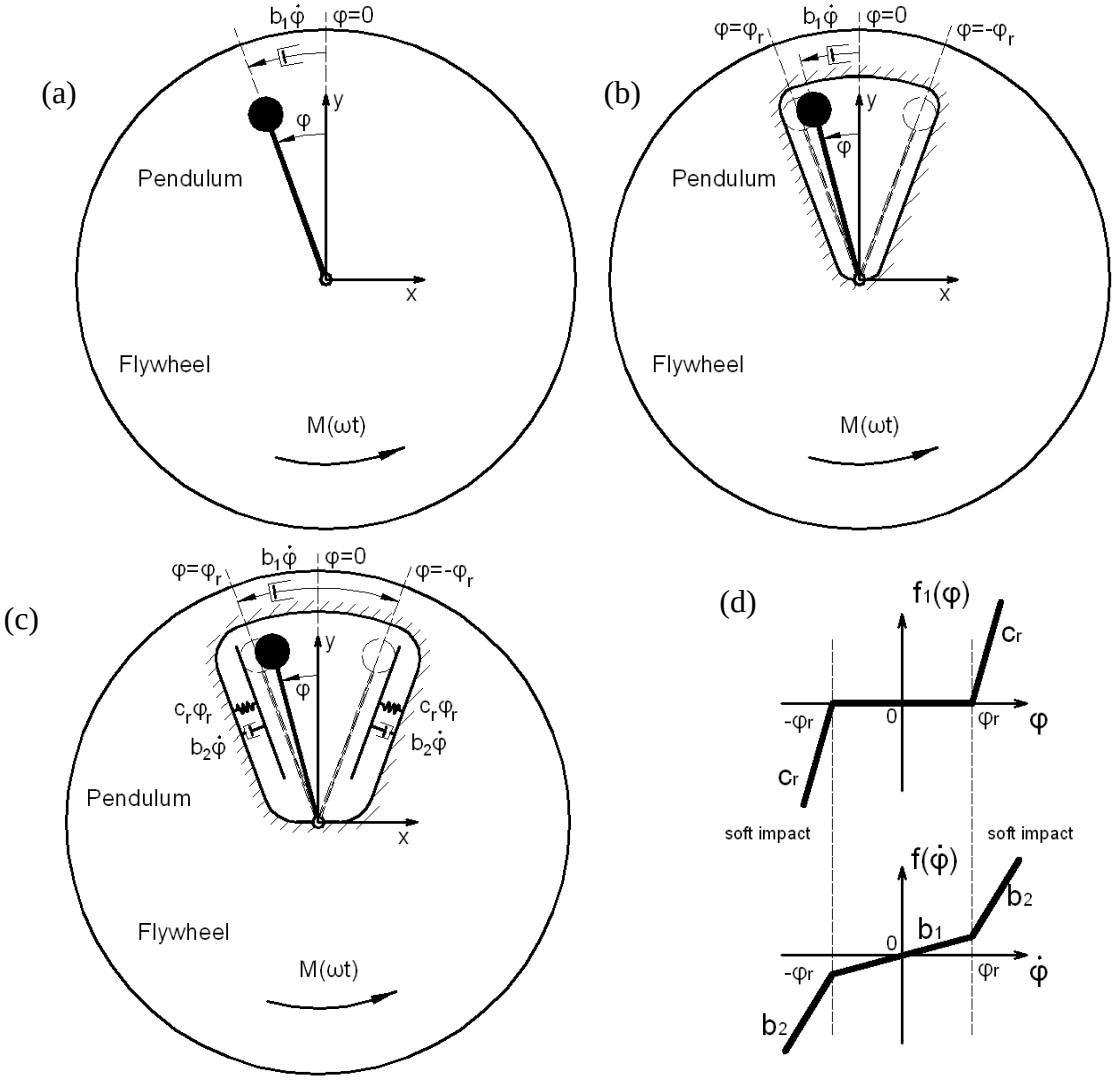

Fig. 3.63. Three cases of a flywheel with pendulum vibration absorber: (a) without impact; (b) with stiff impact; (c) with soft impact; (d) elastic dissipation forces characteristics and dependence of dissipation coefficient on state of system.

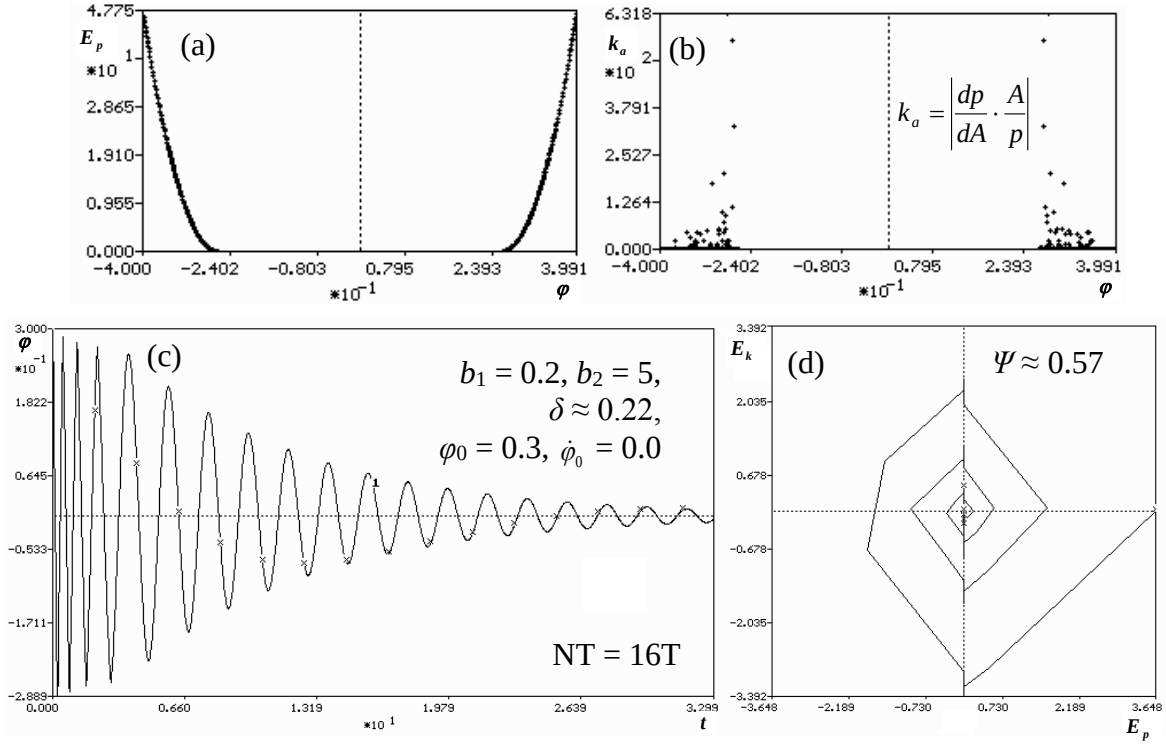

Fig. 3.64. Potential well (a), coefficient of nonlinearity (b), die-away curve of free oscillations for displacement (c) and energy diagram (d) for pendulum vibration absorber system with soft impact. Parameters: $\gamma = 0.1$, $b_1 = 0.2$, $b_2 = 5$, $c_r = 5000$, $\omega = 3$, $d = 0$, $h = 0.5$.

The variable parameter of the pendulum system (Eq.3.7) is moment from the motor $h = 0...1.5$. The base parameters for analysis are: $\gamma = 0.1$, $b_1 = 0.2$, $b_2 = 5$, $c_r = 5000$, $\omega = 3$, $d = 0$, $h = 0.5$. Some results of complete bifurcation analysis of the studied model have been examined in works [145,151]. The possibility of vibration quenching by the pendulum type system is shown in work [58].

With the increase of nonlinearity the amount of nonlinear effects, as a rule, increases. The degree of nonlinearity of resilient description comfortably to estimate through a coefficient [147]:

$$k_a = \left|\frac{dp}{dA}\cdot\frac{A}{p}\right|, \tag{3.9}$$

where p - frequency of free oscillations of the partial system, A – amplitudes of oscillations.

Potential well and coefficient of nonlinearity are shown in Fig.3.64 (a-b). For a system with symmetric trilinear characteristics (Fig.3.63,d) a maximum nonlinearity coefficient can be significantly larger near the break of the elastic characteristics [147] namely less then 631.

The dynamical characteristics of free oscillations in pendulum vibration absorber with soft impact for $b_1 = 0.2$, $b_2 = 5$ are shown by die-away curve for displacement and energy diagram (the kinetic energy E_k relation of the potential energy E_p) in Fig. 3.64 (c-d). The characteristics of linear dissipation, such as the logarithmic decrement of oscillations and the loss coefficient can't

be used to characterize the rate of decay of free oscillations for nonlinear dissipation. These characteristics can be calculated only for concrete region of motion. Logarithmic decrement δ of oscillations and loss coefficient Ψ for the linear dissipation after the first period of excitation force $T = T_\omega$ are:

$$\delta = ln\frac{a_0}{a_1} \approx 0.22,\ \psi = \frac{\Delta P_C}{P_C} \approx 0.57 \tag{3.10}$$

Before the construction of complete bifurcation diagrams, periodic skeleton for base parameters of the pendulum vibration absorber was build.

From the grid of 20×20 = 400 initial conditions (see Fig.3.65) inside the rectangle (-π/12; -1/ π/12; 1) we have obtained periodic skeleton (see Table. 3.4) consisted from 17 periodic attractors (one unstable P1 attractor; one unstable P2 attractor; four P4 attractors – two of them are stable; two unstable P5 attractors; two unstable P6 attractors; one unstable P7 attractor; one unstable P8 attractor; three unstable P9 attractors; one unstable P11 attractor and one unstable, $b_2 = 5$, $c_r = 5000$, $\omega = 3$, $d = 0$, $h = 0.5$ with regime scanning for period from 1 till 16 by using the Newton-Kantorovich method.

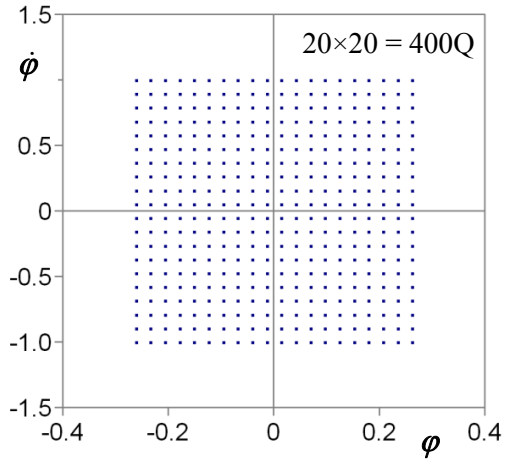

Fig. 3. A grid of 20×20 = 400Q initial conditions inside the rectangle (-π/12;-1 / π/12;1) for construction of periodic skeleton.

By using the Poincaré map founded regimes can be specified by data of the solution (orbit) order, by the number of loops in the projection of the phase trajectories, the coordinates of the fixed point and stability characteristics. For example,

P1 (1/1), Fixed point (-0.185917, -0.502712), $\rho_1 = -0.0781$, $\rho_2 = -4.5831$.

This is the main passport of periodic regime (at a given point of the parameter space of the system). The examples of extended passport of periodic regimes with phase projections and time histories are shown in Table.1. In this table stable solutions (orbits) are plotted by black lines and unstable - by reddish lines (reddish online).

Table. 3.4. Periodic skeleton shows the first 5 of 17 periodic attractors (one unstable P1 attractor; one unstable P2 attractor and two stable P4 attractors) for the base parameters of the centrifugal pendulum vibration absorber.

1	**P1 (1/1) unstable** φ: -0.185917 $\dot{\varphi}$: -0.502712 ρ_1 = -0.0781 ρ_2 = -4.5831	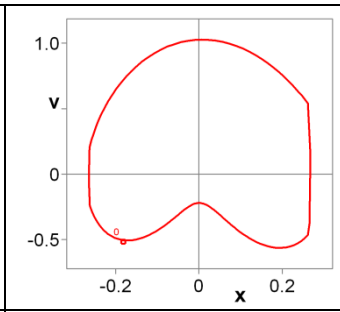	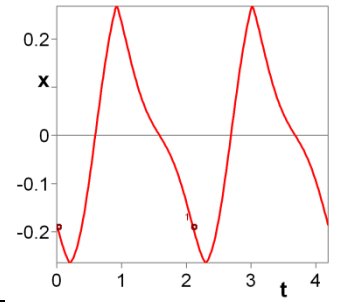
2	**P2 (2/2) unstable** φ: 0.044077, -0.230387 $\dot{\varphi}$: -0.953285, 0.368908 ρ_1 = -0.0552 ρ_2 = -2.2267	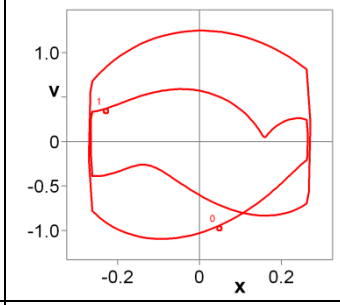	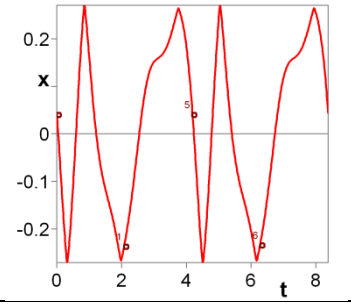
3	**P4 (4/4) unstable** φ: -0.044390, -0.221901, -0.074510, -0.169830 $\dot{\varphi}$: -0.962890, -0.390551, -0.638998, 0.429477 ρ_1 = -0.0026 ρ_2 = -7.7415	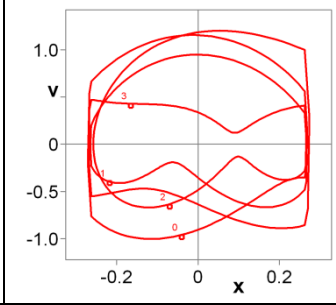	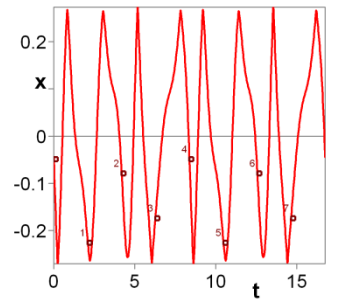
4	**P4 twin (4/4) stable** φ: -0.026677, -0.251735, 0.098861, -0.189815 $\dot{\varphi}$: -0.928878, -0.363381, -0.888374, 0.324743 ρ_1 = -0.0315 ρ_2 = -0.4883	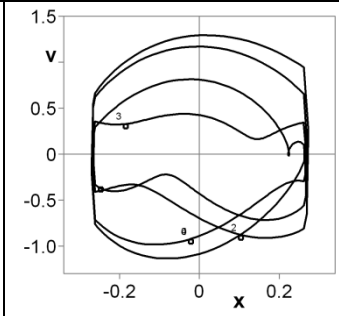	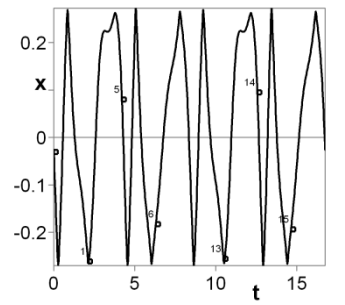
5	**P4 twin (4/4) stable** φ: 0.146848, -0.168306, -0.038020, -0.253032 $\dot{\varphi}$: -0.805198, 0.263888, -0.886517, -0.374921 ρ_1 = -0.0299 ρ_2 = -0.6763	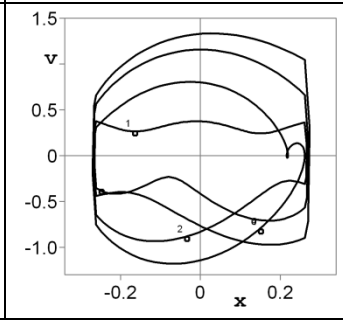	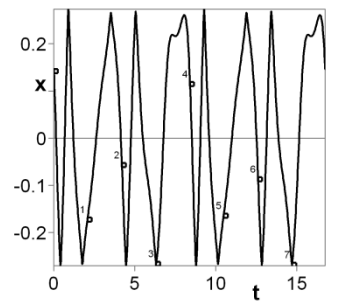

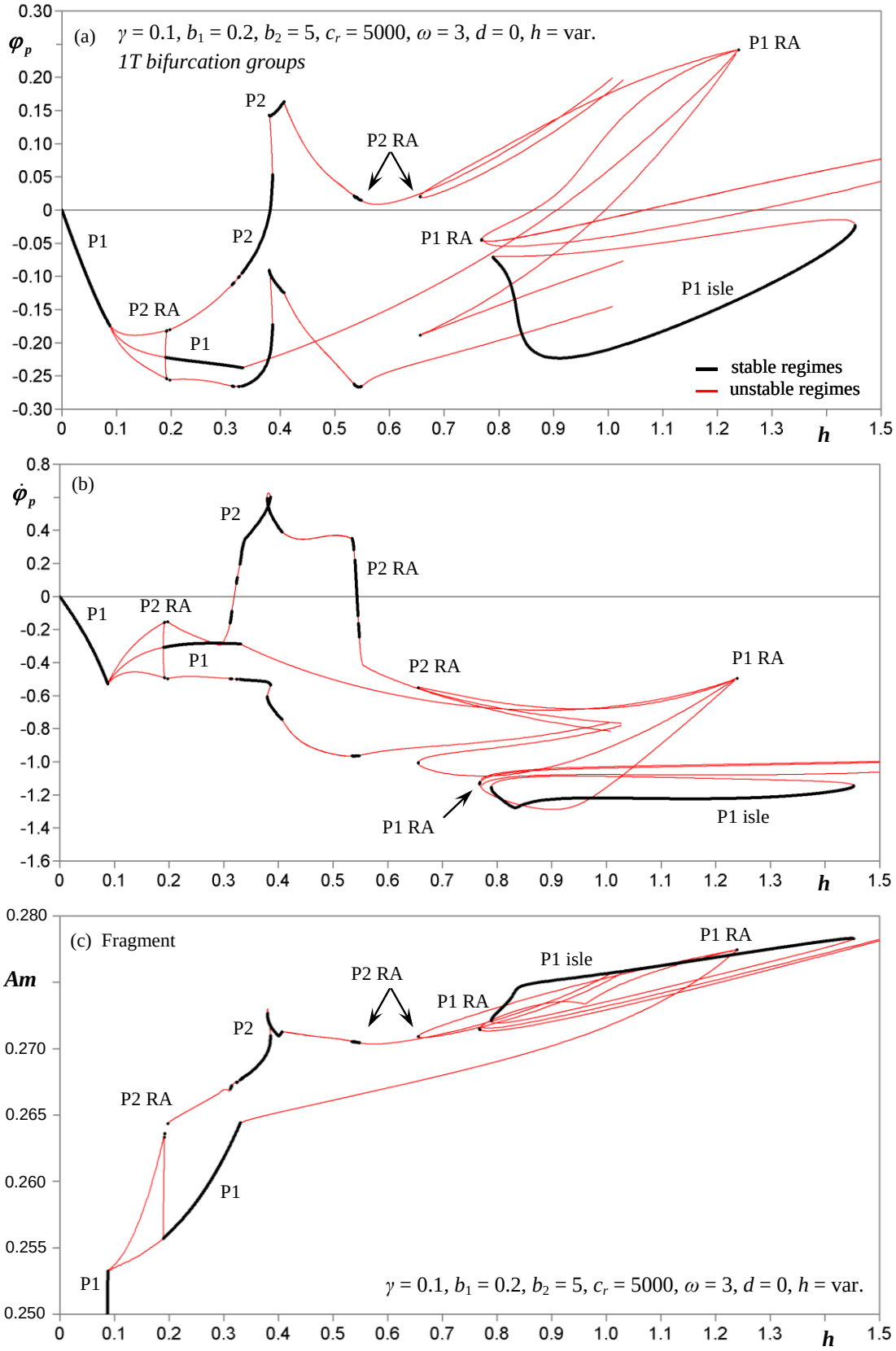

Fig. 3.66. Pendulum vibration absorber with soft impact (Eq.3.7 and Fig.3.63,c). Bifurcation diagrams of the fixed periodic points of the coordinates φ_p, $\dot{\varphi}_p$ and Am versus parameter h. There are two 1T bifurcations groups: 1T (with depth P1-P2) with complex protuberances and 1T isle. The pendulum system has many rare attractors of different kinds. Parameters: $\gamma = 0.1$, $b_1 = 0.2$, $b_2 = 5$, $c_r = 5000$, $\omega = 3$, $d = 0$, h = var.

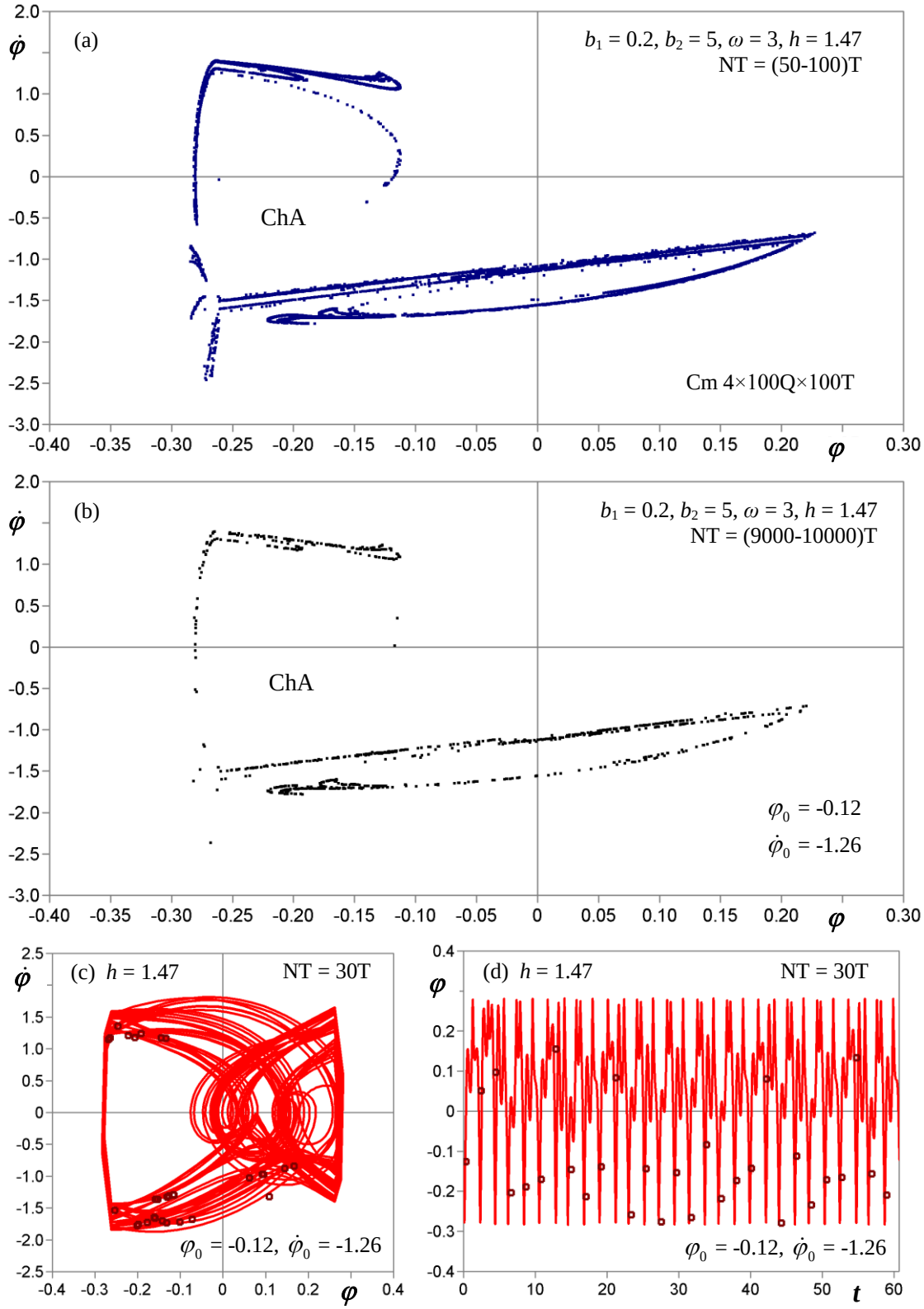

Fig. 3.67. Chaotic attractor in pendulum vibration absorber for cross-section h = 1.47 of bifurcation diagram Fig.3.66: (a)-(b) Poincaré maps - Cm 4×100Q×(50-100)T and NT = (9000-10000)T from initial conditions φ_0 = -0.12, $\dot{\varphi}_0$ = -1.26; (c)-(d) phase projection and time histories with NT = 30T.

The construction of bifurcation diagrams was done by the Runge-Kutta 4-th order with constant integration step: $\Delta t = T_\omega/2^k$, where the period of external force is $T_\omega = 2\pi/\omega$ and coefficient k = 7.

The results of complete bifurcation analysis of the pendulum vibration absorber model are represented in Bifurcation diagrams of the fixed periodic points of the coordinates φ_p, $\dot{\varphi}_p$ and *Am* versus parameter *h* (Fig. 3.66). There are two 1T bifurcations groups: 1T (with depth P1-P2) with complex protuberances and 1T isle. The pendulum system has many RA of different kinds.

In this figure stable solutions are plotted by solid lines and unstable - by thin lines (reddish online). The branches of bifurcation diagram are not completed, because of problem of high instability.

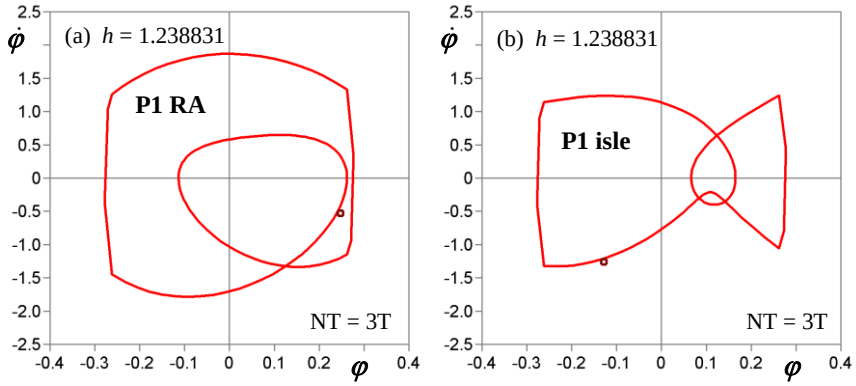

Fig. 3.68. Coexistence of rare attractor P1 RA and P1 isle in cross-section *h* = 1.238831 of diagram Fig.4. Phase projections with NT = 3T.

The example of globally stable chaotic attractor for cross-section *h* = 1.47 of bifurcation diagram (Fig.3.66) obtained using the contour mapping Cm 4×100Q×(50-100)T form a contour (-0.4,-3/ 0.4,2), mapping NT = (9000-10000)T from initial conditions φ_0 = -0.12, $\dot{\varphi}_0$ = -1.26, phase projection and time histories with NT = 30T, is shown in Fig.3.67.

The example of coexistence of rare attractor (P1 RA) with period-1 and P1 isle attractor for cross-section *h* = 1.238831 of bifurcation diagram (Fig.3.66) on phases projections is shown in Fig.3.68. Sometimes oscillation amplitudes of rare attractors are tenfold bigger than oscillating amplitudes of stable P1 regimes [137]. Rare attractor has higher velocity of oscillations than P1 isle. In our case oscillation amplitudes are limited by two elastic detents, which realize soft impacts.

Therefore the MCBG gives robust stability to the studied vibration absorber system by changing the system parameters, which allows saving characteristics of the vibration absorber system and excluding other amazing regimes.

3.9 Conclusions

In this chapter the bifurcation analysis of harmonically driven damped pendulum systems with one degree of freedom was performed. The effectiveness of the method of complete bifurcation groups were discussed for following pendulum driven systems: pendulum with additional linear elastic spring and vibrating point of suspension in both directions, pendulum with harmonic oscillations of the point of suspension in the vertical direction, pendulum with harmonic oscillations of the point of suspension in the horizontal direction, pendulum with harmonic oscillations of the point of suspension at a certain angle to the horizontal, pendulum with external harmonic excitation, rigid body pendulum with linear spring and several equilibrium positions, centrifugal pendulum vibration absorber with impact interactions.

The birth of the previously unknown rare attractors has been shown for different harmonically driven damped systems, and new bifurcation groups with complex protuberances have been obtained. The new types of interaction of different oscillating and rotating orbits have been found as well as rare and chaotic rotational regimes. Also the process of formation of chaotic rotation through the cascade of period-doubling bifurcations for different groups has been studied within the framework of the research.

The method of complete bifurcation groups will be useful for global bifurcation analysis and for search of rare attractors as well as for other pendulum systems with one degree of freedom, which are not presented in this chapter.

4

New Bifurcation Groups and Rare Attractors of the Pendulum Systems with Two Degrees of Freedom

4.1 Introduction

It is known that in the driven nonlinear dynamical system with two-degree-of-freedom (2DOF or with dimension D = 5) can exist new bifurcation groups and new nonlinear phenomena. It means that “new separation of the phase space to trajectories” and new bifurcation groups with unknown before topology, with rare attractors and complex protuberances can appear.

In the previous chapter the most commonly studied models of forced and parametrical oscillations in the harmonically driven damped pendulum systems with one degree of freedom

were discussed. The new types of interaction of different oscillating and rotating orbits have been found as well as rare and chaotic rotational regimes. Also the process of formation of chaotic rotation through the cascade of period-doubling bifurcations for different groups has been studied within the framework of the research.

In the present chapter it is demonstrating how the method of complete bifurcation groups is applied to the global analysis of studied pendulum systems with two degrees of freedom. Among them are pendulum system with a sliding mass and with the external periodic excited moment, and double pendulum with the periodically vibrating point of suspension in vertical direction. The main aims of the research are to investigate the qualitative behaviour of the pendulum systems with 2DOF by varying the parameters of the systems and to obtain the new qualitative results of topology of bifurcation groups with rare regular and chaotic attractors.

4.2 Bifurcation analysis of the driven damped pendulum system with a sliding mass and with the external periodic excited moment

4.2.1 Equations of motion of studied pendulum model

Let us consider the first 2DOF pendulum system with with linear restoring force and linear dissipation (Fig. 4.1). Suspension point is excited by periodical moment. Second sliding mass has linear dissipative and restoring forces. Similar models have been studied in work [18, 58]. Some results of complete bifurcation analysis of the studied model have been examined in the previous works [126, 136].

The first generalized coordinate will be angle of rotation of the pendulum φ, read-out from a vertical line. The second one is the displacement of the sliding mass y, read-out from a quiescent state. Then the Lagrange equations of the second kind have the following form:

$$\begin{cases} \dfrac{d}{dt}\left(\dfrac{\partial E_k}{\partial \dot{\varphi}}\right) - \dfrac{\partial E_k}{\partial \varphi} + \dfrac{\partial E_p}{\partial \varphi} = Q(t), \\ \dfrac{d}{dt}\left(\dfrac{\partial E_k}{\partial \dot{y}}\right) - \dfrac{\partial E_k}{\partial y} + \dfrac{\partial E_p}{\partial y} = 0, \end{cases} \tag{4.1}$$

where φ – angle of rotation of the pendulum; $\dot{\varphi}$ – angular velocity of the pendulum, where $\dot{\varphi} = d\varphi / dt$; t – time; y – displacement of the sliding mass, read-out from a quiescent state; $\dot{y}$ – velocity of the sliding mass, where $\dot{y} = dy / dt$; E_k – kinetic energy; E_p – potential energy; $Q(t)$ – generalized force which describes external periodical moment $M(\omega_1 t)$.

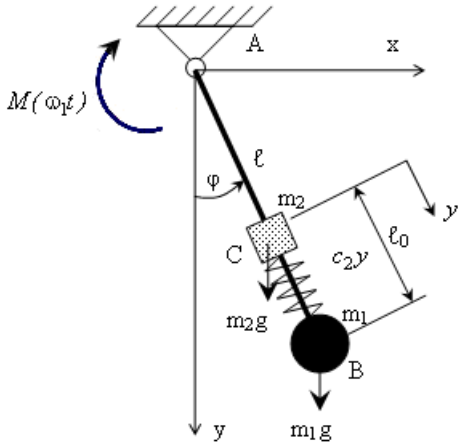

Fig. 4.1. The studied driven damped pendulum model with a sliding mass and with the external periodic excited moment.

For following derivation of equations of motion we will use following expressions:

$$\begin{gathered} x_B = l\sin\varphi\,,\ y_B = l - l\cos\varphi\,; \\ x_C = (l - l_0 + y)\sin\varphi\,,\ y_C = (l - l_0 + y)(1-\cos\varphi), \end{gathered} \tag{4.2}$$

where x_B, y_B, x_C, y_C – coordinates of the centers of gravity of the pendulum B and the sliding mass C accordingly; t – time, read-out from the moment, when the pendulum is coincide with the vertical and sliding mass is at a quiescent state

Thus, potential energy of the system:

$$E_p = \frac{1}{2}c_2\dot{y}^2 + m_1\mu y_B + m_2\mu y_C = \frac{1}{2}c_2 y^2 + m_1\mu[l - l\cos\varphi] + m_2\mu[(l - l_0 + y)(1-\cos\varphi)]. \tag{4.3}$$

Kinetic energy of the system:

$$E_k = \frac{1}{2}m_1\upsilon_B^2 + \frac{1}{2}m_2\upsilon_C^2 + \frac{1}{2}m_2\dot{y}^2\,. \tag{4.4}$$

Projections of the velocities υ_B and υ_C of the centers of gravity of masses B and C are obtained from (4.2):

$$\begin{gathered} \dot{x}_B = l\dot{\varphi}\cos\varphi\,,\ \dot{y}_B = l\dot{\varphi}\sin\varphi\,; \\ \dot{x}_C = (l - l_0 + y)\dot{\varphi}\cos\varphi\,,\ \dot{y}_B = (l - l_0 + y)\dot{\varphi}\sin\varphi\,. \end{gathered} \tag{4.5}$$

Hence:

$$\begin{gathered} \upsilon_B^2 = \dot{x}_B^2 + \dot{y}_B^2 = [l\dot{\varphi}\cos\varphi]^2 + [l\dot{\varphi}\sin\varphi]^2 = l^2\dot{\varphi}^2\,; \\ \upsilon_C^2 = \dot{x}_C^2 + \dot{y}_C^2 = [(l - l_0 + y)\dot{\varphi}\cos\varphi]^2 + [(l - l_0 + y)\dot{\varphi}\sin\varphi]^2 = (l - l_0 + y)^2\dot{\varphi}^2\,. \end{gathered} \tag{4.6}$$

Now substituting (4.6) into (4.4) we get:

$$E_k = \frac{1}{2}m_1 l^2\dot{\varphi}^2 + \frac{1}{2}m_2(l - l_0 + y)^2\dot{\varphi}^2 + \frac{1}{2}m_2\dot{y}^2\,. \tag{4.7}$$

Thus, kinetic energy depends on generalized coordinates (φ, y) and velocities ($\dot{\varphi}$, $\dot{y}$). Then we find partial derivatives of energies:

$$\begin{gathered}\frac{\partial E_p}{\partial \varphi} = m_1 \mu l \sin\varphi + m_2 \mu (l - l_0 + y)\sin\varphi;\ \frac{\partial E_p}{\partial y} = c_2 y + m_2 \mu (1 - \cos\varphi),\\ \frac{\partial E_k}{\partial \dot{\varphi}} = m_1 l^2 \dot{\varphi} + m_2 (l - l_0 + y)^2 \dot{\varphi};\ \frac{\partial E_k}{\partial \dot{y}} = m_2 \dot{y},\\ \frac{d}{dt}\left(\frac{\partial E_k}{\partial \dot{\varphi}}\right) = m_1 l^2 \ddot{\varphi} + m_2 (l - l_0 + y)^2 \ddot{\varphi} + 2 m_2 (l - l_0 + y)\dot{\varphi}\dot{y};\ \frac{d}{dt}\left(\frac{\partial E_k}{\partial \dot{y}}\right) = m_2 \ddot{y},\\ \frac{\partial E_k}{\partial \varphi} = 0;\ \frac{\partial E_k}{\partial y} = m_2 (l - l_0 + y)\dot{\varphi}^2.\end{gathered} \tag{4.8}$$

Substituting obtained solutions into Lagrange equations (4.1), and performing transformations we obtain mathematical model, corresponding to Fig. 4.1:

$$\begin{cases}\left[m_1 l^2 + m_2 (l - l_0 + y)^2\right]\cdot \ddot{\varphi} + b_1 \dot{\varphi} + 2 m_2 (l - l_0 + y)\dot{\varphi}\dot{y} + m_1 \mu l \sin\varphi + \\ \qquad + m_2 \mu (l - l_0 + y)\sin\varphi = M(\omega_1 t), \\ m_2 \ddot{y} + b_2 \dot{y} + c_2 y - m_2 (l - l_0 + y)\dot{\varphi}^2 + m_2 \mu (1 - \cos\varphi) = 0,\end{cases} \tag{4.9}$$

where φ – angle of rotation, read-out from a vertical line; $\dot{\varphi}$ – angular velocity; y – displacement of the sliding mass, read-out from a quiescent state; $\dot{y}$ – velocity of the sliding mass; m_1 – pendulum mass, l – length of the pendulum; m_2 – second mass, l_0 – quiescent state of the sliding mass; μ – gravitational constant; b_1, b_2 – linear damping coefficients of the pendulum and the sliding mass; c_2 – linear stiffness coefficient of the sliding mass.

External periodically excited moment, which acts on suspension point, has the following form:

$$M(\omega_1 t) = h_1 \cos\omega_1 t, \tag{4.10}$$

where h_1 и ω_1 – amplitude and frequency of excitation.

Substituting (4.10) into (4.9) we get following equations of motion:

$$\begin{cases}\left[m_1 l^2 + m_2 (l - l_0 + y)^2\right]\cdot \ddot{\varphi} + b_1 \dot{\varphi} + 2 m_2 (l - l_0 + y)\dot{\varphi}\dot{y} + m_1 \mu l \sin\varphi + \\ \qquad + m_2 \mu (l - l_0 + y)\sin\varphi = h_1 \cos\omega_1 t, \\ m_2 \ddot{y} + b_2 \dot{y} + c_2 y - m_2 (l - l_0 + y)\dot{\varphi}^2 + m_2 \mu (1 - \cos\varphi) = 0,\end{cases} \tag{4.11}$$

In the next sections the variable parameters of the pendulum system are amplitude h_1 and frequency ω_1 of excitation. Other parameters are fixed: m_1 = 1, m_2 = 0.1, l = 1, l_0 = 0.25, b_1 = 0.2, b_2 = 0.1, c_2 = 2, μ = 10.

Therefore, the equations of motion (4.11) of the first studied 2DOF pendulum system with external periodically excited moment were obtained.

4.2.2 Bifurcation diagrams and rare attractors in the pendulum model with a sliding mass with varying frequency of excitation force

As it was mentioned in the second chapter, the method of parameter continuation of periodic regimes is an effective tool for the study of nonlinear dynamical systems with varying parameters. With this method it is easy to search for the regions of existence of an infinite number of unstable periodic solutions (UPI), where there may be irregular movement (see Paragraph 2.7). Therefore, it is given much attention to the construction of bifurcation diagrams. The most obvious is to present the results of bifurcation analysis performed by the parameter continuation of the periodic regimes and by the scanning of phase space on the same diagram. In this case, it is possible to estimate the amplitudes of both periodic and quasi-periodic or chaotic motions. Therefore, we can conclude that construction of two-parameter bifurcation diagram on in the parameter plane for analysis of the behavior of dynamical systems within the given parameter range is the most time consuming, but necessary process [107].

In order to get the basic results needed in the study of regular and chaotic forced oscillations in the pendulum systems with two degrees of freedom and with the external periodic exciting moment the bifurcation analysis of forced oscillations has performed.

At the first stage the stable and unstable periodic P1 regimes (with the coordinates of the fixed points x_p and v_p) with the period of excitation T_ω for several values of $\omega_1 \in (0 \div 5)$ were searching. Then, the solutions of period-1 of 1T bifurcation group were continued by varying the frequency ω_1 from the found fixed points. After this the protuberances with period-2 were built from the bifurcation points of the branches of P1 solutions.

The results of bifurcation analysis in the pendulum system with a sliding mass and with the external periodic excited moment obtained by the method of complete bifurcation groups are presented in Figs. 4.2 and 4.3. Bifurcation diagrams S1(ω_1) and S5(ω_1) of the fixed periodic points of the coordinates φ, $\dot{\varphi}$ and Am_φ of the pendulum versus frequency ω_1 of excitation force are plotted on Fig. 4.2. For the second mass the bifurcation diagrams S1(ω_1) and S5(ω_1) of the fixed periodic points of the coordinates y, $\dot{y}$ and Am_y versus frequency ω_1 of excitation force are plotted on Fig. 4.3. There are symmetry breaking, period doubling, Andronov-Hopf and fold bifurcations in the pendulum system with a sliding mass and with the external periodic excited moment. The tip type subharmonic P5 RA rare attractor was found as well.

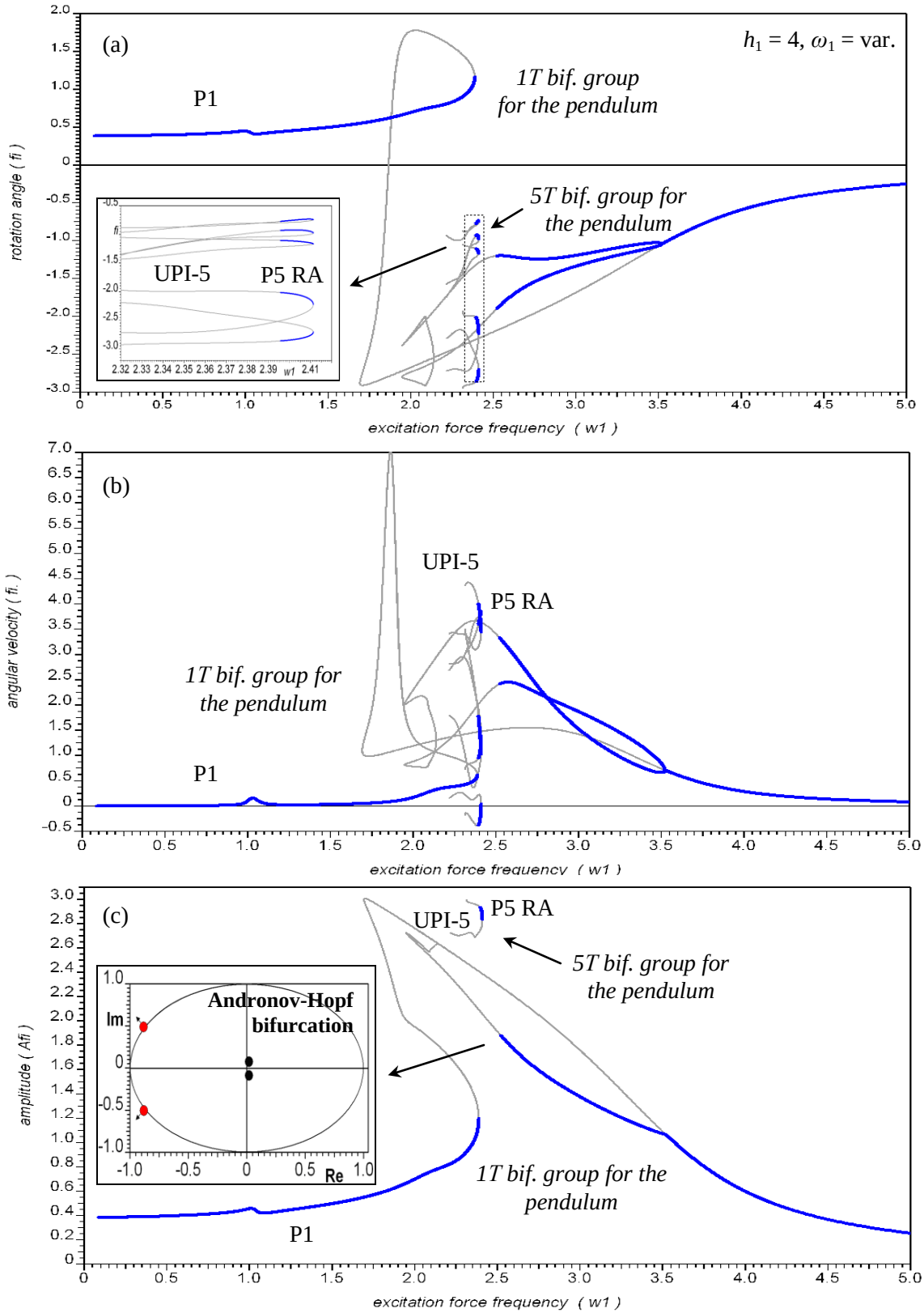

Fig. 4.2. Bifurcation diagrams S1(ω_1) and S5(ω_1) of the fixed periodic points of the coordinates φ, $\dot{\varphi}$ and Am_φ of the pendulum versus frequency ω_1 of excitation force. There are symmetry breaking, period doubling, Andronov-Hopf and fold bifurcations in the pendulum system with a sliding mass and with the external periodic excited moment. There is the tip type subharmonic P5 RA rare attractor. Parameters: m_1 = 1, m_2 = 0.1, l = 1, l_0 = 0.25, b_1 = 0.2, b_2 = 0.1, c_2 = 2, μ = 10, h_1 = 4, ω_1 = var.

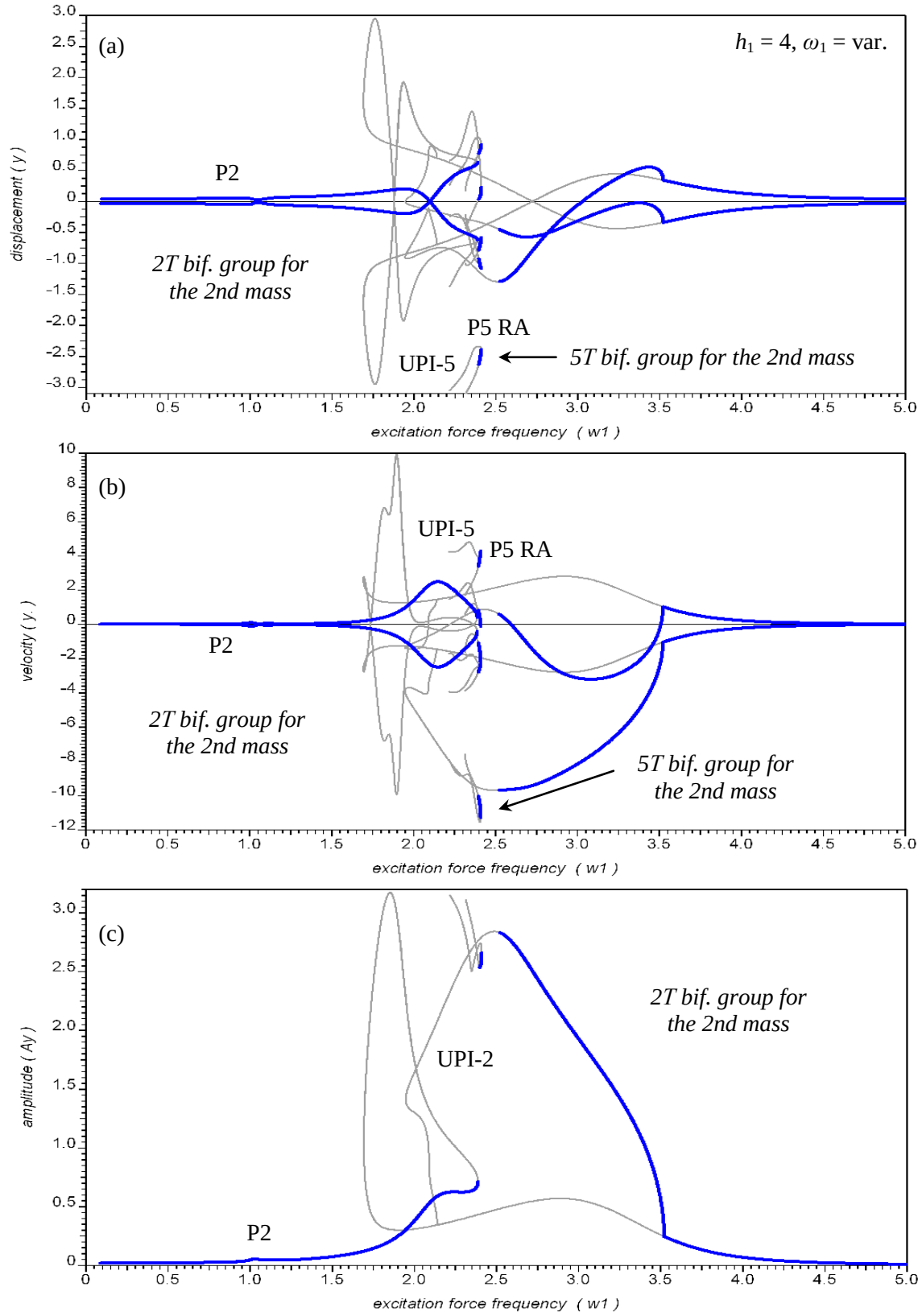

Fig. 4.3. Bifurcation diagrams S1(ω_1) and S5(ω_1) of the fixed periodic points of the coordinates y, $\dot{y}$ and Am_y of the second mass versus frequency ω_1 of excitation force. There are symmetry breaking, period doubling, Andronov-Hopf and fold bifurcations in the pendulum system with a sliding mass and with the external periodic excited moment. There is the tip type subharmonic P5 RA rare attractor. Parameters: m_1 = 1, m_2 = 0.1, l = 1, l_0 = 0.25, b_1 = 0.2, b_2 = 0.1, c_2 = 2, μ = 10, h_1 = 4, ω_1 = var.

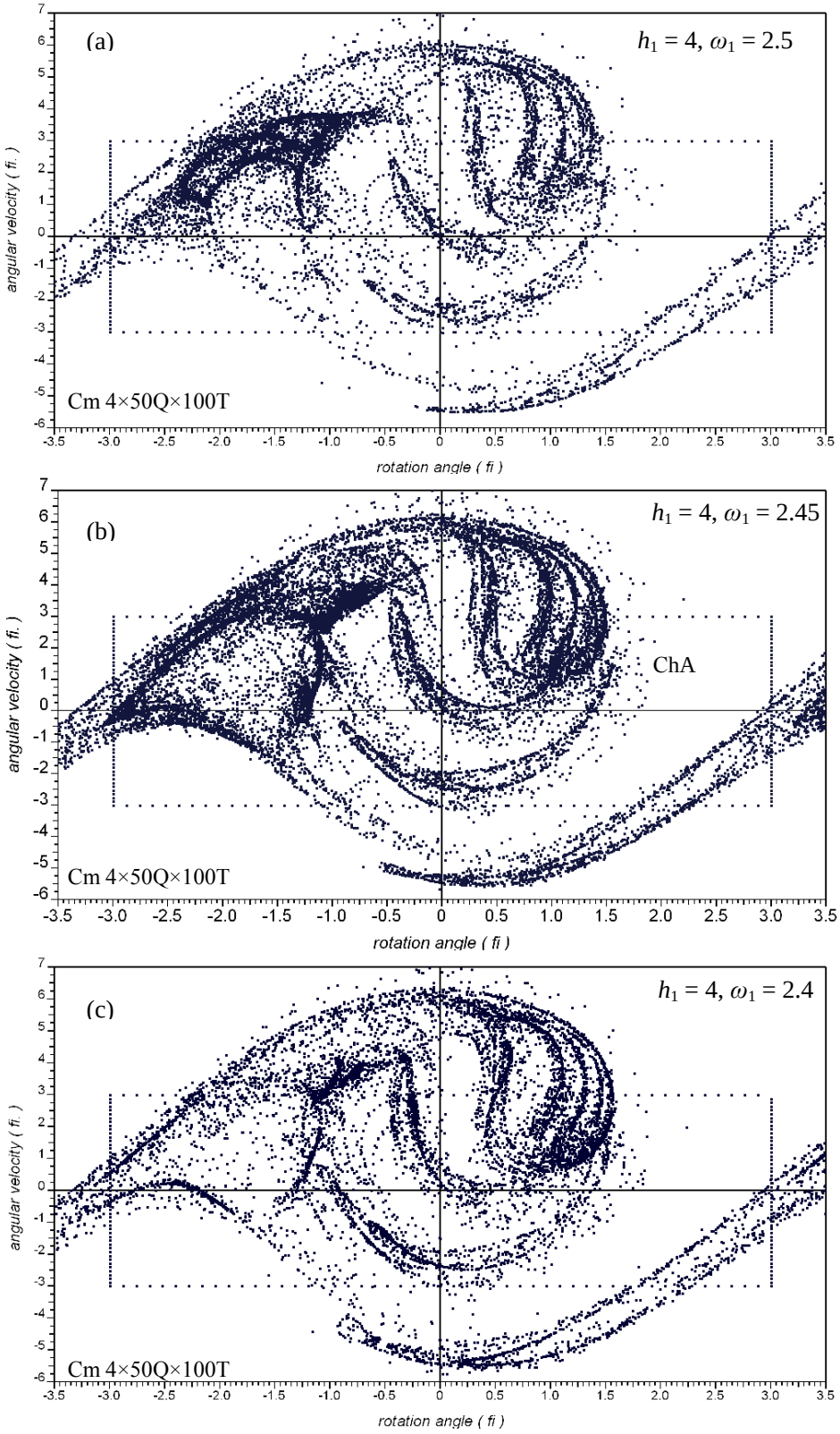

Fig. 4.4. Global chaotic attractor ChA on Poincaré map Cm 4×50Q×250T in the pendulum system with a sliding mass and with the external periodic excited moment (Eq. 4.11) for cross-section of bifurcation diagrams (see Figs.4.2, 4.3). Parameters: $m_1 = 1$, $m_2 = 0.1$, $l = 1$, $l_0 = 0.25$, $b_1 = 0.2$, $b_2 = 0.1$, $c_2 = 2$, $\mu = 10$, $h_1 = 4$, (a) $\omega_1 = 2.5$, (b) $\omega_1 = 2.45$, (c) $\omega_1 = 2.4$.

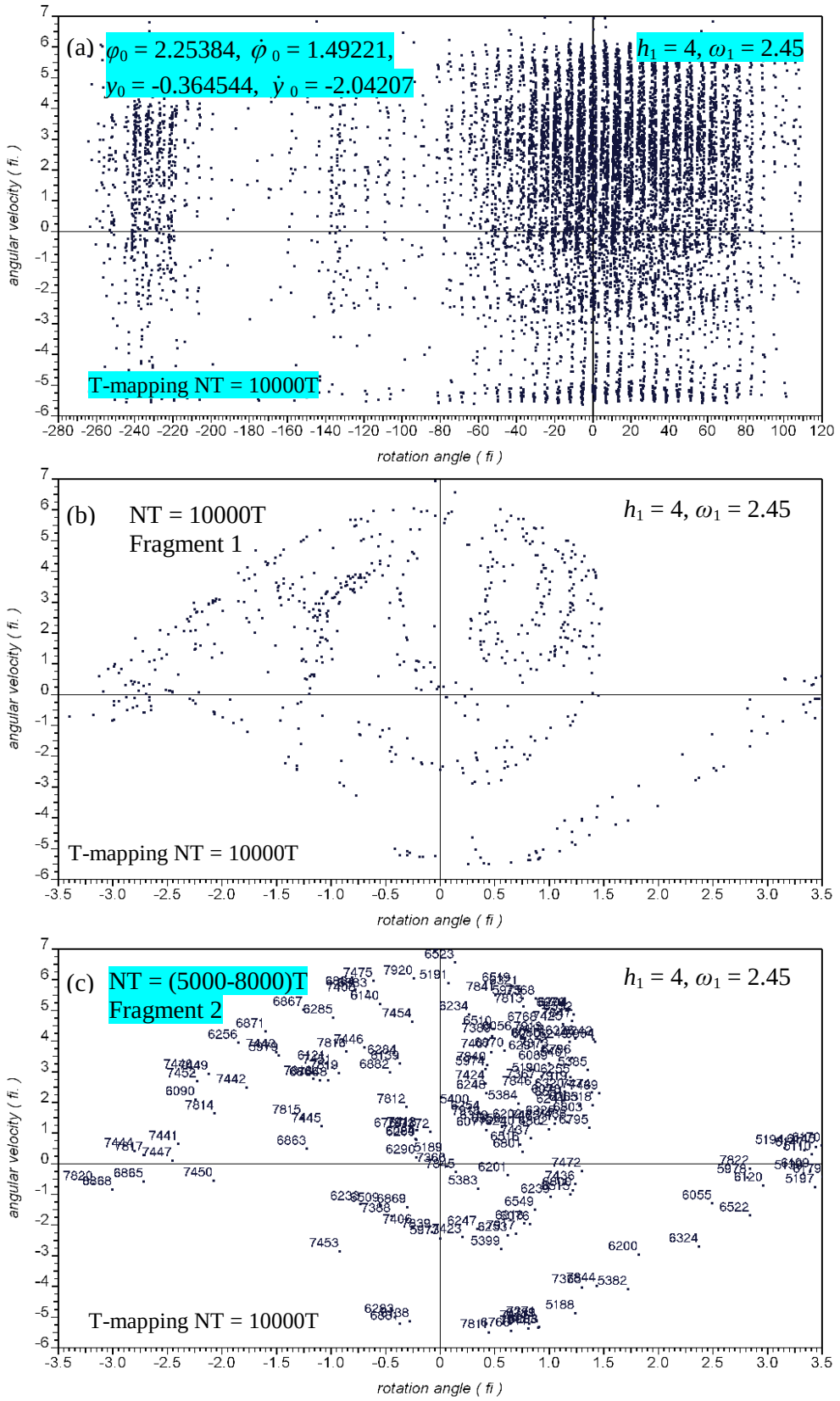

Fig. 4.5. (a) Global chaotic attractor ChA (see Figs. 4.2, 4.4b) obtained by T-mapping on Poincaré map NT = 10000T. (b),(c) Fragments of Poincaré mapping. Parameters: m_1 = 1, m_2 = 0.1, l = 1, l_0 = 0.25, b_1 = 0.2, b_2 = 0.1, c_2 = 2, μ = 10, h_1 = 4, ω_1 = 2.45.

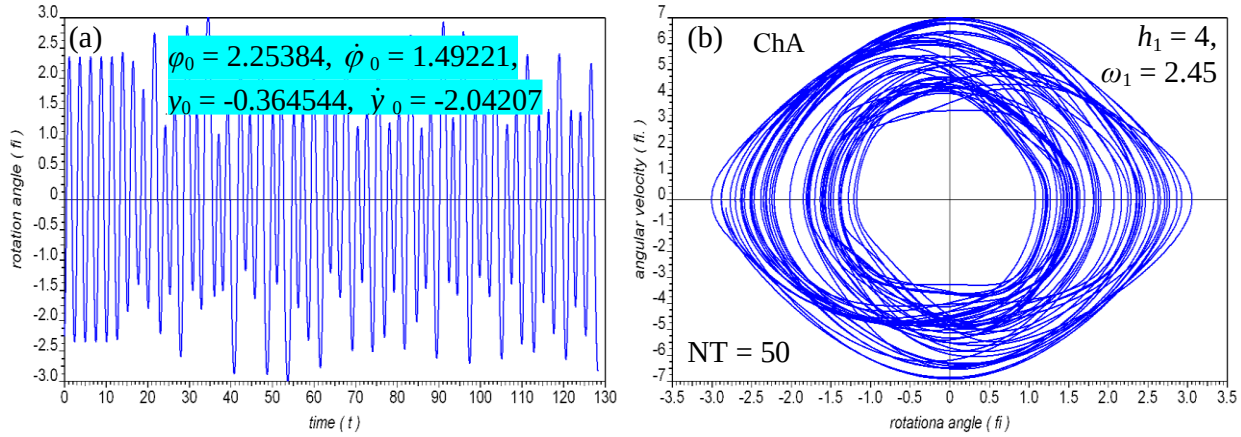

Fig. 4.6. Chaotic attractor ChA-1 (see Figs. 4.2, 4.4b, 4.5) on time history diagram and phase portrait. Parameters: $m_1 = 1$, $m_2 = 0.1$, $l = 1$, $l_0 = 0.25$, $b_1 = 0.2$, $b_2 = 0.1$, $c_2 = 2$, $\mu = 10$, $h_1 = 4$, $\omega_1 = 2.45$.

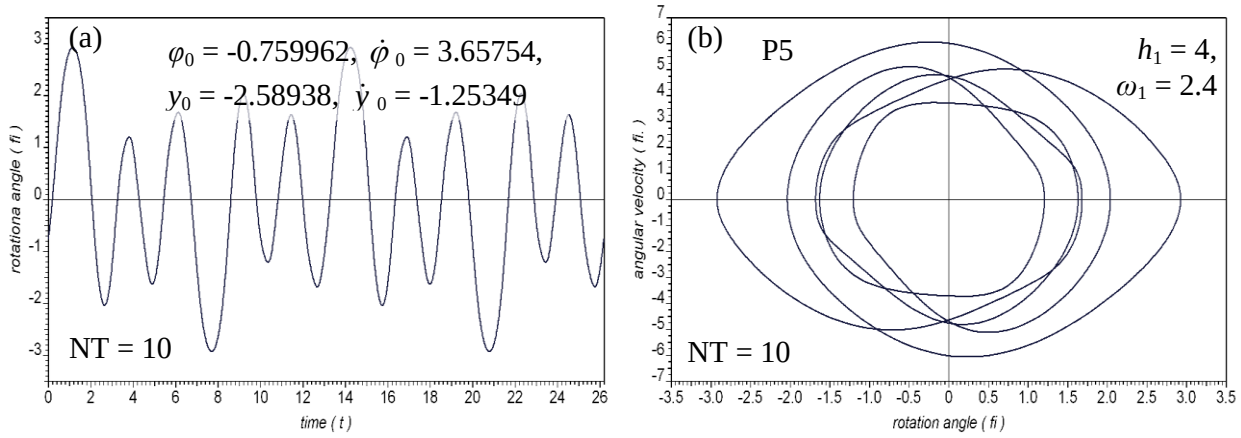

Fig. 4.7. Rare attractor P5 RA (see Figs. 4.2, 4.3) on time history diagram and phase portrait. Parameters: $m_1 = 1$, $m_2 = 0.1$, $l = 1$, $l_0 = 0.25$, $b_1 = 0.2$, $b_2 = 0.1$, $c_2 = 2$, $\mu = 10$, $h_1 = 4$, $\omega_1 = 2.45$.

In the studied pendulum system (4.11) one 1T bifurcation group was found. It has a stable P1 regime with the period T_ω of excitation force and P1 unstable one. This bifurcation group has symmetry breaking, period doubling, Andronov-Hopf and fold bifurcations. As well as in parameter range $\omega_1 \in (2.217 \div 2.411)$ between the fold and Andronov-Hopf bifurcations the new 5T bifurcation group was found. It has tip type rare attractor P5 RA with large amplitudes of oscillations, which is plotted on time history diagram and phase portrait in Fig. 4.7.

The examples for contour mappings on Poincaré map for different values of frequency $\omega_1 = 2.5$; 2.45; 2.4 of excitation in the pendulum system with a sliding mass and with the external periodic excited moment are plotted in Fig. 4.4. The global chaotic attractor ChA is plotted on Poincaré map in Fig.4.5, in time history diagram and phase portrait in Fig. 4.6.

Therefore, the qualitative behavior of the pendulum system with two degrees of freedom by varying the frequency ω_1 of the external periodic exciting moment was investigated. The new qualitative results of the topology of the bifurcation groups with a rare regular P5 RA and chaotic attractor ChA were obtained.

The results of bifurcation analysis in the pendulum system with a sliding mass and with the external periodic excited moment by varying amplitude h_1 of excitation force are presented in the next paragraph.

4.2.3 Bifurcation diagrams and rare attractors in the pendulum model with a sliding mass with varying amplitude of excitation force

The results of bifurcation analysis in the pendulum system with a sliding mass and with the external periodic excited moment obtained by the method of complete bifurcation groups are presented in Figs. 4.8 and 4.9. Bifurcation diagrams S1(h_1) and S2(h_1) of the fixed periodic points of the coordinates φ, $\dot{\varphi}$ and Am_φ of the pendulum versus amplitude h_1 of excitation force are plotted on Fig. 4.8. For the second mass the bifurcation diagrams S1(h_1) and S2(h_1) of the fixed periodic points of the coordinates y, $\dot{y}$ and Am_y versus amplitude h_1 of excitation force are plotted on Fig. 4.9.

In the studied pendulum system (4.11) one 1T bifurcation group was found. It has a stable P1 regime with the period T_ω of excitation force and P1 unstable one. This bifurcation group has symmetry breaking, period doubling and fold bifurcations. As well as in parameter range $h_1 \in (3.375 \div 7.0)$ the new 2T bifurcation group was found. It has tip type rare attractor P2 RA with large amplitudes of oscillations. Coexistence of two P1 RA and P2 RA rare attractors with main stable regime P1 on time history diagram and phase portrait for two different cross-sections of bifurcation diagrams (see Fig. 4.8-4.9) is shown in Fig. 4.10. For the cross-section $h_1 = 1.25$ the amplitudes of oscillations of the pendulum are Am(P1) = 0.193 and Am(P1 RA) = 2.626, but for the cross-section $h_1 = 3.37$ the pendulum has the amplitudes of oscillations Am(P1) = 0.560 and Am(P1 RA) = 2.722.

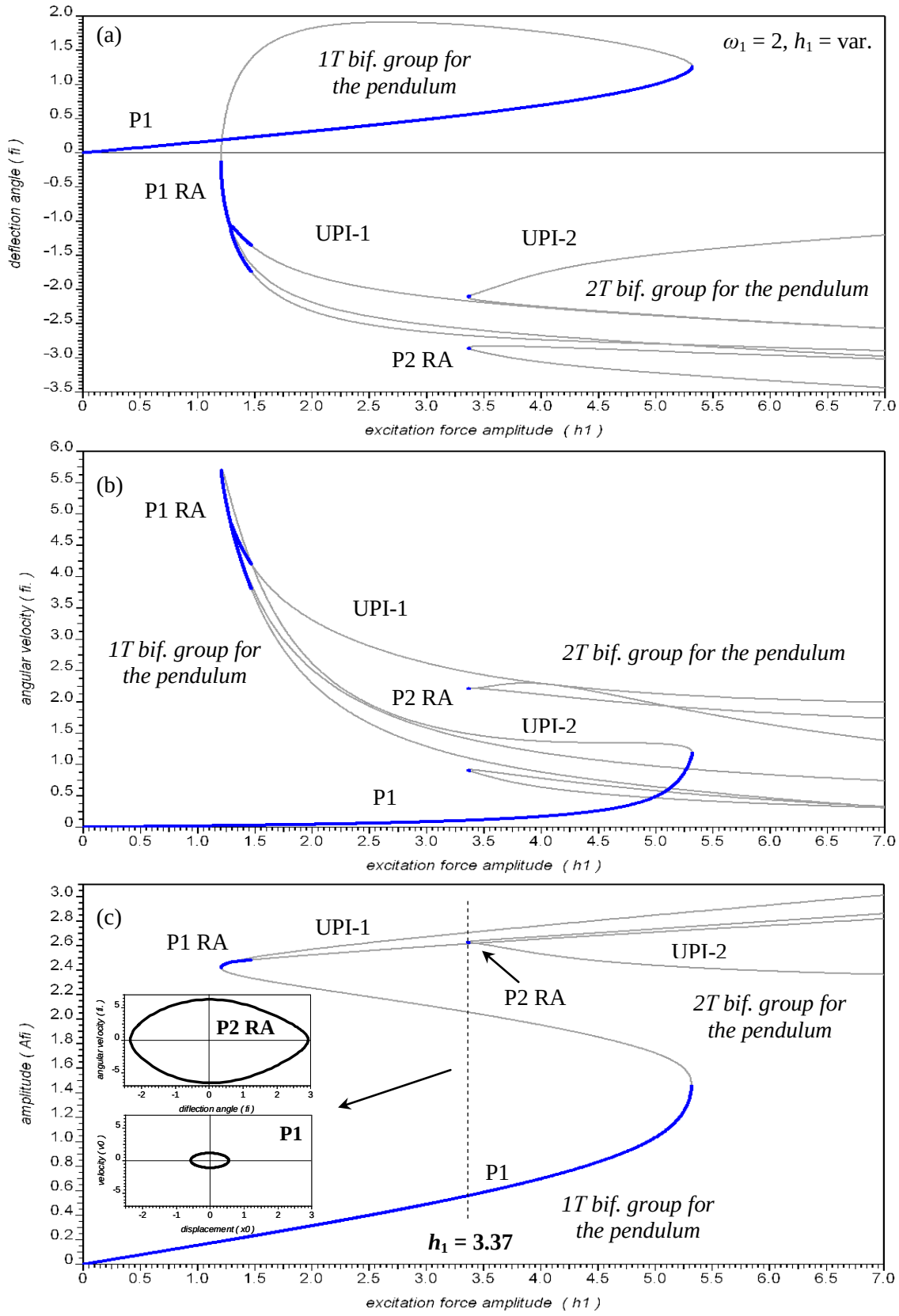

Fig. 4.8. Bifurcation diagrams S1(h_1) and S2(h_1) of the fixed periodic points of the coordinates φ, $\dot{\varphi}$ and Am_φ of the pendulum versus amplitude h_1 of excitation force. The studied pendulum system has symmetry breaking, period doubling and fold bifurcations, as well as tip type P1 RA and P2 RA rare attractors. Parameters: $m_1 = 1$, $m_2 = 0.1$, $l = 1$, $l_0 = 0.25$, $b_1 = 0.2$, $b_2 = 0.1$, $c_2 = 2$, $\mu = 10$, $\omega_1 = 2$, h_1 = var.

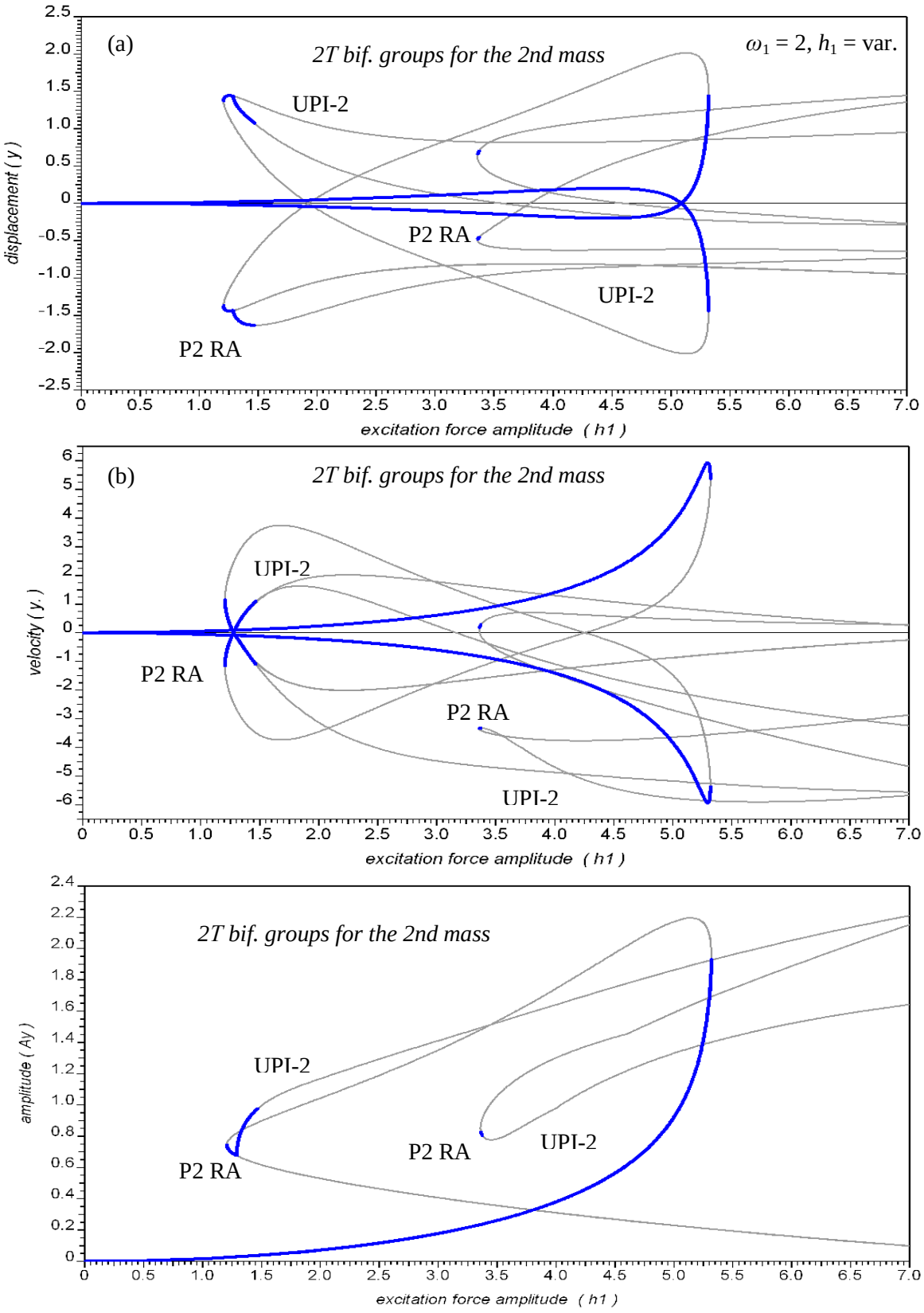

Fig. 4.9. Bifurcation diagrams S1(h_1) and S2(h_1) of the fixed periodic points of the coordinates y, $\dot{y}$ and Am_y of the second mass versus amplitude h_1 of excitation force. The studied pendulum system has symmetry breaking, period doubling and fold bifurcations, as well as tip type P1 RA and P2 RA rare attractors. Parameters: $m_1 = 1$, $m_2 = 0.1$, $l = 1$, $l_0 = 0.25$, $b_1 = 0.2$, $b_2 = 0.1$, $c_2 = 2$, $\mu = 10$, $\omega_1 = 2$, h_1 = var.

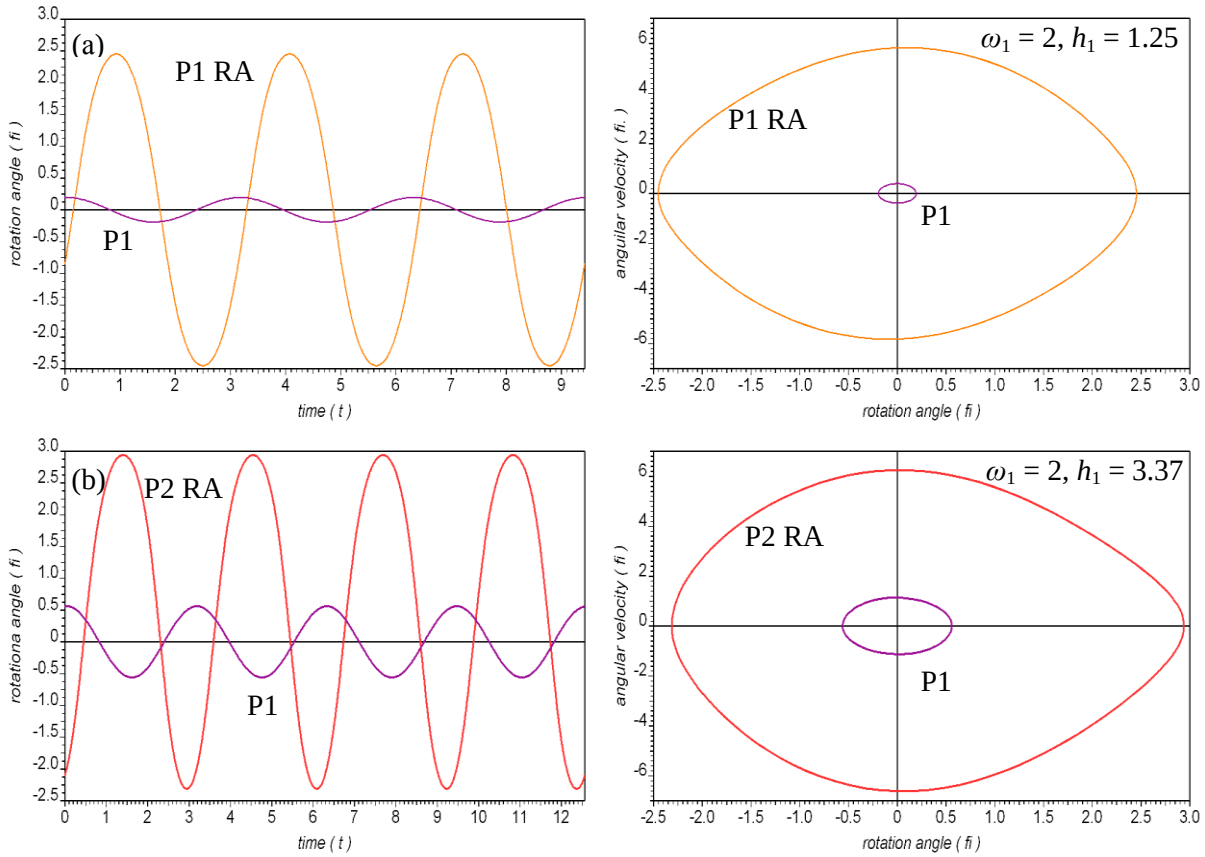

Fig. 4.10. Coexistence of two P1 RA and P2 RA rare attractors with main stable regime P1 on time history diagram and phase portrait for two different cross-sections of bifurcation diagrams (see Fig. 4.8-4.9): (a) for h_1 = 1.25, where the amplitudes of oscillations of the pendulum are *Am*(P1) = 0.193 and *Am*(P1 RA) = 2.626; (b) for h_1 =3.37, where the amplitudes of oscillations of the pendulum are *Am*(P1) = 0.560 and *Am*(P1 RA) = 2.722. Parameters: m_1 = 1, m_2 = 0.1, l = 1, l_0 = 0.25, b_1 = 0.2, b_2 = 0.1, c_2 = 2, μ = 10, ω_1 = 2, (a) h_1 = 1.25, (b) h_1 = 3.37.

Therefore, the qualitative behavior of the pendulum system with a sliding mass and with the external periodic excited moment by varying the frequency ω_1 and the amplitude h_1 of the excitation was investigated using the method of complete bifurcation groups. The new qualitative results of the topology of the bifurcation groups with rare regular P1 RA, P2 RA, P5 RA attractors and chaotic ChA attractor were obtained.

Hence, it is reasonably safe to suggest that there are rare attractors in more complex pendulum-like models of the mechanical systems with two or many degrees of freedom. For example, the dynamical models of satellites, the space tether systems with the engine [18], etc. The usefulness of the study of pendulum systems with 2ODF by the method of complete bifurcation groups is shown using the example of the pendulum system with a sliding mass and with the external periodic excited moment. The obtained results can be useful for the problems of controllability and stability of the spacecraft to avoid catastrophic or unexpected nonlinear phenomena with larger amplitudes [126].

4.3 Bifurcation analysis of the double pendulum with the periodically vibrating point of suspension in vertical direction

4.3.1 Equations of motion of the studied double pendulum

Let us consider the second 2DOF pendulum by the example of double pendulum system (Fig. 4.11). Suspension point periodically vibrates in vertical direction.

The generalized coordinates q will be angles of rotation of the two pendulums φ_1 and φ_2, read-out from a vertical line. Then the Lagrange equations of the second kind have the following form:

$$\begin{cases} \dfrac{d}{dt}\left(\dfrac{\partial L}{\partial \dot{\varphi}_1}\right) - \dfrac{\partial L}{\partial \varphi_1} = 0, \\ \dfrac{d}{dt}\left(\dfrac{\partial L}{\partial \dot{\varphi}_2}\right) - \dfrac{\partial L}{\partial \varphi_2} = 0, \end{cases} \tag{4.12}$$

where φ_1 and φ_2 – angles of rotation of the first and the second pendulums accordingly; $\dot{\varphi}_1$, $\dot{\varphi}_2$ – angular velocities of the first and the second pendulums accordingly, where $\dot{\varphi}_{1,2} = d\varphi_{1,2}/dt$; t – time, read-out from the moment when axis of the pendulums coincide with a vertical line; L – Lagrangian, where $L = E_k - E_p$; E_k and E_p – kinetic and potential energies accordingly.

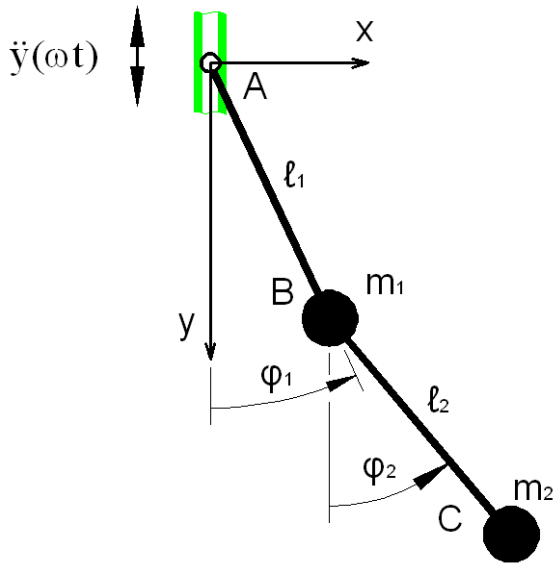

Fig. 4.11. The studied double pendulum with the periodically vibrating point of suspension in vertical direction.

For following derivation of equations of motion we will use following expressions:

$$\begin{gathered} x_B = l_1 \sin\varphi_1,\ y_B = -l_1 \cos\varphi_1 + y(\omega t); \\ x_C = l_1 \sin\varphi_1 + l_2 \sin\varphi_2,\ y_C = -l_1 \cos\varphi_1 - l_2 \cos\varphi_2 + y(\omega t), \end{gathered} \tag{4.13}$$

where x_B, y_B, x_C, y_C – coordinates of the centers of gravity of the first pendulum B and the second pendulum C accordingly; t – time, read-out from the moment when axis of the pendulums coincide with a vertical line.

Thus, potential energy of the system:

$$\begin{gathered} E_p = m_1 \mu y_B + m_2 \mu y_C = m_1 \mu\left[l_1(1-\cos\varphi_1) + y(\omega t)\right] + \\ + m_2 \mu\left[l_1(1-\cos\varphi_1) + l_2(1-\cos\varphi_2) + y(\omega t)\right]. \end{gathered} \tag{4.14}$$

Kinetic energy of the system:

$$E_k = \frac{1}{2} m_1 \upsilon_B^2 + \frac{1}{2} m_2 \upsilon_C^2. \tag{4.15}$$

Projections of the velocities υ_B and υ_C of the centers of gravity of masses B and C are obtained from (4.13):

$$\begin{gathered} \dot{x}_B = l_1 \dot{\varphi}_1 \cos\varphi_1,\ \dot{y}_B = l_1 \dot{\varphi}_1 \sin\varphi_1 + \dot{y}(\omega t); \\ \dot{x}_C = l_1 \dot{\varphi}_1 \cos\varphi_1 + l_2 \dot{\varphi}_2 \cos\varphi_2,\ \dot{y}_B = l_1 \dot{\varphi}_1 \sin\varphi_1 + l_2 \dot{\varphi}_2 \sin\varphi_2 + \dot{y}(\omega t). \end{gathered} \tag{4.16}$$

Hence:

$$\upsilon_B^2 = \dot{x}_B^2 + \dot{y}_B^2 = \left[l_1 \dot{\varphi}_1 \cos\varphi_1\right]^2 + \left[l_1 \dot{\varphi}_1 \sin\varphi_1 + \dot{y}(\omega t)\right]^2 = l_1^2 \dot{\varphi}_1^2 + \dot{y}^2(\omega t) + 2 l_1 \dot{\varphi}_1 \dot{y}(\omega t) \sin\varphi_1;$$

$$\upsilon_C^2 = \dot{x}_C^2 + \dot{y}_C^2 = \left[l_1 \dot{\varphi}_1 \cos\varphi_1 + l_2 \dot{\varphi}_2 \cos\varphi_2\right]^2 + \left[l_1 \dot{\varphi}_1 \sin\varphi_1 + l_2 \dot{\varphi}_2 \sin\varphi_2 + \dot{y}(\omega t)\right]^2 = \tag{4.17}$$

$$= l_1^2 \dot{\varphi}_1^2 + l_2^2 \dot{\varphi}_2^2 + \dot{y}^2(\omega t) + + 2 l_1 \dot{\varphi}_1 \dot{y}(\omega t) \sin\varphi_1 + 2 l_2 \dot{\varphi}_2 \dot{y}(\omega t) \sin\varphi_2 + 2 l_1 l_2 \dot{\varphi}_1 \dot{\varphi}_2 \cos(\varphi_1 - \varphi_2).$$

Now substituting (4.17) into (4.15) we can get the Lagrangian:

$$\begin{gathered} L = E_k - E_p = \frac{m_1}{2}\left[l_1^2 \dot{\varphi}_1^2 + \dot{y}^2(\omega t) + 2 l_1 \dot{\varphi}_1 \dot{y}(\omega t) \sin\varphi_1\right] + \frac{m_2}{2}\left[l_1^2 \dot{\varphi}_1^2 + l_2^2 \dot{\varphi}_2^2 + \dot{y}^2(\omega t)\right. \\ \left. + 2 l_1 \dot{\varphi}_1 \dot{y}(\omega t) \sin\varphi_1 + 2 l_2 \dot{\varphi}_2 \dot{y}(\omega t) \sin\varphi_2 + 2 l_1 l_2 \dot{\varphi}_1 \dot{\varphi}_2 \cos(\varphi_1 - \varphi_2)\right] - \\ - m_1 \mu\left[l_1(1-\cos\varphi_1) + y(\omega t)\right] - m_2 \mu\left[l_1(1-\cos\varphi_1) + l_2(1-\cos\varphi_2) + y(\omega t)\right]. \end{gathered} \tag{4.18}$$

In this case kinetic energy depends on generalized coordinates (φ_1, φ_2) and velocities ($\dot{\varphi}_1$, $\dot{\varphi}_2$) and on time (t). Then we find partial derivatives of energies:

$$\begin{aligned}
&\frac{\partial L}{\partial \dot{\varphi}_1} = m_1\left[l_1^2\dot{\varphi}_1 + l_1\dot{y}(\omega t)\sin\varphi_1\right] + m_2\left[l_1^2\dot{\varphi}_1 + l_1\dot{y}(\omega t)\sin\varphi_1 + l_1 l_2\dot{\varphi}_2\cos(\varphi_1-\varphi_2)\right];\\
&\frac{\partial L}{\partial \dot{\varphi}_2} = m_2\left[l_2^2\dot{\varphi}_2 + l_2\dot{y}(\omega t)\sin\varphi_2 + l_1 l_2\dot{\varphi}_1\cos(\varphi_1-\varphi_2)\right];\\
&\frac{d}{dt}\left(\frac{\partial L}{\partial \dot{\varphi}_1}\right) = m_1\left[l_1^2\ddot{\varphi}_1 + l_1\ddot{y}(\omega t)\sin\varphi_1 + l_1\dot{\varphi}_1\dot{y}(\omega t)\cos\varphi_1\right] + m_2\left[l_1^2\ddot{\varphi}_1 + l_1\ddot{y}(\omega t)\sin\varphi_1 + \right.\\
&\left. + l_1\dot{\varphi}_1\dot{y}(\omega t)\cos\varphi_1 + l_1 l_2\ddot{\varphi}_2\cos(\varphi_1-\varphi_2) - l_1 l_2\dot{\varphi}_2\sin(\varphi_1-\varphi_2)\cdot(\dot{\varphi}_1-\dot{\varphi}_2)\right];\\
&\frac{d}{dt}\left(\frac{\partial L}{\partial \dot{\varphi}_2}\right) = m_2\left[l_2^2\ddot{\varphi}_2 + l_2\ddot{y}(\omega t)\sin\varphi_2 + l_2\dot{\varphi}_2\dot{y}(\omega t)\cos\varphi_2 + \right.\\
&\left. + l_1 l_2\ddot{\varphi}_1\cos(\varphi_1-\varphi_2) - l_1 l_2\dot{\varphi}_1\sin(\varphi_1-\varphi_2)\cdot(\dot{\varphi}_1-\dot{\varphi}_2)\right];\\
&\frac{\partial L}{\partial \varphi_1} = m_1 l_1\dot{\varphi}_1\dot{y}(\omega t)\cos\varphi_1 - m_1\mu l_1\sin\varphi_1 + m_2\left[l_1\dot{\varphi}_1\dot{y}(\omega t)\cos\varphi_1 - \right.\\
&\left. - l_1 l_2\dot{\varphi}_1\dot{\varphi}_2\sin(\varphi_1-\varphi_2) - \mu l_1\sin\varphi_1\right];\\
&\frac{\partial L}{\partial \varphi_2} = m_2\left[l_2\dot{\varphi}_2\dot{y}(\omega t)\cos\varphi_2 - l_1 l_2\dot{\varphi}_1\dot{\varphi}_2\sin(\varphi_1-\varphi_2) - \mu l_2\sin\varphi_2\right]
\end{aligned} \tag{4.19}$$

Substituting (4.19) into (4.12) we obtain the mathematical pendulum model, corresponding to Fig. 4.11:

$$\begin{cases}
(m_1+m_2)\cdot l_1^2\cdot\ddot{\varphi}_1 + m_2 l_1 l_2\cos(\varphi_1-\varphi_2)\cdot\ddot{\varphi}_2 + b_1\dot{\varphi}_1 + b_2(\dot{\varphi}_1-\dot{\varphi}_2) + \\
+ c_1\varphi_1 + c_2(\varphi_1-\varphi_2) + (m_1+m_2)\cdot\mu l_1\sin\varphi_1 + (m_1+m_2)\cdot l_1\ddot{y}(\omega t)\sin\varphi_1 + \\
+ m_2 l_1 l_2\dot{\varphi}_2^2\sin(\varphi_1-\varphi_2) = 0, \\
m_2 l_2^2\cdot\ddot{\varphi}_2 + m_2 l_1 l_2\cos(\varphi_1-\varphi_2)\cdot\ddot{\varphi}_1 + b_2(\dot{\varphi}_2-\dot{\varphi}_1) + c_2(\varphi_2-\varphi_1) + \\
+ m_2\mu l_2\sin\varphi_2 + m_2\cdot l_2\ddot{y}(\omega_2 t)\sin\varphi_2 - m_2 l_1 l_2\dot{\varphi}_1^2\sin(\varphi_1-\varphi_2) = 0,
\end{cases} \tag{4.20}$$

where m_1 and m_2 – mass of the first and the second pendulums accordingly, l_1 and l_2 – length of the first and the second pendulums accordingly; μ – gravitational constant; b_1, b_2 – linear damping coefficients; c_1, c_2 – linear stiffness coefficients of restoring forces; $y(\omega t)$ - periodical excitation, which acts on suspension point in vertical direction; $\ddot{y}(\omega t)$ - acceleration of the suspension point in vertical direction due to the external periodic excitation.

Periodical excitation, which acts on suspension point, has the following form:

$$y(\omega t) = h\cos\omega t, \tag{4.21}$$

where h и ω – amplitude and frequency of excitation.

Substituting (4.21) into (4.21) and transforming by the accelerations we get the following equations of motion discussed below:

$$\begin{cases} \left[(m_1+m_2)l_1^2 - m_2 l_1^2\cos^2(\varphi_1-\varphi_2)\right]\ddot{\varphi}_1 + b_1\dot{\varphi}_1 + b_2(\dot{\varphi}_1-\dot{\varphi}_2)\left[1-\frac{l_1}{l_2}\cos(\varphi_1-\varphi_2)\right] + \\ + c_1\varphi_1 + c_2(\varphi_1-\varphi_2)\left[1-\frac{l_1}{l_2}\cos(\varphi_1-\varphi_2)\right] - \frac{1}{2}m_2 l_1^2\dot{\varphi}_1^2\sin 2(\varphi_1-\varphi_2) - \\ - m_2 l_1 l_2\dot{\varphi}_2^2\sin(\varphi_1-\varphi_2) - \mu l_1\left[(m_1+m_2)\sin\varphi_1 - m_2\sin\varphi_2\cos(\varphi_1-\varphi_2)\right] + \\ + h\omega^2\cos\omega t\left[(m_1+m_2)l_1\sin\varphi_1 - m_2 l_1\sin\varphi_2\cos(\varphi_1-\varphi_2)\right] = 0, \\ \left[m_2 l_2^2 - \frac{m_2^2 l_2^2}{(m_1+m_2)}\cos^2(\varphi_1-\varphi_2)\right]\ddot{\varphi}_2 + b_2(\dot{\varphi}_2-\dot{\varphi}_1)\left[1+\frac{m_2 l_2\cos(\varphi_1-\varphi_2)}{(m_1+m_2)l_1^2}\right] + \\ + c_2(\varphi_2-\varphi_1)\left[1+\frac{m_2 l_2\cos(\varphi_1-\varphi_2)}{(m_1+m_2)l_1^2}\right] - \frac{m_2 l_2 b_1}{(m_1+m_2)l_1}\dot{\varphi}_1\cos(\varphi_1-\varphi_2) - \\ - c_1\varphi_1\frac{m_2 l_2\cos(\varphi_1-\varphi_2)}{(m_1+m_2)l_1^2} - \frac{1}{2}\frac{m_2^2 l_2^2}{(m_1+m_2)}\dot{\varphi}_2^2\sin 2(\varphi_1-\varphi_2) - m_2 l_1 l_2\dot{\varphi}_1^2\sin(\varphi_1-\varphi_2) + \\ + m_2\mu l_2\left[\sin\varphi_2 - \sin\varphi_1\cos(\varphi_1-\varphi_2)\right] - m_2 l_2 h\omega^2\cos\omega t\left[\sin\varphi_2 - \sin\varphi_1\cos(\varphi_1-\varphi_2)\right] = 0 \end{cases} \quad (4.22)$$

In the next paragraphs the variable parameter of the double pendulum system is frequency ω of excitation. Other parameters are fixed: $m_1 = 1$, $m_2 = 0.1$, $l_1 = 1$, $l_2 = 0.5$, $b_1 = 0.2$, $b_2 = 0.1$, $c_1 = 1$, $c_2 = 0.5$, $\mu = 10$, $h = 3$. Similar models have been studied in works [7,51,54].

Therefore, the equations of motion (4.22) of the second studied 2DOF pendulum system with the periodically vibrating point of suspension in vertical direction (Fig. 4.11) were obtained. The construction of this investigated model in the software Spring is considered in the Appendix 2.

The studied double pendulum system can be used in many scientific research and engineering tasks. One of such problems can be the problem of the creation of robotic parts, which are actuated by vibrating suspension. These results can also be useful for the other robotic purposes, for the mixing process, such as liquids, washing machines, etc.

Author does not know any results of the global bifurcation analysis and any serious researches of rare attractors and of rare bifurcation groups in the double pendulum systems, but these studies, of course, are needed to pursue.

4.3.2 Construction of periodic skeleton for the double pendulum system

The example of the construction of periodic skeleton (PSK) in the double pendulum with the periodically vibrating point of suspension in vertical direction (4.22) for oscillating and rotating orbits (regimes, attractors) with order n = (1-2)T (see Table. 4.1) by using the Newton-Kantorovich method from the grid of initial conditions NQ = 20×20Q = 400Q (see Fig.4.12) inside the rectangle (-π, -3.0; π, 3.0) of coordinates φ_i and $\dot{\varphi}_i$ is shown below. The maximum number of iterations is KIN = 64 with precision search of the fixed point EPN = 1e-6 and parameter of discretisation DEN = 1e-5. Active boundaries are $\varphi_{i,\ min}$ = -π, $\varphi_{i,\ max}$ = π, $\dot{\varphi}_{i,min}$ = -10, $\dot{\varphi}_{i,max}$ = 10. For rotational orbits the cylindrical phase space was taken into account with period Lφ = 2π. Time of calculation of periodic skeleton was about 1 hour (the PC characteristics: Intel(R) Core(TM) i3-2120, CPU - 3.30GHz, RAM - 4 GB, Windows 7 SP1).

In the studied double pendulum system (4.22) constructed periodic skeleton for ω = 4 (see Table 4.1) consists of 10 periodic oscillating orbits (regimes, attractors): one stable regime P2 (2/1), one unstable zero regime P1 zero, two unstable P1 twins and two unstable P2 twins..

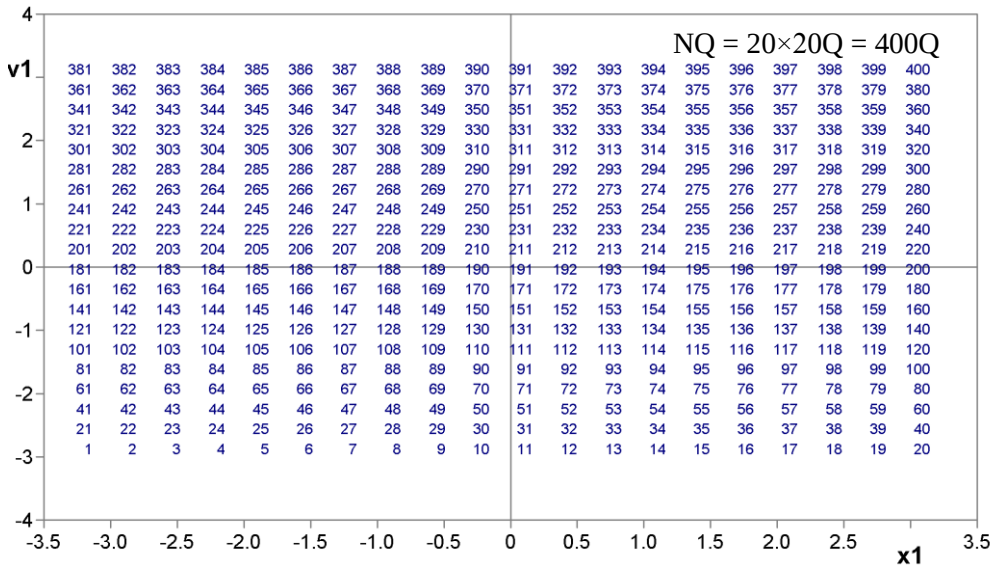

Fig. 4.12. A grid of 20×20 = 400Q initial conditions inside the rectangle (-π; -3.0 / π; 3.0) of coordinates φ_i and $\dot{\varphi}_i$ for construction of periodic skeleton in the double pendulum system (4.22). Parameters: m_1 = 1, m_2 = 0.1, l_1 = 1, l_2 = 0.5, b_1 = 0.2, b_2 = 0.1, c_1 = 1, c_2 = 0.5, μ = 10, h = 3, ω = 4, k = 7.

Table 4.1. Periodic skeleton in the double pendulum system (4.22). It consists of 10 periodic oscillating orbits (regimes, attractors), among them are one stable regime P2 (2/1), one unstable zero regime P1 zero, two unstable P1 twins and two unstable P2 twins. Parameters: $m_1 = 1$, $m_2 = 0.1$, $l_1 = 1$, $l_2 = 0.5$, $b_1 = 0.2$, $b_2 = 0.1$, $c_1 = 1$, $c_2 = 0.5$, $\mu = 10$, $h = 3$, $\omega = 4$, $k = 7$.

Nr.	Orbits	φ_i	$\dot{\varphi}_i$	ρ_{max}
A	P1 zero unstable	$\mathbf{x_1} = 0.0$ $\mathbf{x_2} = 0.0$	$\mathbf{v_1} = 0.0$ $\mathbf{v_2} = 0.0$	$\rho_{max} = -231.78224$
B	P2 (2/1) stable symmetric	$\mathbf{x_1} = 0.276939$ $\mathbf{x_2} = -0.046917$	$\mathbf{v_1} = -10.199898$ $\mathbf{v_2} = -8.719805$	$\rho_{max} = -0.625759$
C_1	P1 left (1/2) unstable, asymmetric	$\mathbf{x_1} = 3.240819$ $\mathbf{x_2} = 2.805736$	$\mathbf{v_1} = -0.158761$ $\mathbf{v_2} = -2.616683$	$\rho_{max} = 16.506502$
C_2	P1 right (1/2) unstable asymmetric	$\mathbf{x_1} = -3.240819$ $\mathbf{x_2} = -2.805736$	$\mathbf{v_1} = 0.158761$ $\mathbf{v_2} = 2.616683$	$\rho_{max} = 16.506502$
D_1	P1 left (1/1) unstable, asymmetric	$\mathbf{x_1} = 3.265967$ $\mathbf{x_2} = 3.701187$	$\mathbf{v_1} = 1.583380$ $\mathbf{v_2} = 3.113184$	$\rho_{max} = -57.091834$
D_2	P1 right (1/1) unstable asymmetric	$\mathbf{x_1} = -3.265967$ $\mathbf{x_2} = -3.701187$	$\mathbf{v_1} = -1.583380$ $\mathbf{v_2} = -3.113184$	$\rho_{max} = -57.091834$
E_1	P2 left (2/1) unstable, asymmetric	$\mathbf{x_1} = 0.014763$ $\mathbf{x_2} = -0.694774$	$\mathbf{v_1} = -5.871255$ $\mathbf{v_2} = -1.547396$	$\rho_{max} = 25.044109$
E_2	P2 right (2/1) unstable asymmetric	$\mathbf{x_1} = -0.014763$ $\mathbf{x_2} = 0.694774$	$\mathbf{v_1} = 5.871255$ $\mathbf{v_2} = 1.547396$	$\rho_{max} = 25.044077$
F_1	P2 left (2/2) unstable, asymmetric	$\mathbf{x_1} = 2.136442$ $\mathbf{x_2} = 2.787340$	$\mathbf{v_1} = 4.522155$ $\mathbf{v_2} = 9.290469$	$\rho_{max} = -73.052264$
F_2	P2 right (2/2) unstable asymmetric	$\mathbf{x_1} = -2.136442$ $\mathbf{x_2} = -2.787340$	$\mathbf{v_1} = -4.522155$ $\mathbf{v_2} = -9.290469$	$\rho_{max} = -73.052391$

Passport of periodic regime A

P1 zero **unstable** ($\rho_{max} = -231.78224$), symmetric

Fixed point

$\mathbf{x_1} = 0.0$ $\mathbf{v_1} = 0.0$
$\mathbf{x_2} = 0.0$ $\mathbf{v_2} = 0.0$

Phase portraits

m_1

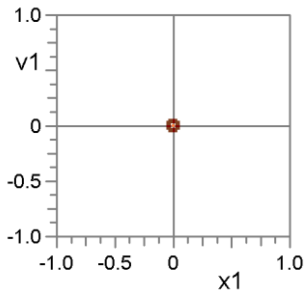

$\mathbf{x_1} = -0.0 \ldots 0.0$
$\mathbf{v_1} = -0.0 \ldots 0.0$
$\mathbf{Ax_1} = 0.0$

m_2

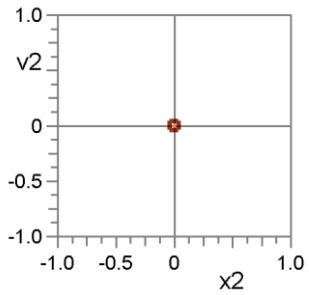

$\mathbf{x_2} = -0.0 \ldots 0.0$
$\mathbf{v_2} = -0.0 \ldots 0.0$
$\mathbf{Ax_2} = 0.0$

Stability

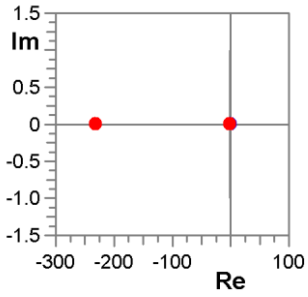

$\boldsymbol{\rho_1} = -0.000516$ $\boldsymbol{\alpha_1} = 180°$
$\boldsymbol{\rho_2} = -0.002844$ $\boldsymbol{\alpha_2} = 180°$
$\boldsymbol{\rho_3} = -1.830919$ $\boldsymbol{\alpha_3} = 180°$
$\boldsymbol{\rho_4} = -231.78224$ $\boldsymbol{\alpha_4} = 180°$

Passport of periodic regime B

P2 (2/1) **stable** (ρ_{max} = -0.625759), symmetric

Fixed point

x_1 = 0.276939 v_1 = -10.199898
x_2 = -0.046917 v_2 = -8.719805

Phase portraits

m_1

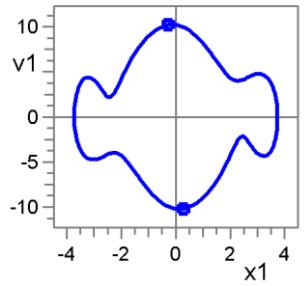

x_1 = -3.731872 … 3.731872
v_1 = -10.239464…10.239464
Ax_1 = 3.731872

m_2

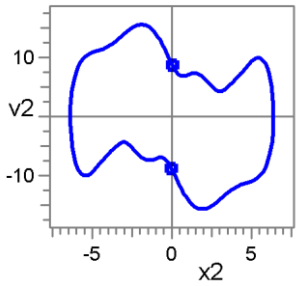

x_2 = -6.391426 … 6.391426
v_2 = -15.627044…15.627044
Ax_2 = 6.391426

Stability

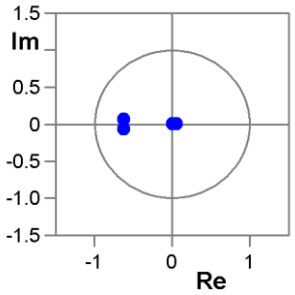

ρ_1 = 0.053987 α_1 = 0°
ρ_2 = 0.000001 α_2 = 0°
ρ_3 = -0.625759 α_3 = -174°
ρ_4 = -0.625759 α_4 = 174°

Passport of periodic regime C_1

P1 (1/2) left **unstable** (ρ_{max} = 16.506502), asymmetric, twin of regime C_2

Fixed point

x_1 = 3.240819 v_1 = -0.158761
x_2 = 2.805736 v_2 = -2.616683

Phase portraits

m_1

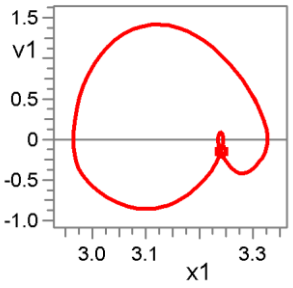

x_1 = 2.964357 … 3.327448
v_1 = -0.862846 … 1.413235
Ax_1 = 0.181546

m_2

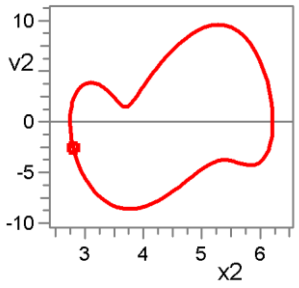

x_2 = 2.748749 … 6.219780
v_2 = -8.646199 … 9.580060
Ax_2 = 1.735516

Stability

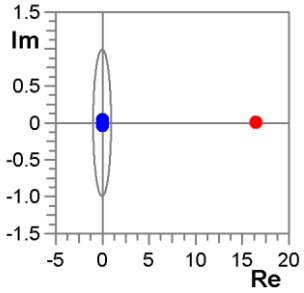

ρ_1 = 16.506502 α_1 = 0°
ρ_2 = 0.019553 α_2 = 0°
ρ_3 = 0.030052 α_3 = 54°
ρ_4 = 0.030052 α_4 = -54°

Passport of periodic regime C_2

P1 (1/2) right **unstable** (ρ_{max} = 16.506502), asymmetric, twin of regime C_1

Fixed point

x_1 = -3.240819 v_1 = 0.158761
x_2 = -2.805736 v_2 = 2.616683

Phase portraits

m_1

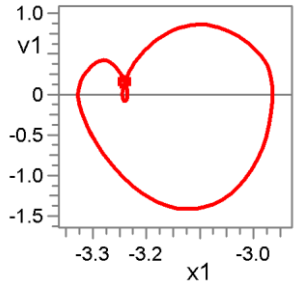

x_1 = -3.327448 … -2.964357
v_1 = -1.413235 …0.862846
Ax_1 = 0.181546

m_2

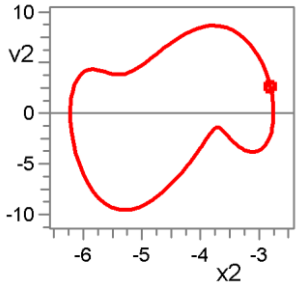

x_2 = -6.219780 … -2.748749
v_2 = -9.58006 … 8.646199
Ax_2 = 1.735516

Stability

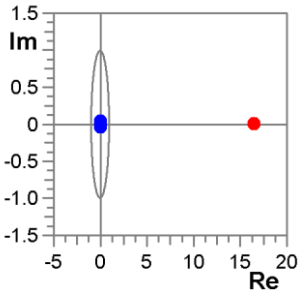

ρ_1 = 16.506502 α_1 = 0°
ρ_2 = 0.019553 α_2 = 0°
ρ_3 = 0.030052 α_3 = 54°
ρ_4 = 0.030052 α_4 = -54°

Passport of periodic regime D_1

P1 (1/1) left **unstable** (ρ_{max} = -57.091834), asymmetric, twin of regime D_2

Fixed point

x_1 = 3.265967 v_1 = 1.583380
x_2 = 3.701187 v_2 = 3.113184

Phase portraits

m_1

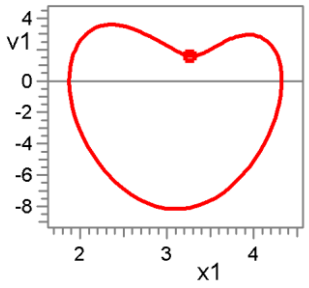

x_1 = 1.873358 … 4.321856
v_1 = -8.174546 … 3.596734
Ax_1 = 1.224249

m_2

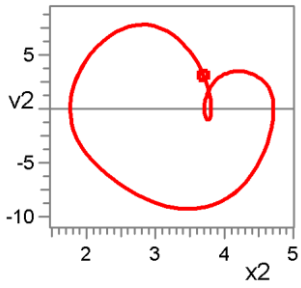

x_2 = 1.766757 … 4.715724
v_2 = -9.279693 … 7.834498
Ax_2 = 1.474483

Stability

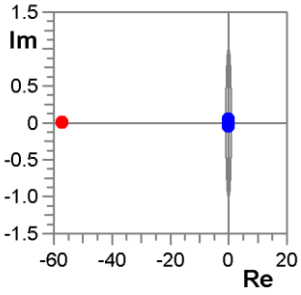

ρ_1 = 0.037467 α_1 = 52°
ρ_2 = 0.037467 α_2 = -52°
ρ_3 = -0.005249 α_3 = 180°
ρ_4 = -57.091834 α_4 = 180°

Passport of periodic regime D_2

P1 (1/1) right **unstable** (ρ_{max} = -57.091834), asymmetric, twin of regime D_1

Fixed point

x_1 = -3.265967 v_1 = -1.583380
x_2 = -3.701187 v_2 = -3.113184

Phase portraits

m_1

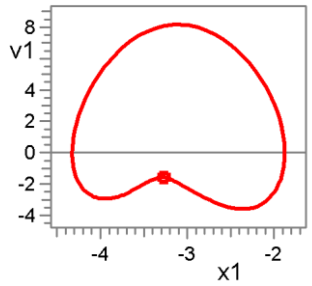

x_1 = -4.321843 … -1.873382
v_1 = -3.596764 … 8.174460
Ax_1 = 1.224231

m_2

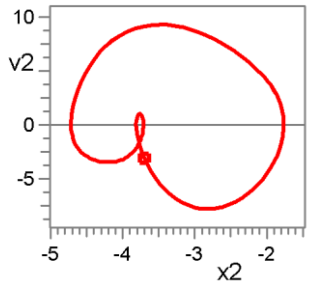

x_2 = -4.715708 … -1.766921
v_2 = -7.833884 … 9.279224
Ax_2 = 1.474394

Stability

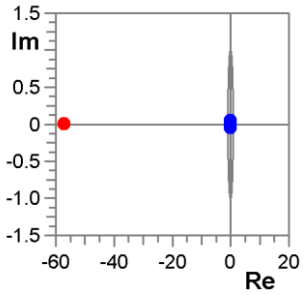

ρ_1 = 0.037467 α_1 = 52°
ρ_2 = 0.037467 α_2 = -52°
ρ_3 = -0.005249 α_3 = 180°
ρ_4 = -57.091834 α_4 = 180°

Passport of periodic regime E_1

P2 (2/1) left **unstable** (ρ_{max} = 25.044109), asymmetric, twin of regime E_2

Fixed point

x_1 = 0.014763 v_1 = -5.871255
x_2 = -0.694774 v_2 = -1.547396

Phase portraits

m_1

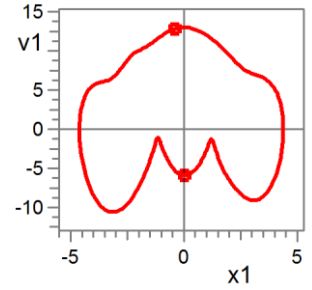

x_1 = -4.621042 … 4.383635
v_1 = -10.560489…13.022296
Ax_1 = 4.502339

m_2

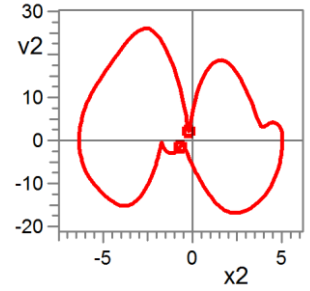

x_2 = -6.352557 … 5.039692
v_2 = -16.910522…26.008221
Ax_2 = 5.696124

Stability

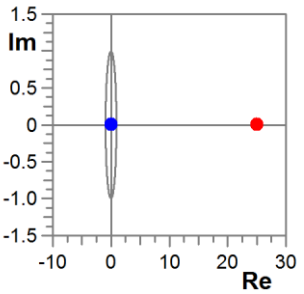

ρ_1 = 25.044109 α_1 = 0°
ρ_2 = 0.064823 α_2 = 0°
ρ_3 = 0.002588 α_3 = 0°
ρ_4 = 0.000121 α_4 = 0°

Passport of periodic regime E_2

P2 (2/1) right **unstable** (ρ_{max} = 25.044077), asymmetric, twin of regime E_1

Fixed point

x_1 = -0.014763 v_1 = 5.871255
x_2 = 0.694774 v_2 = 1.547396

Phase portraits

m_1

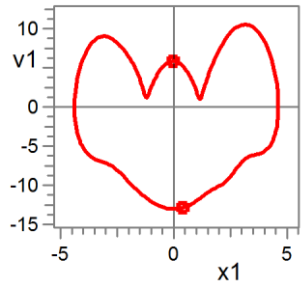

x_1 = -4.383632… 4.621042
v_1 = -13.022293…10.560485
Ax_1 = 4.502337

m_2

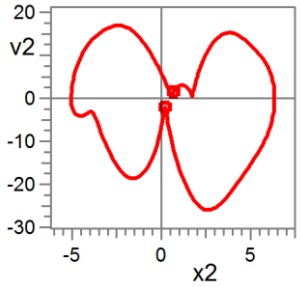

x_2 = -5.039691… 6.352555
v_2 = -26.008222…16.910413
Ax_2 = 5.696123

Stability

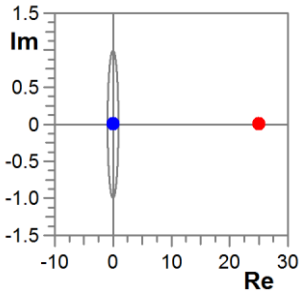

ρ_1 = 25.044077 α_1 = 0°
ρ_2 = 0.064739 α_2 = 0°
ρ_3 = 0.002569 α_3 = 0°
ρ_4 = 0.000091 α_4 = 0°

Passport of periodic regime F_1

P2 (2/2) left **unstable** (ρ_{max} = -73.052264), asymmetric, twin of regime F_2

Fixed point

x_1 = 2.136442 v_1 = 4.522155
x_2 = 2.787340 v_2 = 9.290469

Phase portraits

m_1

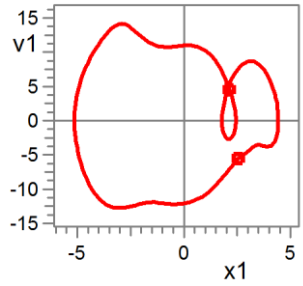

x_1 = -5.134947… 4.428519
v_1 = -12.776173…14.181855
Ax_1 = 4.781733

m_2

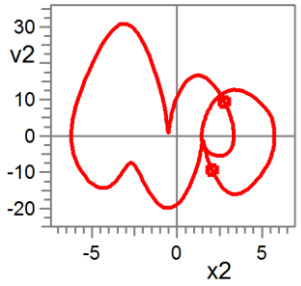

x_2 = -6.231156… 5.733578
v_2 = -19.824205…30.938488
Ax_2 = 5.982367

Stability

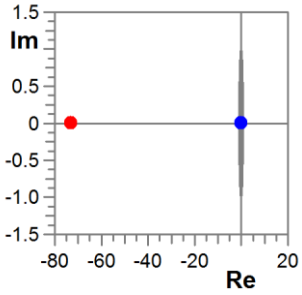

ρ_1 = -0.000157 α_1 = 180°
ρ_2 = -0.003147 α_2 = 180°
ρ_3 = -0.029106 α_3 = 180°
ρ_4 = -73.052264 α_4 = 180°

Passport of periodic regime F_2

P2 (2/2) right **unstable** (ρ_{max} = -73.052391), asymmetric, twin of regime F_1

Fixed point

x_1 = -2.136442 v_1 = -4.522155
x_2 = -2.787340 v_2 = -9.290469

Phase portraits

m_1

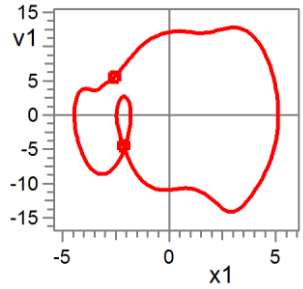

x_1 = -4.428519… 5.134947
v_1 = -14.181895…12.776174
Ax_1 = 4.781733

m_2

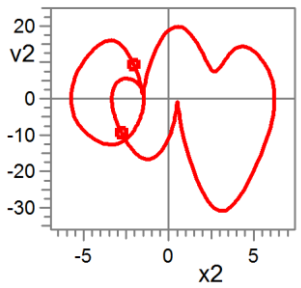

x_2 = -5.733578… 6.231156
v_2 = -30.938627…19.824218
Ax_2 = 5.982367

Stability

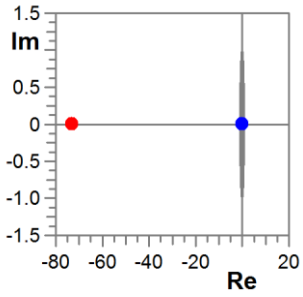

ρ_1 = -0.000154 α_1 = 180°
ρ_2 = -0.003931 α_2 = 180°
ρ_3 = -0.024624 α_3 = 180°
ρ_4 = -73.052391 α_4 = 180°

Therefore the periodic skeleton for the base parameters in the double pendulum with the periodically vibrating point of suspension in vertical direction was constructed. In the next paragraph the periodic skeleton will be used for performing the global bifurcation analysis by the method of complete bifurcation groups.

4.3.3 New bifurcation groups and rare attractors in the double pendulum

In order to get the basic results needed in the study of regular and chaotic forced oscillations in the double pendulum with the periodically vibrating point of suspension in vertical direction the bifurcation analysis of forced oscillations has performed. Global bifurcation analysis is performed by the method of complete bifurcation groups from the periodic skeleton (Table 4.1) obtained in the previous paragraph. These solutions with the found fixed points will be continued by varying the frequency of excitation.

The results of bifurcation analysis in the double pendulum with the periodically vibrating point of suspension in vertical direction obtained by the method of complete bifurcation groups are presented in Figs. 4.13 and 4.15.

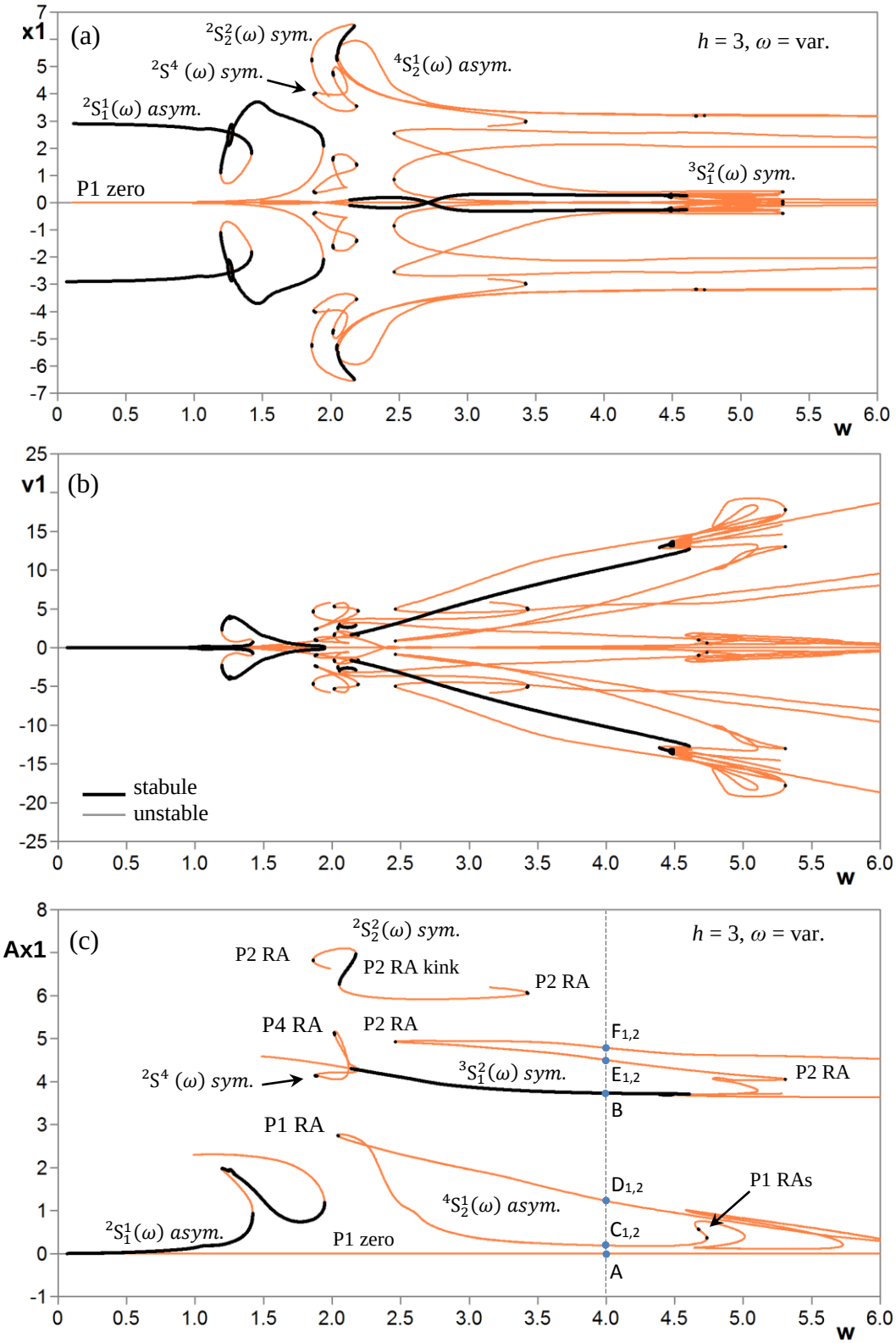

Fig. 4.13. Bifurcation diagrams S1(ω), S2(ω) and S4(ω) of the fixed periodic points of the coordinates φ_{1p}, $\dot{\varphi}_{1p}$ and $Am_{\varphi 1}$ of the first pendulum versus excitation force frequency ω. There are 8 different symmetric and asymmetric (twins) bifurcation groups with complex protuberances, with their own rare attractors of different types and UPIs. Parameters: $m_1 = 1$, $m_2 = 0.1$, $l_1 = 1$, $l_2 = 0.5$, $b_1 = 0.2$, $b_2 = 0.1$, $c_1 = 1$, $c_2 = 0.5$, $\mu = 10$, $h = 3$, ω = var.

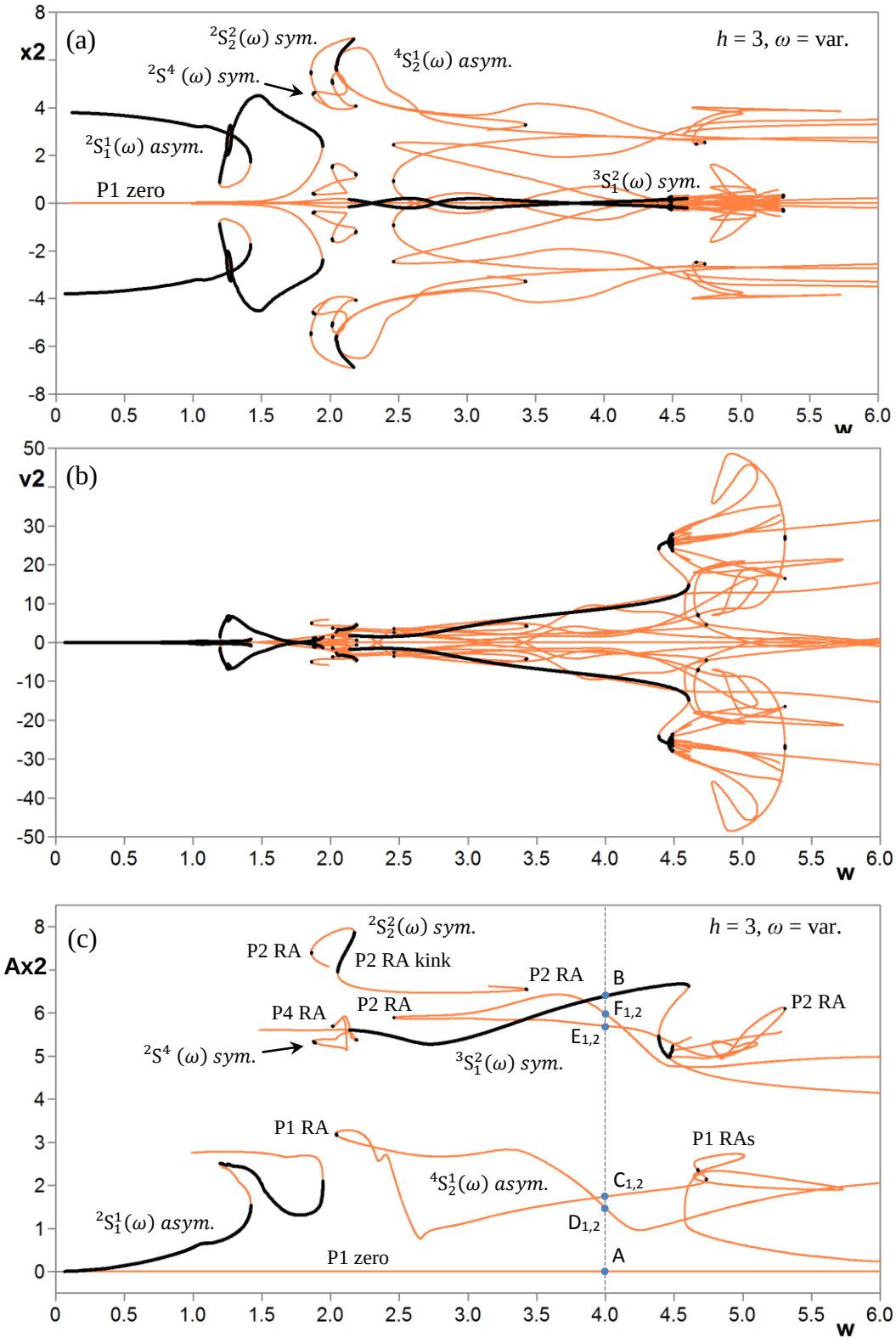

Fig. 4.14. Bifurcation diagrams S1(ω), S2(ω) and S4(ω) of the fixed periodic points of the coordinates φ_{2p}, $\dot{\varphi}_{2p}$ and $Am_{\varphi 2}$ of the second pendulum versus excitation force frequency ω. There are 8 different symmetric and asymmetric (twins) bifurcation groups with complex protuberances, with their own rare attractors of different types and UPIs. Parameters: $m_1 = 1$, $m_2 = 0.1$, $l_1 = 1$, $l_2 = 0.5$, $b_1 = 0.2$, $b_2 = 0.1$, $c_1 = 1$, $c_2 = 0.5$, $\mu = 10$, $h = 3$, ω = var.

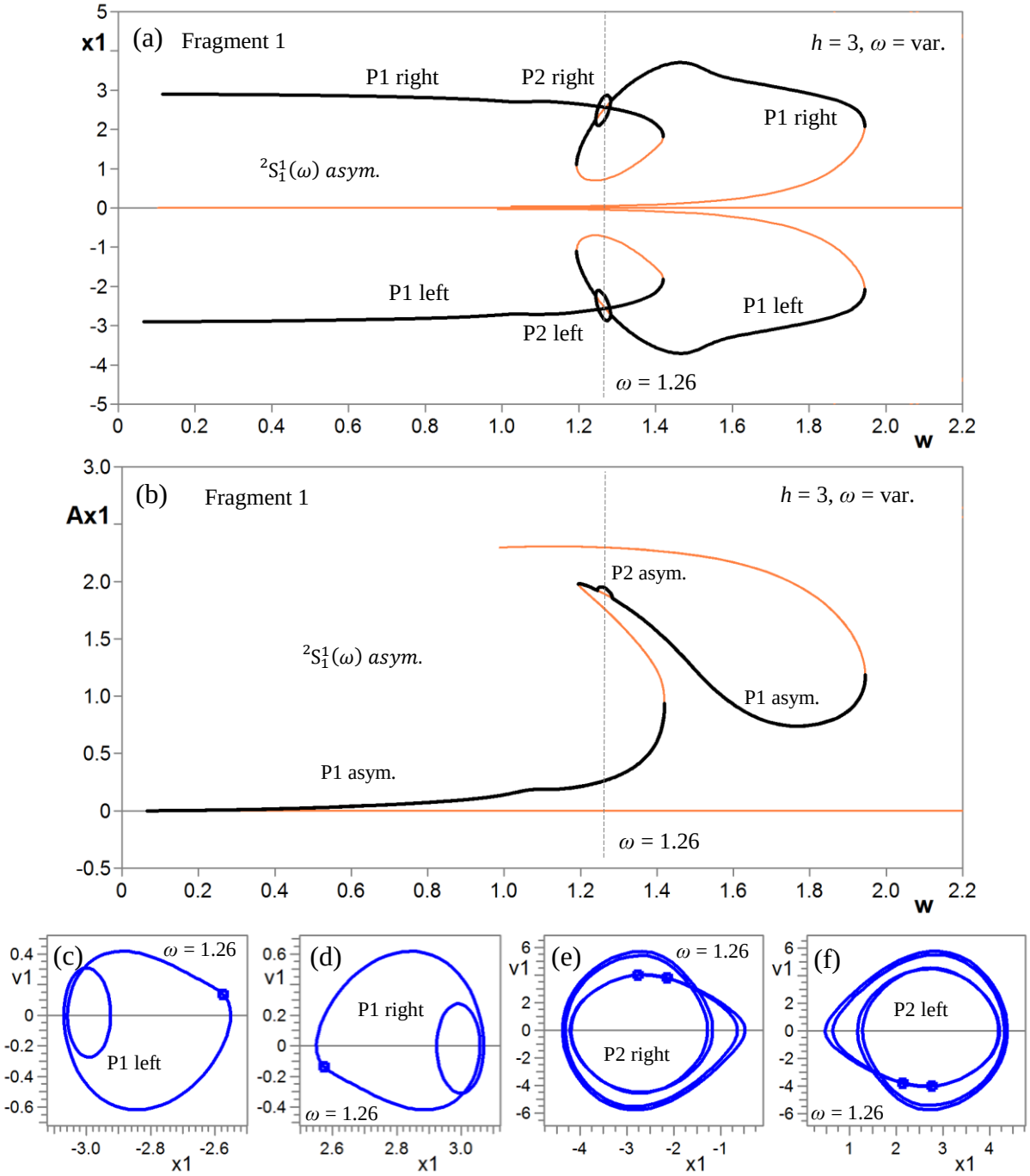

Fig. 4.15. Fragment 1 of bifurcation diagrams S1(ω) of the fixed periodic points of the coordinates φ_{1p} and $Am_{\varphi 1}$ of the first pendulum versus excitation force frequency ω. There are two asymmetric (twin) 1T bifurcation groups with fold and period doubling bifurcations. The hysteresis effect was found as well. Parameters: $m_1 = 1$, $m_2 = 0.1$, $l_1 = 1$, $l_2 = 0.5$, $b_1 = 0.2$, $b_2 = 0.1$, $c_1 = 1$, $c_2 = 0.5$, $\mu = 10$, $h = 3$, (a)-(b) ω = var., (c)-(f) $\omega = 1.26$.

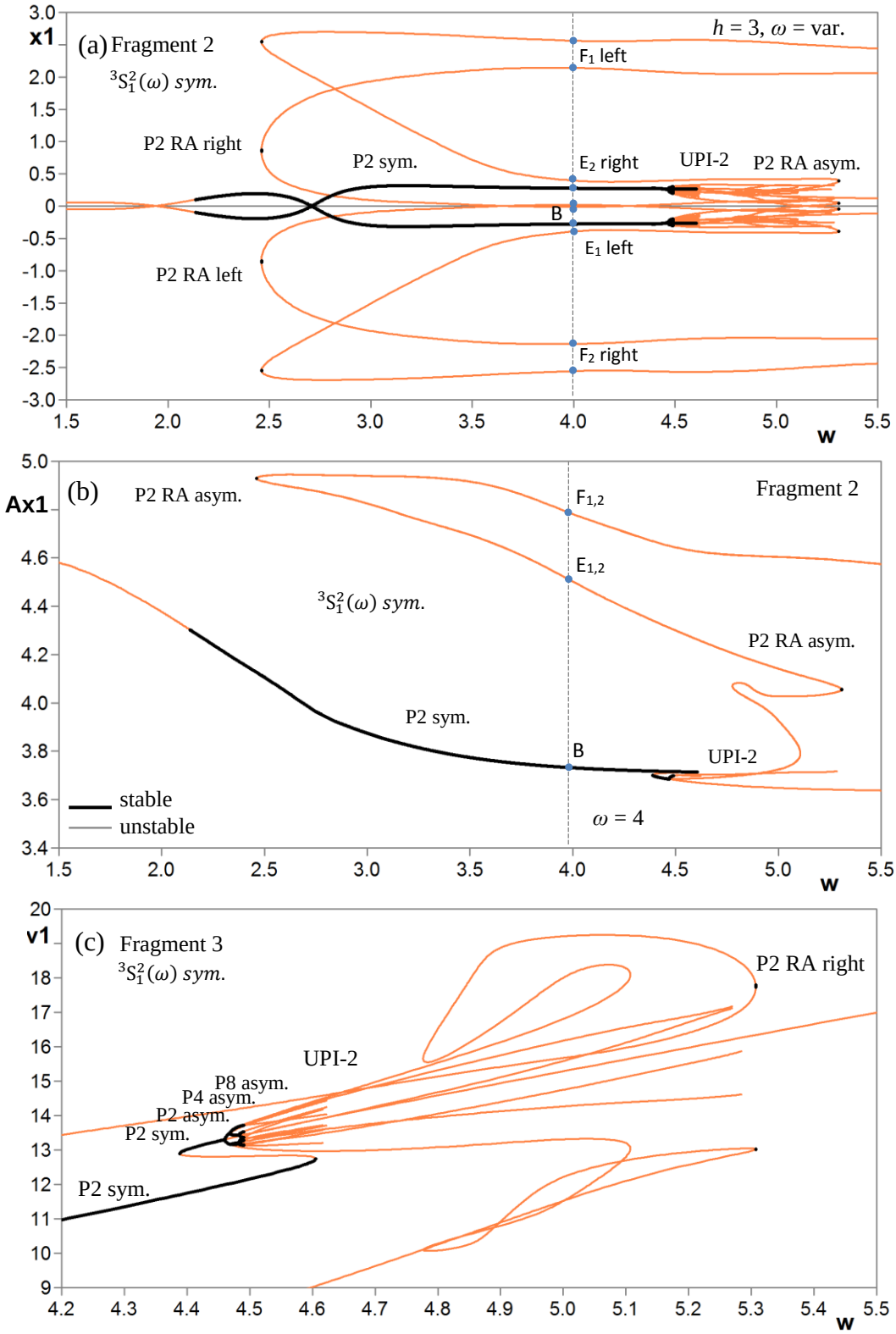

Fig. 4.16. Bifurcation diagrams S2(ω) of the fixed periodic points of the coordinates φ_{1p}, $\dot{\varphi}_{1p}$ and $Am_{\varphi 1}$ versus excitation force frequency ω. Subharmonic 2T symmetric bifurcation group with fold and period doubling bifurcations was found. There are rare attractors and UPIs. Parameters: $m_1 = 1$, $m_2 = 0.1$, $l_1 = 1$, $l_2 = 0.5$, $b_1 = 0.2$, $b_2 = 0.1$, $c_1 = 1$, $c_2 = 0.5$, $\mu = 10$, $h = 3$, ω = var.

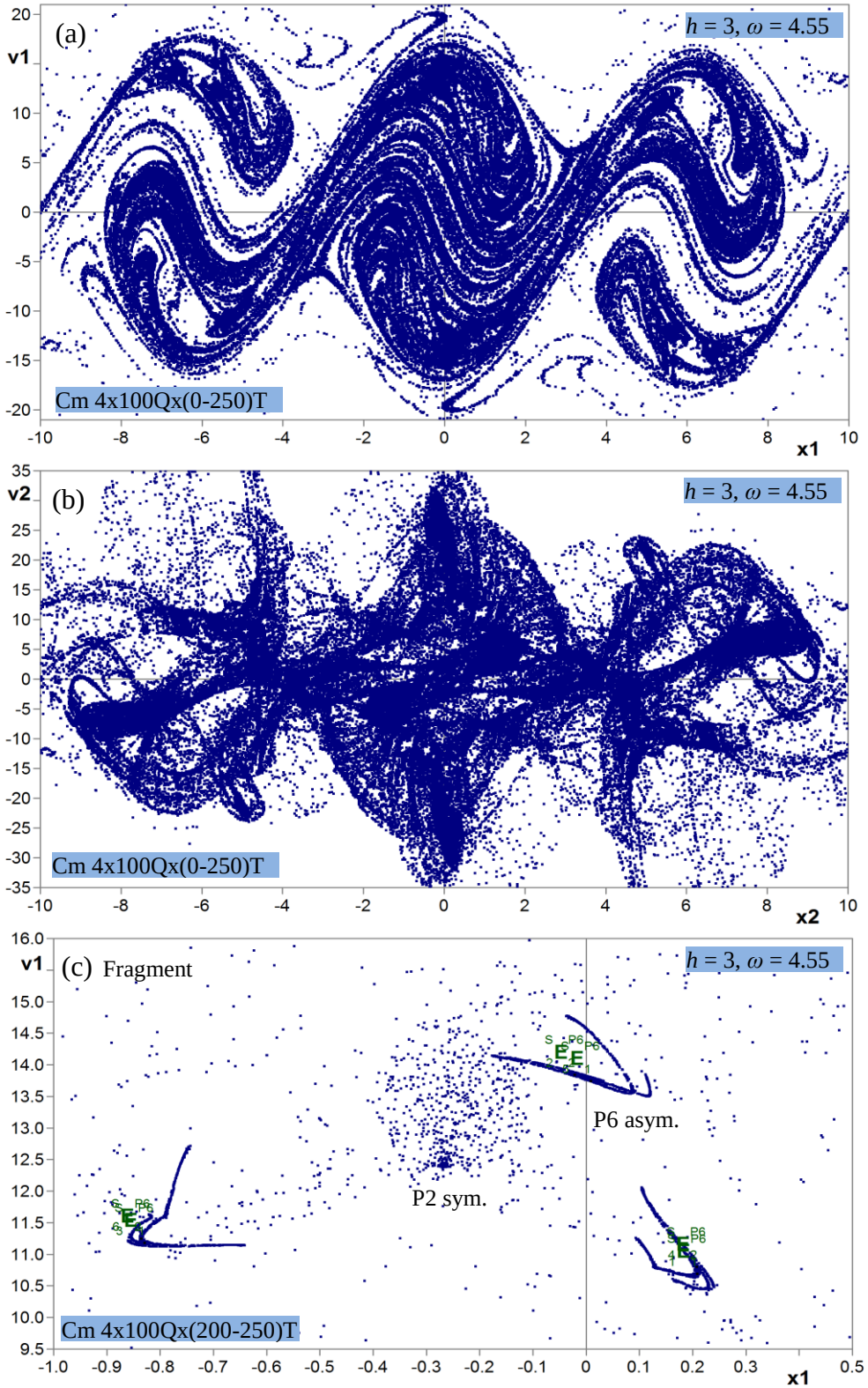

Fig. 4.17. Coexistence of P2 symmetric attractor and P6 asymmetric (twin) attractor on Poincaré map Cm 4×100Q×(0-250)T in the double pendulum with the periodically vibrating point of suspension in vertical direction (4.22) for cross-section of bifurcation diagrams (see Figs.4.13, 4.14, 4.16) for $\omega = 4.55$. Phase portraits with FPs of found orbits are shown in Fig. 4.18. Parameters: $m_1 = 1$, $m_2 = 0.1$, $l_1 = 1$, $l_2 = 0.5$, $b_1 = 0.2$, $b_2 = 0.1$, $c_1 = 1$, $c_2 = 0.5$, $\mu = 10$, $h = 3$, $\omega = 4.55$.

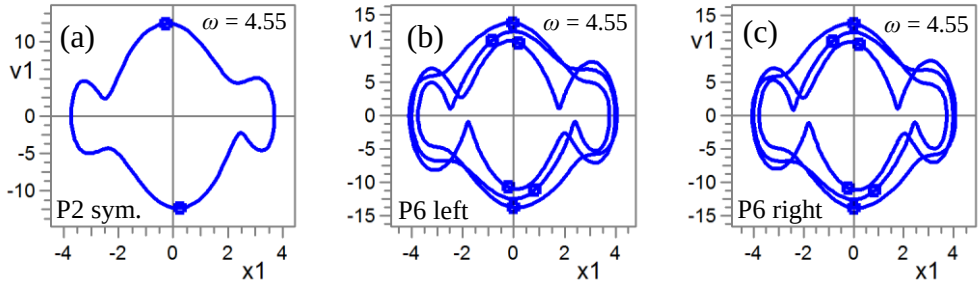

P2 stable sym.	P6 stable left	P6 stable right
x_{11} = 0.266697 v_{11} = -12.379578 x_{21} = -0.176390 v_{21} = -12.596349	x_{11} = -0.208782 v_{11} = -10.689317 x_{21} = -0.581509 v_{21} = -14.398329	x_{11} = 0.208782 v_{11} = 10.689316 x_{21} = 0.581509 v_{21} = 14.398326
x_{12} = -0.266698 v_{12} = 12.379576 x_{22} = 0.176390 v_{22} = 12.596348	x_{12} = -0.020959 v_{12} = 13.837486 x_{22} = 0.182371 v_{22} = 7.682676	x_{12} = 0.020959 v_{12} = -13.837487 x_{22} = -0.182371 v_{22} = -7.682675
ρ_1 = 0.499110 α_1 = 0° ρ_2 = 0.000008 α_2 = 0° ρ_3 = -0.359134 α_3 = 124° ρ_4 = -0.359134 α_4 = -124°	x_{13} = 0.828544 v_{13} = -11.178458 x_{23} = 0.730496 v_{23} = -8.923723	x_{13} = -0.828544 v_{13} = 11.178457 x_{23} = -0.730496 v_{23} = 8.923726
	x_{14} = 0.208094 v_{14} = 10.800691 x_{24} = 0.598033 v_{24} = 14.623089	x_{14} = 0.208094 v_{14} = 10.800691 x_{24} = 0.598033 v_{24} = 14.623089
	x_{14} = 0.208094 v_{14} = 10.800691 x_{24} = 0.598033 v_{24} = 14.623089	x_{14} = -0.208094 v_{14} = -10.800693 x_{24} = -0.598033 v_{24} = -14.623091
	x_{15} = -0.009000 v_{15} = -13.741950 x_{25} = -0.260793 v_{25} = -7.678622	x_{15} = 0.009000 v_{15} = 13.741948 x_{25} = 0.260794 v_{25} = 7.678622
	x_{16} = -0.835260 v_{16} = 11.247137 x_{26} = -0.736317 v_{26} = 8.630023	x_{16} = 0.835260 v_{16} = -11.247138 x_{26} = 0.736317 v_{26} = -8.630019
	ρ_1 = 0.447190 α_1 = 47° ρ_2 = 0.447190 α_2 = -47° ρ_3 = 0.000012 α_3 = 0° ρ_4 = 2.866738e-7 α_4 = 0°	ρ_1 = 0.447018 α_1 = 47° ρ_2 = 0.000008 α_2 = -47° ρ_3 = 0.000012 α_3 = 0° ρ_4 = 4.115449e-7 α_4 = 0°

Fig. 4.18. Phase portraits and fixed points (FP) with stability characteristics (multipliers) of coexisting P2 symmetric attractor, P6 asymmetric (twin) attractor in the double pendulum (4.22) for cross-section of bifurcation diagrams (see Figs.4.13, 4.14, 4.16, 4.21) for frequency ω = 4.55 of excitation force. The coexistence of these attractors on Poincaré map is shown in Fig. 4.17. Parameters: m_1 = 1, m_2 = 0.1, l_1 = 1, l_2 = 0.5, b_1 = 0.2, b_2 = 0.1, c_1 = 1, c_2 = 0.5, μ = 10, h = 3, ω = 4.55.

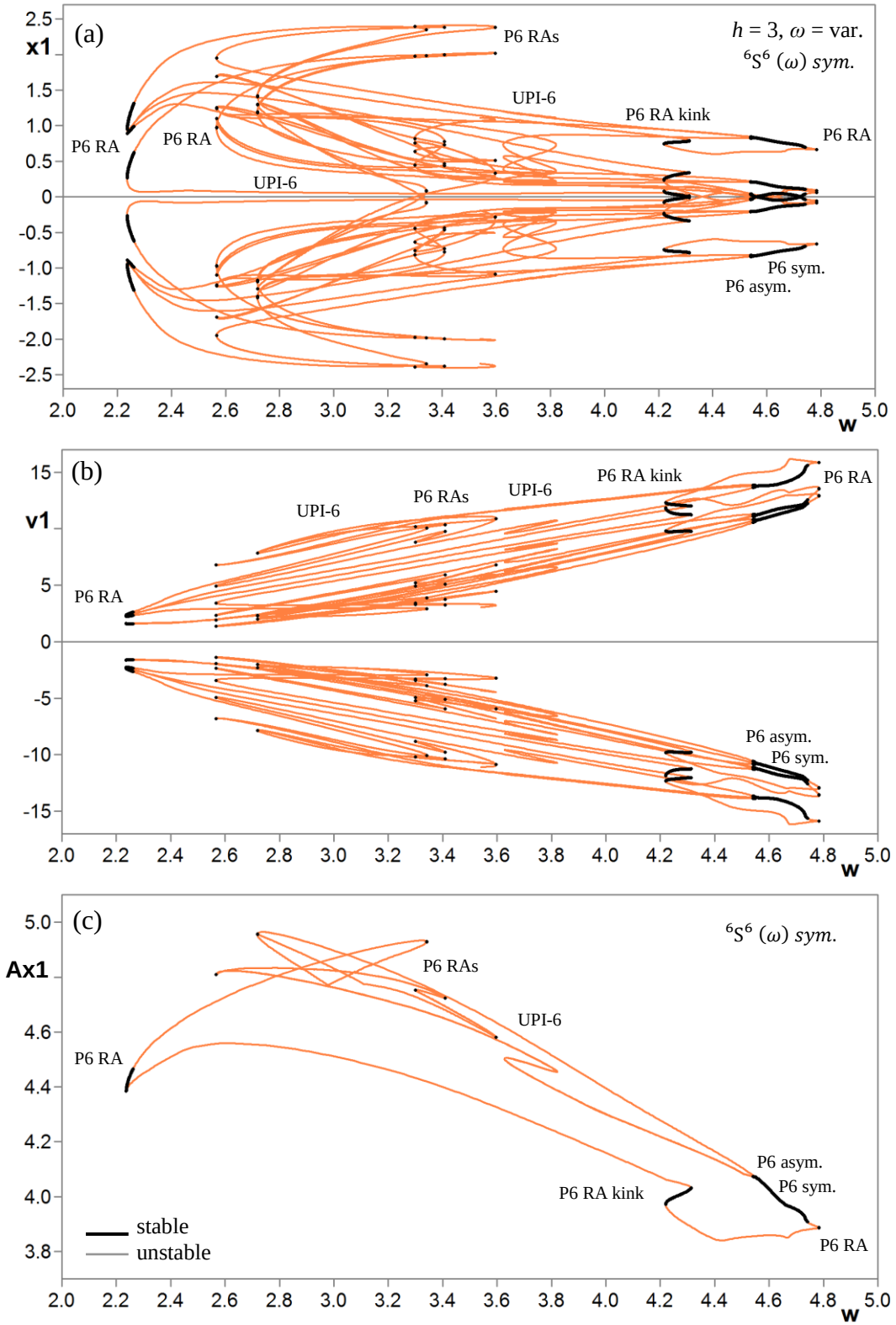

Fig. 4.19. Bifurcation diagrams S6(ω) of the fixed periodic points of the coordinates φ_{1p}, $\dot{\varphi}_{1p}$ and $Am_{\varphi 1}$ of the first pendulum versus excitation force frequency ω. There is 6T symmetric isle bifurcation group with complex protuberances, with their own rare attractors of different types and UPIs. For construction of this subharmonic bifurcation group the P6 asymmetrical attractors (Fig. 4.18) were found by the mapping from a contour on Poincaré map (Fig. 4.17). Parameters: m_1 = 1, m_2 = 0.1, l_1 = 1, l_2 = 0.5, b_1 = 0.2, b_2 = 0.1, c_1 = 1, c_2 = 0.5, μ = 10, h = 3, ω = var.

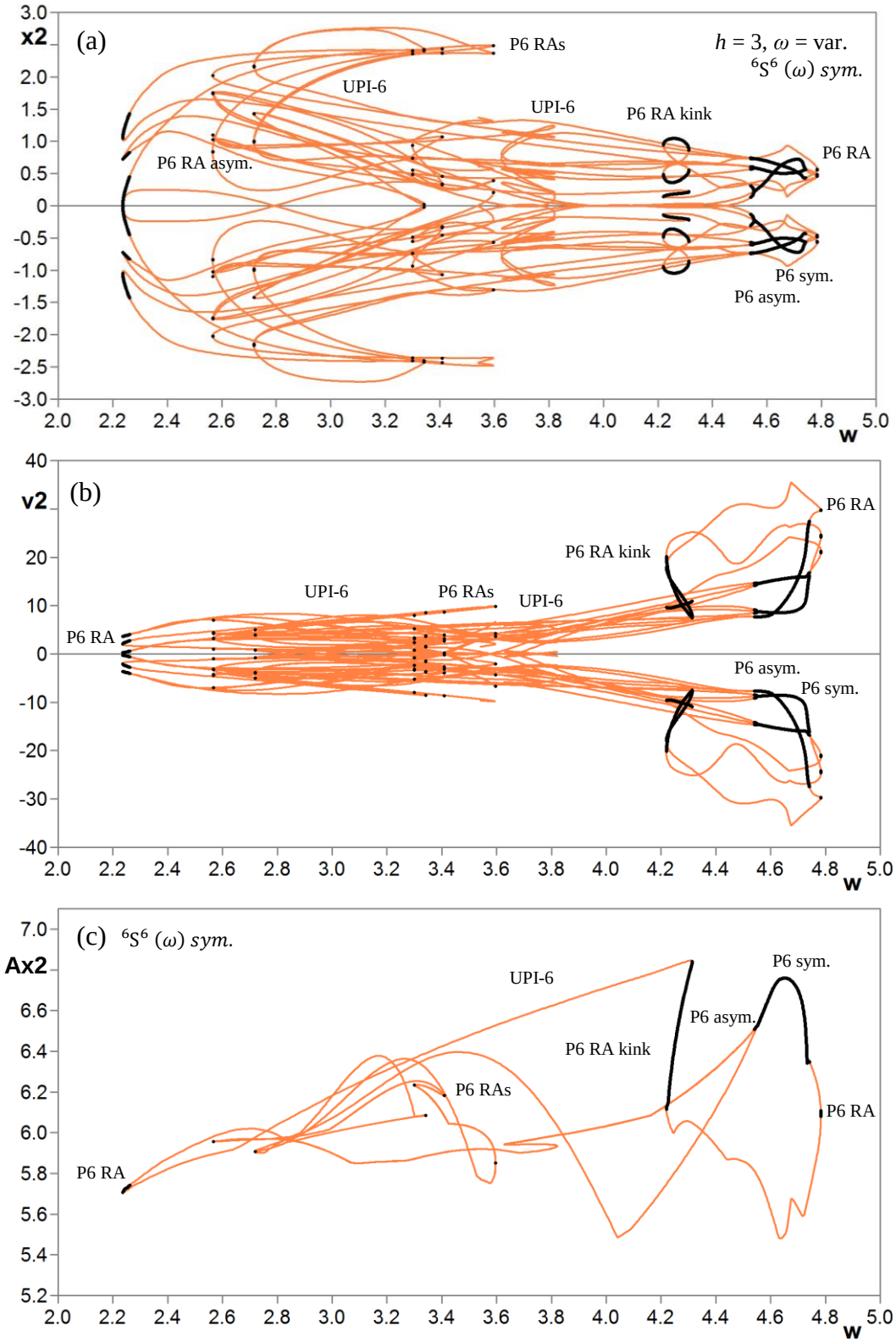

Fig. 4.20. Bifurcation diagrams S6(ω) of the fixed periodic points of the coordinates φ_{2p}, $\dot{\varphi}_{2p}$ and $Am_{\varphi 2}$ of the second pendulum versus excitation force frequency ω. There is 6T symmetric isle bifurcation group with complex protuberances, with their own rare attractors of different types and UPIs. For construction of this subharmonic bifurcation group the P6 asymmetrical attractors (Fig. 4.18) were found by the mapping from a contour on Poincaré map (Fig. 4.17). Parameters: $m_1 = 1$, $m_2 = 0.1$, $l_1 = 1$, $l_2 = 0.5$, $b_1 = 0.2$, $b_2 = 0.1$, $c_1 = 1$, $c_2 = 0.5$, $\mu = 10$, $h = 3$, ω = var.

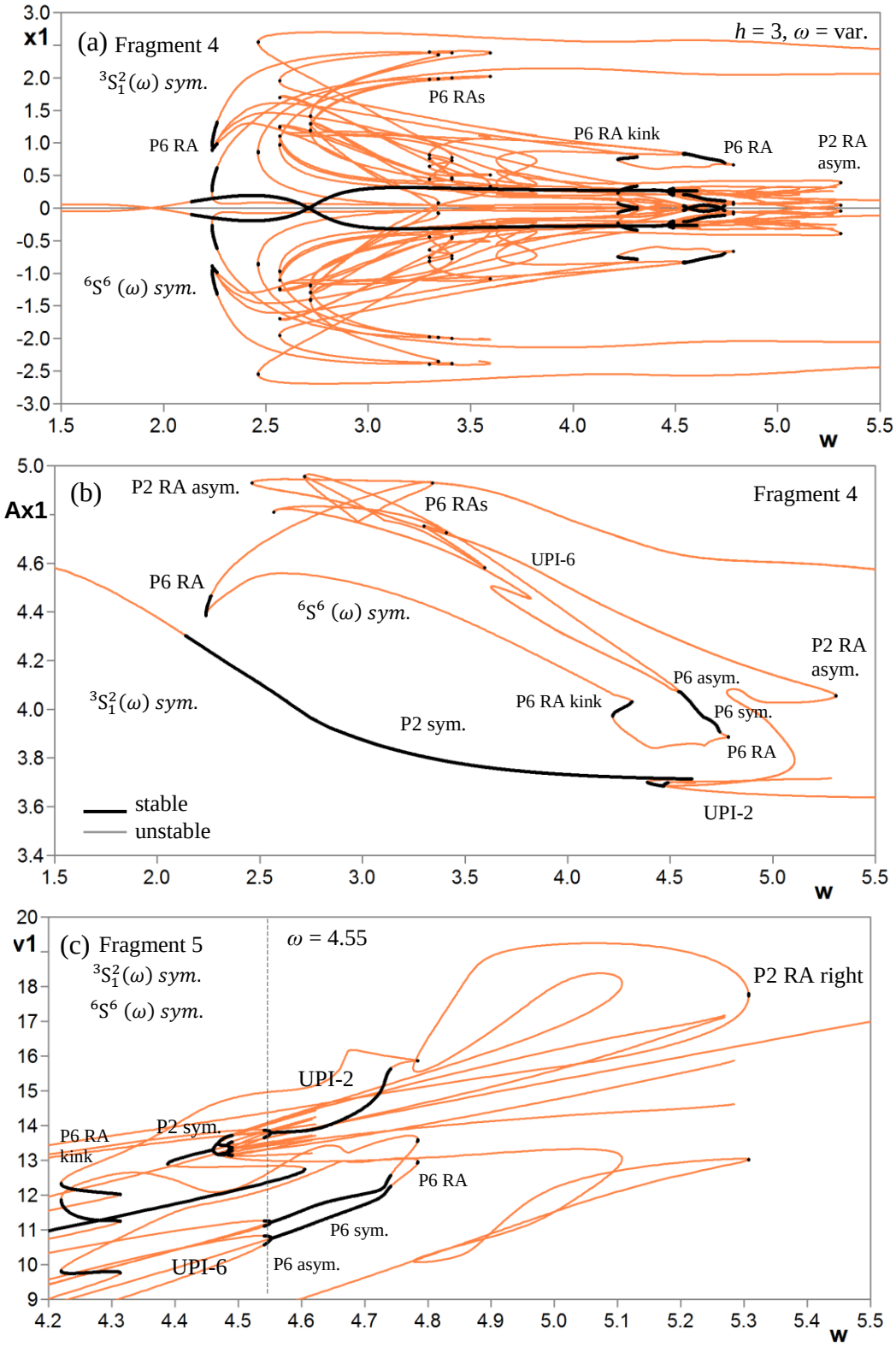

Fig. 4.21. Bifurcation diagrams S2(ω) and S6(ω) of the fixed periodic points of the coordinates φ_{1p}, $\dot{\varphi}_{1p}$ and $Am_{\varphi 1}$ versus excitation force frequency ω. The coexistence of subharmonic 2T bifurcation group (Fig. 4.16) and 6T symmetric isle bifurcation group (Fig. 4.19-4.20) is presented. Diagram illustrates the complex protuberances, with their own rare attractors of different types and UPIs. Parameters: m_1 = 1, m_2 = 0.1, l_1 = 1, l_2 = 0.5, b_1 = 0.2, b_2 = 0.1, c_1 = 1, c_2 = 0.5, μ = 10, h = 3, ω = var.

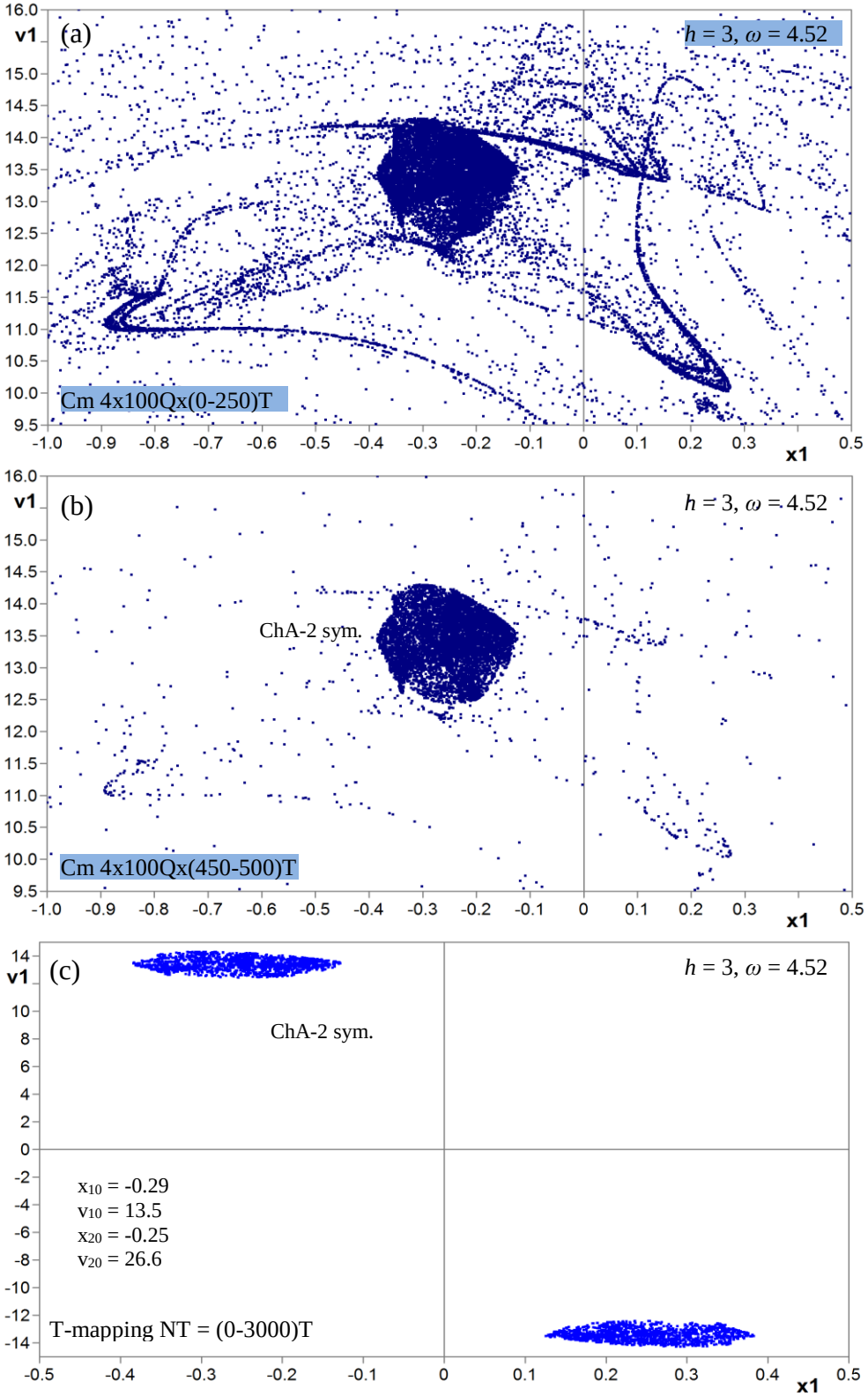

Fig. 4.22. Subharmonic symmetric chaotic attractor ChA-2 and transient chaos ChA-6 in the double pendulum (4.22) for cross-section of bifurcation diagrams (see Figs.4.13, 4.14, 4.16, 4.21) for ω = 4.52. (a)-(b) Mappings Cm 4x100Qx(0-500)T from contours x_1, v_1 (-0.5, -3.0; 0.5, 0.0), x_2, v_2 (-0.5, -3.0; 0.5, 0.0); (c)T-mapping NT = (0-3000)T on Poincaré map, the fragment of which is presented in Fig. 4.23(a). The phase portraits NT= 50T subharmonic symmetric chaotic attractors ChA-2 from the same initial conditions are plotted in Figs. 4.23(b-c).Parameters: m_1 = 1, m_2 = 0.1, l_1 = 1, l_2 = 0.5, b_1 = 0.2, b_2 = 0.1, c_1 = 1, c_2 = 0.5, μ = 10, h = 3, ω = 4.52.

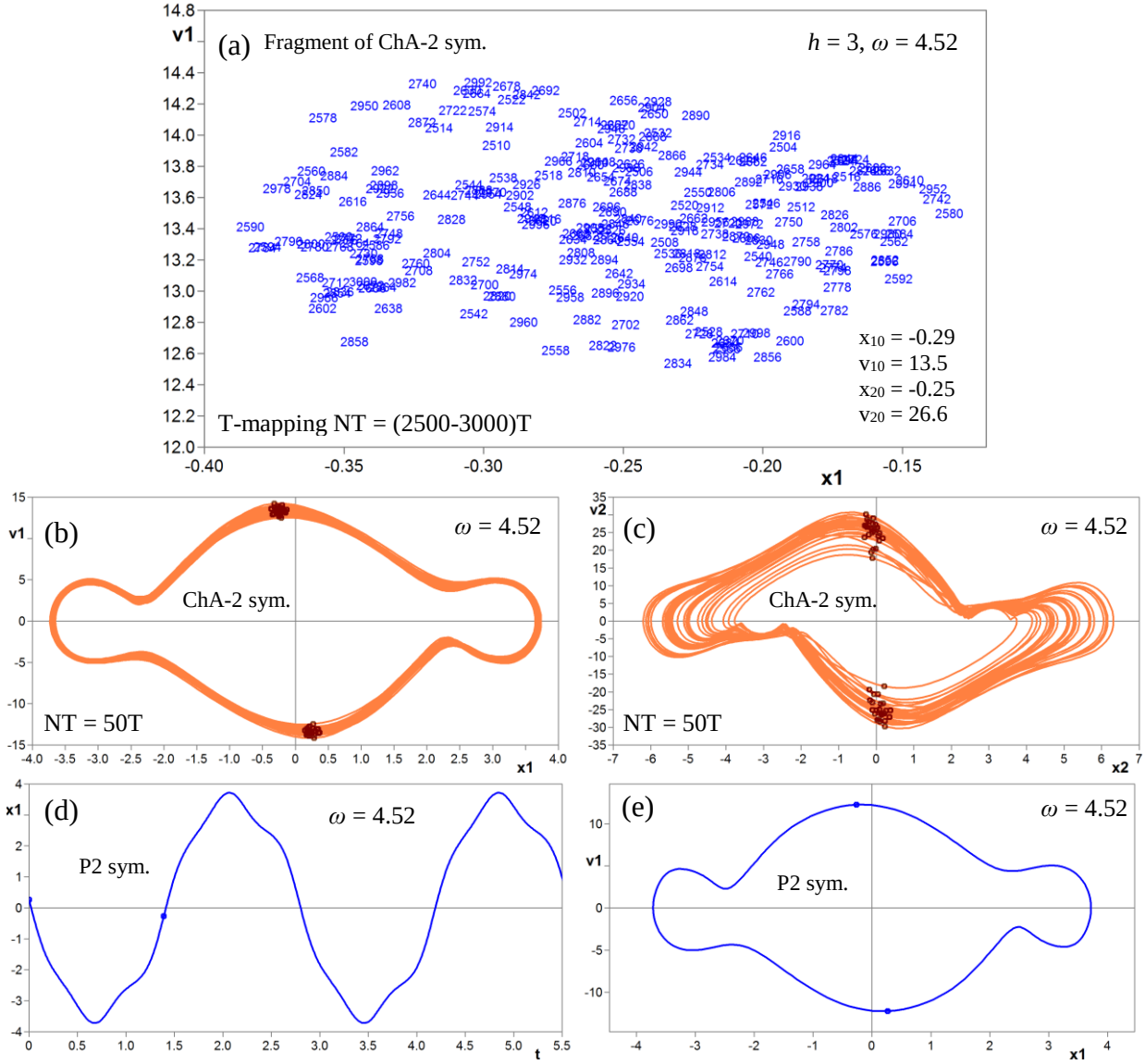

Fig. 4.23. Coexisting subharmonic symmetric chaotic attractor ChA-2 and stable subharmonic symmetric P2 attractor in the six body driven symmetric pendulum system (5.3): (a) fragment NT = (2500-3000)T of T-mapping on Poincaré map shown in Fig. 4.22(a) for ChA-2 attractor; (b) – (c) phase portraits NT= 50T for ChA-2 attractor from the initial conditions x_{10} = -0.29, v_{10} = 13.5, x_{20} = -0.25, v_{20} = 26.6; (d) – (e) time history and phase portrait for P2 symmetric attractor. Parameters: m_1 = 1, m_2 = 0.1, l_1 = 1, l_2 = 0.5, b_1 = 0.2, b_2 = 0.1, c_1 = 1, c_2 = 0.5, μ = 10, h = 3, ω = 4.52.

Bifurcation diagrams S1(ω), S2(ω) and S4(ω) of the fixed periodic points of the coordinates φ_{1p}, $\dot{\varphi}_{1p}$ and $Am_{\varphi 1}$ of the first pendulum versus frequency ω of excitation force are plotted on Fig. 4.13. For the second pendulum the bifurcation diagrams S1(ω), S2(ω) and S4(ω) of the fixed periodic points of the coordinates φ_{2p}, $\dot{\varphi}_{2p}$ and $Am_{\varphi 2}$ versus frequency ω of excitation force are plotted on Fig. 4.14. There are 8 different symmetric and asymmetric (twins) bifurcation groups with complex protuberances, with their own rare attractors of different types and UPIs. Two asymmetric (twin) 1T bifurcation groups with fold and period doubling

bifurcations are shown on Fragment 1 (Fig. 4.15). The hysteresis effect was found as well. There is a multiplicity in the frequency range $\omega \in (1.19 \div 1.94)$. Phase portraits of non-resonant P1 asymmetric and resonant P2 asymmetric attractors for ω = 1.26 are shown in Fig. 4.15 (c)-(f).

Bifurcation diagrams S2(ω) of the fixed periodic points of the coordinates φ_{1p}, $\dot{\varphi}_{1p}$ and $Am_{\varphi 1}$ versus excitation force frequency ω force are plotted on Fig. 4.16. Subharmonic 2T symmetric bifurcation group with fold and period doubling bifurcations was found. There are complex protuberances, rare attractors and UPI in this bifurcation group.

Coexistence of P2 symmetric attractor and P6 asymmetric (twin) attractor on Poincaré map Cm 4×100Q×(0-250)T in the double pendulum with the periodically vibrating point of suspension in vertical direction (4.22) for cross-section of bifurcation diagrams (see Figs.4.13, 4.14, 4.16, 4.21) for ω = 4.55 was presented in Fig. 4.17. Phase portraits with fixed points of found orbits are shown in Fig. 4.18.

Bifurcation diagrams S6(ω) of the fixed periodic points of the coordinates of the both pendulums versus excitation force frequency ω are plotted on Figs. 4.19-4.20. Subharmonic 6T symmetric isle bifurcation group with complex protuberances, with their own rare attractors of different types and UPIs are found. For construction of this subharmonic bifurcation group the P6 asymmetrical attractors (Fig. 4.18) were found by the mapping from a contour on Poincaré map (Fig. 4.17).

Subharmonic symmetric chaotic attractor ChA-2 and transient chaos ChA-6 in the double pendulum with the periodically vibrating point of suspension in vertical direction (4.22) for cross-section of bifurcation diagrams (see Figs.4.13, 4.14, 4.16, 4.21) for frequency ω = 4.52 of excitation force is shown in Fig. 4.22. These two coexisting chaotic motions were found using the mappings Cm 4x100Qx(0-500)T from such contours x_1, v_1 (-0.5, -3.0; 0.5, 0.0), x_2, v_2 (-0.5, -3.0; 0.5, 0.0) shown in Figs. 4.22(a-b) and using the T-mapping NT = (0-3000)T from such initial conditions x_{10} = -0.29, v_{10} = 13.5, x_{20} = -0.25, v_{20} = 26.6 shown in Fig. 4.22(c). The fragment NT = (2500-3000)T of T-mapping (see Fig. 4.22,c) on Poincaré map for ChA-2 attractor is presented in Fig. 4.23(a). The phase portraits NT= 50T of subharmonic symmetric chaotic attractor ChA-2 from the same initial conditions are plotted in Figs. 4.23(b-c). Moreover the time history and phase portrait for coexisting stable subharmonic symmetric P2 attractor are presented in Fig. 4.23(d-e).

Therefore, the qualitative behavior of the double pendulum with the periodically vibrating point of suspension in vertical direction with varying the frequency ω of the excitation was investigated using the method of complete bifurcation groups. The new qualitative results of the

topology of the bifurcation groups with complex protuberances, UPIs, with many different rare regular P1 RA asym., P2 RA sym., P2 RA kink sym., P4 RA sym., P6 RA kink sym. and P6 RA attractors, chaotic transients ChA-6 and chaotic ChA-2 attractor were obtained.

4.4 Conclusions

In this chapter two different pendulum systems with two degrees of freedom were investigated. The possibility of using the method of complete bifurcation groups for the global analysis of the pendulum system with a sliding mass and with the external periodic excited moment, and double pendulum with the periodically vibrating point of suspension in vertical direction is demonstrated.

The main qualitative results of topology of bifurcation groups with rare regular and chaotic attractors for the pendulum systems with two degrees of freedom were obtained with varying the frequency ω of the excitation. The subharmonic, chaotic and rare periodic behaviour were investigated. There are complex protuberances with many rare regular attractors of different types, chaotic transients and chaotic motions.

Hence, it is reasonably safe to suggest that there are rare attractors in more complex pendulum-like models of the mechanical systems with two or many degrees of freedom. For example, the dynamical models of satellites, the space tether systems with the engine, etc. The usefulness of the study of pendulum systems with 2ODF by the method of complete bifurcation groups is shown using the example of the pendulum system with a sliding mass and with the external periodic excited moment, and double pendulum with the periodically vibrating point of suspension in vertical direction. The obtained results can be useful for the problems of controllability and stability of the spacecraft to avoid catastrophic or unexpected nonlinear phenomena with larger amplitudes.

5

Analysis of Forced Oscillations in the Pendulum Systems with Several Degrees of Freedom

5.1 Introduction

It is known that in the system with several degrees of freedom with an external excitation exist the new bifurcation groups and new nonlinear effects. That is, "a new partition of the phase space into the trajectories" and the appearance of new bifurcation groups and bifurcation groups with previously unknown topology with rare attractors and complex protuberances.

In the third chapter studying the forced and parametrical oscillations of the pendulum systems with one degree of freedom a new class of stable periodic orbits, called rotational rare attractors, was found [147,149]. In the fourth chapter bifurcation analysis of pendulum systems

with two degrees of freedom and with external harmonic excitation was conducted. Studies of these systems were conducted using the new methods of new bifurcation theory, which also are intended to solve the pendulum systems with several degrees of freedom.

This chapter provides the bifurcation analysis of the pendulum system with several degrees of freedom, with several equilibrium positions and with an external harmonic excitation.

5.2 Bifurcation analysis of six body symmetric driven pendulum system with several equilibrium positions

5.2.1 The model of six body pendulum with additional restoring force

In the previous chapters, the pendulum systems with one or two degrees of freedom were investigated. The bifurcation diagrams of these systems contain such phenomena as rare regular and chaotic attractors. At the same time, all of the real dynamical systems are not limited to a single degree of freedom [56,107]. Therefore, in this section the possibilities of the applying the methods of analysis of nonlinear dynamical systems to the systems with several degrees of freedom are discussed.

Let us consider the nonlinear dynamical system with six degrees of freedom, e.g. six body symmetric pendulum system with several equilibrium positions and with external harmonic excitation (Fig. 5.1). Such models have been studied theoretically and practically in works (Andrievsky et al., 1998, 2002; Andrievsky and Boykov, 2001; Fradkov et al., 2005) [e.g. Fradkov A.L., Andrievsky B.R. "*Control of wave motion in the chain of pendulums*". Proc. of the 17th World Congress "The International Federation of Automatic Control", Seoul, Korea, 2008, pp. 3136-3141.]. The studied nonlinear dynamical pendulum model with six degrees of freedom (6DOF) or with dimension D = 13 is described by such system of differential equations:

$$\begin{cases} m_1 l_1^2 \ddot{\varphi}_1 = Fv_2 + Fx_2 - Fv_1 - Fx_1 - Fg_1 + F_t, \\ m_2 l_2^2 \ddot{\varphi}_2 = Fv_3 + Fx_3 - Fv_2 - Fx_2 - Fg_2, \\ m_3 l_3^2 \ddot{\varphi}_3 = Fv_4 + Fx_4 - Fv_3 - Fx_3 - Fg_3, \\ m_4 l_4^2 \ddot{\varphi}_4 = Fv_5 + Fx_5 - Fv_4 - Fx_4 - Fg_4, \\ m_5 l_5^2 \ddot{\varphi}_5 = Fv_6 + Fx_6 - Fv_5 - Fx_5 - Fg_5, \\ m_6 l_6^2 \ddot{\varphi}_6 = -Fv_6 - Fx_6 - Fg_6. \end{cases} \tag{5.1}$$

The studied model consists from linear dissipative forces $Fv_{1,i+1}$ between pendulums, pendulum's restoring forces Fg_i, additional linear elastic forces $Fx_{1,i+1}$ and harmonic excitation Ft, applied to the first pendulum:

$$
\begin{aligned}
&Fv_1 = b_1\dot{\varphi}_1,\\
&Fx_1 = c_1\varphi_1,\\
&Fg_i = m_i g l_i \sin\varphi_i,\ i = 1,2...6,\\
&Fx_{i+1} = c_{i+1}(\varphi_{i+1} - \varphi_i),\ i = 1,2...5,\\
&Fv_{i+1} = b_{i+1}(\dot{\varphi}_{i+1} - \dot{\varphi}_i),\ i = 1,2...5,\\
&Ft = h\cos(\omega t + \phi_0),
\end{aligned}
\tag{5.2}
$$

where $m_1 = m_2 = m_i$ – masses of pendulums (i = 1, 2…6),

$l_1 = l_2 = l_i$ – lengths of pendulums (i = 1, 2…6),

g – gravitation constant,

$b_1 = b_2 = b_i$ – coefficients of linear dissipation between pendulums (i = 1, 2…6),

$c_1 = c_2 = c_i$ – stiffness coefficients of linear elastic forces between pendulums (i = 1, 2…6),

ω, h, ϕ_0 – frequency, amplitude and initial phase of excitation force, applied to the first pendulum, in these investigations $\phi_0 = 0$.

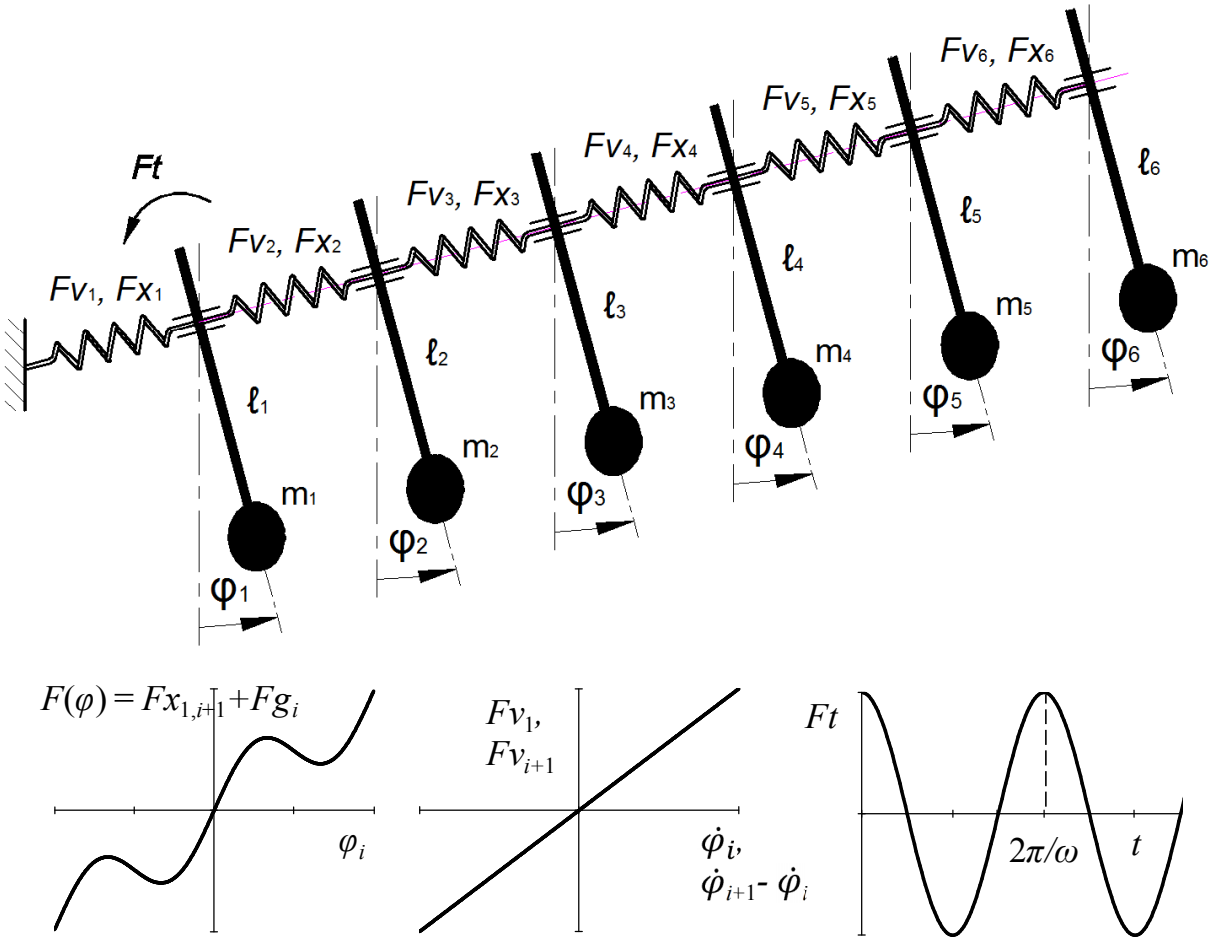

Fig. 5.1. Six body driven symmetric pendulum system with several equilibrium positions, linear dissipative forces $Fv_{1,i+1}$ between pendulums, pendulum's restoring forces Fg_i, additional linear elastic forces $Fx_{1,i+1}$ and harmonic excitation Ft, applied to the first pendulum.

The model of six body driven symmetric pendulum system with several equilibrium positions and external harmonic excitation described by these differential equations (5.1) is shown in Figure 5.1. Also on this figure the linear dissipative forces, pendulum's restoring forces, additional linear elastic forces and harmonic excitation are shown.

Substituting (5.2) in (5.1) we obtain the mathematical model of the studied pendulum:

$$\begin{cases} m_1 l_1^2 \ddot{\varphi}_1 = b_2(\dot{\varphi}_2 - \dot{\varphi}_1) + c_2(\varphi_2 - \varphi_1) - b_1\dot{\varphi}_1 - c_1\varphi_1 - m_1 g l_1 \sin\varphi_1 + h\cos(\omega t + \phi_0), \\ m_2 l_2^2 \ddot{\varphi}_2 = b_3(\dot{\varphi}_3 - \dot{\varphi}_2) + c_3(\varphi_3 - \varphi_2) - b_2(\dot{\varphi}_2 - \dot{\varphi}_1) - c_2(\varphi_2 - \varphi_1) - m_2 g l_2 \sin\varphi_2, \\ m_3 l_3^2 \ddot{\varphi}_3 = b_4(\dot{\varphi}_4 - \dot{\varphi}_3) + c_4(\varphi_4 - \varphi_3) - b_3(\dot{\varphi}_3 - \dot{\varphi}_2) - c_3(\varphi_3 - \varphi_2) - m_3 g l_3 \sin\varphi_3, \\ m_4 l_4^2 \ddot{\varphi}_4 = b_5(\dot{\varphi}_5 - \dot{\varphi}_4) + c_5(\varphi_5 - \varphi_4) - b_4(\dot{\varphi}_4 - \dot{\varphi}_3) - c_4(\varphi_4 - \varphi_3) - m_4 g l_4 \sin\varphi_4, \\ m_5 l_5^2 \ddot{\varphi}_5 = b_6(\dot{\varphi}_6 - \dot{\varphi}_5) + c_6(\varphi_6 - \varphi_5) - b_5(\dot{\varphi}_5 - \dot{\varphi}_4) - c_5(\varphi_5 - \varphi_4) - m_5 g l_5 \sin\varphi_5, \\ m_6 l_6^2 \ddot{\varphi}_6 = -b_6(\dot{\varphi}_6 - \dot{\varphi}_5) - c_6(\varphi_6 - \varphi_5) - m_6 g l_6 \sin\varphi_6. \end{cases} \tag{5.3}$$

This model six body symmetric pendulum system with several equilibrium positions and with external harmonic excitation can be used in many scientific research and engineering tasks. One of such problems can be the design of prospective laboratory equipment for control education, e.g. the "*Chain of Pendulums*" mechatronic set-up, created in the IPME RAS, Saint Petersburg (Fradkov et al., 2008). These results can also be useful for the vibration absorbing systems, for the mixing process, such as liquids, washing machines, etc.

Author does not know any results of the global bifurcation analysis and any serious researches of rare attractors and of rare bifurcation groups in the many pendulum systems, but these studies, of course, are needed to pursue.

5.2.2 Construction of periodic skeleton for the six body driven pendulum system

The example of the construction of periodic skeleton (PSK) in six body symmetric pendulum system with several equilibrium positions and with external harmonic excitation (5.3) for oscillating and rotating orbits (regimes, attractors) with order n = (1-16)T (see Table. 5.1) by using the Newton-Kantorovich method from the grid of initial conditions NQ = 20×20Q = 400Q (see Fig.5.2) inside the rectangle (-π, -5.0; π, 5.0) of coordinates φ_i and $\dot{\varphi}_i$ is shown below. The maximum number of iterations is KIN = 64 with precision search of the fixed point EPN = 1e-6 and parameter of discretisation DEN = 1e-5. Active boundaries are $\varphi_{i,\ min}$ = -π, $\varphi_{i,\ max}$ = π, $\dot{\varphi}_{i,min}$ = -10, $\dot{\varphi}_{i,max}$= 10. For rotational orbits the cylindrical phase space was taken into account with period Lφ = 2π. Time of calculation of periodic skeleton was about 1 hour (the PC characteristics: Intel(R) Core(TM) i3-2120, CPU - 3.30GHz, RAM - 4 GB, Windows 7 SP1).

Periodic skeleton (see Table 5.1) consists from 3 periodic oscillating orbits (regimes, attractors), among them are two stable regimes P1 (1/1) (resonant and non-resonant) and one unstable regime P1 (1/1) for construction of periodic skeleton in the six body driven symmetric pendulum system (5.3). The construction of this investigated model in the software Spring is considered in the Appendix 3.

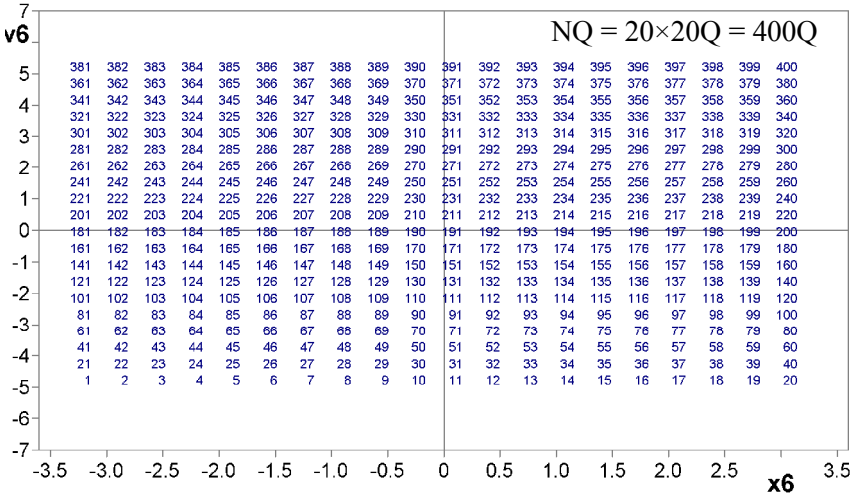

Fig. 5.2. A grid of 20×20 = 400Q initial conditions inside the rectangle ($-\pi$; -5.0 / π; 5.0) of coordinates φ_i and $\dot{\varphi}_i$ for construction of periodic skeleton in the six body driven symmetric pendulum system (5.3). Parameters: $m_1 = m_2 = \ldots = m = 1$, $b_1 = b_2 = \ldots = b = 0.2$, $c_1 = c_2 = \ldots = c = 10$, $l_1 = l_2 = \ldots = l = 0.5$, $\omega = 4$, $h = 3$, $\varphi_0 = 0$, $g = 10$, $k = 7$.

Table 5.1. Periodic skeleton consists of 3 periodic oscillating orbits (regimes, attractors), among them are two stable regimes P1 (1/1) (resonant and non-resonant) and one unstable regime P1 (1/1) for construction of periodic skeleton in the six body driven symmetric pendulum system (5.3).

Nr.	Orbits	φ_i	$\dot{\varphi}_i$	ρ_{max}
A	P1 (1/1) stable resonant	$\mathbf{x_1}$ = 0.001226 $\mathbf{x_2}$ = -0.297601 $\mathbf{x_3}$ = -0.625689 $\mathbf{x_4}$ = -0.988623 $\mathbf{x_5}$ = -1.340830 $\mathbf{x_6}$ = -1.570854	$\mathbf{v_1}$ = 0.929288 $\mathbf{v_2}$ = 1.860250 $\mathbf{v_3}$ = 2.907649 $\mathbf{v_4}$ = 4.000139 $\mathbf{v_5}$ = 4.962034 $\mathbf{v_6}$ = 5.527472	ρ_{max} = 0.944668
B	P1 (1/1) unstable	$\mathbf{x_1}$ = 1.396726 $\mathbf{x_2}$ = 0.38462 $\mathbf{x_3}$ = 0.030276 $\mathbf{x_4}$ = -1.274929 $\mathbf{x_5}$ = -2.420837 $\mathbf{x_6}$ = -3.280096	$\mathbf{v_1}$ = 0.407374 $\mathbf{v_2}$ = -1.431633 $\mathbf{v_3}$ = -0.655393 $\mathbf{v_4}$ = 1.814081 $\mathbf{v_5}$ = 0.786257 $\mathbf{v_6}$ = -1.38399	ρ_{max} = 1.380530
C	P1 (1/1) stable non-resonant	$\mathbf{x_1}$ = 0.221727 $\mathbf{x_2}$ = -0.166794 $\mathbf{x_3}$ = -0.128102 $\mathbf{x_4}$ = -0.101835 $\mathbf{x_5}$ = -0.085649 $\mathbf{x_6}$ = -0.077964	$\mathbf{v_1}$ = 0.059383 $\mathbf{v_2}$ = -0.033715 $\mathbf{v_3}$ = -0.018908 $\mathbf{v_4}$ = 0.009416 $\mathbf{v_5}$ = 0.003253 $\mathbf{v_6}$ = -0.001023	ρ_{max} = 0.964142

Passport of periodic regime A

P1 **stable resonant** (ρ_{max} = 0.944668), symmetric

Fixed point

x_1 = 0.001226	v_1 = 0.929288
x_2 = -0.297601	v_2 = 1.860250
x_3 = -0.625689	v_3 = 2.907649
x_4 = -0.988623	v_4 = 4.000139
x_5 = -1.34083	v_5 = 4.962034
x_6 = -1.570854	v_6 = 5.527472

Phase portraits

m_1

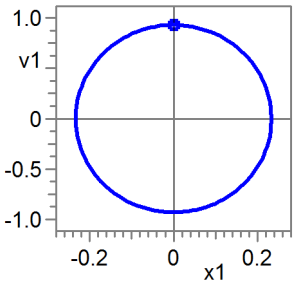

x_1 = -0.232892 … 0.232892
v_1 = -0.929288 … 0.929288
Ax$_1$ = 0.232892

m_2

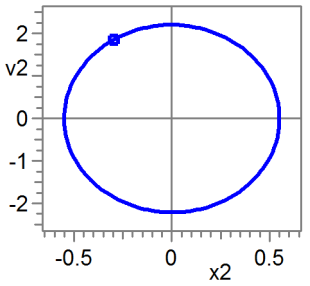

x_2 = -0.550911 … 0.550911
v_2 = -2.205702 … 2.205702
Ax$_2$ = 0.550911

m_3

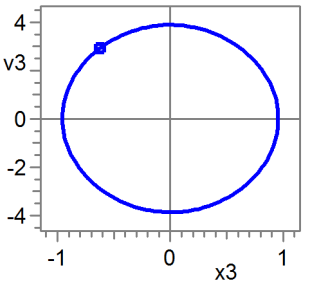

x_3 =-0.957180 … 0.957180
v_3 = -3.876684 … 3.876684
Ax$_3$ = 0.957180

m_4

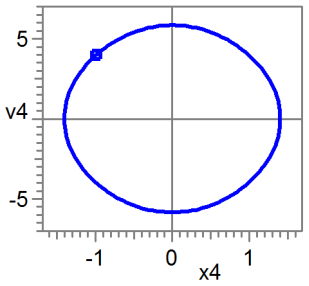

x_4 = -1.405814 … 1.405814
v_4 = -5.841293 … 5.841293
Ax$_4$ = 1.405814

m_5

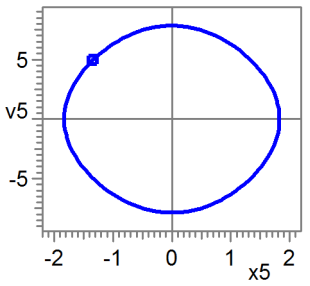

x_5 = -1.828880 … 1.828880
v_5 = -7.840457 … 7.840457
Ax$_5$ = 1.828880

m_6

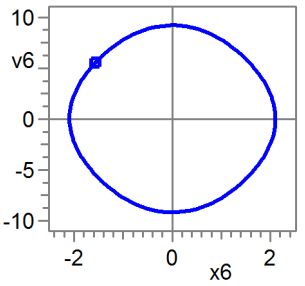

x_6 = -2.097804 … 2.097804
v_6 = -9.194004 … 9.194004
Ax$_6$ = 2.097804

Stability

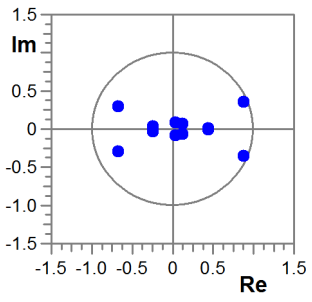

ρ_1 = 0.944668	α_1 = -21°	ρ_7 = 0.244518	α_7 = 173°
ρ_2 = 0.944668	α_2 = 21°	ρ_8 = 0.244518	α_8 =-173°
ρ_3 = 0.735605	α_3 = -156°	ρ_9 = 0.139233	α_9 =-28°
ρ_4 = 0.735605	α_4 = 156°	ρ_{10} = 0.139233	α_{10} = 28°
ρ_5 = 0.445425	α_5 = -0.77°	ρ_{11} = 0.094548	α_{11} = -69°
ρ_6 = 0.445425	α_6 = 0.77°	ρ_{12} = 0.094548	α_{12} = 69°

Passport of periodic regime B

P1 **unstable resonant** (ρ_{max} = 1.380530), symmetric

Fixed point

x_1 = 1.396726	v_1 = 0.407374
x_2 = 0.38462	v_2 = -1.431633
x_3 = 0.030276	v_3 = -0.655393
x_4 = -1.274929	v_4 = 1.814081
x_5 = -2.420837	v_5 = 0.786257
x_6 = -3.280096	v_6 = -1.38399

Phase portraits

m_1

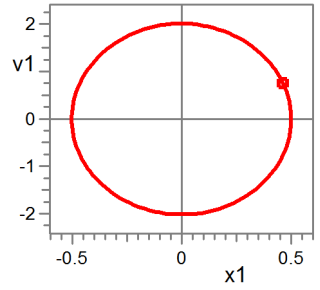

x_1 = -0.501874 … 0.501874
v_1 = - 2.013275 … 2.013275
Ax$_1$ = 0.501874

m_2

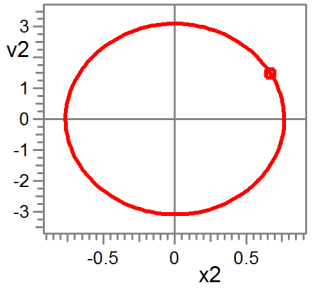

x_2 = -0.765633 … 0.765633
v_2 = -3.095370 … 3.095370
Ax$_2$ = 0.765633

m_3

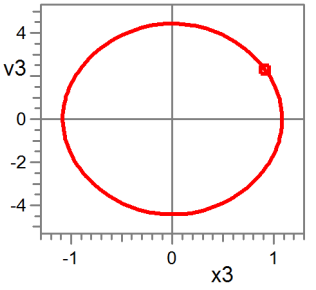

x_3 = -1.082101 … 1.082101
v_3 = -4.428233 … 4.428233
Ax$_3$ = 1.082101

m_4

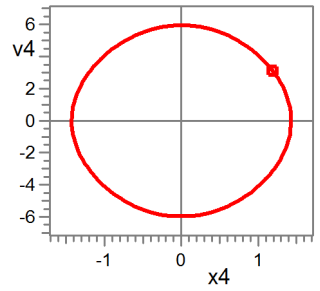

x_4 = -1.428143… 1.428143
v_4 = -5.959546… 5.959546
Ax$_4$ = 1.428143

m_5

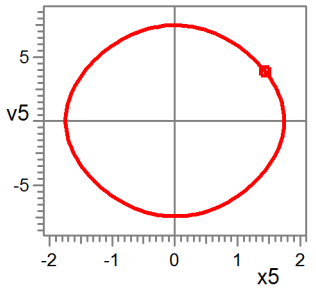

x_5 = -1.745314 … 1.745314
v_5 = -7.451887 … 7.451887
Ax$_5$ = 1.745314

m_6

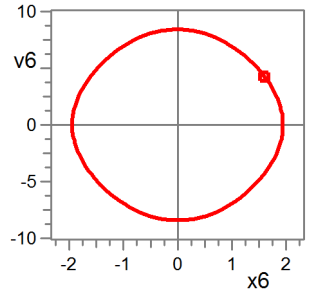

x_6 = -1.941643 … 1.941643
v_6 = -8.419533 … 8.419533
Ax$_6$ = 1.941643

Stability

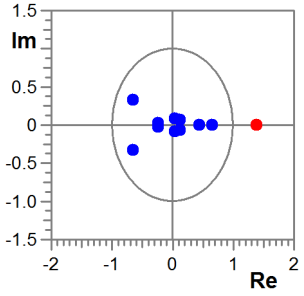

ρ_1 = 1.380530	α_1 = 0°	ρ_7 = 0.24455	α_7 = 173°
ρ_2 = 0.655249	α_2 = 0°	ρ_8 = 0.24455	α_8 =-173°
ρ_3 = 0.733316	α_3 = -153°	ρ_9 = 0.139207	α_9 = 28°
ρ_4 = 0.733316	α_4 = 153°	ρ_{10} = 0.139207	α_{10} = -28°
ρ_5 = 0.445088	α_5 = 0.28°	ρ_{11} = 0.09428	α_{11} = -66°
ρ_6 = 0.445088	α_6 = -0.28°	ρ_{12} = 0.09428	α_{12} = 66°

Passport of periodic regime C

P1 **stable non-resonant** (ρ_{max} = 0.964142), symmetric

Fixed point

x_1 = 0.221727	v_1 = 0.059383
x_2 = -0.166794	v_2 = -0.033715
x_3 = -0.128102	v_3 = -0.018908
x_4 = -0.101835	v_4 = 0.009416
x_5 = -0.085649	v_5 = 0.003253
x_6 = -0.077964	v_6 = -0.001023

Phase portraits

m_1

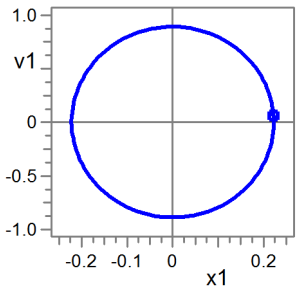

x_1 = -0.222189 … 0.222189
v_1 = -0.890471 … 0.890471
Ax_1 = 0.222189

m_2

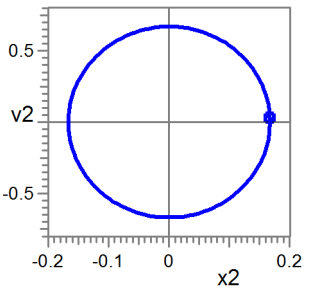

x_2 = -0.167007 … 0.167007
v_2 = -0.668996 … 0.668996
Ax_2 = 0.167007

m_3

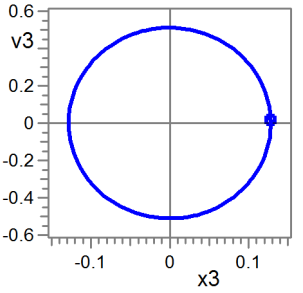

x_3 = -0.128179 … 0.128179
v_3 = -0.512197 … 0.512197
Ax_3 = 0.128179

m_4

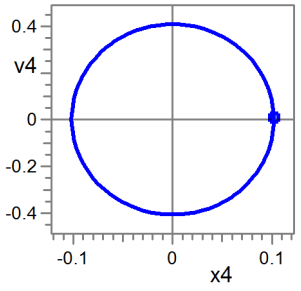

x_4 = -0.101835 … 0.101835
v_4 = -0.407599 … 0.407599
Ax_4 = 0.101835

m_5

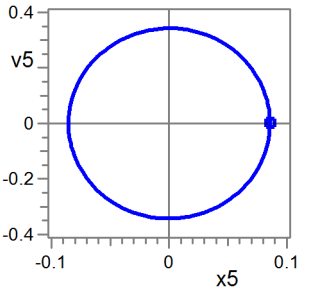

x_5 = -0.085649 … 0.085649
v_5 = -0.342929 … 0.342929
Ax_5 = 0.085649

m_6

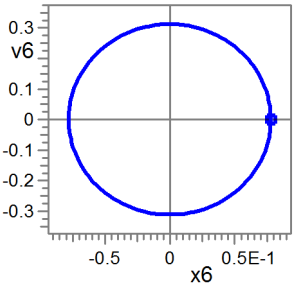

x_6 = -0.077964 … 0.077964
v_6 = -0.311722 … 0.311722
Ax_6 = 0.077964

Stability

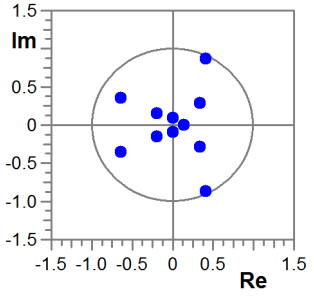

ρ_1 = 0.964142	α_1 = -64°	ρ_7 = 0.244608	α_7 = -141°
ρ_2 = 0.964142	α_2 = 64°	ρ_8 = 0.244608	α_8 = 141°
ρ_3 = 0.729037	α_3 = -150°	ρ_9 = 0.139393	α_9 = 0.9°
ρ_4 = 0.729037	α_4 = 150°	ρ_{10} = 0.139393	α_{10} = -0.9°
ρ_5 = 0.444402	α_5 = -39°	ρ_{11} = 0.093548	α_{11} = -88°
ρ_6 = 0.444402	α_6 = 39°	ρ_{12} = 0.093548	α_{12} = 88°

5.2.3 *Bifurcation analysis of six body pendulum system with varying frequency of excitation force*

In the previous paragraph the periodic skeleton for the six body symmetric driven pendulum systems with several equilibrium positions was constructed and it will be used for performing the global bifurcation analysis in this section by the method of complete bifurcation groups.

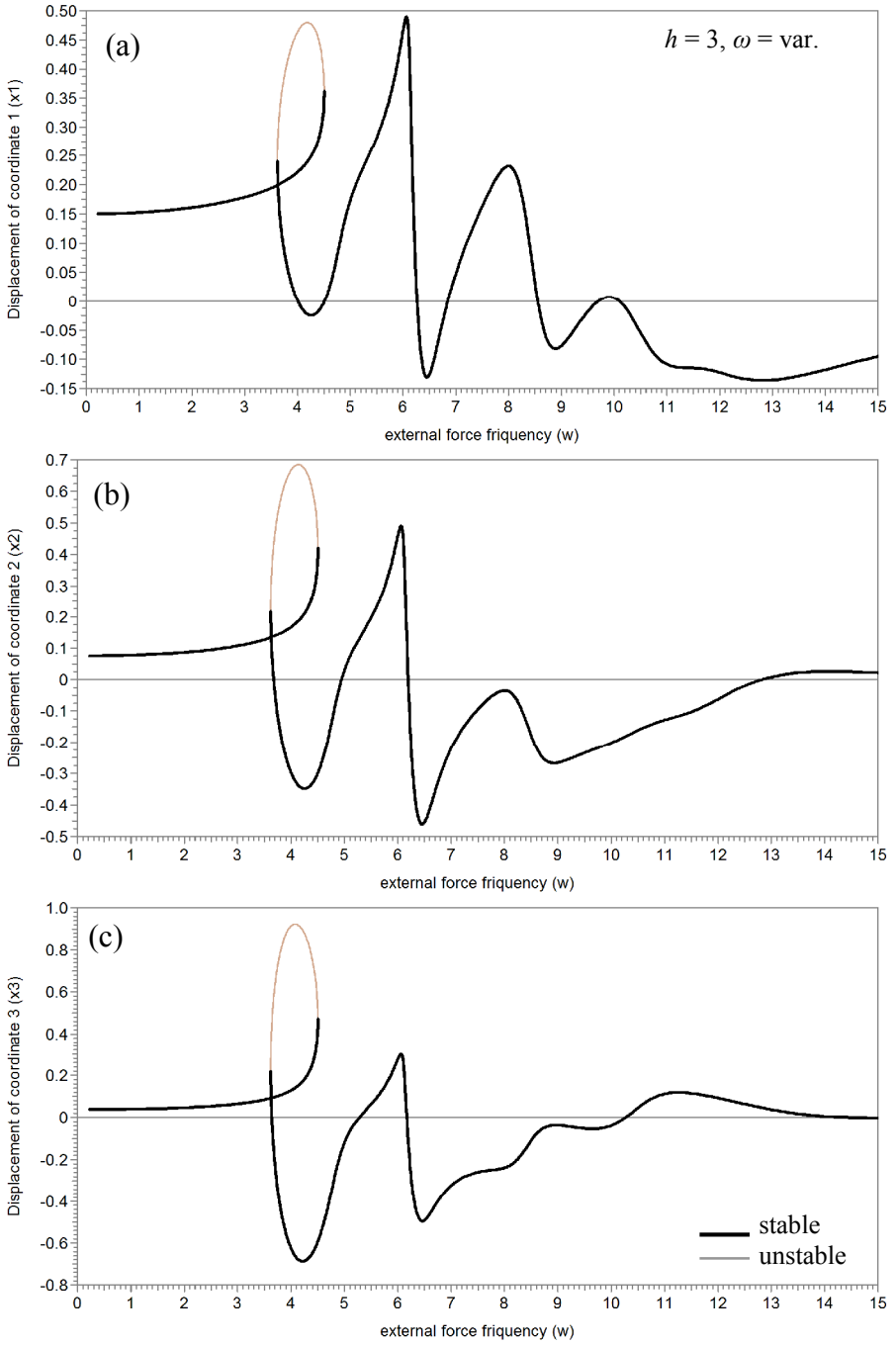

Fig. 5.3. Bifurcation diagrams S1(ω) of the fixed periodic points of the coordinates φ_{ip} versus excitation force frequency ω. There is 1T bifurcation group with hysteresis effect in the six body driven symmetric pendulum system (5.3). Parameters: $m_1 = m_2 = \ldots = m = 1$, $b_1 = b_2 = \ldots = b = 0.2$, $c_1 = c_2 = \ldots = c = 10$, $l_1 = l_2 = \ldots = l = 0.5$, ω = var., $h = 3$, $\varphi_0 = 0$, $g = 10$, $k = 7$.

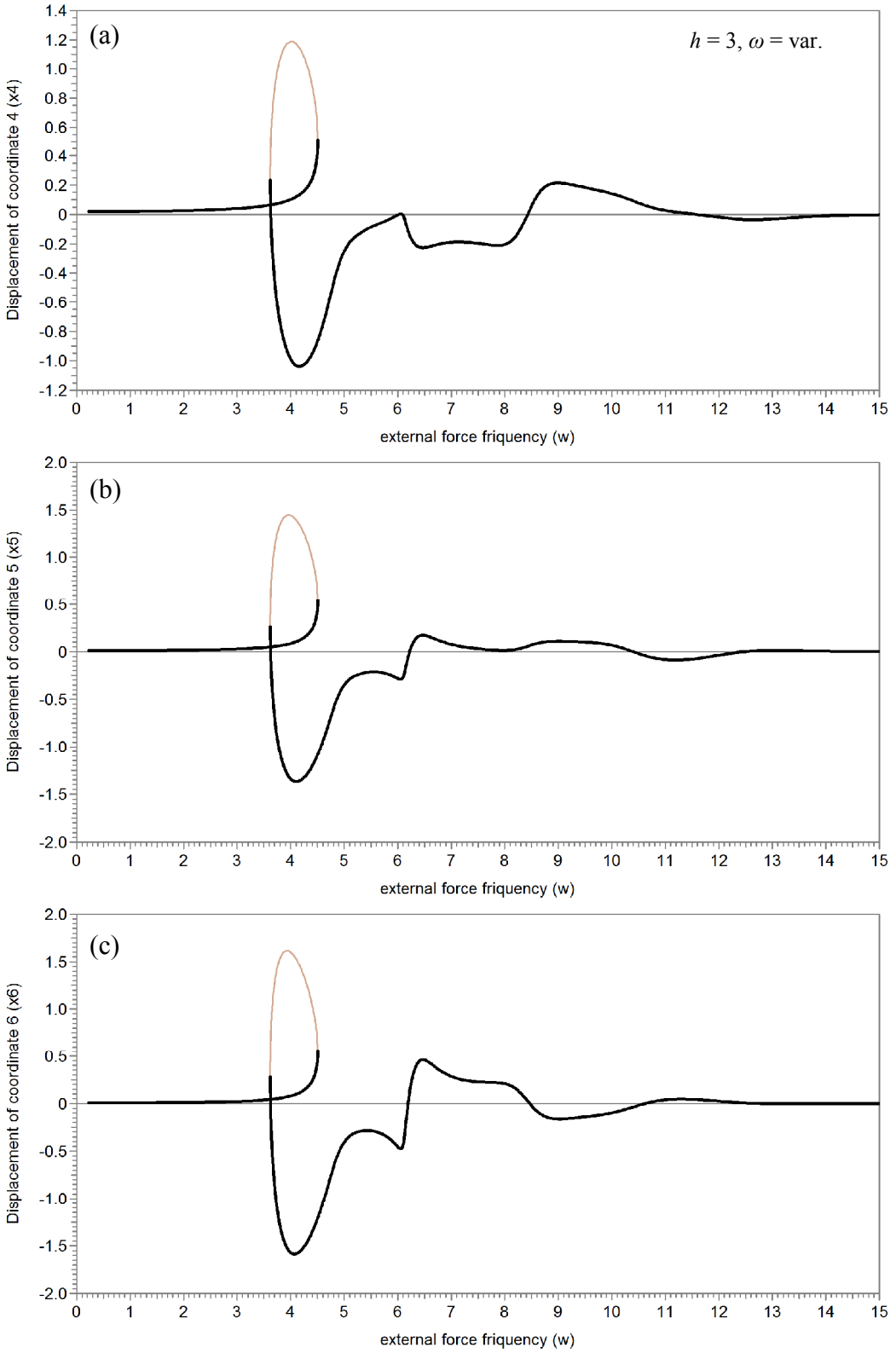

Fig. 5.4. Bifurcation diagrams S1(ω) of the fixed periodic points of the coordinates φ_{ip} versus excitation force frequency ω. There is 1T bifurcation group with hysteresis effect in the six body driven symmetric pendulum system (5.3). Parameters: $m_1 = m_2 = \ldots = m = 1$, $b_1 = b_2 = \ldots = b = 0.2$, $c_1 = c_2 = \ldots = c = 10$, $l_1 = l_2 = \ldots = l = 0.5$, ω = var., $h = 3$, $\varphi_0 = 0$, $g = 10$, $k = 7$.

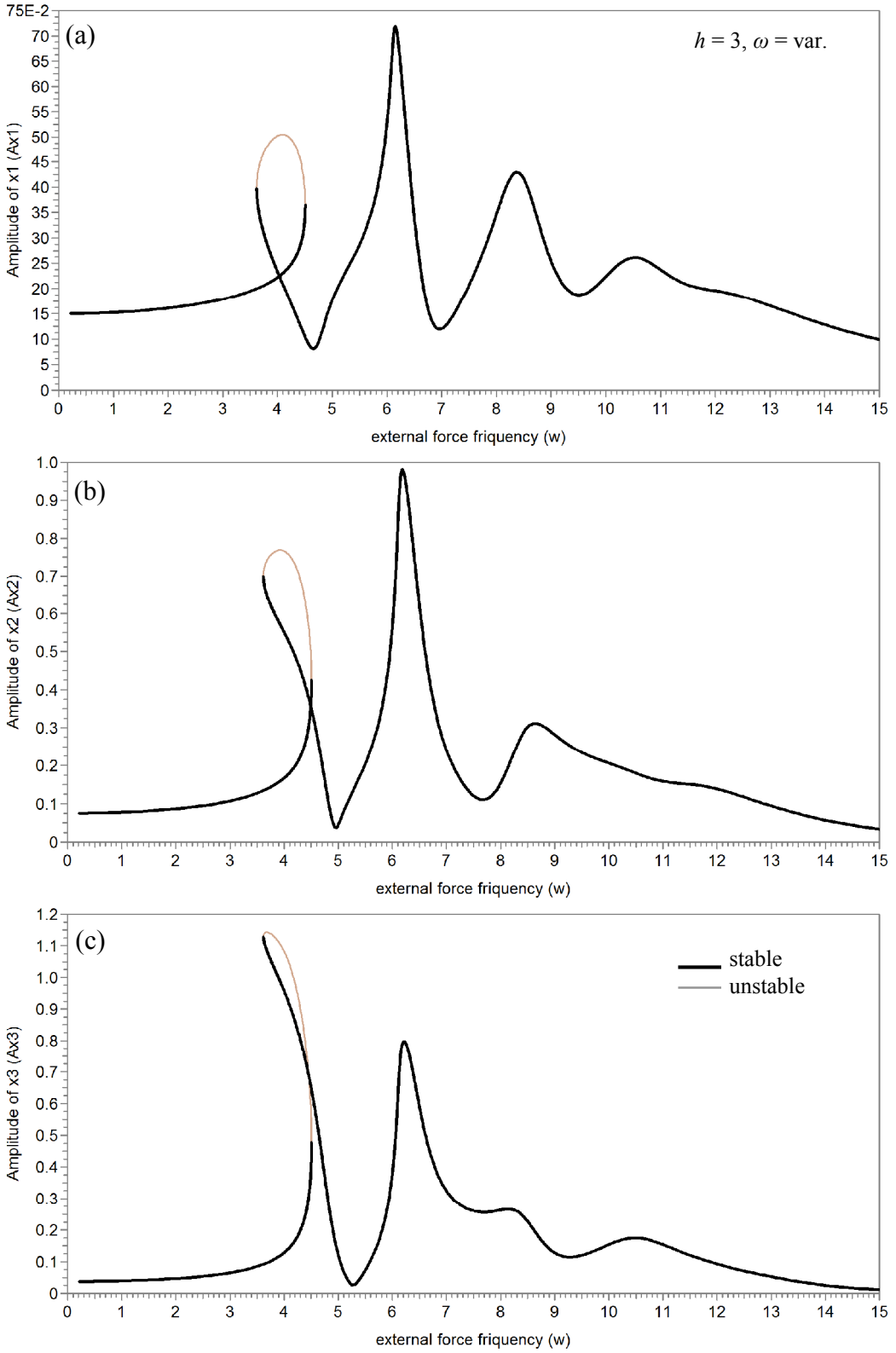

Fig. 5.5. Bifurcation diagrams S1(ω) of the fixed periodic points of the amplitude of rotation Am_{ip} versus excitation force frequency ω. There is 1T bifurcation group with hysteresis effect in the six body driven symmetric pendulum system (5.3). Parameters: $m_1 = m_2 = \ldots = m = 1$, $b_1 = b_2 = \ldots = b = 0.2$, $g = 10$, $c_1 = c_2 = \ldots = c = 10$, $l_1 = l_2 = \ldots = l = 0.5$, ω = var., $h = 3$, $\varphi_0 = 0$, $k = 7$.

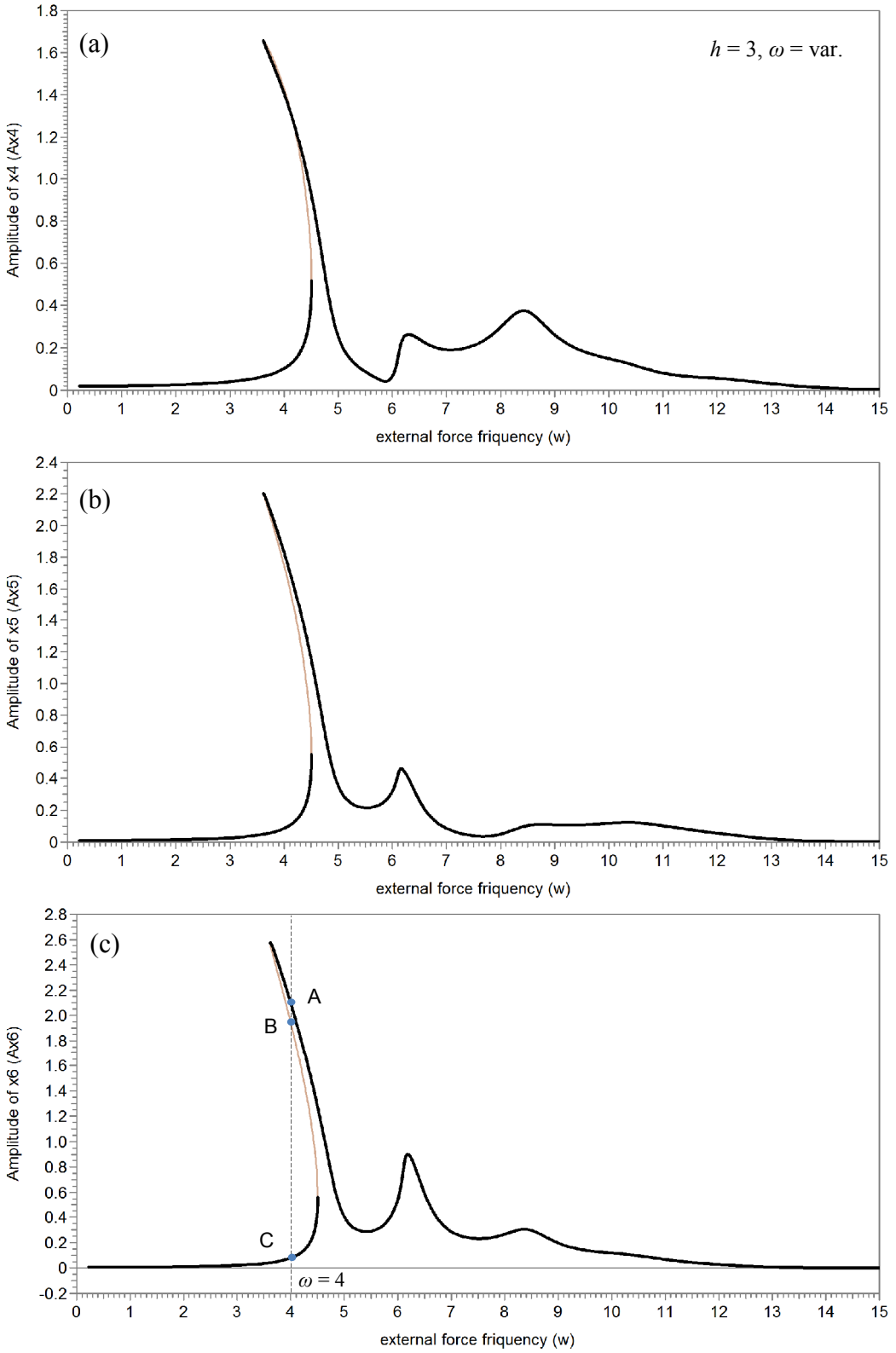

Fig. 5.6. Bifurcation diagrams S1(ω) of the fixed periodic points of the amplitude of rotation Am_{ip} versus excitation force frequency ω. There is 1T bifurcation group with hysteresis effect in the six body driven symmetric pendulum system (5.3). Parameters: $m_1 = m_2 = \ldots = m = 1$, $b_1 = b_2 = \ldots = b = 0.2$, $g = 10$, $c_1 = c_2 = \ldots = c = 10$, $l_1 = l_2 = \ldots = l = 0.5$, ω = var., $h = 3$, $\varphi_0 = 0$, $k = 7$.

In the studied pendulum system (5.3) one 1T bifurcation group was found. Bifurcation diagrams S1(ω) of the fixed periodic points of the coordinates φ_{ip} versus excitation force frequency ω are shown on Figs. 5.3-5.4. Bifurcation diagrams S1(ω) of the fixed periodic points of the amplitude of rotation Am_{ip} versus excitation force frequency ω are shown on Figs. 5.5-5.6. The stable solutions on bifurcation diagrams are plotted by black solid lines, but unstable solutions are plotted by reddish thin lines.

The studied six body driven symmetric pendulum system has a stable P1 regime with the period T_ω of excitation force and P1 unstable one. This bifurcation group has two fold bifurcations. As well as in parameter range $\omega \in (3.6 \div 4.5)$ such nonlinear phenomenon as hysteresis was found. The amplitudes of rotation of resonant regime are larger than the non-resonant has. For example for the cross-section of bifurcation diagram (Fig. 5.6) for $\omega = 4$ the stable periodic non-resonant symmetric regime C has the rotation amplitudes of sixth mass $Ax_6 = 0.077964$, but the stable periodic resonant symmetric regime A - $Ax_6 = 2.097804$. It means that the amplitudes are 27 times bigger. The switching between these two stable periodic regimes can be done by changing initial conditions.

5.3 Conclusions

In this chapter the most commonly studied model of forced oscillations in the driven damped pendulum systems with several degrees of freedom was investigated. The possibility of using the method of complete bifurcation groups for the global analysis of the six body symmetric driven pendulum systems with several equilibrium positions is demonstrated.

The possible applications of six body symmetric driven pendulum systems with several equilibrium positions are design of prospective laboratory equipment for control education, vibration absorbing systems, mixing (liquids, washing machines), etc.

6

Experimental Investigations and Tests of the Pendulum Systems by the Method of Complete Bifurcation Groups

6.1 Introduction

Practice convincingly shows that a carefully designed experimental design allows fully comprehending the experiment, foreseeing the amount of work and avoiding any mistakes, which is key to its success [5].

The author does not know any serious experimental studies of rare attractors and rare bifurcation groups, but these experiments are, of course, necessary.

As mentioned above, the main task of the doctoral thesis is a theoretical and practical study of the nonlinear dynamics of the pendulum system based on the method of complete bifurcation groups, which allow conducting the global bifurcation analysis and finding new bifurcation groups, rare periodic and chaotic attractors both oscillating and rotating. The results can provide guidance on the use of complex regular and chaotic regimes on real objects in vibroengineering, robotics, space dynamics, medicine etc.

Note that the theoretical and experimental results obtained in this chapter should be considered preliminary in the development of real objects. They also can serve as a basis for the development of more complex pendulum-like models than considered in the present doctoral thesis. These complex models can take into account the technological application, additional degrees of freedom of the model, the dry friction effect, the influence of external factors (magnetic fields, the correct way of experimental data collection through the microcontroller, etc.), the dynamic characteristics of the exciter and control system.

In previous chapters, the use of the method of complete bifurcation groups allowed finding new complex rare regular and chaotic (oscillating, oscillating-rotating and rotating) regimes in the study of the driven damped pendulum systems with one or several degrees of freedom. These regimes can be used on real objects on real objects in technics: for the robotic purposes, in space dynamics, for the mixing process, such as liquids, washing machines, etc.

The purpose of this chapter is showing the possibility of performance of the experimental investigations in more realistic models of pendulum systems, which were discussed in the present doctoral thesis. The visualization possibility of the founded regimes by the method of complete bifurcation groups in the pendulum systems is discussed as well.

For these purposes, the experimental setup for natural experimental investigations in the simplest pendulum system with the periodically vibrating point of suspension in vertical direction was developed and produced. The construction and description of this setup is presented in Paragraph 6.2. The experimental results of bifurcation analysis in studied pendulum system are discussed in Paragraph 6.3. Comparison with theoretical investigations is described in paragraph 6.4 as well. The demonstration of nonlinear effects, complex subharmonic oscillating and rotating regimes, chaotic and transient processes with animation software “Parametrically Excited Pendulum”, created by the author of present doctoral thesis using Pascal programming language, is presented in Paragraph 6.5.

The experimental investigations were performed with help of colleagues from the Faculty of Electronics and Telecommunications of RTU.

6.2 Experimental setup of the pendulum with vertical vibrations of the support

For the experimental investigations of the behavior of the pendulum system with the periodically vibrating point of suspension in vertical direction the experimental setup (Fig. 6.1) was produced. The model of this setup can be described by the pendulum system with one degree of freedom. The mathematical model of this system and the results of complete bifurcation analysis by the method of complete bifurcation groups are presented in the Paragraph 3.3. As a result, rare regular and chaotic attractors and some other new nonlinear phenomena, such as co-existence of different types of periodic and chaotic attractors (rotation R1, P1 hilltop, subharmonic solutions and chaotic oscillations) and rare and chaotic rotational regimes (with a period of excitation, subharmonic and chaotic ones), oscillatory-rotational regimes, have been found for the pendulum system (3.2).

The investigated in this chapter pendulum system was first described by A. Stephenson, who found that the small oscillations near upper unstable equilibrium position of the pendulum might be stable when the driving frequency is fast [53] But P. Kapitza was the first who introduced the experimental investigations of the pendulum with periodically vibrating point of suspension in vertical direction [76] He carried out a number of experimental studies to improve the existence of the hilltop regimes. This pendulum model has attracted attention of many researchers, e.g. [8, 11, 13, 15, 19, 42, 44, 49, 51, 56 and many others]. As a rule, to carry out such kind of experiments a technological infrastructure is required, for example, the laboratory of the vibrational mechanics of the Institute of mechanical engineering of Russian academy of science and "Mechanobr-Tekhnika" in St. Petersburg, the head of which is Professor, Doctor of Sci. (Phys. and Math.) I. Blekhman, the laboratory of vibromechanics of Blagonravov Mechanical engineering institute of RAS, the head of which is Professor, Dr.habil.sc.ing., Grigory Panovko, the laboratory of the Institute of Mechanics of Riga Technical University and the laboratory "Nonlinear effects of oscillating systems" under the guidance of Professor, Dr.habil.sc.ing., S. Tsyfansky.

The equation of motion of the experimental setup for the pendulum system (Fig.6.1) is such:

$$m\ell^2\ddot{\varphi} + b\dot{\varphi} + m\ell\left(g - h\omega^2\cos\omega t\right)\sin\varphi = 0\,, \qquad (6.1)$$

where φ – angle of the pendulum, read-out from a vertical line; $\dot{\varphi}$ - angular velocity, where $\dot{\varphi} = d\varphi / dt$; t – time; m and ℓ– mass and length of the pendulum accordingly; g – gravitation constant; b – linear damping coefficient; h and ω – vertical vibrating amplitude and frequency of the support, where $\omega = 2\pi\nu$; ν - frequency of excitation measured by optocoupler in Hz .

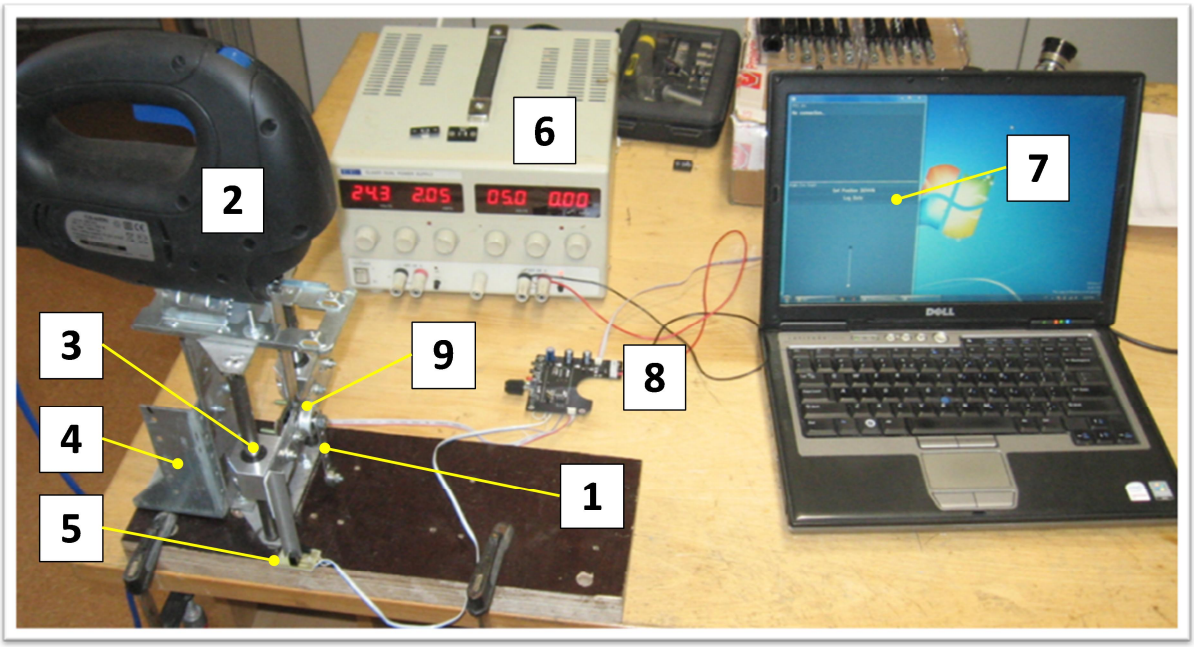

Fig. 6.1. General view of experimental setup of the pendulum with vertical vibrations of the support consisted of 1-pendulum; 2-exciter; 3-slides with special linear bearings; 4-frame; 5-optocoupler for measuring the frequency of excitation; 6-power supply, 5V; 7-software for experimental data collection and animation; 8-AVR microcontroller; 9-pendulum's support by ball bearing and Hall-effect 360° angle position encoder with a 14-bit high resolution output and measuring accuracy 0.05.

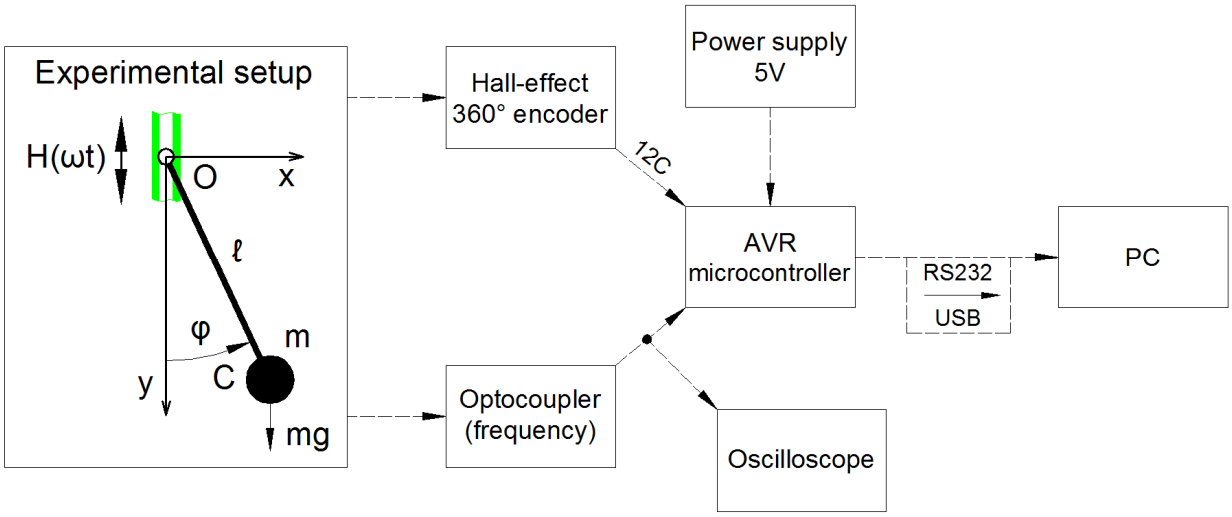

Fig. 6.2. Block-diagram of the experimental setup of the pendulum model with the periodically vibrating point of suspension in vertical direction.

Table 6.1. Parameters of experimental setup of the pendulum with vertical vibrations of the support

Parameters	Values
l – length of the pendulum [m]	0.060
m – mass of the pendulum [kg]	0.0076
b – computed linear damping coefficient in the support	0.000035
h – amplitude of excitation [m]	0.009
v – frequency range of excitation [Hz]	10-30

The physical parameters of the studied experimental setup are shown in Table 6.1. The mechanical part of experimental setup of the pendulum with vertical vibrations of the support consists from pendulum (1) with length l = 0.060 [m] and mass m = 0.0076 [kg]. Vibroexciter (2) converts the rotational motion of the motor into reciprocating in vertical direction. The amplitude of excitation is h = 0.009 [m]. The frequency range of the vertical vibrations of the support is ν = 10-30 [Hz] or ω = 62.8-188.5[rad/s]. The support of the pendulum slides along a guide beam using special linear bearings (3). The frame (4) rigidly fixes the setup to the base. Frequency measurements are done by optocoupler "Omron" (5) and are controlling with oscilloscope as well. Data transfer and controlling is performed by the AVR microcontroller (8) with power supply 5V (6). Using Pascal programming language the software (7) for experimental data collection and animation is written. It helps to save the experimental data and to animate the real time position of pendulum. The pendulum (1) is supported by ball bearing and its angle of rotations is measured by the Hall-effect 360° angle position encoder with a 14-bit high resolution output and measuring accuracy 0.05 of degree. At the first stage of the experiment the free damped oscillations were obtained (Fig. 6.3). Data processing allow estimating the logarithmic decrement, $\delta = \ln(a_0 / a_1)$. For the studied setup it is equal $\delta \approx 0.31$, which approximately corresponds to linear damping coefficient b = 0.000035. Differences in this parameter definition appeared due to the effect of dry friction.

Experimentally the multiplicity of P1 hilltop and P1 zero attractors, and two period-1 rotations in clockwise and counter-clockwise direction were investigated (Figs. 6.4-6.5). Constructing these regimes the frequency of excitation ν = 19.56 Hz or ω = 122.9 [rad/s] and the concrete initial conditions were set. The time interval for the data readout from the Hall-effect position encoder was about 16 ms.

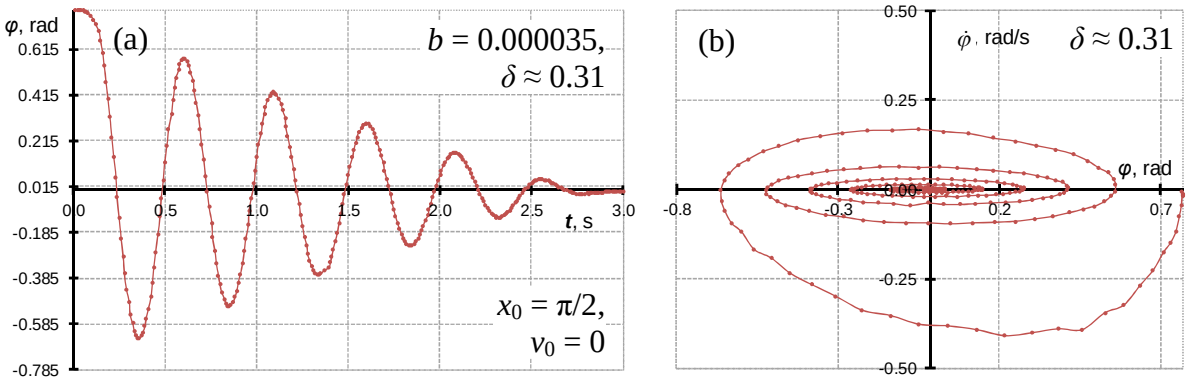

Fig. 6.3. Free damped oscillations of the experimental setup (Fig. 6.1) of the pendulum model with the periodically vibrating point of suspension in vertical direction. The logarithmic decrement is equal $\delta = \ln(a_0/a_1)$.

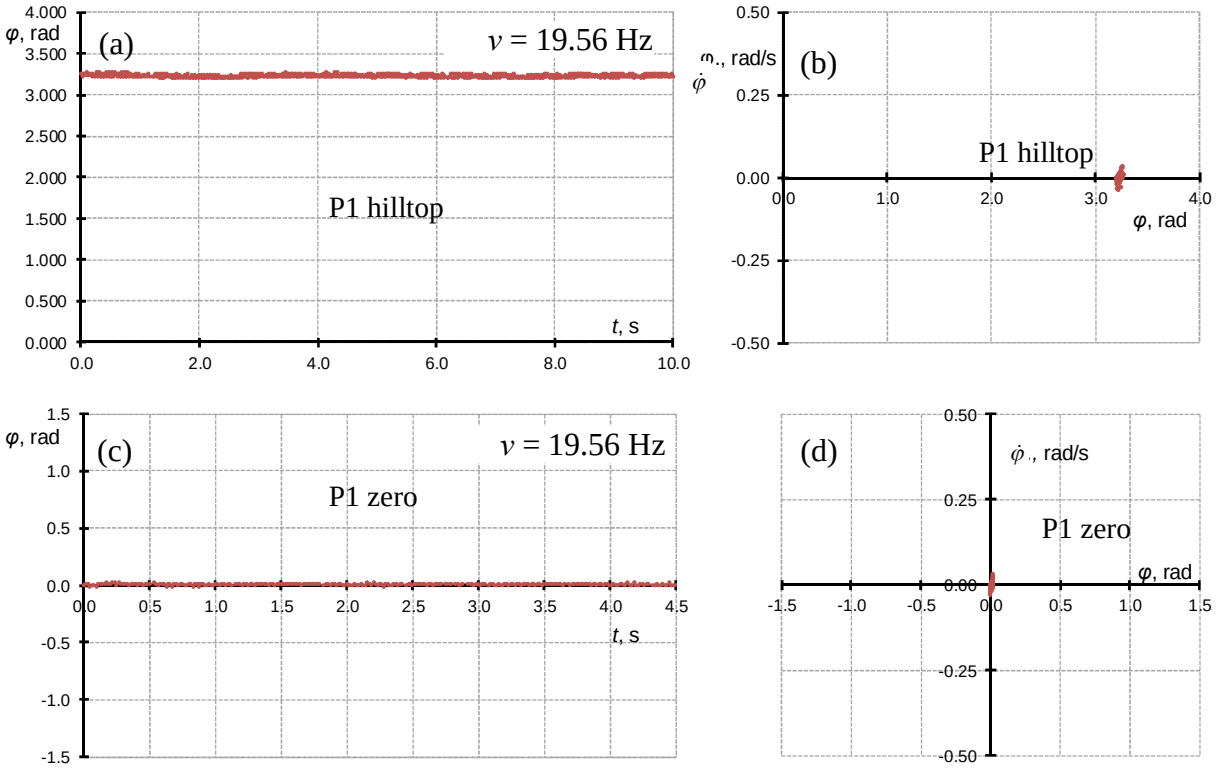

Fig. 6.4. Examples of periodic P1 hilltop and P1 zero regimes obtained by the experimental investigations for frequency ν = 19.56 Hz of excitation. (a)-(b) Time history and phase portrait for stable P1 hilltop regime; (c)-(d) time history and phase portrait of stable P1 zero regime.

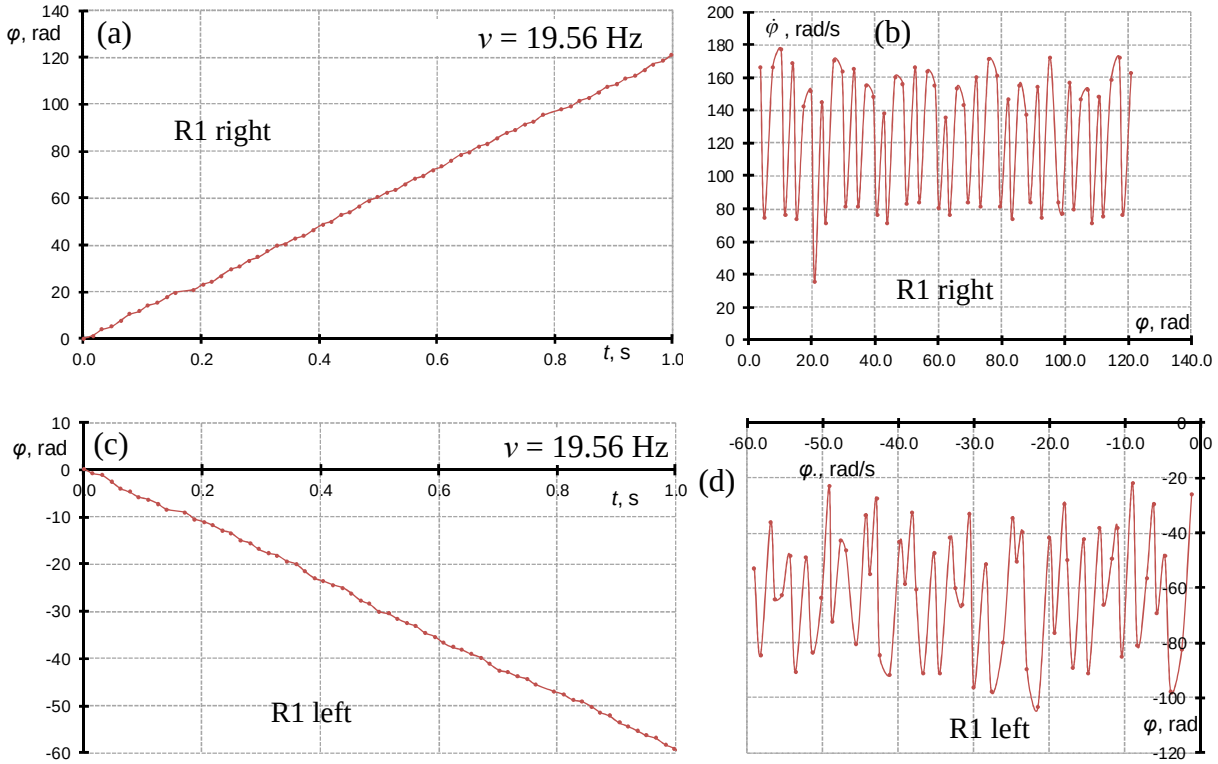

Fig. 6.5. Examples of periodic R1 right and R1 left rotations obtained by the experimental investigations for frequency ν = 19.56 Hz of excitation. (a)-(b) Time history and phase portrait for R1 right rotation; (c)-(d) time history and phase portrait of R1 left rotation.

6.3 Experimental results of bifurcation analysis in the pendulum with vertical vibrations of the support

For the construction of the experimental bifurcation diagrams the data were readout according to the period of excitation force $T_\omega = 2\pi/\omega$. The frequency of excitation force was varying in range ν = 10-30 [Hz] or ω = 62.8-188.5[rad/s], starting from the larger value and decreasing the parameter. Experimental bifurcation diagrams S1(ω) of the coordinate φ of the pendulum versus frequency ω of excitation force are shown in Fig.6.6. There is the coexistence of two different bifurcation groups P1 zero and P1 hilltop. Time histories and phase portraits of these regimes are shown Fig. 6.4-6.5. In the next paragraph the experimental results will be compared with theoretical investigations (see Paragraph 6.4)

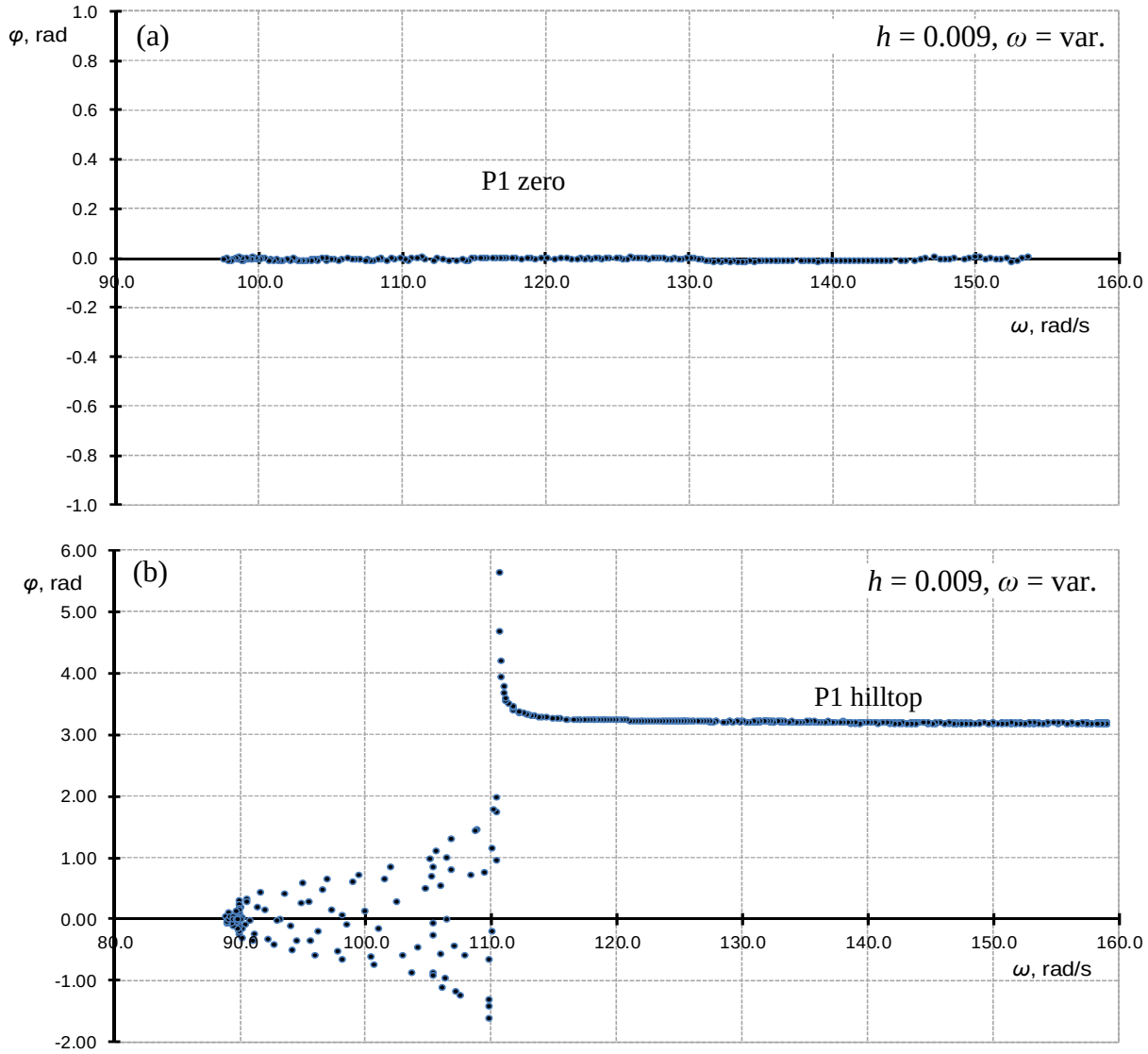

Fig. 6.6. Experimental bifurcation diagrams S1(ω) of the coordinate φ of the pendulum versus frequency ω of excitation force. There is the coexistence of two different bifurcation groups P1 zero and P1 hilltop. Parameters: m = 0.0076, l = 0.06, b = 0.000035, g = 9.81, h = 0.009, ω = var.

6.4 Comparison of experimental results with theoretical investigations

Bifurcation analysis of the studied pendulum model (6.1) was performed by the method of complete bifurcation groups and using the software SPRING [107]. Bifurcation diagrams S1(ω) of the coordinate φ of the pendulum versus frequency ω of excitation force are shown on Fig. 6.7. Diagram (a) shows the results of bifurcation analysis only for oscillating regimes, but diagram (b) – interaction of oscillating and rotating bifurcation groups. There is the coexistence of four different bifurcation groups with regimes P1 zero, P1 hilltop, R1 left and R1 right.

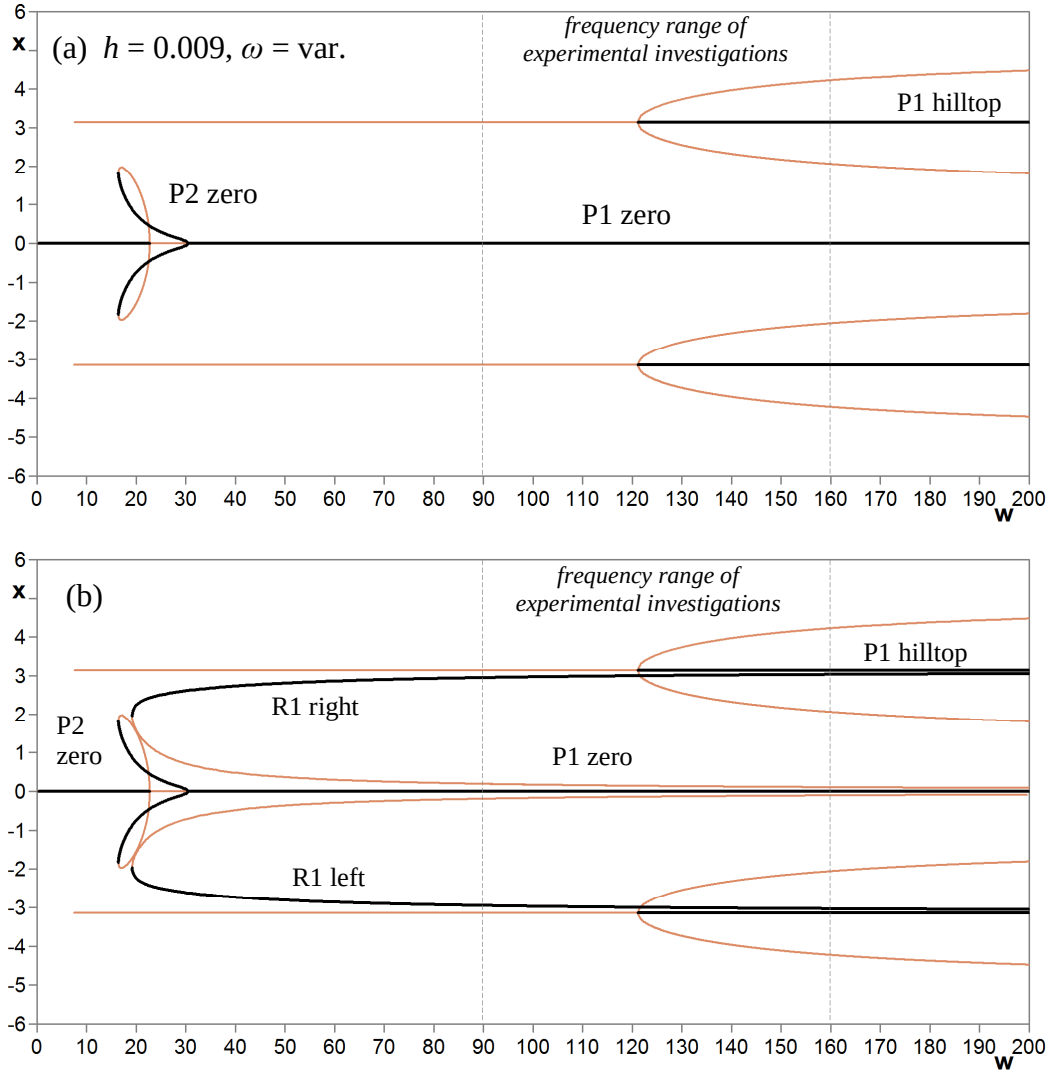

Fig. 6.7. Bifurcation diagrams S1(ω) of the coordinate φ of the pendulum versus frequency ω of excitation force. Diagram (a) shows the results of bifurcation analysis only for oscillating regimes, but diagram (b) – interaction of oscillating and rotating bifurcation groups. There is the coexistence of four different bifurcation groups with regimes P1 zero, P1 hilltop, R1 left and R1 right. Parameters: m = 0.0076, l = 0.06, b = 0.000035, g = 9.81, h = 0.009, ω = var.

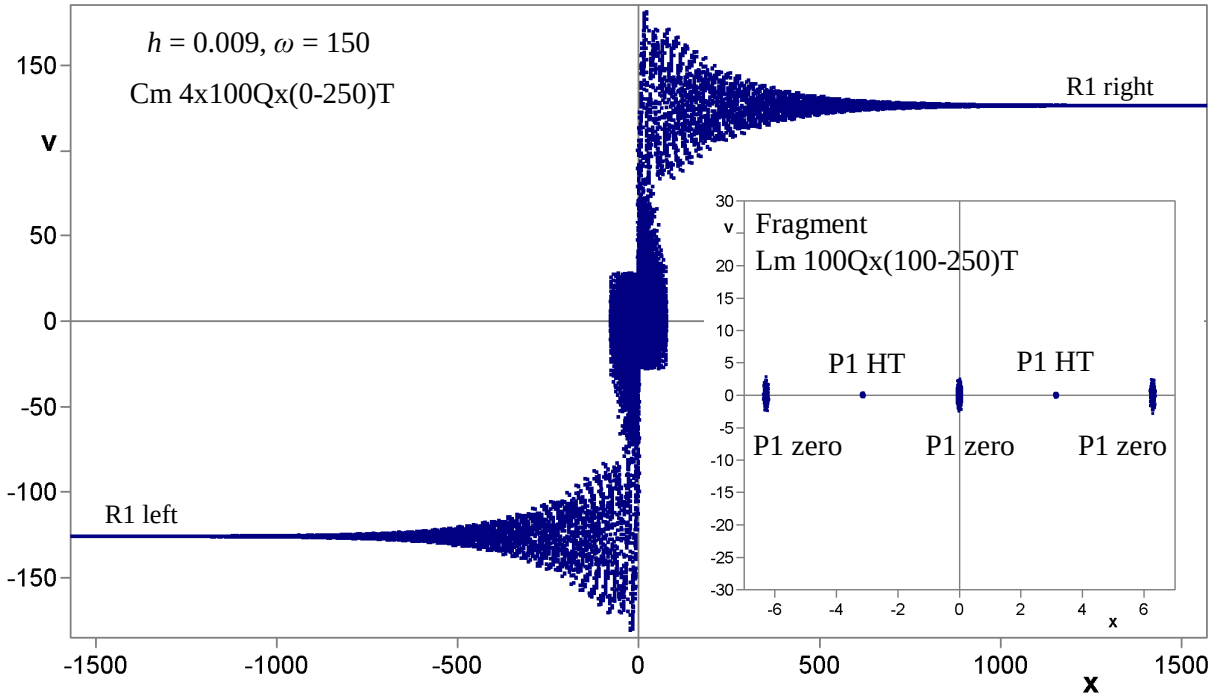

Fig. 6.8. Coexistence of P1 zero and P1 hilltop attractors, R1 left and R1 right rotations on Poincaré map obtained by the mapping Cm 4×100Q×(0-250)T from a contour ($-\pi$, -100; π, 100) without taking into account cyclicality for cross-section of bifurcation diagrams (see Fig.6.7) for ω = 150. Fragment of mapping Lm 100Qx(100-250)T from a line (-2π, 0.0; 2π, 0.0) is shown as well. Parameters: m = 0.0076, l = 0.06, b = 0.000035, g = 9.81, h = 0.009, ω = 150.

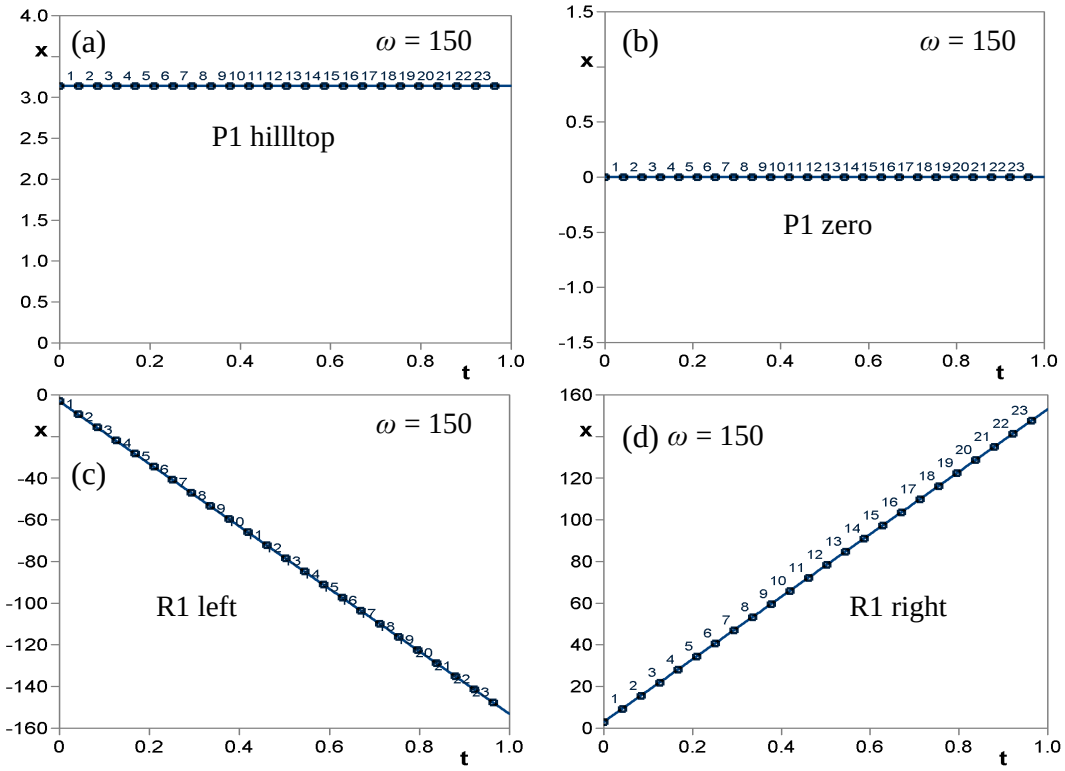

Fig. 6.9. Time histories of coexisting P1 zero and P1 hilltop attractors, and R1 left and R1 right rotations. The mappings on Poincaré map for these regimes are shown in Fig. 6.8. Parameters: m = 0.0076, l = 0.06, b = 0.000035, g = 9.81, h = 0.009, ω = 150.

Coexistence of P1 zero and P1 hilltop attractors, R1 left and R1 right rotations on Poincaré map obtained by the mapping Cm 4×100Q×(0-250)T from a contour (-π, -100; π, 100) without taking into account cyclicality for cross-section of bifurcation diagrams (see Fig.6.7) for ω = 150 is shown in Fig. 6.8. Fragment of mapping Lm 100Qx(100-250)T from a line (-2π, 0.0; 2π, 0.0) is shown as well. Time histories of theses coexisting P1 zero and P1 hilltop attractors, R1 left and R1 right rotations for cross-section of bifurcation diagrams (see Fig.6.7) for ω = 150 are shown in Fig. 6.9.

Thus, the experimentally founded regimes have qualitative agreement with the theoretical investigations. The four different regimes were found in both cases: P1 zero, P1 hilltop, R1 left and R1 right attractors (see Figs. 6.4, 6.5, 6.8, 6.9). Bifurcation diagrams (Fig. 6.6) also corresponds to the results of numerical simulations. Near the subcritical period doubling bifurcation point of P1 hilltop solutions by the small parameter changing the non-ideal construction of experimental setup and other external factors have influence on the system's behaviour. Probably, the quantitative differences appear due to the dry friction effect, the influence of external factors (magnetic fields, the correct way of experimental data collection through the microcontroller, etc.) and the unheeded dynamic characteristics of the exciter (motor). These influences require further study. Therefore, as it was mentioned before the theoretical and experimental results obtained in this chapter should be considered preliminary. In the future it is planned to conduct the more detailed analysis of dynamics of the pendulum systems including the described above influences on the studied system. The possible applications of founded regimes in the driven pendulum systems with the periodically vibrating point of suspension in vertical direction may be the energy extraction [41], mixing (liquids, washing machines), robotics [60], communication and orientation systems of the spacecraft (antenna) [18,126], etc.

6.5 Animation software "Parametrically Excited Pendulum"

The animation of the dynamics of the investigated pendulum systems can provide better understanding of the obtained results. For these proposes it is possible to use the commercial software, such as Working Model [*www.design-simulation.com*], Simulation X [*www.itisim.com/simulationx*], Universal Mechanism [*www.universalmechanism.com*] and other.

The main aim of this paragraph is to show the possibility of visualization of the founded regimes by the method of complete bifurcation groups in the pendulum systems discussed in the

present doctoral thesis. The animation of nonlinear phenomena of pendulum systems can be useful not only for student as methodological material, but also for engineers who are working with real pendulum-like systems. As an example in this paragraph the software for animation of parametrically excited pendulum in vertical direction it shown.

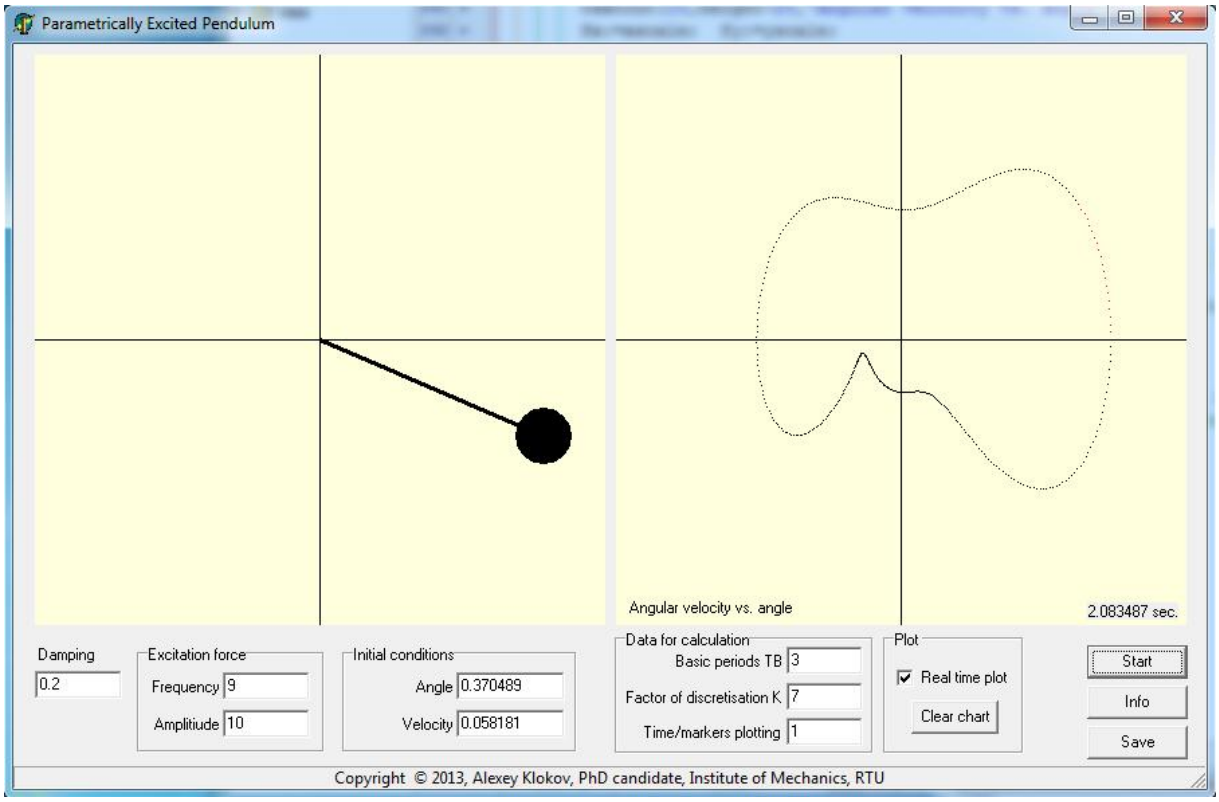

Fig. 6.10. The animation software “Parametrically Excited Pendulum” for the pendulum system with the periodically vibrating point of suspension in vertical direction (Fig. 3.15 and Eq.3.2).

The software was created using Pascal programming language. The software part, which describes the equation of motion (3.2) of the studied pendulum system with the periodically vibrating point of suspension in vertical direction, is look such:

```
…
Function TForm1.PendFunc(T,X,XPrime:Float):Float;
begin
  Result:=-Damping*XPrime-(1+ Amp*cos(omega*T))*sin(Pi*X);
end;
…
```

The software illustrates the pendulum system’s behaviour and draws it phase portrait. As an example, in Fig. 6.10 the phase portrait of P3 RA (3/1) right oscillating rare attractor

(Fig. 3.25, a) for the system's parameters b = 0.2, h = 10, ω = 9 is shown. In this system also coexist period-1 zero attractor, period-1 hilltop attractor, subharmonic P3 twin attractors, left and right rotations of period-1. It is declared by the one-parameter (see Fig.3.21) and two-parameter bifurcation diagram (Fig. 3.24).

6.6 Conclusions

This chapter shows the possibility of performance of the experimental investigations in more realistic models of pendulum systems, which were discussed in the present doctoral thesis. For these purposes, the experimental setup for natural experimental investigations in the simplest pendulum system with the periodically vibrating point of suspension in vertical direction was developed and produced. The experimental and theoretical investigations were performed for the simple pendulum driven system, in which founded regimes have qualitative agreement with the theoretical investigations. The four different oscillating and rotating regimes were found in both cases. Bifurcation diagrams also correspond to the results of numerical simulations. Near the bifurcation points of the non-ideal construction of experimental setup and other external factors have influence on the system's behaviour. Probably, the quantitative differences appear due to the dry friction effect, the influence of external factors (magnetic fields, the correct way of experimental data collection through the microcontroller, etc.) and the unheeded dynamic characteristics of the exciter (motor). These influences require further study. Therefore, as it was mentioned before the theoretical and experimental results obtained in this chapter should be considered preliminary. In the future it is planned to conduct the more detailed analysis including the described above influences on the studied pendulum system.

The visualization possibility of the founded regimes by the method of complete bifurcation groups in the pendulum systems is shown as well. It is implemented by the animation software created using Pascal programming language. The animation of nonlinear phenomena of pendulum systems can be useful not only for student as methodological material, but also for engineers who are working with real pendulum-like systems.

The possible applications of founded regimes in the driven pendulum systems with the periodically vibrating point of suspension in vertical direction may be the energy extraction, mixing (liquids, washing machines), robotics, communication and orientation systems of the spacecraft (antenna), etc.

Conclusion

The main task of the doctoral thesis is a theoretical and practical study of the nonlinear dynamics of the pendulum systems with one or several degrees of freedom by the method of complete bifurcation groups, which allow conducting the global bifurcation analysis and finding new bifurcation groups, unknown before rare periodic and chaotic attractors both oscillating and rotating. The results can provide guidance on the use of complex regular and chaotic regimes on real objects in vibroengineering, robotics, space dynamics, medicine etc.

In the present doctoral thesis such main results were obtained:

1. Apparently, rare regular and chaotic rotational regimes have been found in the pendulum systems with or several degrees of freedom for the first time within the framework of this research. These nonlinear phenomena define a great theoretical and practical interest of studies of nonlinear dynamics in the pendulum systems.
2. It is shown that the use of the method of complete bifurcation groups allows conducting the qualitative global bifurcation analysis of the pendulum systems and finding the new bifurcation groups and previously unknown regular and chaotic oscillating, oscillating-rotating and rotating orbits (regimes, attractors) by the example of the simplest systems with one or more degrees of freedom. The qualitative topology of different bifurcation groups is investigated and new periodic and chaotic orbits are found.
3. The birth of the previously unknown rare attractors has been shown for different harmonically driven damped systems using the method of complete bifurcation groups, and new bifurcation groups with complex protuberances have been obtained. The new types of interaction of different oscillating and rotating orbits have been found as well as rare and chaotic rotational regimes.

4. Apparently, the process of formation of chaotic rotation through the cascade of period-doubling bifurcations for different groups has been found for the first time and studied within the framework of the research.
5. The interaction of different bifurcation groups in the pendulum systems with one or several degrees of freedom is investigated. Two-parameter bifurcation diagrams were constructed. It is shown, that the existence of bifurcation subgroup with unstable periodic infinitium (UPI) always leads to chaotic behavior of the system: chaotic attractor or transient chaos
6. The main qualitative results of topology of bifurcation groups with rare regular and chaotic attractors for the pendulum systems with two degrees of freedom were investigated. The subharmonic, chaotic and rare periodic behaviour were investigated. There are complex protuberances with many rare regular attractors of different types, chaotic transients and chaotic motions.
7. The possibility of using the method of complete bifurcation groups for the global analysis of the six body symmetric driven pendulum systems with several equilibrium positions is demonstrated.
8. The possibility of performance of the experimental investigations in more realistic models of pendulum systems, which were discussed in the present doctoral thesis, is shown. The visualization possibility of the founded regimes by the method of complete bifurcation groups in the pendulum systems is investigated as well.

Thus, in the doctoral thesis it is shown, that the method of complete bifurcation groups allows conducting the global bifurcation analysis of the pendulum systems with one or several degrees of freedom and finding new nonlinear phenomena, new bifurcation groups, unknown before rare periodic and chaotic attractors both oscillating and rotating. The possibility of usage of new obtained results in real objects is discussed as well.

The author is of the opinion that the method of complete bifurcation groups will be useful for global bifurcation analysis and for search of rare attractors as well as for other pendulum systems.

Bibliography

1. Andronov, A.A., Vitt, E.A., Khaiken, S.E. Theory of Oscillators. Oxford: Pergamon Press, 1966.
2. Andronov, A.A., Leontovich, E.A., Gordon, I.I., Maier, A.G. Theory of Bifurcations of Dynamic Systems on a Plane, Israel Program of Scientific Translations, Jerusalem, 1971.
3. Andronov, A.A., Leontovich, E.A., Gordon, I.I., Maier, A.G. Theory of Dynamic Systems on a Plane, Israel Program of Scientific Translations, Jerusalem, 1973.
4. Astashev, V.K., Babitsky, V.I. Ultrasonic cutting as a nonlinear (vibro-impact) process. // Ultrasonics, No.6, pp. 89-96, 1998.
5. Auzins J., Janushe Experimental design and analysis. Riga: RTU publ. house, 2007, 255 p. [in Latvian].
6. Auzins J., Boiko A. Various approaches for the simulation of mechanisms with flexible beams. E. Lavendelis and M. Zakrzhevsky (eds.), IUTAM/IFToMM Symposium on Nonlinear Dynamical Systems, Solid Mechanics and its Applications. Vol. 73, Dordrecht, Boston, London: Kluwer Academic Publishers. 2000, pp. 49-56.
7. Awrejcewicz, J., Ludwicki, M.. Dynamics of 3-D physical pendulums with nonautonomous system universal joints. // Proceedings of 10th Conference on Dynamical Systems – Theory and Applications, vol. 1, pp. 421-428, Lodz, Poland, 2009.
8. Awrejcewicz J., Pryk S. Nonlinear Dynamics of Three-Degree-of-Freedom Manipulator's Model. In: Lavendelis E., Zakrzhevsky M. Editors, IUTAM/IFToMM Symposium on Synthesis of Nonlinear Dynamical Systems, Kluwer Academic Publishers, 2000, pp. 57-66.
9. Balthazar, J.M., Felix, J.L.P., Dantas ,M.J.H. Searching of periodic solutions in a nonlinear electromechanical vibration absorber with a magneto-rheological damper and excited by a non-ideal motor. // Proceedings of 10th Conference on Dynamical Systems – Theory and Applications, vol. 1, pp. 429-438, Lodz, Poland, 2009.
10. Beletsky, V.V., Rodnikov, A.V. On evolution of libration points similar to Eulerian in the model problem of the binary-asteroids dynamics. // Journal of Vibroengineering - JVE 10, Issue 4, 12 (2008), pp. 550-556.
11. Belyakov A.O., On rotational solutions for elliptically excited pendulum. Physics Letters A. 2011, Vol. 375, Issue 25, pp. 2524-2530.
12. Birkhoff, G.D. Dynamical Systems, A.M.S. Publications, Providence, 1927.
13. Bishop, S.R. Impact oscillators, Phil. Trans. Roy. Soc. A, 347:347-351, 1994.
14. Blekhman, I.I. Vibrational Mechanics. Singapore: World Scientific, 2000 (in Russian: Nauka, Moscow, 1994).
15. Blekhman I.I., Kuznetsova L.P. Rare events – rare attractors; formalization and examples – Journal of Vibroengineering JVE, December 2008, Vol. 10, Issue 4, p. 418-420.
16. Butikov E I 2001 On the dynamic stabilization of an inverted pendulum Am. J. Phys. 69 (7) 755 – 768.
17. Butikov E. Regular and Chaotic Motions of the Parametrically Forced Pendulum: Theory and Simulations. Computational Science – ICCS 2002, Springer Verlag, LNCS 2331, pp. 1154 – 1169, 2002.
18. Cartmell, M.P., D'Arrigo, M.C. Simultaneous forced and parametric excitation of a space tether. // Proceedings of the 33rd Summer School on Advanced Problems in Mechanics, St. Petersburg: Russian Academy of Sciences, pp. 347-355, 2005.
19. De Paula, A., Savi, MA., Vaziri, V., Wiercigroch, M. & Pavlovskaia, EE. (2013). 'Numerical and Experimental Bifurcation Control in a Parametrically Excited Pendulum'. in MA Savi (ed.), Proceedings of the XV International Symposium on Dynamic Problems of Mechanics. ABCM, diname, Buzios, Brazil, 17-22 June.
20. Di Bernardo, M., Budd, C.J., Champneys, A.R., Kowalczyk, P. Piecewise-Smooth Dynamical Systems. Theory and Applications. Applied Mathematical Sciences, vol. 163, London: Springer-Verlag, 2008.
21. Fritzkowski P., Kamiński H. A discrete model of a rope with bending stiffness or viscous damping, Acta Mechanica Sinica, 27(1):108-113, 2011.
22. Galan J, Fraser W.B., Acheson D.J., Champneys A.R. The parametrically excited upside-down rod: an elastic jointed pendulum model, Journal of Sound and Vibration, 280 (2005), 359–377.

23. Guckenheimer, J. and Holmes, P. Nonlinear Oscillations, Dynamical Systems, and Bifurcations of Vector Fields. Applied Mathematical Sciences, vol. 42, New York: Springer-Verlag, 1983.
24. Horton , B. , Sieber , J. , Thompson , J. M. T. and Wiercigroch , M. Dynamics of the elliptically excited pendulum. Cornell University Library , arXiv:0803.1662 (math.DS) , 2008.
25. Hsu C. S. Cell-to-Cell Mapping: A Method of Global Analysis for Nonlinear Systems. Springer-Verlag. New York. 1987.
26. Kovacic, I., Brennan, M.J. The Duffing Equation: Nonlinear Oscillators and Their Behaviour. Wiley, 2011.
27. Krause T., Kremer E., Movlazada P., Theory and Simulation of Centrifugal Pendulum Absorber with Trapezoidal Suspension // Proceedings of the 10th International Conference on Vibration Problems, September 5-8, 2011, Prague, Czech Republic, pp. 322-327.
28. Kuznetsov, Yu.A. Elements of Applied Bifurcation Theory (third edition). Applied Mathematical Sciences, vol. 112, New York: Springer-Verlag, 2004.
29. Landa, P.S. Regular and Chaotic Oscillations, Berlin: Springer-Verlag, 2001.
30. Lenci S., Rega G., 2011, "Load carrying capacity of systems within a global safety perspective. Part I: Robustness of stable equilibria under imperfections," Int. J. Non-Linear Mech., 46, 1232-1239.
31. Lenci S., Rega G., 2011, "Load carrying capacity of systems within a global safety perspective. Part II: Attractor/basin integrity under dynamic excitations," Int. J. Non-Linear Mech., 46, 1240-1251.
32. Leonov, G.A. Strange Attractors and Classical Stability Theory. St. Petersburg: St. Petersburg University Press, 2008.
33. Leine, R.I., van Campen, D.H. Discontinuous fold bifurcations in mechanical systems. Archive of Applied Mechanics, 72 (2-3):138-146, April 2002.
34. Li, T. Y., Yorke, J. A. Period Three Implies Chaos. 1975; Yorke J. A. Period Doubling. 2010; Private Communication, 2010.
35. Luo, A.C.J., Menon, S. Global chaos in a periodically forced, linear system with a dead-zone restoring force. Chaos, Solitons and Fractals 19(5):1189-1199, 2004.
36. Mikhlin, Yu.V., Avramov, K.V., Rudnyeva, G.V. Analytical Methods for Analysis of Transitions to Chaotic Vibrations in Mechanical Systems. // An International Journal of Research and Surveys "Nonlinear Dynamics and Systems Theory", vol. 9, No. 3, pp. 375-406, 2009.
37. Moon, F.C. Chaotic Vibrations. Wiley, 2004.
38. Mosekilde, E. Topics in Nonlinear Dynamics: Applications to Physics, Biology and Economic Systems. Singapore: World Scientific, 1996.
39. Naess, A., Mo, E. A numerical study of the existence and stability of some chaotic attractors by path integration. // Journal of Vibroengineering - JVE 10, Issue 4, 12 (2008), 541-549.
40. Najdecka, AJ., Vaziri, V. & Wiercigroch, M. (2013). 'Dynamics, Synchronization and Control of Parametric Pendulums'. Proceedings of the IUTAM Symposium on Nonlinear Dynamics for Advanced Technologies and Engineering Design, Aberdeen, UK, 27-30 July 2010. vol. 32, Springer, pp. 185-193.
41. Nandakumar K., Wiercigroch M., Chatterjee A. Optimum energy extraction from rotational motion in a parametrically excited pendulum. Mechanics Research Communications, vol. 43, 2012, 7-14. [
42. Nordmark, A.B. Non-periodic motion caused by grazing incidence in impact oscillators. Sound and Vibrations, 2:279-297, 1991.
43. Pavlovskaia E., Horton B., Wiercigroch M., Lenci S., Rega G., Approximate rotational solutions of pendulum under combined vertical and horizontal excitation. International Journal of Bifurcation and Chaos, 22(2012) 1250100 (13 pages).
44. Peterka, F., Vacik, J. Transition to chaotic motion in mechanical systems with impacts. Sound and Vibration, 154(1):95-115, 1992.
45. Poincaré, H. Mémoire sur les cóurbes definies par les équations différentielles I-VI, Oeuvre I, Gauthier-Villar, Paris, 1880-1890.
46. Ragulskis, K., Ragulskis, L. Dynamical directivity and chaos in some systems with supplementary degrees of freedom. // Journal of Vibroengineering - JVE 10, Issue 4, 12 (2008), 500-509.
47. Rega, G., Lenci, S. Recent advanced in control of complex dynamics in mechanical and structural systems. Series on Stability Vibration and Control of Systems, Series B "Recent progress in controlling chaos" - vol. 16, pp.189-237, 2010.
48. Shaw, S.W., Holmes, P.J. A periodically forced piecewise linear oscillator. Sound and Vibration, 90(1):129-155, 1983.
49. Skiadas, C. H., Skiadas, C. Chaotic Modelling and Simulation: Analysis of Chaotic Models, Attractors and Forms, CRC / Taylor & Francis, 2009.
50. Skiadas, C.H. Von Karman Streets Chaotic Simulation. WSPC – Proc., pp. 309-313, 2009.
51. Stachowiak T., Okada T.. "A numerical analysis of chaos in the double pendulum", Chaos, Solitons & Fractals, vol. 29, pp.417–422, 2006.

52. Starrett J and Tagg R 1995 Control of a chaotic parametrically driven pendulum Phys. Rev. Lett. 74, (11) 1974-1977.
53. Stephenson, A. On a new type of dynamic stability. Memoirs and Proceedings of the Manchester Literary and Philosophical Society 52(8): 1-10, 1908.
54. Strizak T.G. Methods of dynamical pendulum type systems research - Alma-Ata: Science KazSSR, 1981, p. 256 (in Russian).
55. Szemplinska-Stupnicka W., Tyrkiel E. The oscillation-rotation attractors in the forced pendulum and their peculiar properties. I. J. Bifurcation and Chaos 12(1):159-168 (2002).
56. Thompson, J.M.T. and Stewart, H.B. Nonlinear Dynamics and Chaos. 2nd ed., Wiley, 2002.
57. Thomsen, J.J. Vibrations and Stability. Berlin: Springer-Verlag, 2nd edition, 2003.
58. Tondl A., Kotek V., Kratochvil C.: Vibration Quenching of Pendulum Type Systems by Means of Absorbers, CERN akad. naklad., Brno, 2001
59. Ueda, Y. The Road to Chaos - II, Aerial Press Inc. - Santa Cruz, 2001.
60. Viba J., Kruusmaa M., Fointaine J. Robotic fish motion control optimization – XVI Symposium “Dynamics of Vibroimpact Systems” (“DYVIS-2009”), Moscow, Russia, 24-30 May, 2009, pp. 469-478.
61. Warmiñski J., Litak G., Lipski J., Wiercigroch M., Cartmell M. Chaotic vibrations in the regenerative cutting process. In: Lavendelis E., Zakrzhevsky M. Eds., IUTAM/IFToMM Symposium on Synthesis of Nonlinear Dynamical Systems, Kluwer, 2000, pp. 275-284.
62. Xu X., Wiercigroch M., Cartmell M.P. Rotating orbits of a parametrically-excited pendulum. Chaos, Solitons and Fractals 23 (5) (2005) 1537–1548.
63. Yurchenko D, Naess A, Alevras P (2013) Pendulum's rotational motion governed by a stochastic Mathieu equation. Probabilist Eng Mech 31:12-18.
64. Yurchenko D., Alevras P., Stochastic Dynamics of a parametrically base excited rotating pendulum, Procedia IUTAM 6 (2013) 160 – 168.
65. Zambrano, S., Allaria, E., Brugioni, S., Leyva, I., Meucci, R., Sanjuan, M., Arecchi, F. Numerical and experimental exploration of phase control of chaos. Chaos, 16:013111, 2006.
66. Zevin, A.A. Some amazing phenomena in stability of nonlinear dynamical systems. Proceedings of the 6th European Nonlinear Dynamics Conference ENOC-2008, 4 p., 2008.
67. Андрианов И.В., Грабенцев Р.Г., Маневич Л.И. Асимптотическая математика и синергетика: путь к целостной простоте. М.: Едиториал УРСС, 2004. – 304 с.
68. Анищенко В.С. Сложные колебания в простых системах. М.: Наука, 1990. – 312 с.
69. Анищенко В.С., Вадивасова Т.Е., Астахов В.В. Нелинейная динамика хаотических и стохастических систем. Фундаментальные основы и избранные проблемы. Саратов: Изд-во ГосУНЦ «Колледж», 2003. – 136 с.
70. Баталова З. С., Белякова Г. В. О колебательных движениях маятника с вибрирующей точкой подвеса // Динамика систем (оптимизация и адаптация). – Горький: Изд-во ГГУ, 1982. – С. 145 – 170.
71. Белецкий В. В. Очерки о движении космических тел. М.: Наука, 1977 (2-е изд.) – 430 с.
72. Бутиков Е.И. Маятник с осциллирующим подвесом (к 60-летию маятника Капицы). СПб.: Санкт-Петербургский государственный университет, 42 с.
73. Вульфсон И.И. Колебания в машинах. Учеб. пособие для втузов. Изд. 2-ое, доп. / СПб.: СПГУТД, 2006. – 260с.
74. Ганиев Р.Ф., Кононенко В.О. Колебания твердых тел. М.:Наука, 1976. – 432 с.
75. Гуськов А.М., Пановко Г.Я., Чан Ван Бинь. Динамика автопараметрического гасителя колебаний (часть 2) // Наука и образование. Инженерное образование. E-Journal (http://technomag.edu.ru/doc/87802.html). - 2008.- №4.
76. Данилов Ю.А. Лекции по нелинейной динамике. М.: Постмаркет, 2001. – 437 с.
77. Диаку Ф., Холмс Ф. Небесные встречи. Истоки хаоса и устойчивости. Москва-Ижевск: НИЦ «Регулярная и хаотическая динамика», 2004. – 304 с.
78. Капица П.Л. Динамическая устойчивость маятника при колеблющейся точке подвеса. // Журн. эксперим. и теорет. физики, 1951. т.21. вып.5. с. 588-597.
79. Капица С.П., Кудрюмов С.П., Малинецкий Г.Г. Синергетика и прогнозы будущего. Изд. 2-е. М.: Едиториал УРСС, 2001. – 288 с.
80. Кельзон А.С., Циманский Ю.П., Яковлев В.И. Динамика роторов в упругих опорах. М., 1982. – 280 с.
81. Краснопольская Т.С., Щвец А.Ю. Регулярная и хаотическая динамика систем с ограниченным возбуждением. Москва: Ижевск: R&CD, 2008. – 280 с.
82. Крылов Н. М., Боголюбов Н. Н. Введение в нелинейную механику. Киев: Изд. АН УССР, 1937.
83. Кузнецов А.П, Кузнецов С.П., Рыскин Н.М. Нелинейные колебания. Учеб. Пособие для вузов. М.: Издательство физико-математической литературы, 2002. – 292 с.
84. Лавендел Э. Э. Синтез оптимальных вибромашин. Рига: Зинатне, 1970. – 252 с.

85. Магницкий Н.А., Сидоров С.В. Новые методы хаотической динамик. М.: Изд-во УРСС, 2004. – 320 с.
86. Малинецкий Г.Г.,Потапов А.Б Нелинейная динамика и хаос. М.: Эдиториал УРСС, 2006. – 240 с.
87. Митулис А. А. Влияние начальных параметров движения на условия вибрационного возбуждения синхронного вращения маятника. Дис. канд. техн. наук. Рига, 1966. – 224с.
88. Морозов А.Д. Глобальный анализ в теории нелинейных колебаний. Монография. Н.Новгород: изд-во ННГУ, 1995. – 292 с.
89. Неймарк Ю. И. Метод точечных отображений в теории нелинейных колебаний. М., 1972. – 472 с.
90. Неймарк Ю. И., Ланда П. С. Стохастические и хаотические колебания. - М.: Наука. Гл. ред. ред. физ.-мат. лит., 1987. - 424 с.
91. Пановко Я. Г., Губанова И. И. Устойчивость и колебания упругих систем. М.: Наука. Гл. ред. физ.-мат. лит., 1987. – 352 с.
92. Пановко Г.Я. Динамика вибрационных технологических процессов. М. – Ижевск: НИЦ «Регулярная и хаотическая динамика», Инст. комп. исследований, 2006. – 176 с.
93. Рабинович М.И., Трубецков Д.И. Введение в теорию колебаний и волн. М.: Наука, 1984.
94. Трубецков Д.И. Введение в синергетику. Колебания и волны. Изд. 2-е. М.: Едитор. УРСС, 2003. – 224 с.
95. Фейгин М.И. Вынужденные колебания систем с разрывными нелинейностями. М., 1994. – 288 с.
96. Хаяси Т. Нелинейные колебания в физических системах. М.: Мир, 1968. – 432 с.
97. Шустер Г. Детерминированный хаос: Введение: Пер. с англ. М.: Мир, 1998. – 240 с.

List of works of the research group “Nonlinear dynamics, chaos, complexity and control” of the Institute of Mechanics, Riga Technical University

98. Zakrzhevsky, M.V. The nonlinear way of thinking and education problems in nonlinear dynamics. // Proceedings of the 2nd European Nonlinear Oscillations Conference. Prague, Vol.2, pp. 255-260, 1996.
99. Zakrzhevsky, M.V., Frolov, V. Bifurcation analysis of the stable forced oscillations near unstable equilibrium position. // Proceeding of the 2nd ENOC, Prague, Vol.2, pp. 265-267, 1996.
100. Zakrzhevsky M., Ivanov Yu., Frolov V. NLO: Universal Software for Global Analysis of Nonlinear Dynamics and Chaos. // Proceeding of the 2nd ENOC, Prague 1996. v.2. p.261-264.
101. Zakrzhevsky, M.V., Frolov, V. Hilltop effect: the global stable oscillations near unstable equilibrium positions. Proceedings of the 3rd EUROMECH Solid Mechanics Conference, Stockholm, Sweden, pp. 225, 1997.
102. Zakrzhevsky, M.V. The energy coordinates and energy phase space in nonlinear dynamics. // Proceedings of the 3rd EUROMECH Solid Mechanics Conference. Stockholm, pp. 226, 1997.
103. Zakrzhevsky, M.V. Global Stable Oscillations Near Unstable Equilibrium Positions: The Hilltop Effect, in F.C. Moon (ed.), Proceedings of the IUTAM Symposium on New Applications of Nonlinear and Chaotic Dynamics in Mechanics, held in Ithaca, USA, Kluwer Academic Publishers, pp. 117-124, 1998.
104. Zakrzhevsky, M.V. Stable Forced Hilltop Oscillations, in E. Lavendelis and M. Zakrzhevsky (eds.), Proceedings of the IUTAM Symposium on Synthesis of Nonlinear Dynamical Systems, held in Riga, Latvia, 1997, Kluwer Academic Publishers, pp. 285-294, 2000.
105. Zakrzhevsky, M.V. Nonlinear Oscillatory and Vibro-Impact Systems: Rare Attractors, in V.K. Astashev and V.L. Krupenin (eds.) The Dynamics of Vibroimpact (Strongly Nonlinear) Systems. Russian Academy of Sciences, Moscow-Zvenigorod, pp. 156-162, 2001.
106. Smirnova, R.S. Regular and Chaotic Forced Oscillations in Piecewise Linear Systems with Nonlinear Dissipation. Ph.D Thesis, RTU, Riga: Daugavpils, 2002, 189 p. [in Russian].
107. Schukin, I.T. Development of the methods and algorithms of simulation of nonlinear dynamics problems. Bifurcations, chaos and rare attractors. PhD Thesis, Riga: Daugavpils, 2005, 205 p. [in Russian].
108. Zakrzhevsky, M. V. Method of Bifurcation Groups (MBG) and Prediction of Rare Dangerous Phenomena in Machine Dynamics, 2007. Arctic Summer Conference on Dynamics, Vibrations and Control, August 6-10, Ivalo, Finland, pp. 36-38, 2007.
109. Zakrzhevsky, M.V. New concepts of nonlinear dynamics: complete bifurcation groups, protuberances, unstable periodic infinitiums and rare attractors. // Journal of Vibroengineering - JVE 10, Issue 4, 12 (2008), pp. 421-441.
110. Schukin, I.T., Zakrzhevsky, M.V., Ivanov, Yu.M., Kugelevich, V.V., Malgin, V.E., Frolov, V.Yu. Realization of Direct Methods and Algorithms for Global Analysis of Nonlinear Dynamical Systems. // Journal of Vibroengineering - JVE 10, Issue 4, 12 (2008), 510-518.
111. Zakrzhevsky, M.V. Global nonlinear dynamics based on the method of complete bifurcation groups and rare attractors. // Proceedings of the ASME 2009 (IDETC/CIE 2009), San Diego, USA, p. 8, 2009.
112. Yevstignejev, V.Yu. Application of the Complete Bifurcation Groups Method for Analysis of Strongly Nonlinear Oscillators and Vibro-Impact Systems. PhD thesis, Riga, 2008.

113. Zakrzhevsky, M.V., Frolov, V. ABC NDC: new software for global analysis of nonlinear dynamics and chaos. // Proceedings of the 2nd International Symposium RA'11 on “Rare Attractors and Rare Phenomena in Nonlinear Dynamics”, May 17 - 20, 2011, Jurmala, Latvia, pp. 11-15.
114. Smirnova, R., Zakrzhevsky, M., Schukin, I., Yevstignejev, V. The influence of nonlinear dissipation on the birth of rare attractors in dynamic systems. // Proceedings of the 2nd International Symposium RA'11 on “Rare Attractors and Rare Phenomena in Nonlinear Dynamics”, May 17-20, 2011, Jurmala, Latvia, pp. 31-34.
115. Yevstignejev, V.Yu., Zakrzhevsky, M. Clusters of submerged subharmonic isles with rare attractors in two parameters bifurcation diagrams. // Proceedings of the 2nd International Symposium RA'11 on “Rare Attractors and Rare Phenomena in Nonlinear Dynamics”, May 17-20, 2011, Jurmala, Latvia, pp. 35-38.
116. Yevstignejev, V.Yu., Zakrzhevsky M., Toporensky A., On the Possibility of Rare Attractors in Scalar Field Cosmology. // Proceedings of the 2nd International Symposium RA'11 on “Rare Attractors and Rare Phenomena in Nonlinear Dynamics”, May 17 - 20, 2011, Jurmala, Latvia, pp. 39-42.
117. Schukin, I.T. Global analysis of nonlinear regular, transient and chaotic dynamics. // Proceedings of the 1st International School for Young Scientists “Nonlinear Dynamics of Machines” and of the XVII Symposium “Dynamics of Vibroimpact Systems” (“DYVIS-2012”), Moscow-Klin, 20 - 26 May, 2012, pp. 252-260.
118. Smirnova, R.S. The transition to chaos and criteria of chaotic behavior in dynamical systems with linear and nonlinear damping. // Proceedings of the same conferences (“School-NDM” and “DYVIS-2012”), Moscow-Klin, 20 - 26 May, 2012, pp. 261-267.
119. Закржевский М.В. Колебания существенно-нелинейных механических систем. Рига: Зин., 1980. – 189 с.
120. Кугелевич В. В. Применение метода Ньютона-Канторовича для отыскания и продолжения по параметру периодических движений динамических систем. //Вопросы динамики и прочности. -Рига, 1981. вып. 49, с. 43-50.
121. Кугелевич В.В. Автоматизированный расчет вынужденных колебаний нелинейных вибромашин на основе метода точечных отображений. Дис. канд. техн. наук. Рига, РПИ, 1987. – 198с.
122. Фролов В.Ю. Усовершенствование методов и алгоритмов расчета существенно-нелинейных колебательных систем. Диссертация, Рига, 1997 г. – 181 с.
123. Шилван Э.П., Закржевский М.В. Динамика клапанной системы при вынужденных колебаниях. Бифуркационный анализ и редкие регулярные и хаотические аттракторы. // Сборник трудов первой международной школы молодых ученых "Нелинейная динамика машин" (School-NDM) и XVII Симпозиума по динамике виброударных (сильно нелинейных) систем (DYVIS-2012), Москва – Клин, 20 – 26 мая, 2012, с. 220-227.

List of works with the participation of author

124. Klokov A., Viba J. Modeling of mixed excitation system // Scientific Journal of RTU. 6. series., Transport and Enineering. - 28. vol. (2008), pp. 55-62. [in Latvian].
125. Klokov A. Vibration and noise quenching of aviation engines by the methods of nonlinear dynamics. – Bachelor Thesis, Riga: RTU, 2007, 120 p. [in Latvian].
126. Klokov A. Research of the typical spacecraft models by the methods of nonlinear dynamics. Master Thesis, Riga: RTU, 2009, 90 p. [in Latvian].
127. Klokov A., Zakrzhevsky M. Rare attractors in the spacecraft dynamics. // XVI Symposium “Dynamics of Vibroimpact Systems” (“DYVIS-2009”), Moscow, Zvenigorod, 2009, pp. 183-192. [in Russian].
128. Zakrzhevsky M., Smirnova R., Schukin I., Yevstignejev V., Kugelevich V., Frolov V., Klokov A., Shilvan E. Method of complete bifurcation groups and its application in nonlinear dynamics. // Scientific Journal of RTU. 6. series., Transport and Enineering: Anniversary edition. - 31. vol. (2009), pp. 27-34.
129. Klokov A., Zakrzhevsky M. Bifurcation analysis and rare attractors in the parametrically excited pendulum system. // 10th Conference on Dynamical Systems Theory and Applications, Poland, Lodz, 7.-10. December, 2009. - pp 623-628.
130. Klokov A., Zakrzhevsky M. Bifurcation analysis and rare attractors in driven damped pendulum systems. // JVE Journal of Vibroengineering. – December 2010, Volume 12, Issue 4, pp. 369-374.
131. Klokov A. Application of the Method of Complete Bifurcation Groups in Parametrically Excited Pendulum Systems // Scientific Journal of RTU. 6. series., Transport and Enineering. - 33. vol. (2010), pp. 43-48.
132. Zakrzhevsky M., Klokov A. Complete bifurcation analysis of a pendulum with a vibrating support. // Proceedings of „16th US National Congress of Theoretical and Applied Mechanics”, June 27 - July 2, 2010, State College, Pennsylvania, USA, CD, 2 p.
133. Zakrzhevsky M., Schukin I., Smirnova R., Yevstigņejev V., Frolov V., Klokov A., Shilvan E. Global nonlinear dynamics: new novel concepts and their realization based on the method of complete bifurcation groups. // Proceedings of „16th US National Congress of Theoretical and Applied Mechanics”, June 27 - July 2, 2010, State College, Pennsylvania, USA, CD, 2 p.

134. Zakrzhevsky M., Klokov A. Rare attractors and method of complete bifurcation groups in tasks of dynamics of machine and mechanisms. // The extended paper publishing of the best presentations of XXII International Innovation Conference of Young Scientists and Students (IICYSS-2010) “Future of Russian Mechanical Engineering” (October 26 - 29, 2010), Moscow, Russia, 2011, 58-65 p. [in Russian].
135. Kraģis A., Zakrževskis M., Klokovs A. Svārsta tipa kosmiska moduļa nelineāra dinamika. Par jauna veida pārvietošanas iespēju.// 51. RTU studentu zinātniskas un tehniskas konferences materiāli II (Mašīnzinības), 2010. gada aprīlī, RTU Izd., lpp. 110-111.
136. Zakrzhevsky M., Klokov A., Yevstigņejev V., Shilvan E., Kragis A. Nonlinear Dynamics and Rare Attractors in driven damped pendulum systems. Proceedings of the 7th International DAAAM Baltic Conference "Industrial engineering", 22-24 April 2010, Tallin, Estonia, Vol. 1, pp.136-141.
137. Klokov A., Zakrzhevsky M. Parametrically excited pendulum systems with several equilibrium positions. Bifurcation analysis and rare attractors. // International Journal of Bifurcation and Chaos, Vol. 21, No. 10 (2011) pp. 2825-2836.
138. Zakrzhevsky M., Klokov A., Yevstigņejev V., Shilvan E. Complete bifurcation analysis of the driven damped pendulum systems. // Estonian Journal of Engineering. - Mar2011, Vol. 17, Issue 1, pp. 76-87.
139. Klokov A., Zakrzhevsky M. Theoretical and Experimental investigation of the Parametrically Excited Pendulum Systems. // Proceedings of International Scientific Practical Conference "The role and opportunities of youth in the development of engineering sciences", April 28, 2011, Daugavpils, Latvia, pp. 49-52.
140. Klokov A., Pikulin D., Zakrzhevsky M. Rare Attractors in Discrete Nonlinear Dynamical Systems. // Proceedings of International Scientific Practical Conference "The role and opportunities of youth in the development of engineering sciences", April 28, 2011, Daugavpils, Latvia, pp. 45-48.
141. Klokov A., Zakrzhevsky M. Nonlinear Dynamics and Rare Attractors of the Pendulum with the Vertical Vibrating Point of Suspension. // Proceedings of the 2nd International Symposium RA’11 on “Rare Attractors and Rare Phenomena in Nonlinear Dynamics”, May 16 - 20, 2011, Riga - Jurmala, Latvia, pp. 16-20.
142. Zakrzhevsky M., Schukin I., Frolov V., Klokov A., Yevstignejev V., Smirnova R., Pikulin D. Rare Attractors in Discrete Nonlinear Dynamical Systems. // Proceedings of the 2nd Symposium RA’11 on “Rare Attractors and Rare Phenomena in Nonlinear Dynamics”, May 16 - 20, 2011, Riga - Jurmala, Latvia, pp. 21-25.
143. Zakrzhevsky M., Schukin I., Smirnova R., Yevstignejev V., Klokov A., Shilvan E., New Methods of Global Bifurcation Analysis in Nonlinear Machine Dynamics. // Proceedings of the 10th International Conference on Vibration Problems “ICOVP 2011”, September 5-8, 2011, Prague, Czech Republic, pp. 100-105.
144. Klokov A., Zakrzhevsky M., Schukin I. Shilvan E. Rare and chaotic oscillating and rotating attractors in pendulum systems. // Proceedings of the 1st International school for young scientists “Nonlinear dynamics of machines” (School-NDM) and of the XVII Symposium “Dynamics of Vibroimpact Systems” (“DYVIS-2012”), Moscow-Klin, 20-26 May, 2012, pp.100-111. [in Russian].
145. Kremer E., Zakrzhevsky M., Klokov A. Complete Bifurcation Analysis with Rare Attractors of a Pendulum Vibration Absorber // Proceedings of the 4th IEEE International Conference on Nonlinear Science and Complexity “NSC 2012”, August 6-11, 2012 Budapest, Hungary, pp. 205-210.
146. Yevstignejev V., Klokov A., Smirnova R., Schukin I. Rare Attractors in Typical Nonlinear Discrete Dynamical Models // Proceedings of the 4th IEEE International Conference on Nonlinear Science and Complexity “NSC 2012”, August 6-11, 2012 Budapest, Hungary, pp. 229-234.
147. Zakrzhevsky M., Smirnova R., Schukin I., Yevstignejev V., Frolov V., Klokov A., Shilvan E. Nonlinear Dynamics and Chaos. Bifurcation Groups and Rare Attractors. – Riga: RTU Publishing House, 2012 – 181 p. [in Russian].
148. Zakrzhevsky M.V., Pikulin D.A., Klokov A.V., Smirnova R.S., Yevstignejev V.Yu., Schukin I.T.. Rare attractors in discrete nonlinear dynamical systems. – Riga: RTU, 2013. – 105 lpp.
149. Zakrzhevsky M. and Klokov A. How to find rare attractors and chaos in nonlinear dynamical systems by the method of complete bifurcation groups. The collection of bifurcation diagrams in the pendulum driven systems. – Riga, 2013 – 310 p.
150. Zakrzhevsky M., Schukin I., Yevstignejev V., Frolov V., Smirnova R., Klokov A., Shilvan E. Nonlinear Dynamics and Chaos. Complete Bifurcation Analysis and Rare Attractors. – Riga: RTU Publishing House, 2013. – 210 p. (in print).
151. Kremer E., Zakrzhevsky M., Schukin I., Klokov A. Bifurcation Analysis for a Quasi-linear Centrifugal Pendulum Absorber. Proceedings of the 11th Biennial International Conference on Vibration Problems (ICOVP-2013), September 9 - 12, 2013, Lisbon, Portugal, CD, 6 p.
152. Zakrzhevsky M., Schukin I., Klokov A., Shilvan E. Periodic Skeletons of Nonlinear Dynamical Systems in the Problems of Global Bifurcation Analysis. Proceedings of the International Conference VIBROENGINEERING 2013, 18–20 September, 2013, Druskininkai, Lithuania, 6 p. (in print).

List of notations and abbreviations

S – structure of the pendulum system;
P – parameters of the pendulum system;
Q – state of the pendulum system;
p – generalized notation of the system's parameter during bifurcation analysis;
x – phase coordinate;
$v = \dot{x}$ - phase velocity;
x_p – coordinate of fixed point after one period of excitation force; v_p – velocity of fixed point after one period of excitation force; in the diagrams coordinates of fixed points are defined by $x = x_p$ and $v = \dot{x}_p$;
c – coefficient of elastic characteristic;
b – the linear dissipation coefficient;
h – the amplitude of external excitation;
ω – the frequency of external excitation;
T_ω – the period of external excitation;
k – the coefficient characterizing the step of numeric integration $\Delta t = T_\omega / 2^k$;
Ψ – the loss coefficient for the linear viscous damping on energy plane after one period T_ω of excitation, $\psi = \Delta P_c / P_c$;
k_x – the coefficient of nonlinearity of elastic characteristic, $k_x = \left| dp/dA \cdot A/p \right|$ (see Paragraph 2.6);
1*T*, 2*T*, … *nT* – the bifurcation group of order 1, 2, … *n*;
*P*1, *P*2, … *Pn* – the periodic oscillating orbit with period 1, 2, … *n* of excitation, for the solutions of subharmonic type – *P*2, *P*3, *P*4, etc. *P*4 (2/4) *u* notation of the periodic unstable orbit of the period-4, which has 2 loops on the phase portrait, while for stable attractors the notation "*s*" is used;
*R*1, *R*2, … *Rn* – the rotating orbit with period 1, 2, … *n* of excitation, for the solutions of subharmonic type – *R*2, *R*3, *R*4, etc. The sign "+" denotes counter-clockwise or right rotation of the pointer, while the sign "-" – clockwise or left rotation. The notation "*u*" denotes unstable rotation, while the notation "*s*" – stable rotational attractor.
*OR*1, *OR*2, … *ORn* – the oscillating-rotating orbit with period 1, 2, … *n* of excitation, for the solutions of subharmonic type – *OR*2, *OR*3, *OR*4, etc. The sign "+" denotes counter-clockwise or right oscillation-rotation of the pointer, while the sign "-" – clockwise or left oscillation-

rotation. The notation "*u*" denotes unstable oscillation-rotation, while the notation "*s*" – stable oscillating-rotating attractor;

ChA – chaotic attractor; *ChA*-3, *ChA-n* – chaotic attractor of the bifurcation group *n;*

RA – rare attractor; *P*1 *RA*, *P*2 *RA*, *PnRA* – rare attractor with period 1, 2, 3, …, *n*; *R*4 *RA*+ denotes a rare attractor of subharmonic counter-clockwise rotational regime of order 4. Rare attractors can be in the form of egg (egg-shaped) or dumbbell, kink or hysteresis or in the form of small isolated island (isola isle);

Twins – asymmetric, but mutually symmetric orbits (oscillatory or rotational) exist only in symmetric systems; in diagrams these orbits are defined as left and right;

HT – hilltop periodic orbit (regime, attractor), which exists near unstable equilibrium position;

FP – fixed point;

UPI – infinite number of unstable periodic regimes;

UPI-1, *UPI*-2, *UPI*-3, …, *UPI-n* – infinite number of unstable periodic regimes for bifurcation group *n*;

DW – dynamical well;

Core of attraction – set of points (initial conditions) in phase space near the FP, from which after the transient process in the system the particular orbit (regime, attractor) implements;

L – cyclicity of the pendulum by coordinate *x* is 2;

$\rho_1, \rho_2, \ldots, \rho_i,$ – values of multiplicators, characterizing the stability of periodic regimes;

Cm – contour mapping on Poincaré plane;

Lm – line mapping on Poincaré plane;

Lm 50Q×100T – line mapping on Poincaré plane from 50 initial conditions along the 100 periods of external excitation force for each point;

NQ – number of initial points;

PSK – periodic skeleton;

KIN – maximum number of iterations;

EPN – precision search of the fixed point;

DEN – parameter of discretization;

—— – stable solutions on bifurcation diagrams are plotted by black solid lines;

—— – unstable solutions on bifurcation diagrams are plotted by reddish thin lines.

● – rare attractors on the bifurcation diagrams;

×, ▲ – marker that defines the location of stable FP of periodic regime on Poincaré plane;

o – unstable fixed point of periodic regime on the Poincaré plane;

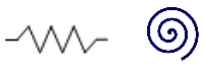 – elastic restoring forces on figures of pendulum driven damped models;

${}^{4}E^{3}$ – stable fixed point of the periodic orbit with period-3, which has 4 loops;

${}^{4}\overline{E}^{3}$ – unstable fixed point of the periodic orbit with period-3, which has 4 loops;

${}^{4}_{1}E^{3}_{2}$ – the 1-st stable fixed point of the 2-nd periodic orbit with the period-3, which has 4 loops;

${}^{4}_{1}\overline{E}^{3}_{2}$ – the 1-st unstable fixed point of the 2-nd periodic orbit with the period-3, which has 4 loops;

${}^{3}S^{2}_{1}(p)$ – notation of the 1-st 2T bifurcation group, which has 2×3 folds.

Index of terms

Glossary

This glossary contains a list of some basic definitions and terms of Bifurcation Theory. Terms, which are proposed by the research group "Nonlinear dynamics, chaos, catastrophes and control" of the Institute of Mechanics of RTU under the guidance of Prof. M. Zakrzhevsky, are marked with a sign (*).

A **Andronov-Hopf bifurcation** – a birth of quasi-periodic oscillations from the periodic one by varying parameter of dynamical system.

Attractor – a point or collection of points in the phase space, where all the initial states tend to approach the steady-state. There are several types of attractors, such as a point attractor, a periodic or quasi-periodic attractor, chaotic attractor or rare attractor.

B **Basin of attraction** – a collection of points in the phase space (initial conditions), from which a concrete regime (attractor) is realized after a transient process (see Paragraph 2.10).

Bifurcation – a qualitative change in the topology of the phase space by varying a bifurcation parameter of dynamical system.

Bifurcation analysis – an analysis of behaviour of a dynamical system by varying a bifurcations parameter.

Bifurcation analysis (complete)* – complete analysis of behaviour of a dynamical system by varying a bifurcations parameter, whereby complete bifurcation groups are constructing (see Paragraph 2.1).

Bifurcation group (complete)* – all stable and unstable branches of periodic orbits, the branches of which are connected to each other at a bifurcation points (see Paragraph 2.3).

Bifurcation parameter – a parameter of a dynamical system, by varying of which a bifurcation occurs.

C **Chaos** – irregular oscillations of a deterministic system, which have a high sensitivity to initial conditions.

Chaotic attractor – the same as *chaos*.

D **Dynamical system (DS)** – a dynamic continuous or discrete model, behavior of which unambiguously and deterministically depends on it structure (S), parameters (P) and states (initial conditions Q_0)

E **Equilibrium state** – see *fixed point.*

F **Fixed point (FP)** – a singular point on Poincaré plane, which corresponds to stable or unstable periodic solutions, i.e. to closed phase trajectories. There are four types of fixed points: node, focus, saddle and center.

Fold bifurcation – a bifurcation, where stable and unstable branches of a same regime mutually eliminates.

I **Initial conditions** – a vector of generalized coordinates (displacement, velocity, initial phase of external influence), which is used to describe a mathematical model of a dynamical system at the initial time t_0.

Island* – a closed branch of periodic regime in a limited region of varied parameter in the bifurcation diagram.

L **Linear dissipation** – a friction force is proportional to the velocity.

M **Method of Complete Bifurcation Group (MCBG)*** – a complex of approaches used for the global bifurcation analysis of dynamical systems for variable parameter values. MCBG is applied to find all stable and unstable periodic solutions for given parameter and phase space region (see Paragraph 2.1).

Multiplicity – a nonlinear phenomenon of coexistence of different stationary regimes (attractors) in phase space with the same parameters of the system and the invariance of its structure. An implementation of concrete regime depends on initial conditions.

N **Node** – an equilibrium state, which corresponds to the stability or instability of particular fixed point of the phase plane. Roots of the characteristic equation (multipliers) – real negative (positive) numbers.

P **Passport of a periodic orbit*** – includes the information about the order of regime, initial conditions or coordinates of its fixed points, multipliers characterizing the stability of found regimes, number of loops in phase projection closed curve and some additional information, if necessary. Data included in periodic skeleton allow complete reconstruction of the regime, preserving all its characteristics (see Paragraph 2.4).

Period doubling bifurcation – a local bifurcation in which a limit cycle of the system changes into a cycle of twice the period as a bifurcation parameter is varied.

Periodic regime – a stable or unstable periodic solution of differential equation or closed phase trajectory, which are assigned by fixed points of the corresponding T-mapping.

Periodic skeleton* – all stable and unstable periodic regimes with their passport for all bifurcation groups and UPI subgroups found for the fixed parameter value (see Paragraph 2.5).

Phase portrait – a portrait of regime, structure of partitioning of the phase space on trajectories for regime in studied dynamical system.

Poincaré mapping – see *T-mapping*.

Poincaré section – section, obtained by a strobe of dynamical variables (displacement x_p and velocity $\dot{x}_p = v_p$) after a period of excitation force T_ω.

Protuberance* – on the bifurcation diagram- the set of stable and unstable branches of periodic regimes, corresponding to one bifurcation group, restricted by period doubling or some other bifurcations of the same order.

Q **Quasi-periodic oscillations** – oscillations with two or more incommensurable frequencies.

R **Regular oscillations** – regular attractors (except chaotic one): point, periodic, quasi-periodic.

Rare attractors* – periodic regime, which exist, as a rule, in quite narrow ranges of system varied parameters. The types of rare attractors can be such: tip, egg-like or dumbbell, kink or hysteresis, small isolated island (isola isle) (see Paragraph 2.9).

Regime – characteristic of dynamical process. There are stationary and transient regimes.

S **Saddle** – an equilibrium state, which corresponds to an unstable fixed point of particular phase plane. Roots of the characteristic equation (multipliers) – real numbers, one of which is in absolute value greater than one.

Separatrix – stable and unstable manifolds (invariant curves) passing through a singular point of the saddle.

Simple island* – island, which has one stable and one unstable branch.

Stationary chaos – chaotic behaviour of the system that was established after the decay of transients in a dissipative dynamical system, the same as chaotic attractor.

Symmetry breaking bifurcation – a global bifurcation in which a symmetrical attractor is replaced by two coexisting asymmetrical attractors (twins).

T **T-mapping** – mapping, obtained on the Poincaré section by a strobe of dynamical variables (displacement x_p and velocity $\dot{x}_p = v_p$) after a period of excitation force T_ω.

Transient chaos – chaotic behavior that was established in the system during the transition to some regular stationary regime.

Transient process – nonstationary process that is describing the motion of the system from an initial state at time t_0 during time t of the transition to some steady state.

Twins* – periodic regimes, which appear in symmetrical systems as a result of symmetry breaking bifurcation.

U **Unstable periodic infinitium (UPI)*** – bifurcation subgroup with the infinite number of unstable periodic regimes corresponding to nT bifurcation group (see Paragraph 2.7).

Appendices

Appendix 1
Open problems

1. More detailed global bifurcation analysis of the pendulum systems with two, three and more bodies.
2. Improvement of algorithm for global bifurcations analysis of the pendulum systems. As it shown present doctoral thesis the computer performance and optimization in choosing of initial conditions for construction of periodic skeleton play an important role in research process. For example, for construction of periodic skeleton of rigid body pendulum (3.6) on Intel 4 CPU 2.66GHz personal computer the time calculation was 2 hours 13 minutes, but on Intel Core i3 CPU 3.30GHz it was 1 hour 20 minutes. More pronounced deference in time calculation of basins of attraction by Cell-to-Cell mapping was obtained. For the first PC it was about 21 hours, but for the second – 4 hours. Also it will be useful to take another method for choosing the initial conditions for construction of periodic skeleton. In this work it was done by the rectangle of grid of initial conditions as uniform distributed points. The possible way of hanging of finding the fixed points can be achieved for example using the Monte Carlo method.
3. The process of formation of chaotic rotation should be investigated by in-depth research.
4. Construction of basisns of attraction for the models with demiension $D \geq 4$. The task of a core of basin of attraction.
5. Applications of nonlinear effects of studied pendulums for the systems of different type.
6. Nonlinear dynamics of the pendulum systems are not fully investigated and due to this any results of the global bifurcation analysis and any serious researches of rare attractors and of rare bifurcation groups are not known. But these studies, of course, are needed to pursue.
7. More detailed experimental investigations of the pendulum systems including the dry friction effect, the influence of external factors (magnetic fields, the correct way of experimental data collection through the microcontroller, etc.) and the unheeded dynamic characteristics of the exciter (motor).

Appendix 2
Double pendulum in the software Spring

In the present appendix the construction of double pendulum model (4.22) with the periodically vibrating point of suspension in vertical direction in the software Spring is considered. The results of complete bifurcation analysis are presented in Paragraph 4.3.

Transforming the system of equations (4.22) by the accelerations and moving all forces acting on each of the pendulums to the right side of equations we get the following:

$$\ddot{\varphi}_1 = (Fb1 + Fx1 + F11 + F12 + Fg1 + Ft1) \Big/ \left[(m_1 + m_2)l_1^2 - m_2 l_1^2 \cos^2(\varphi_1 - \varphi_2)\right],$$

where $Fb1 = -b_1\dot{\varphi}_1 - b_2(\dot{\varphi}_1 - \dot{\varphi}_2)\left[1 - \dfrac{l_1}{l_2}\cos(\varphi_1 - \varphi_2)\right];$

$$Fx1 = -c_1\varphi_1 - c_2(\varphi_1 - \varphi_2)\left[1 - \frac{l_1}{l_2}\cos(\varphi_1 - \varphi_2)\right];$$

$$F11 = \frac{1}{2}m_2 l_1^2\dot{\varphi}_1^2 \sin 2(\varphi_1 - \varphi_2);$$

$$F12 = m_2 l_1 l_2\dot{\varphi}_2^2 \sin(\varphi_1 - \varphi_2);$$

$$Fg1 = \mu l_1\left[(m_1 + m_2)\sin\varphi_1 - m_2 \sin\varphi_2 \cos(\varphi_1 - \varphi_2)\right];$$

$$Ft1 = -l_1 h\omega^2 \cos\omega t\left[(m_1 + m_2)\sin\varphi_1 - m_2 \sin\varphi_2 \cos(\varphi_1 - \varphi_2)\right];$$

$$\ddot{\varphi}_2 = (Fb2 + Fx2 + F21 + F22 + Fg2 + Ft2) \Big/ \left[m_2 l_2^2 - \frac{m_2^2 l_2^2}{(m_1 + m_2)}\cos^2(\varphi_1 - \varphi_2)\right],$$

where $Fb2 = -b_2(\dot{\varphi}_2 - \dot{\varphi}_1)\left[1 + \dfrac{m_2 l_2 \cos(\varphi_1 - \varphi_2)}{(m_1 + m_2)l_1^2}\right] + \dfrac{m_2 l_2 b_1}{(m_1 + m_2)l_1}\dot{\varphi}_1 \cos(\varphi_1 - \varphi_2);$

$$Fx2 = -c_2(\varphi_2 - \varphi_1)\left[1 + \frac{m_2 l_2 \cos(\varphi_1 - \varphi_2)}{(m_1 + m_2)l_1^2}\right] + c_1\varphi_1 \frac{m_2 l_2 \cos(\varphi_1 - \varphi_2)}{(m_1 + m_2)l_1^2};$$

$$F21 = \frac{1}{2}\frac{m_2^2 l_2^2}{(m_1 + m_2)}\dot{\varphi}_2^2 \sin 2(\varphi_1 - \varphi_2);$$

$$F22 = m_2 l_1 l_2\dot{\varphi}_1^2 \sin(\varphi_1 - \varphi_2);$$

$$Fg2 = -m_2\mu l_2\left[\sin\varphi_2 - \sin\varphi_1 \cos(\varphi_1 - \varphi_2)\right];$$

$$Ft2 = m_2 l_2 h\omega^2 \cos\omega t\left[\sin\varphi_2 - \sin\varphi_1 \cos(\varphi_1 - \varphi_2)\right].$$

The model of double pendulum (4.22) for performing of the complete bifurcation analysis using the software Spring has such form:

```
PWM: Double pendulum with vibrating point of suspension in vertical direction

DOF 2

[Variables]
w = 4 is ' vertical external force frequency ' with range from 0 to 100
m1 = 1 is ' 1st pendulum mass ' with range from 0.0001 to 100
m2 = 0.1 is ' 2nd pendulum mass ' with range from 0.0001 to 100
b1 = 0.2 is ' friction coefficient of 1st pendulum ' with range from 0 to 10000
b2 = 0.1 is ' friction coefficient of 2nd pendulum ' with range from 0 to 10000
c1 = 1 is ' stiffnes coefficient of 1st pendulum ' with range from 0 to 10000
c2 = 0.5 is ' stiffnes coefficient of 2nd pendulum ' with range from 0 to 10000
h = 3 is ' vertical external force amplitude ' with range from 0 to 40000
l1 = 1 is ' 1st pendulum lenght ' with range from 0.0001 to 100000
l2 = 0.5 is ' 2nd pendulum lenght ' with range from 0.0001 to 100000
mju = 10 is ' free fall acceleration ' with range from 0.0001 to 100000
k = 7 is ' coefficient of integration step ' with range from 2 to 15

[markers]
Poincare w = w fi = 0

[options]
integration dt = (2*pi/w) / 2^k

[options]
;periodic x1 min -2*pi max 2*pi
;periodic x2 min -2*pi max 2*pi

[limitations]
x1 minimum -2*pi
x1 maximum 2*pi
v1 minimum -10
v1 maximum 10
x2 minimum -2*pi
x2 maximum 2*pi
v2 minimum -10
v2 maximum 10

[force Fb1]
Fb1 = -b1*v1 - b2*(v1-v2)*( 1 - (l1*cos(x1-x2)/l2) )

[force Fx1]
Fx1 = -c1*x1 - c2*(x1-x2)*( 1 - (l1*cos(x1-x2)/l2) )

[force F11]
F11 = 0.5*m2*l1*l1*v1*v1*sin(2*(x1-x2))

[force F12]
F12 = m2*l1*l2*v2*v2*sin(x1-x2)

[force Fg1]
Fg1 = mju*l1*( (m1+m2)*sin(x1) - m2*sin(x2)*cos(x1-x2) )

[force Ft1]
Ft1 = -l1*h*w*w*cos(w*t)*( (m1+m2)*sin(x1) - m2*sin(x2)*cos(x1-x2) )

[force Fb2]
Fb2 = -b2*(v2-v1)*( 1 + (m2*l2*cos(x1-x2)/((m1+m2)*l1*l1) )) +
(m2/((m1+m2)*l1))*l2*b1*v1*cos(x1-x2)
```

```
[force Fx2]
Fx2 = -c2*(x2-x1)*( 1 + (m2*l2*cos(x1-x2)/((m1+m2)*l1*l1) )) +
(m2/((m1+m2)*l1*l1))*l2*c1*x1*cos(x1-x2)

[force F21]
F21 = 0.5*m2*m2*l2*l2*v2*v2*sin(2*(x1-x2))/(m1+m2)

[force F22]
F22 = m2*l1*l2*v1*v1*sin(x1-x2)

[force Fg2]
Fg2 = -m2*mju*l2*( sin(x2) - sin(x1)*cos(x1-x2) )

[force Ft2]
Ft2 = m2*l2*h*w*w*cos(w*t)*( sin(x2) - sin(x1)*cos(x1-x2) )

[Equations]
a1 = (Fb1+Fx1+F11+F12+Fg1+Ft1) / ( (m1+m2)*l1*l1 - m2*l1*l1*cos(x1-x2)*cos(x1-x2) )
a2 = (Fb2+Fx2+F21+F22+Fg2+Ft2) / ( m2*l2*l2 - m2*m2*l2*l2*cos(x1-x2)*cos(x1-
x2)/(m1+m2) )
```

Appendix 3
Six body pendulum system in the software Spring

In this appendix the six body symmetric pendulum system with several equilibrium positions and with external harmonic excitation (Fig. 5.1) described by the system of equations (5.3) in the software Spring is look such:

Model for simulation in SPRING:

```
pwm: Pend 6 dof

DOF 6

[variables]
g=10    is 'gravitaional constant' with range from 0 to 100
h=2     is 'external force amplitude' with range from 0 to 150
w=3     is 'external force friquency' with range from 0 to 1000
b=0.2   is 'coefficient of linear damping' with range from 0 to 10
c=1     is 'stiffness coefficient of linear elastic force' with range from 0 to
5000
l=0.5   is 'length of pendulum' with range from 0 to 100
m=1     is 'mass of pendulum' with range from 0 to 100
k=7     is 'coefficient of integration step, dt=2pi/w/2^k' with range from 2 to
15

[options]
integration dt = (2*pi/w)/2^k

[markers]
Poincare w=w fi=0

[equations]
a1 = (b*(v2-v1)+c*(x2-x1)-b*v1-c*x1-m*g*l*sin(x1)+h*cos(w*t))/(m*l*l)
a2 = (b*(v3-v2)+c*(x3-x2)-b*(v2-v1)-c*(x2-x1)-m*g*l*sin(x2))/(m*l*l)
a3 = (b*(v4-v3)+c*(x4-x3)-b*(v3-v2)-c*(x3-x2)-m*g*l*sin(x3))/(m*l*l)
a4 = (b*(v5-v4)+c*(x5-x4)-b*(v4-v3)-c*(x4-x3)-m*g*l*sin(x4))/(m*l*l)
a5 = (b*(v6-v5)+c*(x6-x5)-b*(v5-v4)-c*(x5-x4)-m*g*l*sin(x5))/(m*l*l)
a6 = (-b*(v6-v5)-c*(x6-x5)-m*g*l*sin(x6))/(m*l*l)
```

Were used SPRING tools:

Fixed point	*for searching all periodic solutions and construction of the periodic skeleton*
Bifurcation diagram	*for construction of the bifurcation diagrams*

The results of complete bifurcation analysis, construction of periodic skeleton and basins of attraction is presented in Chapter 5.